THE UNIVERSITY *of* EDINBURGH

WT1 IN THE ADULT KIDNEY: PODOCYTE MAINTENANCE AND THE EPITHELIAL-MESENCHYMAL BALANCE

Eve Victoria Miller-Hodges

Ph.D.

The University of Edinburgh

2013

DECLARATION

This thesis has been composed by me and is entirely my own work. The experiments described within this thesis have also been carried out by me, unless stated otherwise. This work has not been submitted for any other degree or professional qualification. The publications arising from this thesis are included in the appendices, with permission from the joint authors.

Eve V Miller-Hodges

ACKNOWLEDGEMENTS

Firstly I would like to thank my supervisors, Nick Hastie and Peter Hohenstein, for all their help and input towards this project. To Nick for providing insight, perspective and for always asking the pertinent questions, and to Peter for offering vital practical support in techniques and methodologies, especially in the early months of making the transition from the ward to the lab.

Secondly, this project would not have been possible without the support of the ECAT programme and sponsorship from the Wellcome Trust. The ECAT programme provided me with this individual opportunity as well as fostering a clinical-academic community in which knowledge and experience was freely shared and encouraged, via the CATRIP meetings and networking opportunities.

Thirdly I would like to thank Moin Saleem, for the DDS cell lines and for offering thought and insight into the project.

I would also like to acknowledge all the help I received from the Hastie Lab group and other staff of the MRC HGU. Particular thanks should go to Anna Thornburn and Rachel Berry for all their help with animal experiments; to Paul Devenney for transgenics; to Lizzie Freyer for FACS and to Karamjit Singh-Dolt for work towards the Podocin-Cre construct. I would also like to thank the staff of the BRF and TF for the animal husbandry and for the practical support they provided.

When writing up, Karen Mackenzie offered excellent advice as to producing a focused thesis.

Finally, I would like to thank my partner Chris, for all his support, both emotional and practical, while attempting to complete experiments and write a thesis while heavily pregnant, and my daughter Iris, who despite adding a certain extra challenge to the situation, reminded me there was more to life than *WT1*.

ABSTRACT

Glomerular diseases are the leading cause of end stage kidney disease worldwide. Podocyte injury plays a key role in the initiation and development of such diseases, which follow a progressive course due to the limited capacity of podocytes to regenerate. Podocytes are highly specialised, terminally differentiated cells, which play a vital role in the glomerular filtration barrier. They are also the main sites of expression of the Wilms Tumour Suppressor gene, *WT1*, in the adult. *WT1* is a complex gene, which plays an essential role in renal development by controlling the process of mesenchymal to epithelial transition that forms the nephron. Adult podocytes maintain both epithelial and mesenchymal features and continue to express high levels of *WT1*. Little is known about the role of *WT1* in adult podocytes as previous studies have been limited due to the confounding developmental effects and embryonic lethality of existing animal models.

This thesis sought to investigate the hypothesis that *WT1* is an essential gene in adult kidney and plays a fundamental role in the adult podocyte. Given its role in nephron development, *WT1* loss was hypothesised to result in dedifferentiation and an alteration of the epithelial-mesenchymal balance in the podocyte, affecting its specialised function. Using an inducible, conditional animal model of *Wt1* loss, *Wt1* was deleted from the adult, confirming its essential role in adult kidney. *Wt1* deletion resulted in severe podocyte injury and failure of the glomerular filtration barrier, as well as loss of expression of key podocyte genes. Preliminary analysis suggests this was not simply due to podocyte apoptosis and/or detachment, supporting a role for *Wt1* in podocyte differentiation. This was corroborated by *in vitro* studies that demonstrated a requirement for *Wt1* for podocyte differentiation. Significantly, *Wt1* loss resulted in a marked change in the expression of epithelial and mesenchymal markers in podocytes, with upregulation of mesenchymal characteristics, in keeping with a transitional stage consistent with an earlier developmental form. To investigate the mechanism behind these findings a conditionally immortalised podocyte cell line was generated as a model of *Wt1* loss *in vitro*. In order to confirm and specifically analyse the podocyte phenotype, BAC recombineering was utilised to produce a promoter-reporter transgene construct to attempt to generate a fluorescent-labelled, podocyte specific animal model of *Wt1* loss.

The findings of this thesis establish that *Wt1* is essential for adult podocyte function, and appears to be a key upstream regulator of podocyte differentiation. Extension of this work may allow the identification of potential targets to promote podocyte differentiation and/or regeneration in the setting of acquired and progressive glomerular disease.

Table of Contents

Declaration 2

Acknowledgements 3

Abstract 4

Abbreviations 17

1 Introduction: *Wt1* is essential for adult podocyte maintenance and for regulation of their epithelial –mesenchymal balance 20

1.1 Overview 20

1.2 The Wilms' Tumour Suppressor Gene, WT1 22

1.3 WT1 mutations in disease 26

1.3.1 Wilms' Tumour 26

1.3.2 WAGR Syndrome 26

1.3.3 Denys Drash Syndrome 27

1.3.4 Frasier Syndrome 28

1.3.5 Renal Disease 29

1.4 The role of WT1 in renal development and how this may indicate potential roles for WT1 in the adult 32

1.5 WT1 and the epithelial-mesenchymal balance 37

1.5.1 Epithelial-mesenchymal transitions during development 37

1.5.2 Epithelial-mesenchymal transitions in cancer 39

1.5.3 Epithelial-mesenchymal transitions in scarring and fibrosis 39

1.6 The role of podocyte damage in glomerular disease and progressive kidney disease 42

1.6.1 Foot Process Effacement 44

1.6.2 Abnormalities of the slit diaphragm 45

1.6.3 Podocyte loss 45

1.7 Current knowledge about the role of WT1 in the podocyte 47

1.8 A role for WT1 in adult tissue maintenance and regeneration 49

1.9 Conclusion and hypothesis 51

2 Using human WT1-mutant podocyte cell lines to analyse the role of WT1 in the podocyte 52

2.1 Introduction 52

2.1.1 WT1 Mutations in Denys Drash Syndrome 52

2.1.2 Aims 54

2.1.3 Experimental approach 54

2.2 Generation of human cell lines from patients with DDS 55

2.3 DDS podocytes exhibit a more mesenchymal phenotype 56

2.4 *WT1* expression is altered in DDS podocytes 56
2.5 The epithelial-mesenchymal balance is disturbed in DDS podocytes 61
2.6 Conclusion: Summary of experimental findings 66
2.6.1 Human podocytes from patients with DDS shown downregulation of Wt1 upon differentiation 66
2.6.2 Human podocytes from patients with Denys Drash Syndrome exhibit variable disturbance of the epithelial-mesenchymal balance 66
2.7 Discussion 67
2.7.1 Human podocytes from patients with DDS shown downregulation of Wt1 upon differentiation 67
2.7.2 Human podocytes from patients with Denys Drash Syndrome exhibit variable disturbance of the epithelial-mesenchymal balance 68
2.8 Concluding Remarks 69
3 Generating an in vitro model of podocyte Wt1 loss 70
3.1 Introduction 70
3.1.1 Using conditionally immortalized podocyte cell lines to study podocyte biology in vitro 70
3.1.2 Limitations and drawbacks of in vitro podocyte culture systems 72
3.1.3 Aims 75
3.1.4 Experimental Approach 75
3.2 Generating a conditionally immortalized podocyte cell line from the CreER*Wt1*$^{co/GFP}$ mouse 76
3.3 Characterising the conditionally immortalized podocyte cell line from the CreER*Wt1*$^{co/GFP}$ mouse 78
3.3.1 CreERWt1$^{co/GFP}$ conditionally immortalized podocytes and "wild-type" conditionally immortalized podocytes can differentiate and express appropriate markers of mature podocytes 78
3.3.2 Tamoxifen-induced Cre-recombination causes Wt1 deletion in Podo32.1 cells 84
3.3.3 No macroscopic phenotype is evident following tamoxifen-mediated Cre-recombination 87
3.3.4 Evidence of significant Wt1 loss at either the mRNA or protein level cannot be demonstrated. 87
3.3.5 Wt1-deletion does not cause cell death or detatchment 92
3.3.6 Wt1$^{co/GFP}$ conditionally immortalised cells express only low levels of Wt1 96
3.4 Alternative Methods to achieve Wt1 loss in podocytes in vitro: Achieving Stable Wt1 knockdown using RNAi in cultured podocytes 100
3.4.1 Introduction 100
3.4.2 Using the Thermo Scientific Open Biosystems Expression Arrest GIPZ Lentiviral shRNAmir kit to knockdown Wt1 in podocytes. 100

3.4.3 Efficient transduction of both undifferentiated and differentiated podocytes is achieved using the pGIPZ Lentiviral Vector 102
3.4.4 Wt1 knockdown cannot be detected in undifferentiated cells 105
3.4.5 Putative Wt1-knockdown podocytes are unable to differentiate. 112
3.4.6 Using previously established Wt1-knockdown and controls in the pGIPZ Vector to validate results 116
3.4.7 Optimising the system in M15 cells 117
3.4.8 Effective Wt1 knockdown is achieved in conditionally immortalised podocytes 120
3.4.9 Wt1 is required for differentiation of conditionally immortalised podocytes in culture 123
3.5 Conclusion: Summary of experimental findings 127
3.5.1 CreERWt1$^{co/GFP}$ conditionally immortalised podocytes do not provide a robust model to study the effects of Wt1 loss in podocytes in vitro 127
3.5.2 RNAi can be used to stably knock down Wt1 in podocytes in vitro 127
3.5.3 Wt1 is necessary for differentiation of podocytes in culture 127
3.6 Discussion 128
3.6.1 CreERWt1$^{co/GFP}$ conditionally immortalised podocytes do not provide a robust model to study the effects of Wt1 loss in podocytes in vitro 128
3.6.2 RNAi can be used to stably knock down Wt1 in podocytes in vitro and Wt1 is necessary for differentiation of podocytes in culture 130
3.7 Concluding Remarks 132
4 *Wt1* is critical for glomerular function in adult kidney 133
4.1 Introduction 133
4.2 Aims 134
4.3 Experimental approach 134
4.4 Optimizing the analysis of *Wt1*-deleted kidneys 142
4.5 Using a low dose tamoxifen protocol to delete *Wt1* in the *CreERWt1$^{co/co}$* model 145
4.5.1 Using a very low dose tamoxifen protocol to delete Wt1 in the CreER Wt1$^{co/co}$ model 149
4.6 Clinical consequences of *Wt1* deletion 151
4.6.1 Early Death 151
4.6.2 Wt1 deleted mice develop severe albuminuria and serum hypoalbuminaemia 156
4.7 Tamoxifen-induced Cre-recombination leads to *Wt1*-deletion and significant *Wt1*-loss 163
4.8 *Wt1* deletion causes severe glomerular injury. 168
4.8.1 There is no evidence of significant nephron loss in Wt1-deleted glomeruli ... 177
4.9 *Wt1* deletion leads to the loss of major podocyte proteins 179

4.10 *Wt1* deletion does not lead to significant podocyte loss or detatchment...187
4.10.1 CreERWt1$^{co/GFP}$ mice exhibit strong GFP expression in the renal podocytes.187
4.11 *Wt1* loss affects the epithelial to mesenchymal balance in adult kidney ...192
4.12 Wt1-deletion leads to re-expression of Wnt4, consistent with earlier developmental pathways 197
4.13 Summary of findings....198
4.14 Discussion 199
4.14.1 Overview of analysis 199
4.14.2 Why didn't reducing the tamoxifen dose always significantly improve survival?....201
4.14.3 Why did the mice die?....202
4.14.4 Wt1 deletion causes significant albuminuria and hypoalbuminaemia, consistent with failure of the glomerular filtration barrier 203
4.14.5 Altering the tamoxifen dose did not appear to alter the degree of Wt1 loss.204
4.14.6 Wt1 deletion in the kidney leads to both podocyte and PEC damage and tubular injury 205
4.14.7 Why does Wt1-deletion lead to loss of podocyte specific proteins**?**....206
4.14.8 Wt1 loss affects the epithelial to mesenchymal balance in adult kidney....208
4.14.9 Wt1 loss leads to re-expression of Wnt 4. 209
4.14.10 How does Wt1 deletion compare with other genetic models of podocyte injury? 210
4.15 Concluding Remarks 212
5 Generating a Podocyte Specific In Vivo Model of Wt1-loss 213
5.1 Introduction....213
5.1.1 WT1 expression in the adult 213
5.1.2 Limiting Wt1 deletion to the kidney 215
5.2 Aims....218
5.3 Experimental approach 218
5.3.1 Using Gateway Recombineering to generate a BAC transgenic mouse 221
5.4 Generating the Gateway Construct 223
5.4.1 Step 1: Constructing the Entry Clone....226
5.4.2 Step 2: Regenerating the Destination Vector 226
5.4.3 Step 3: Generating the new Expression Clone 228
5.4.4 Step 3: Generating the new Expression Clone #2....230
5.5 Recombineering the GFP-CreERT2-IRES-puro-BAC Expression Clone into the Podocin BAC....232
5.5.1 Amplifying the Recombineering Arms....232
5.5.2 Cloning the 5' Recombineering Arm into the GFP-CreERT2-IRES-puro-BAC (GCT2iP) vector 237

5.5.3 Cloning the 3' Recombineering Arm into the GFP-CreERT2-IRES-puro-BAC (GCT2iP 5') vector 237
5.5.4 Electroporation of BAC DNA into EL350 cells 238
5.5.5 Recombineering the GCT2iP5'3' vector into the Podocin BAC 238
5.5.6 Confirmation of correct integration of the recombineering arms 238
5.5.7 Removal of the BAC LoxP site 243
5.6 Generation of the Podocin-GFPCreERT2 Mouse 247
5.6.1 BAC DNA Microinjection 247
5.6.2 Random integration of BAC into ES cells 251
5.6.3 Endogenous Targeting of GCT2iP-Podocin BAC into Embryonic Stem Cells 251
5.7 Using *Nestin*-CreERT2 as a method of glomerular-specific Cre-recombination 255
5.8 Discussion 257
5.8.1 BAC recombineering was unsuccessful in generating an inducible podocyte-specific Cre transgenic line. 257
5.8.2 Alternative approaches to generating a podocyte-specific model of Wt1 loss 259
5.8.3 Using the Podocin-iCreERT2 transgenic line to generate a podocyte specific model of Wt1 loss 259
5.9 Concluding Remarks 261
6 General Discussion 262
6.1 The findings from this thesis can be summarised as follows: 262
6.1.1 The generation and In-vitro analysis of Wt1-mutant podocytes: 262
6.1.2 Using a dose-limited model of conditional Wt1-deletion in the adult mouse, it was established that: 263
6.1.3 Podocyte-specific Wt1 deletion in-vivo 264
6.2 How do the findings from this thesis build upon previous work and how can they contribute to further understanding of podocyte biology? 265
6.3 Future Work 267
6.3.1 Podocyte-specific Wt1-deletion 267
6.3.2 Further investigation of the effects of Wt1 deletion on the epithelial-mesenchymal characteristics of podocytes 268
6.3.3 Further Investigation of the effects of Wt1 deletion on podocyte differentiation 269
6.3.4 How does Wt1-loss cause the effects demonstrated 269
6.3.5 Generation of a useable model of Wt1-loss in podocytes in vitro 270
6.4 Concluding Remarks 272
7 Materials and Methods 273
7.1 Methods Overview 273
7.1.1 Cell Culture 273

7.1.2 Animal Experiments 273
7.1.3 Cloning 273
7.1.4 Analysis 274
7.2 Experiments done by others 274
7.2.1 Cell Culture 274
7.2.2 Animal Experiments 274
7.2.3 Cloning 274
7.2.4 Analysis 274
7.3 Cell Culture 275
7.3.1 Generation of human podocyte cell lines 275
7.3.2 Generation of murine podocyte cell lines 276
7.3.3 Podocyte Cell Culture 276
7.3.4 Splitting Cells 277
7.3.5 Cryopreservation 277
7.3.6 Induction of Cre-Recombinase 277
7.3.7 Caspase Apoptosis Assay 278
7.3.8 Time-lapse photography 278
7.3.9 FACS analysis of cell cultures 279
7.3.10 M15 Cell Culture 279
7.4 RNA interference 280
7.4.1 Lentiviral RNA interference using the Expression Arrest GIPZ Lentiviral shRNAmir kit. 280
7.4.2 Optimised Lentiviral RNAi using alternative pGIPZ vectors 281
7.5 Mouse Lines 283
7.5.1 CreERWt1$^{co/co}$ 283
7.5.2 CreERWt1$^{co/GFP}$ 283
7.5.3 CreER 283
7.5.4 CreERR26R$^{YFP/YFP}$ 283
7.5.5 NestinCreERT2 R26R$^{YFP/YFP}$ 284
7.6 Animal Experiments 285
7.6.1 Animal Husbandry 285
7.6.2 Tamoxifen administration 285
7.6.3 Clinical assessment following tamoxifen administration (Wt1 deletion) 286
7.6.4 Urine and Serum Analysis 286
7.6.5 Tissue harvesting 288
7.6.6 Glomerular isolation 288
7.6.7 FACS analysis of kidney cells 289
7.7 Cloning using Gateway Recombineering 293
7.7.1 PCR amplification of the eGFPCreERT2 construct 293
7.7.2 BP Reaction 293
7.7.3 LR Reaction 293

7.7.4 PCR amplification of the Recombineering Arms 294
7.7.5 Recombineering 295
7.8 Generating the Podocin-GFPCreERT2 Mouse 298
7.8.1 Microinjection of BAC DNA into the pronucleus of fertilised mouse oocytes. 298
7.8.2 Gene targeting in ES cells 300
7.9 Microbiology 302
7.9.1 Culture Methods 302
7.9.2 Bacterial Transformation via heat shock 302
7.9.3 Bacterial transformation via electroporation 303
7.9.4 Reagents prepared by the MRC HGU Core Scientific Services 303
7.9.5 Maintenance of ES cells in Culture 304
7.10 RNA 305
7.10.1 RNA Analysis 305
7.10.2 RNA isolation 305
7.10.3 Measuring RNA Concentration 305
7.10.4 cDNA Synthesis 306
7.10.5 Real Time PCR 306
7.11 Protein 308
7.11.1 Protein Extraction 308
7.11.2 Measuring Protein Concentration 308
7.11.3 Western Blot 308
7.12 DNA 311
7.12.1 Isolation of Genomic DNA for Genotyping of Experimental Animals 311
7.12.2 Isolation of Genomic DNA from Tissues stored in RNA Later 311
7.12.3 DNA Extraction 312
7.12.4 Measuring DNA Concentration 313
7.12.5 DNA Precipitation 313
7.12.6 Digestion with Restriction Enzymes 314
7.12.7 DNA Ligation 314
7.12.8 DNA purification 314
7.13 Polymerase Chain Reaction (PCR) 316
7.13.1 Deoxyribonucleotide triphosphates (dNTPs) 316
7.13.2 Primers 316
7.13.3 Other Reagents 316
7.13.4 Purification of PCR Products 316
7.13.5 Gel Electrophoresis 320
7.14 Histology 321
7.14.1 Paraffin Fixation 321
7.14.2 Cryopreservation 321
7.14.3 Histological Staining 322
7.14.4 Immunohistochemistry 325

7.15 Microscopy **328**
7.15.1 Quantification of Cre-recombination events 328
7.15.2 Quantification of Wt1 staining 328
7.15.3 Glomerular Injury 328
7.15.4 Histological score 328
7.16 Bioinformatics **329**
7.17 Statistical Methods **329**
7.18 Solutions prepared by the MRC HGU Core Scientific Services **331**

Appendix **333**
Conference Presentations and publications during the course of this thesis **333**

References **334**

FIGURES AND TABLES

FIGURE 1.1: THE WT1 PROTEIN (TAKEN FROM SCHOLZ & KIRSCHNER, 2005) 22
FIGURE 1.2: THE WT1 GENE (TAKEN FROM HOHENSTEIN & HASTIE, 2006) 23
FIGURE 1.3: *WT1* EXPRESSION IN THE DEVELOPING KIDNEY 34
FIGURE 2.1: LIGHT MICROSCOPY OF UNDIFFERENTIATED (PROLIFERATING) AND DIFFERENTIATED 'WILD-TYPE' AND DDS HUMAN PODOCYTES 58
FIGURE 2.2: QUANTITATIVE RT-PCR FOR *WT1* MRNA EXPRESSION IN UNDIFFERENTIATED (33) AND DIFFERENTIATED (37) HUMAN PODOCYTES 59
FIGURE 2.3: QUANTITATIVE RT-PCR FOR MRNA EXPRESSION OF EPITHELIAL-MESENCHYMAL DRIVERS 62
FIGURE 2.4: QUANTITATIVE RT-PCR FOR MRNA EXPRESSION OF MESENCHYMAL MARKERS 63
FIGURE 2.5: QUANTITATIVE RT-PCR ANALYSIS FOR MRNA EXPRESSION OF EPITHELIAL-MESENCHYMAL GENES PRESENTED ACCORDING TO CELL LINE 64
FIGURE 3.1: LIGHT MICROSCOPY OF CULTURED PODOCYTES 71
FIGURE 3.2: EXPRESSION OF NEPHRIN AND WT1 IN DIFFERENT PODOCYTE CELL LINES (CHITTIPROL, CHEN ET AL. 2011) 74
FIGURE 3.3: SCHEMATIC OF $Wt1^{co/GFP}$ MODEL 77
FIGURE 3.4: DIFFERENTIATION OF POD32.1 AND WTPODO CONDITIONALLY IMMORTALIZED PODOCYTES 80
FIGURE 3.5: QUANTITATIVE PCR OF KEY PODOCYTE MARKERS IN UNDIFFERENTIATED AND DIFFERENTIATED WT PODO AND PODO 32.1 CELLS 81
FIGURE 3.6: QUANTITATIVE PCR OF KEY PODOCYTE MARKERS IN UNDIFFERENTIATED AND DIFFERENTIATED WT PODO AND PODO 32.1 CELLS RELATIVE TO MURINE KIDNEY CORTEX AND ISOLATED GLOMERULI 82
FIGURE 3.7: IMMUNOFLUORESCENCE OF DIFFERENTIATED PODOCYTES 83
FIGURE 3.8: TRIPLE PRIMER PCR TO DEMONSTRATE CRE-RECOMBINATION AND *WT1*-LOSS AT THE DNA LEVEL 85
FIGURE 3.9: DIFFERENTIATED PODOCYTES FOLLOWING WT1-DELETION 88
FIGURE 3.10: QUANTITATIVE RT-PCR FOR *WT1* EXPRESSION IN "WT1-DELETED" CELLS 89
FIGURE 3.11: WESTERN BLOT FOR WT1 90
FIGURE 3.12: WT1 DELETION IN VIVO 91
FIGURE 3.13: *WT1*-DELETION DOES NOT CAUSE CELL DEATH OR DETACHMENT 94
FIGURE 3.14: QUANTITATIVE RT-PCR FOR *WT1* MRNA EXPRESSION 98
FIGURE 3.15: FACS ANALYSIS FOR GFP EXPRESSION IN *CREERWT1*$^{co/GFP}$ PODOCYTES 99
FIGURE 3.16: PGIPZ LENTIVIRAL SHRNA EXPRESSION VECTOR 101
FIGURE 3.17: FACS SORT FOR GFP EXPRESSION OF UNDIFFERENTIATED WTPODO CELLS TRANSDUCED WITH THE DIFFERENT LENTIVIRAL VECTORS 103
FIGURE 3.18: FACS SORT FOR GFP EXPRESSION OF DIFFERENTIATED WTPODO CELLS TRANSDUCED WITH THE DIFFERENT LENTIVIRAL VECTORS 104
FIGURE 3.19: REPRESENTATIVE QPCR ASSAY FOR WT1 EXPRESSION (ASSAY DETECTING EXONS 8&9) IN UNDIFFERENTIATED CELLS FOLLOWING LENTIVIRAL TRANSDUCTION IN THE UNDIFFERENTIATED (PROLIFERATING) STATE 106
FIGURE 3.20 AMPLIFICATION CURVES FOR Q-RT-PCR WT1 ASSAY OF UNDIFFERENTIATED WTPODO CDNA 107
FIGURE 3.21: Q-RT-PCR FOR WT1 EXPRESSION FOLLOWING RNAI TO DIFFERENTIATED CELLS 110
FIGURE 3.22: Q-RT-PCR FOR WT1 EXPRESSION FOLLOWING LENTIVIRALLY MEDIATED RNAI TO M15 CELLS 111
FIGURE 3.23: PUTATIVE *WT1*-KNOCKDOWN CELLS ARE UNABLE TO DIFFERENTIATE 113

FIGURE 3.24: Q-RT-PCR FOR *WT1* MRNA EXPRESSION FOLLOWING WT1 KNOCKDOWN IN UNDIFFERENTIATED CELLS, WHICH WERE THEN DIFFERENTIATED OVER A PERIOD OF 14 DAYS 115
FIGURE 3.25: FACS ANALYSIS FOR GFP EXPRESSION IN TRANSDUCED M15 CELLS 118
FIGURE 3.26: Q-RT-PCR FOR WT1 MRNA EXPRESSION IN M15 CELLS 119
FIGURE 3.27: FACS ANALYSIS FOR GFP EXPRESSION IN TRANSDUCED PODOCYTES 121
FIGURE 3.28: Q-RT-PCR FOR *WT1* MRNA EXPRESSION IN UNDIFFERENTIATED WTPODO CELLS 122
FIGURE 3.29" WT1 KNOCKDOWN PODOCYTES ARE UNABLE TO DIFFERENTIATE 124
FIGURE 3.30: CELL DEATH OCCURS IN DIFFERENTIATING WT1-KNOCKDOWN PODOCYTES 125
FIGURE 4.1: EXPERIMENTAL TIMELINE 136
FIGURE 4.2: UBIQUITOUSLY-EXPRESSED VS PODOCYTE-SPECIFIC CRE LINES 137
FIGURE 4.3 MOUSE MODELS USED IN THE ANALYSIS OF WT1 DELETION IN THE ADULT 139
FIGURE 4.4: QUANTITATIVE RT-PCR OF MRNA EXPRESSION OF MAJOR PODOCYTE GENES IN KIDNEY CORTEX AND ISOLATED GLOMERULI. 143
FIGURE 4.5: TESTING THE EFFICIENCY OF CRE-RECOMBINATION IN THE KIDNEY USING DIFFERENT DOSES OF TAMOXIFEN 146
FIGURE 4.6: DISEASE-FREE SURVIVAL FOLLOWING WT1 DELETION, USING TAMOXIFEN AT 1MG/40G BODYWEIGHT FOR 5 DAYS, IN *CREERWT1$^{CO/CO}$* AND *CREERWT1$^{CO/GFP}$* MICE 148
FIGURE 4.7: DISEASE-FREE SURVIVAL FOLLOWING *WT1* DELETION USING TAMOXIFEN AT 1MG/40G BODYWEIGHT FOR 3 DAYS 150
FIGURE 4.8: ASSESSING HEALTH / DISTRESS USING A MODIFIED BODY SCORE 154
FIGURE 4.9: ALBUMIN CREATININE RATIO FOLLOWING TAMOXIFEN TREATMENT TO DELETE *WT1* 158
FIGURE 4.10: SERUM ALBUMIN, UREA AND CREATININE FOLLOWING WT1 DELETION 161
FIGURE 4.11: WT1 LOSS FOLLOWING CRE-RECOMBINATION 167
FIGURE 4.12: HISTOLOGICAL CHANGES FOLLOWING *WT1* DELETION 169
FIGURE 4.13: GLOMERULAR INJURY FOLLOWING WT1-DELETION 173
FIGURE 4.14: APOPTOSIS AND PROLIFERATION FOLLOWING WTI-DELETION 175
FIGURE 4.15: TOTAL GLOMERULAR NUMBER FOLLOWING *WT1*-DELETION 178
FIGURE 4.16: PODOCYTE MARKER EXPRESSION FOLLOWING *WT1* DELETION 185
FIGURE 4.17: USING THE *WT1$^{CO/GFP}$* MOUSE TO ESTIMATE PODOCYTE LOSS FOLLOWING *WT1* DELETION 191
FIGURE 4.18: QUANTITATIVE RT-PCR FOR MRNA EXPRESSION OF KEY EPITHELIAL AND MESENCHYMAL MARKERS IN WT1 DELETED GLOMERULI 196
FIGURE 4.19: QUANTITATIVE RT-PCR FOR MRNA EXPRESSION OF WNT4 IN WT1 DELETED GLOMERULI. 197
FIGURE 5.1: SCHEMATIC OF *PODOCIN*-GFP-CREERT2 TRANSGENIC LINE 219
FIGURE 5.2: SCHEMATIC ILLUSTRATING THE STEPS TO GENERATE THE PODOCIN-GFP-CREERT2 EXPRESSION CLONE 224
FIGURE 5.3: THE EXISTING EXPRESSION CLONE: GFP-CRE-IRES-PURO-BAC, CONTAINING A GFP-CRE CASSETTE 225
FIGURE 5.4: CONSTRUCTING THE ENTRY CLONE 227
FIGURE 5.5: MODIFIED DESTINATION VECTOR, WITH ALTERED MULTIPLE CLONING SITE 229
FIGURE 5.6: COMPLETED GFP-CREERT2-IRES-PURO CONSTRUCT 231
FIGURE 5.7: PODOCIN BAC 233
FIGURE 5.8: DESIGNING THE PRIMERS FOR AMPLIFICATION OF THE RECOMBINEERING ARMS 234
FIGURE 5.9: DESIGNING THE RECOMBINEERING ARMS 235
FIGURE 5.10: VERIFYING THE INCORPORATION OF THE RECOMBINEERING ARMS 239
FIGURE 5.11: RECOMBINEERING IN THE 3' ARM 240
FIGURE 5.12: CONFIRMING THE PODOCIN BAC 241

FIGURE 5.13: RECOMBINEERING THE VECTOR INTO THE PODOCIN BAC 242
FIGURE 5.14: REMOVING THE LOXP SITES 244
FIGURE 5.15: VERIFYING THE CORRECT INTEGRATION OF AMPICILLIN USING PCR 244
FIGURE 5.16: THE RECOMBINEERED BAC 246
FIGURE 5.17: CRE GENOTYPING OF POTENTIAL FOUNDERS 249
FIGURE 5.18: ENDOGENOUS TARGETING 253
FIGURE 5.19: VALIDATING THE PROBES 254
FIGURE 5.20: IMMUNOFLUORESCENCE FOR YFP EXPRESSION FOLLOWING CRE-INDUCTION IN *NESTIN*-CRERT2 YFP/YFP MICE 256

TABLE 1.1: RENAL DISEASES INVOLVING WT1 MUTATIONS 31
TABLE 2.1: HUMAN PODOCYTE CELL LINES 55
TABLE 3.1: PODOCYTE MARKERS 78
TABLE 5.1: MICROINJECTION INTO WILD TYPE (CD1) 248
TABLE 5.2: MICROINJECTION INTO *WT1*$^{co/co}$ 248
TABLE 7.1: LENTIVIRAL SHRNAMIR KIT KNOCKDOWN VECTORS 280
TABLE 7.2: OPTIMISED LENTIVIRAL RNAI KNOCKDOWN VECTORS 281
TABLE 7.3: RECOMBINEERING PRIMERS 296
TABLE 7.4: EGFP-CRERT2 SEQUENCING PRIMERS 297
TABLE 7.5: ENDOGENOUS TARGETING PRIMERS 301
TABLE 7.6: Q-RT-PCR HUMAN PRIMERS 307
TABLE 7.7: Q-RT-PCR MOUSE PRIMERS 307
TABLE 7.8: ANTIBODIES USED IN WESTERN BLOT 310
TABLE 7.9: RESTRICTION DIGESTS 315
TABLE 7.10: PCR PRIMERS 317
TABLE 7.11: PCR CONDITIONS 318
TABLE 7.12: ANTIBODIES 327
TABLE 7.13: BIOINFORMATICS 330

ABBREVIATIONS

ACR	Albumin/Creatinine Ratio (mg/mmol)
cDNA	Complementary DNA
CKD	Chronic Kidney Disease
Cre	Cre-Recombinase
CreER	Tamoxifen-inducible Cre-recombinase
DDS	Denys Drash Syndrome
DMS	Diffuse Mesangial Sclerosis
dNTPs	Deoxyribonucleotide triphosphates
dpc	days post coital
EMT	Epithelial to Mesenchymal Transition
ESKD	End Stage Kidney Disease
FACS	Fluorescence Activated Cell Sorting
FCS	Foetal Calf Serum
FSGS	Focal Segmental Glomeruslosclerosis
GFP	Green Fluorescent Protein
HEK293	Human Embryonic Kidney 293 Cell Line
HIVAN	HIV Associated Nephropathy
IDMS	Isolated Diffuse Mesangial Sclerosis
IF	Immunofluorescence

IFN-γ	Interferon-gamma
IHC	Immunohistochemistry
IP	Intra-peritoneal
LB	Lennox-Bertani Broth
M15	Mouse mesonephric cell line
MET	Mesenchymal to Epithelial Transition
MPGN	Membranoproliferative Glomerulonephritis
mRNA	Messenger RNA
NHS	National Health Service
PBS	Phosphate Buffered Saline
PCR	Polymerase Chain Reaction
PDGF	Platelet Derived Growth factor
PEC	Parietal Epithelial Cell
Q-RT-PCR	Quantitative Reverse Transcriptase PCR
RNAi	RNA interference
RRT	Renal Replacement Therapy
RT-PCR	Reverse-Transcriptase PCR
shRNA	Small Hairpin RNA
siRNA	Small Interfering RNA
SRNS	Steroid Resistant Nephrotic Syndrome

TGF	Transforming Growth factor
VEGF	Vascular Endothelial Growth Factor
Wt1	Murine Wilms' Tumour Suppressor Gene 1
WT1	Human Wilms' Tumour Suppressor Gene 1
$Wt1^{co/co}$	Homozygous Wt1 conditional mouse
$Wt1^{co/GFP}$	Heterozygous Wt1 conditional, Wt1-GFP mouse

1 INTRODUCTION: *WT1* IS ESSENTIAL FOR ADULT PODOCYTE MAINTENANCE AND FOR REGULATION OF THEIR EPITHELIAL – MESENCHYMAL BALANCE

1.1 OVERVIEW

Chronic Kidney Disease (CKD) is a major global health burden and prevalence rates are increasing worldwide (Coresh, Astor et al. 2003, Hamer and El Nahas 2006). Although early detection and aggressive management of hypertension, hyperglycaemia and the primary disease can slow progression, many of these patients with CKD will progress to end stage kidney disease, requiring costly and demanding renal replacement therapy. In the UK renal replacement therapy requirements have increased by 50% over the past decade, directly costing the NHS £1.45 billion per annum (approximately 1.3% of the total NHS budget). CKD also carries a significant burden of associated co-morbidity, particular cardiovascular disease, and these excess cardiovascular events account for a further £174-178 million cost to the NHS. Most significantly, CKD causes more than 45,000 deaths per year, which is more than both breast and lung cancer combined (Kerr, Bray et al. 2012).

Glomerular disease is the leading cause of end stage kidney disease worldwide (USRDS). Podocyte injury is the major cause of this progressive glomerular damage (Shankland 2006). As a consequence, there has been a surge of interest in podocyte biology over recent years, leading to the identification of a number of key genes and pathways involved in podocyte function and injury. One such gene is the Wilms' Tumour Suppressor gene, *WT1*, a complex gene involved in transcriptional regulation, RNA splicing and translation. *WT1* is highly expressed in the adult podocyte.

WT1 is an essential gene involved extensively in mammalian development, particularly renal development, where it controls the process of mesenchymal to epithelial transition that forms the nephron.

However, the expression of *WT1*in adult tissue is limited, and focused upon the adult podocyte. Until now the role of *WT1* in adult kidney has been difficult to study, as the *Wt1*-null mouse is embryonically lethal (Kreidberg, Sariola et al. 1993) and transgenic models carrying germ line *Wt1*-mutations exhibit significant and confounding developmental phenotypes (Hammes, Guo et al. 2001, Hastie 2001, Menke, A et al. 2003, Patek, Fleming et al. 2003, Gao, Maiti et al. 2004, Ratelade, Arrondel et al. 2010).

Using an inducible *Wt1*-conditional mouse model, this project aimed to analyse the effects of *Wt1*-deletion in adult kidney, to study the role of *Wt1* in adult kidney maintenance whilst avoiding any confounding developmental effects. Furthering the understanding of the functions of WT1 in the adult podocyte would contribute towards the field of podocyte biology, in order to identify potential mechanisms and targets to prevent or reverse the progression of glomerular disease.

This introduction will therefore aim to put this project in context, and will cover

- General overview of the *WT1* gene
- *WT1* mutations in disease
- The role of *WT1* in renal development and how this may infer potential roles for *WT1* in the adult
- *WT1* and the epithelial-mesenchymal balance
- The role of podocyte damage in glomerular disease and progressive kidney disease
- Current knowledge about the role of *WT1* in the podocyte
- A role for *WT1* in adult tissue maintenance and regeneration

1.2 The Wilms' Tumour Suppressor Gene, WT1

The Wilms' Tumour Suppressor Gene, *WT1,* was first identified in 1990, mapping to chromosome 11p13 (Haber, Buckler et al. 1990). Subsequently, *WT1* mutations have been found to account for up to 15-20% of Wilms' Tumours, a form of childhood developmental kidney cancer.

The human *WT1* gene consists of approximately 45 kb of genomic DNA, comprising 11 exons. It encodes a 52-54kDa nuclear protein, with an NH2-terminal proline and glutamine rich transactivation domain, and a COOH-terminal zinc-finger nucleic acid binding domain, containing four zinc-fingers, characteristic of transcription factors (Figure 1.1).

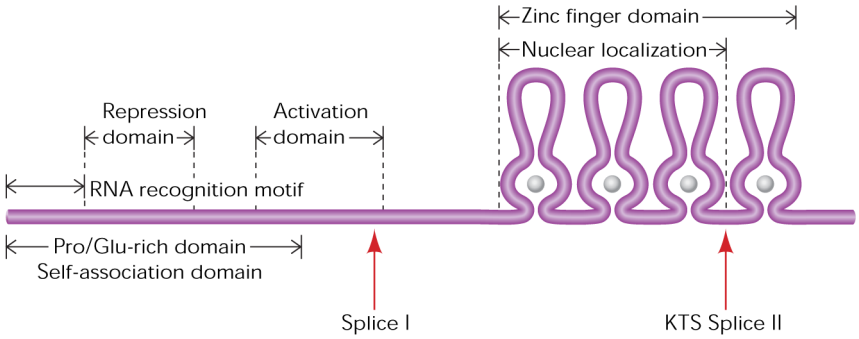

FIGURE 1.1: THE WT1 PROTEIN (TAKEN FROM SCHOLZ & KIRSCHNER, 2005)

WT1 is a complex gene with multiple isoforms. The combination of alternative splice sites, alternative start sites and alternative exons confer up to 36 theoretical isoform configurations, although the majority of these have not yet been characterised (Hohenstein and Hastie 2006) (Figure 1.2). Of all these isoforms, the most well studied are +/- exon 5, expressed only in mammals, which adds 17 amino acids between the transactivation domain and zinc finger DNA binding domain and +/- KTS, which adds three amino acids (lysine, threonine and serine) between the third and fourth zinc finger (Morrison, Viney et al. 2008). As discussed in more

detail below, the ratio and concentrations of these different splice isoforms appear critical for *WT1* function (Hammes, Guo et al. 2001).

.

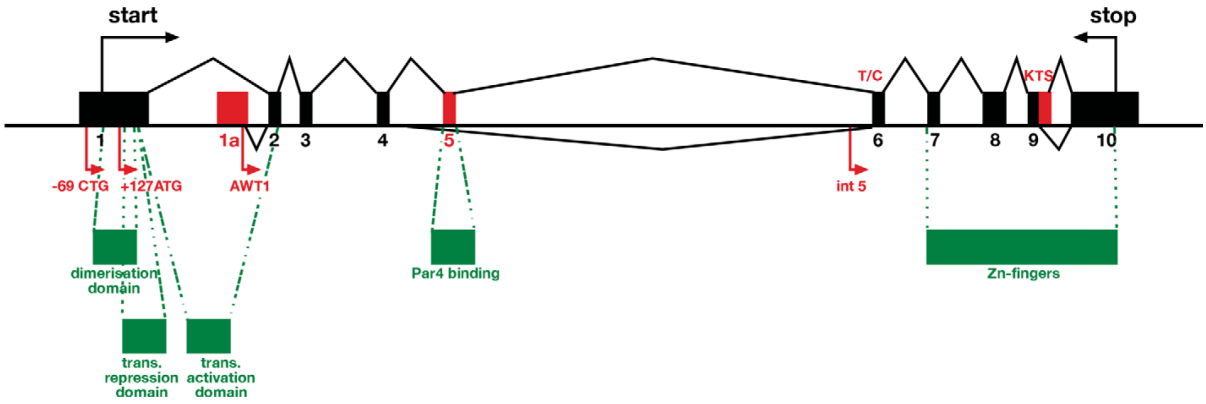

FIGURE 1.2: THE WT1 GENE (TAKEN FROM HOHENSTEIN & HASTIE, 2006)

The +/- exon 5 isoform variants are conserved throughout mammals. Transgenic mice lacking exon 5 develop normally, however, and are fertile (Natoli, McDonald et al. 2002). In contrast, transgenic models specifically lacking either the +KTS or –KTS isoforms demonstrate different phenotypes in the homozygous state, in keeping with distinct roles for these isoforms. Although given that neither of these models recapitulates the severity of the *WT1*-null mouse, a degree of redundancy must be present (Hastie 2001).

Heterozygous 'Frasier Mice' (unable to express the +KTS isoform and equivalent to human Frasier Syndrome) develop severe albuminuria and die of renal failure after a few months. Homozygous Frasier animals exhibited abnormal renal developmental with small shrunken glomeruli, impaired podocyte foot process formation and reduced synpatopodin expression resulting in death within 24 hours of birth (Hammes, Guo et al. 2001).

Correspondingly, homozygous 'KTS' animals (unable to express the –KTS isoform) demonstrate an even more severe phenotype, with small kidneys containing an increased

proportion of stroma (rather than epithelialized nephrons), few glomeruli and streak gonads. Again these mice survived only 24 hours after birth (Hammes, Guo et al. 2001).

In adult podocytes, little is known about the expression and function of the different *WT1* isoforms. Reduced expression of the +KTS isoform in Frasier syndrome leads to abnormal glomerular development and FSGS in early life. This indicates a specific physiological role for *WT1*+KTS, which is supported by the different renal phenotypes displayed by the KTS-mutant transgenic animals described above. However, as both these situations primarily affect podocyte development, it can only be inferred that the different KTS isoforms are likely to be of individual importance in the adult.

The +KTS isoform's functions appear to be mainly post-transcriptional, as they localise to the splicing speckles and directly bind splicing factors (Larsson, Charlieu et al. 1995, Davies, Calvio et al. 1998, Ladomery, Slight et al. 1999). *WT1*+KTS appears to preferentially bind specific sequences within the *Igf-2* RNA transcript, via the zinc-finger regions (Caricasole, Duarte et al. 1996). However, no further *WT1* RNA targets have subsequently been identified.

Although mainly a nuclear protein (in keeping with its established role in transcriptional regulation) both +KTS and –KTS *WT1* isoforms have been shown to shuttle from the nucleus to the cytoplasm, where it is localised to functional polysomes. These functions are reliant upon *WT1* directly interacting with the actin cytoskeleton (Vajjhala, Macmillan et al. 2003, Niksic, Slight et al. 2004, Dudnakova, Spraggon et al. 2010).

Searches for target genes of the +KTS isoform using micro-arrays and in vitro binding site selection screens had proved unsuccessful until recently (Lee and Haber 2001). However, a recent study has identified the planar cell polarity gene *SCRIBBLE* as a potential *WT1*+KTS target (Wells, Rivera et al.). Using 'ChIP-cloning' to perform a genome-wide binding site screen, the authors identified a number of genes preferentially bound by *WT1*+KTS. Further analysis confirmed Scribble and WT1 shared both temporal and spatial expression patterns, confined to the adult podocyte, and *in vitro* studies revealed modest upregulation of *Scribble* expression by *WT1*+KTS. *SCRIBBLE* regulates epithelial cell migration in mammalian cells, and misexpression of *SCRIBBLE* has been implicated in breast cancer tumourigenesis. This would be consistent with a role in the epithelial-mesenchymal balance, as a potential downstream target of *WT1*.

In contrast, the *WT1*-KTS isoform has been shown to act as a transcriptional regulator, and a number of transcriptional targets have been identified in the kidney, including *podocalyxin, nephrin, Wnt4* and *VEGF* (Palmer, Kotsianti et al. 2001, Wagner, Wagner et al. 2004, Rigby, Leitch et al. 2008, McCarty, Awad et al. 2011). Of particular importance is that this transcriptional regulation appears to vary in a cell-type and temporal context, with *WT1* acting as a transcriptional activator in one context and as a repressor in another (Rigby, Leitch et al. 2008, Martinez-Estrada, Lettice et al. 2010).

The mechanisms behind these paradoxical effects on transcriptional regulation have been elegantly characterised in relation to *Wnt4*, a gene is essential for renal development. In developing kidney *Wt1* activates *Wnt4*, whereas in developing heart it represses *Wnt4* expression. These occur as *Wt1* is able to switch the chromatin configuration of the *Wnt4* locus depending on the developmental context. In developing kidney, *Wt1* recruits the co-activators Cbp and p300 and maintains chromatin at the *Wnt4* locus in an active state. However, in the developing heart, *Wt1* recruits Basp1 as a co-repressor and the chromatin is reciprocally switched to a repressed state (Rigby, Leitch et al. 2008).

In summary, *WT1* is a complex gene encoding for multiple isoforms with multifunctional roles, including context-specific transcriptional regulation, post-transcriptional regulation and interaction with the actin cytoskeleton. It has been the subject of intense study for over 2 decades, in multiple scientific fields, including development, cancer, haematology and renal disease. This project aims to study the role of *WT1* specifically in adult kidney.

1.3 WT1 MUTATIONS IN DISEASE

As mentioned above, *WT1* was originally identified as the causative gene in familial Wilms' Tumours, in which it acts as a tumour suppressor gene. Subsequently, a number of other human diseases have also been identified which are associated with abnormal expression of *WT1*.

1.3.1 WILMS' TUMOUR

The eponymous Wilms' Tumour, in which *WT1* mutations are thought to cause 15-20% of cases, is the archetypal example of aberrant development leading to neoplasia (Coppes-Zantinga and Coppes 1999). In this context, WT1 behaves as a classic tumour suppressor gene. Germline cases demonstrate loss of the wild type allele, and non-familial cases show bi-allelic somatic WT1 loss (Hohenstein and Hastie 2006) . Wilms' Tumours are triphasic, consisting of epithelial, blastemal and stromal elements, and occasionally express differentiated ectopic tissues such as bone and cartilage, in keeping with abnormal developmental pathways. Most relevantly, Wilms' Tumours are associated with the presence of nephrogenic rests, which are embryonic kidney structures that persist in the adult kidney (Park, Bernard et al. 1993). Activating b-catenin mutations are also often found in conjunction with WT1 loss, demonstrating involvement of another key pathway in renal development (Li, Kim et al. 2004).

1.3.2 WAGR SYNDROME

WAGR Syndrome (Wilms Tumour, Aniridia, Genito-urinary malformation, Mental Retardation) was the first *WT1*-associated disease to be identified. It is caused by deletions of 11p13, which remove both *WT1* and *Pax6*. The associated renal disease (usually FSGS) was originally thought to be a secondary phenomenon following nephron loss and glomerular hyperfiltration as a consequence of nephrectomy for Wilms' Tumour. However, rates of renal disease (40%) are much higher following nephrectomy in WAGR syndrome than in patients who have undergone nephrectomy for isolated non-familial Wilms' Tumour, implying an underlying vulnerability as a consequence of the loss of one *WT1* allele (Fischbach, Trout et al. 2005). Abnormal, small, glomeruli have been identified in patients with WAGR syndrome (Dahan, Kamal et al. 2007)

and a study looking at serial renal biopsies in a small number of children who had WAGR syndrome without nephrectomy or treatment for Wilms' Tumour demonstrated the development of FSGS. This could not be as a secondary effect, implying the glomerular injury was primarily due to loss of a *WT1* allele and not a resultant phenomenon (Iijima, Someya et al. 2012). These findings are in keeping with the phenotype of the Wt1-heterozygous mouse, which develops glomerular sclerosis with ageing (Guo, Menke et al. 2002, Menke, A et al. 2003)

1.3.3 DENYS DRASH SYNDROME

Denys Drash Syndrome (DDS) is normally caused by point (missense) mutations in exons 8 or 9, encoding the DNA-binding zinc finger regions of the WT1 protein. These mutations lead to alterations in the DNA-binding properties of WT1 and are exacerbated as the mutant WT1 protein is thought to act in a dominant negative manner by forming heterodimers with the wild-type protein to prevent normal function (Little, Williamson et al. 1993, Moffett, Bruening et al. 1995). Denys Drash Syndrome results in a triad of Wilms Tumour, rapidly progressive renal failure (reaching end-stage in the first few years of life) and ambiguous genitalia or male pseudohermaphroditism (Niaudet and Gubler 2006). The characteristic renal lesion is one of diffuse mesangial sclerosis, assumed to be a developmental or paracrine effect, given that *WT1* is not expressed in mesangial cells (although is expressed in their glomerular precursors).

There is also increasing evidence for an abnormal podocyte phenotype in DDS, with podocyte hypertrophy and foot process effacement, increased proliferation and overexpression of PDGFα and TGFβ, normally associated with pathological epithelial to mesenchymal transitions (Yang, Chen et al. 2004). More recently, evidence has emerged indicating that podocytes in DDS resemble an earlier developmental stage, having not differentiated fully. DDS podocytes continue to express the stimulatory form of VEGF-A (VEGF165), which is normally only expressed from the S-shaped body stage of nephron development, and stimulates glomerular endothelial cell proliferation, migration and differentiation (Robert, Zhao et al. 2000). Upon differentiation, mature podocytes begin to express an inhibitory form of VEGF (VEGF165b). This is completely lacking in DDS podocytes (Schumacher, Jeruschke et al. 2007). This study also revealed that glomerular basement membrane constituents in DDS patients also resemble those at the S-shaped body developmental stage, with high levels of collagen α1(IV) and laminin

β1 and a relative lack of collagen α4(IV) and laminin β2, which are normally found in normal adult glomeruli. The authors interpret this to mean that DDS podocytes are halted in development and do not proceed fully through differentiation.

1.3.4 FRASIER SYNDROME

Frasier Syndrome is almost always caused by splice site mutations in exon 9, which prevent correct expression of the +KTS *WT1* isoform. This leads to male pseudohermaphroditism, predisposition to gonadoblastoma and glomerular disease (usually FSGS), which causes renal failure within the first two decades of life. The risk of Wilms' Tumour is much lower than in DDS (Barbaux, Niaudet et al. 1997, Barbosa, Hadjiathanasiou et al. 1999, Auber, Jeanpierre et al. 2009).

It must be highlighted that these genotype-phenotype correlations in DDS and Frasier Syndrome are not precise. Although the general associations are as described, intron 9 mutations have been described in patients with DDS, but without Wilms' Tumour (Little and Wells 1997) and intron 9 mutations, which should not affect splicing, have been found in patients with clinical Frasier Syndrome (Kohsaka, Tagawa et al. 1999). This implies there must be some degree of redundancy between the main *WT1* isoforms. The type of mutation does appear to correlate closely with the risk of Wilms' Tumour, as the exon 8/9 missense or nonsense mutations usually associated with DDS are associated with a high risk of Wilms' Tumour but splice site mutations only confer a very low risk (Chernin, Vega-Warner et al. 2010). Although not proven, this may be due to the dominant negative effect of DDS mutations dramatically reducing the availability of wild-type WT1 protein needed to proceed through development (Patek, Little et al. 1999, Rivera and Haber 2005).

1.3.5 RENAL DISEASE

Over recent years there has been increased recognition of the role of *WT1* mutations in non-syndromic renal diseases with *WT1* mutations identified in a number of cases of isolated diffuse mesangial sclerosis (IDMS), focal segmental glomerulosclerosis (FSGS) and membranoproliferative glomerulonephritis (MPGN) (Table 1).

Sizeable cohort studies have revealed *WT1* mutations to be a significant cause of steroid resistant nephrotic syndrome (SRNS) in children and young adults, with an incidence ranging from 6-7% in a worldwide cohort of 300 paediatric patients with SRNS (Ruf, Schultheiss et al. 2004) to 12% of cases of SRNS in a cohort of females under 18 years of age (Aucella, Bisceglia et al. 2006). This compares with a prevalence of 10-26% for *NPHS2* (podocin) mutations in SRNS, the most common genetic cause (Ruf, Lichtenberger et al. 2004).

Intriguingly, unlike other genetic causes, SRNS due to *WT1* mutations appears to be amenable to treatment with ciclosporin A. Although patient numbers are limited, a number of cases have been reported which demonstrate a favourable response to treatment with a combination of steroids, ciclosporin A and ACE inhibitors, with significant reductions in proteinuria and preservation of renal function. These children had a variety of previously described *WT1* mutations, varying presentations, and either DMS or FSGS histologically (Stefanidis and Querfeld 2011). In this context, ciclosporin treatment is thought to prevent calcineurin-mediated dephosphorylation and degradation of synaptopodin, thus maintaining podocyte cytoskeletal architecture (Faul, Donnelly et al. 2008).

Cicloporin A has also been reported to induce total remission of proteinuria in a patient with diffuse mesangial sclerosis in the context of DDS, maintained for more than a year (Wasilewska, Kuroczycka-Saniutycz et al. 2011). Again, in this context, it is suggested that cyclosporine activity leads to stabilization of the podocyte actin cytoskeleton, by preventing degradation of synaptopodin. The efficacy of ciclosporin in this context implies that the renal diseases associated with *WT1* mutations are due to a podocyte defect leading to loss of cytoskeletal architecture.

These findings also demonstrate the importance of correct identification of SRNS associated with *WT1* mutations, in order to guide treatment, and postpone the need for renal replacement therapy.

Alterations in *WT1* expression can be seen in a number of renal diseases, with increasing evidence of a role for *WT1* mutations in non-syndromic renal disease. *WT1* plays an essential role in renal development, so it is possible that these diseases arise solely from a failure of correct renal differentiation. However, the variety of disease phenotypes and delayed onset of pathology in some cases is in keeping with an on-going role for *WT1* in adult kidney, as would be expected with its persisting expression in the podocyte.

TABLE 1.1: RENAL DISEASES INVOLVING WT1 MUTATIONS

Renal Disease	**Study**	**Reference**
Isolated FSGS	Molecular analysis of exons 8 & 9 was carried out in 5 members from 3 generations of a family with adult onset proteinuria and isolated FSGS, progressing to end stage kidney disease in 3 individuals. A novel sequence variant c.1208G>A in WT1 exon 9 was identified, predicted to affect zinc-finger DNA-binding interactions.	(Benetti, Caridi et al.)
	Four phenotypically normal female patients were found to carry de novo WT1 mutations. Three had FSGS on renal biopsy and one DMS, without the development of Wilms Tumour	(Megremis, Mitsioni et al.)
Isolated DMS	Two cases of isolated DMS associated with WT1 mutations in exons 8 & 9, without other features of DMS	(Hahn, Cho et al. 2006)
	Four out of 10 patients with isolated DMS carried WT1 mutations, without genital abnormalities	(Jeanpierre, Denamur et al. 1998)
Membranoproliferative glomerulonephritis	Case study of a female child who developed membranoproliferative GN following treatment for Wilms Tumour associated with a c1168C>T; p.Arg390X mutation that introduced a stop codon at amino acid 390.	(Bockenhauer, van't Hoff et al. 2009)

1.4 THE ROLE OF WT1 IN RENAL DEVELOPMENT AND HOW THIS MAY INDICATE POTENTIAL ROLES FOR WT1 IN THE ADULT

The roles of *WT1* in both renal and non-renal development have been studied extensively. These functions may imply potential roles for *WT1* in adult kidney, so are of significance when investigating the effects of *WT1* loss in the adult.

WT1 is essential for mammalian development, and *Wt1*-null mice die at mid-gestation, almost certainly from cardiac failure as a consequence of abnormal cardiac development and pericardial haemorrhage (Kreidberg, Sariola et al. 1993). A number of other severe developmental abnormalities are also evident, including diaphragmatic hernia, abnormalities of liver, spleen, retinal, genital and adrenal development and complete renal agenesis. The kidney fails to form due to apoptosis of the metanephric blastema, the early renal precursor cells. All these tissues arise from the intermediate or lateral plate mesoderm, which gives rise to mesenchymal cell populations (Chau and Hastie 2012).

Subsequent to these discoveries, the role of *WT1* in kidney development has been the subject of intense research and is probably the most well understood area of *WT1* biology. However, the embryonic lethality of the *Wt1*-null mouse meant animal models have provided only limited information about the role of *Wt1* in later stages of renal development.

WT1 is expressed throughout the course of renal development. The kidney forms due to reciprocal interactions between two tissues, the metanephric mesenchyme, which forms the nephron, and the epithelial ureteric bud, which forms the collecting duct system. *WT1* is initially expressed at low levels in the uninduced mesenchyme, which gives rise to the metanephric kidney. Nephrogenesis initiates when the ureteric bud invades the metanephric mesenchyme, which condenses around the ureteric bud. This mesenchyme is induced, in response to *Wnt9b* signalling, to start the process of mesenchymal to epithelial transition (MET) to form the nephron (Karner, Das et al. 2011) During this MET process, the epithelial structures of the comma-shaped and S-shaped bodies are formed, which mature to form the adult nephron. *WT1* expression increases in the induced mesenchyme, and persists throughout the comma-shaped and S-shaped body stage (where *WT1* expression is at it's highest), until it becomes focused on the

proximal nephron and eventually the mature podocyte (Figure 1.3) (Greka and Mundel 2012). *WT1* is not expressed in the ureteric bud or collecting duct.

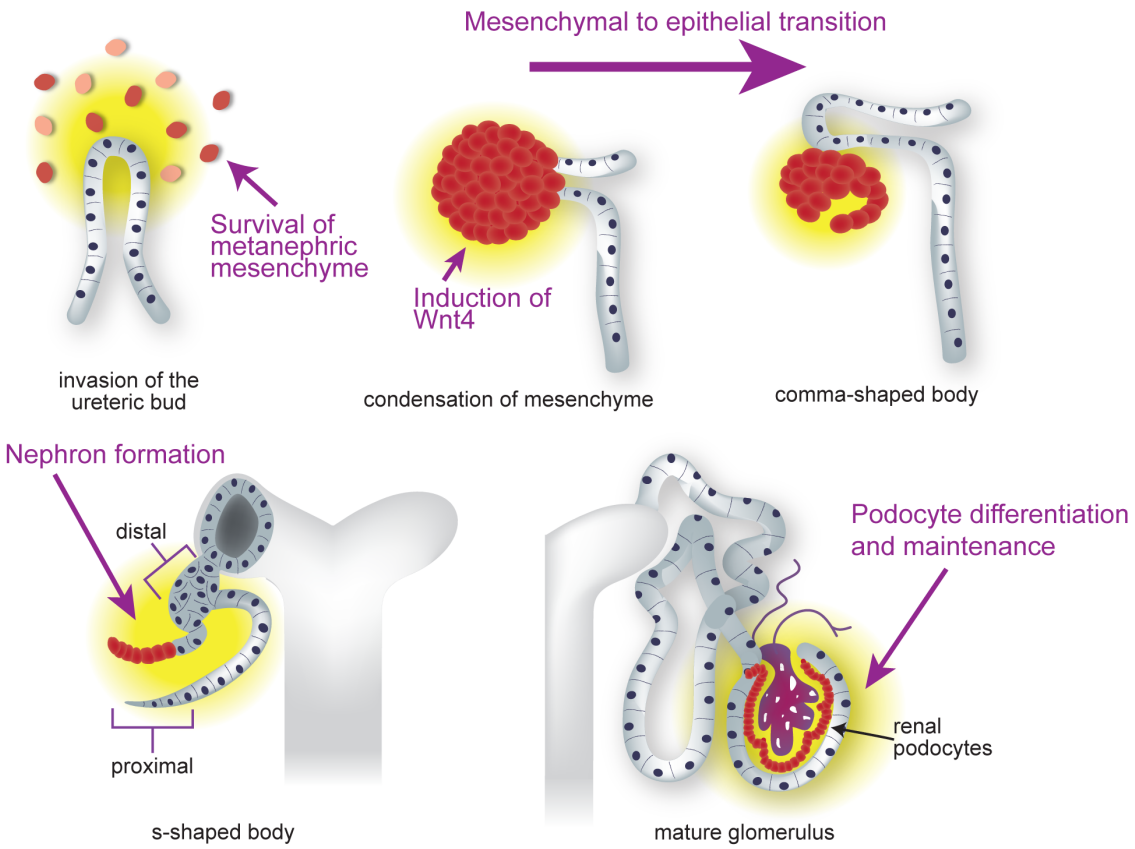

FIGURE 1.3: *WT1* EXPRESSION IN THE DEVELOPING KIDNEY

Low-level *Wt1* expression is seen in the metanephric mesenchyme, which increases as the mesenchyme condenses around the ureteric bud tips. Subsequently, *Wt1* expression becomes focused on the proximal nephron, through the comma-shaped and S-shaped body stages, before being confined to the mature glomerulus. Image created with the help of Craig Nichol, MRC HGU.

Given the embryonic lethality of the *Wt1*-null mouse, initial studies to analyse the role of *Wt1* later in renal development have used an *ex vivo* organ culture approach, using RNAi to knock down *Wt1* in embryonic kidney (Davies, Ladomery et al. 2004). This has demonstrated that *Wt1* is essential for nephron development, as *Wt1* knockdown from E11.5 prevents nephron formation and allows abnormal cell proliferation. Ureteric bud branching is unaffected. This phenocopies the effects of *Wnt4* loss. However, when *Wnt4* is knocked down, *Wt1* expression is maintained, confirming that *Wt1* lies upstream of *Wnt4*, and regulates *Wnt4* expression in the developing mesenchyme (Sim, Smith et al. 2002, Rigby, Leitch et al. 2008).

Subsequent to this work, the use of the *Wt1*-conditional mouse in combination with a *Nestin*-Cre line has confirmed the essential role of *Wt1* in nephron MET *in vivo*. Conditional deletion of *Wt1* in the renal mesenchyme markedly reduced nephrogenesis, producing an excess of mesenchyme, consistent with a failure to proceed through MET (Rigby, Leitch et al. 2008). This has been confirmed using other Cre-lines that delete Wt1 from the kidney at different stages of development (Berry *et al* manuscript in preparation).

As discussed earlier, animal models carrying *Wt1* mutations or only expressing specific isoforms, also exhibit abnormalities in renal development. Mouse models only able to express either the +KTS or –KTS *Wt1* isoforms exhibit severe and differing renal developmental abnormalities in the homozygous state, leading to early post-natal death.

Mice heterozygous for *Wt1* are born at Mendelian frequencies and appear normal in early life, but approximately half then die from renal failure from about 6 months of age, with severe and diffuse glomerulosclerosis, and significant albuminuria (Menke, A et al. 2003). However, heterozygous *Wt1*-null mice have been shown to express nearly 95% of normal wild-type *Wt1* mRNA levels (Guo, Menke et al. 2002), which may explain the limited phenotype in these animals.

This ‘dose effect’ was further confirmed by using a YAC transgenic model in which the human *Wt1* locus is expressed via a YAC transgene to rescue *Wt1*-null mice. Analysis of this model (Guo, Menke et al. 2002) revealed that reduced *Wt1* expression levels lead to mesangial sclerosis or crescentic glomerulosclerosis depending on the relative reduction in gene expression.

A number of mouse models of Denys Drash Syndrome have confirmed the causative role of *WT1* mutations in this condition. Mice carrying a *Wt1*tmT396 mutation (which disrupts zinc finger 3 and truncates the protein to delete the KTS insert and zinc finger 4) in the heterozygous or chimeric state develop features characteristic of Denys Drash Syndrome, including mesangial sclerosis, male genital abnormalities, and, in one case, Wilms' Tumour (Patek, Little et al. 1999). Further analysis of this model showed evidence of podocyte dedifferentiation, with prominent Pax2 expression (usually absent from differentiated adult glomeruli), novel TGFβ expression, loss of Zo-1 and reduced vimentin (which is expressed after the S-shaped body stage during podocyte differentiation), synaptopodin, nephrin and a-actinin 4 expression (Patek, Fleming et al. 2003).

A different model, which carries a heterozygous missense R394W mutation, identified in human DDS, had normal kidney development until 4 months of age, but male mice then developed proteinuria and glomerulosclerosis. Moderate loss of nephrin, podocin and synaptopodin was noted at birth, and increased expression of TGFβ and IGF-1 at 2-4 months of age (Gao, Maiti et al. 2004).

Taken together, these various models provide strong evidence of the importance of *Wt1* during renal development, and the phenotypes following birth suggest a continued need for *Wt1* in the adult. However, as they are all expressed constitutively, and thus affect renal development from its initiation, they cannot prove that *WT1* is required in adult kidney, or be used to study the role of *WT1* in adult podocytes. This highlights the need for an inducible and conditional model of *Wt1* loss.

1.5 WT1 AND THE EPITHELIAL-MESENCHYMAL BALANCE

A major role for *WT1* is in regulation of the epithelial-mesenchymal balance, and during development it controls both epithelial to mesenchymal and mesenchymal to epithelial transitions in a tissue specific manner (Chau and Hastie 2012, Miller-Hodges and Hohenstein 2012) Epithelial and mesenchymal transitions have been the subject of intense interest over recent years, as potential pathological mechanisms behind tissue fibrosis and cancer metastasis. Evidence has been presented for such transitions occurring within both kidney tubular cells and podocytes (Liu , Ivanova, Butt et al. 2008). Although the contributions of such mechanisms to progressive renal diseases remain the subject of intense debate, investigating a potential role for *WT1* in influencing these tissue states appears worthwhile.

1.5.1 EPITHELIAL-MESENCHYMAL TRANSITIONS DURING DEVELOPMENT

During early embryonic development, *WT1* is expressed in the coelomic epithelium, which contributes progenitor cells to the genital ridge, adrenals, and mesothelial cell population, and in the septum transversum, which contributes to the diaphragm, liver mesothelium and epicardial cells (Chau and Hastie 2012). It is this diverse expression pattern in the early embryo that may explain the variety of profound developmental phenotypes seen in the *Wt1*-null mouse. Meacham syndrome, a rare congenital syndrome of male pseudohermaphroditism, abnormal internal female genitalia, congenital heart defects and diaphragmatic hernia, demonstrates obvious similarities with that of the *Wt1*-null mouse, and several cases have been identified which are caused by heterozygous mutations of *WT1*. It has been hypothesised that these abnormalities are due to defective EMT processes in the coelomic epithelium and septum transversum caused by the mutant *WT1* (Suri, Kelehan et al. 2007). The analysis of a number of foetuses with bilateral renal agenesis and cardiac malformation have also shown reduced *Wt1* expression in the liver mesothelium, consistent with a *Wt1*-related failure of epithelial-mesenchymal transitions during development and mirroring the findings in the *Wt1*-null mouse (Loo, Pereira et al. 2012).

As discussed above, *WT1* is essential for renal development, which occurs via a process of mesenchymal to epithelial transition. *WT1* likewise plays a vital role in cardiac development, where, in contrast, it controls the epithelial to mesenchymal transition of epicardial cells to form epicardially derived precursor cells which migrate into the heart to form the coronary vasculature (Zhou, Ma et al. 2008). Epicardial specific *WT1* loss during development does not affect the epithelial cells of the epicardium, but leads to a dramatic reduction in the number of epicardially-derived mesenchymal cells, so the coronary vasculature fails to form. This process occurs through *WT1* mediated transcriptional activation of *Snail* and repression of *E-cadherin* (Martinez-Estrada, Lettice et al. 2010)

WT1 is also expressed in the mesothelial cells of the developing liver, and, via an epithelial to mesenchymal transition, these cells invade the liver parenchyma to contribute to the hepatic stellate cell population (Ijpenberg, Perez-Pomares et al. 2007) and are thought to influence hepatocyte growth and development (Wang, Yao et al. 2010, Asahina, Zhou et al. 2011). It is thought the abnormal liver phenotype in the *Wt1*-null mouse may arise from failure of this process.

Wt1 is expressed in the mesothelial cells of the developing lung as well, and lineage tracing experiments have demonstrated these cells also invade the lung parenchyma to contribute to the vascular smooth muscle cell population, presumably after undergoing an EMT (Que, Wilm et al. 2008).

Thus, *WT1* has been shown to play a key role in processes requiring regulation of the epithelial-mesenchymal balance during the development of various organs. In adult life, *WT1* expression is mainly limited to a subset of cells which, importantly, maintain both epithelial and mesenchymal characteristics (Chau and Hastie 2012). These include the podocyte (discussed in more detail below), the Sertoli cells of the testis, and the mesothelial cells, which form a polarised layer of cells, adjoined by tight junctions, around the organs, but also express mesenchymal proteins such as vimentin.

1.5.2 *EPITHELIAL-MESENCHYMAL TRANSITIONS IN CANCER*

WT1 is also thought to play a potential role in the pathological EMTs occurring in cancer (Kalluri and Weinberg 2009). As discussed above, *WT1* acts as a classical tumour suppressor gene in the context of Wilms' Tumour but in other cancers, novel *WT1* expression suggests it may be acting as an oncogene. In some solid tumours, including breast, colorectal and brain tumours, novel *WT1* activation has been detected, despite the fact the tissues of origin do not normally express *WT1*, even in development (Hohenstein and Hastie 2006). In haematological malignancies the situation is slightly different, as *WT1* continues to be expressed in a small subset of haematopoietic cells in the adult (Hosen, Shirakata et al. 2007). However, *WT1* overexpression and/or mutations have been described in a number of haematological malignancies, including leukaemia and myelodysplasia (Sugiyama 2002, Cilloni, Gottardi et al. 2003) so it has been identified as a useful therapeutic target for immunotherapy (Sugiyama 2010) In cancer biology, epithelial to mesenchymal transition is an essential process for metastatic invasion, as tumour epithelial cells need to acquire mesenchymal characteristics in order to invade locally and spread to distant sites, and the activation of genes that promote EMT, including *WT1*, confers a poorer prognosis (Hohenstein and Hastie 2006). Although this has yet to be proven experimentally, strong circumstantial evidence exists for a role for *WT1* in epithelial-mesenchymal transitions in cancer.

1.5.3 *EPITHELIAL-MESENCHYMAL TRANSITIONS IN SCARRING AND FIBROSIS*

Pathological epithelial-mesenchymal transitions have also been widely researched as a mechanism leading to tissue fibrosis and progressive organ dysfunction. Some years ago, EMT of tubular epithelial cells was proposed as a source of activated myofibroblasts in fibrotic kidney diseases (Ivanova, Butt et al. 2008). A similar phenomenon has also been described in podocytes (Liu 2010) Incubation of cultured podocytes with TGFβ, a key mediator of EMT, resulted in loss of slit diaphragm proteins (a specialised type of adherens junction) and increased expression of mesenchymal markers such as desmin and fibronectin, and upregulation of the mesenchymal driver, Snail (Li, Kang et al. 2008). These changes appear to have functional effects as they increase the permeability of podocytes to albumin, as measured by an *in vitro* albumin influx assay. Similar findings have been reported when cultured podocytes were incubated with mesangial media from patients with IgA nephropathy, resulting in loss of epithelial markers (Zo-

1 and P-cadherin), loss of slit diaphragm proteins (podocin) and upregulation of mesenchymal markers (desmin, FSP-1 and α-SMA). Again this resulted in increased albumin influx using an *in vitro* albumin influx assay (Wang, Liu et al. 2012). However, as with much research into epithelial to mesenchymal transitions in disease, this work is in an *in vitro* environment, so does not fully recapitulate the *in vivo* situation (Kriz, Kaissling et al. 2011) Nevertheless, observational work in human diseases does confirm similar changes in proteinuric kidney diseases such as diabetes and FSGS. The study described above confirms upregulation of α-SMA in the glomeruli of patients with heavily proteinuric IgA nephropathy, consistent with the *in vitro* findings (Li, Kang et al. 2008, Wang, Liu et al. 2012) In diabetic nephropathy, epithelial-mesenchymal transition has been proposed as a mechanism of podocyte detachment, with marked upregulation of FSP-1 detected in patients with diabetic kidney disease (Yamaguchi, Iwano et al. 2009). Immunohistochemical analysis of glomerular proteins also revealed loss of Zo-1 in advanced stages of diabetic nephropathy and upregulation of Snail, even at early stages. Similar findings have also been reported in patients with FSGS (Kretzler, Teixeira et al. 2001, Samejima, Nakatani et al. 2012)

Changes consistent with an EMT in podocytes have also been reported in animal models of glomerular injury. In experimental puromycin aminonucleoside (PAN) nephrosis, podocyte injury results in upregulation of several mesenchymal markers (desmin, vimentin and nestin) (Zou, Yaoita et al. 2006). Using genetically tagged podocytes in a model of anti-GBM nephritis to lineage trace the fate of podocytes in crescentic GN, Moeller and colleagues demonstrated that cells derived from the podocyte lineage contribute to crescent formation and completely lose expression of *Wt1* and slit diaphragm proteins, consistent with a profound phenotypic switch in the context of injury (Moeller, Soofi et al. 2004).

However, it must be emphasised that the concept of podocyte EMT remains very controversial, especially given that podocytes are not 'true' epithelial cells, but maintain mesenchymal elements, and that the majority of research in this area is limited to *in vitro* studies or observational data. A major limitation of these studies is the reliance upon epithelial and mesenchymal markers, which are more straightforward to measure, yet may not be truly specific, so may not correctly identify the cellular changes (Zeisberg and Duffield 2010) However, as yet, few formal *in vivo* lineage-tracing experiments exist to clarify this issue. Certainly, in the field of kidney fibrosis, elegant lineage tracing provides convincing evidence to support a role for renal

pericytes as the source of activated myofibroblasts and matrix deposition in kidney fibrosis, rather than transformed tubular cells (Humphreys, Lin et al. 2010). *Wt1*-expressing mesothelial cells contribute to the pericyte population in both liver (Ijpenberg, Perez-Pomares et al. 2007) and lung (Que, Wilm et al. 2008). This has not, however, been confirmed in the kidney, and the lineage tracing experiments performed by Duffield and colleagues would suggest kidney pericytes originate from the *Wt1*-negative stromal component (Humphreys, Lin et al. 2010). However, podocytes themselves have been described as a type of pericyte (Hirschberg, Wang et al. 2008, Saleem, Zavadil et al. 2008, Greka and Mundel 2012) and both podocytes and pericytes originate from *WT1*-expressing tissues and continue to express *WT1*. Therefore, although a specific role for *WT1* has not yet been established, there is strong developmental and functional rationale for a role for *WT1* in such cell transitions, be they of pericytes or podocytes, which warrants further investigation.

In summary, *WT1* plays a key role in regulation of the epithelial-mesenchymal balance in a number of situations. The most well-characterised role is in development, however, early evidence exists for a role in pathological changes in the epithelial-mesenchymal balance in cancer and potentially in tissue fibrosis. In adult tissue, *WT1* continues to be expressed in specialised cells that maintain both epithelial and mesenchymal characteristics, implying a fundamental role in maintaining this balance.

1.6 THE ROLE OF PODOCYTE DAMAGE IN GLOMERULAR DISEASE AND PROGRESSIVE KIDNEY DISEASE

As discussed above, glomerular disease is the leading cause of end stage kidney disease worldwide, and podocyte injury is the major mechanism of progressive glomerular damage (Shankland 2006). The podocyte is the main site of *WT1* expression in the adult.

Podocytes are highly specialised, terminally differentiated cells, with a quiescent phenotype, that form a key part of the glomerular filtration barrier (GFB). They are pericyte-like cells that consist of a polarised cell body attached to the glomerular basement membrane, and a complex series of inter-digitating foot processes, which envelop the glomerular capillaries. Slit diaphragms, which are modified adherens junctions, form between adjacent foot processes to provide a selectively permeable barrier to the glomerular filtrate. Podocytes originate from cells of the metanephric mesenchyme, which undergo a mesenchymal to epithelial to transition to form the adult nephron. At the S-shaped body stage of kidney development, podocyte precursors take the form of undifferentiated epithelial cells, with apically localised tight junctions (Greka and Mundel). It is at this point that expression of *WT1* is at its highest (Mundlos, Pelletier et al. 1993). As these precursors progress through the capillary loop stage of development, they lose their mitotic activity and start to develop the complex foot process architecture. Migration of ZO-1 from its apical location begins the process of forming the slit diaphragm (Reeves, Caulfield et al. 1978, Reiser, Kriz et al. 2000). It is at this point that the maturing podocytes begin to express the intermediate filament protein vimentin, characteristic of mesenchymal cells, which persists in the fully differentiated adult podocyte (Holthofer, Miettinen et al. 1984).

Thus, podocytes form from mesenchymal cells, which undergo a mesenchymal to epithelial transition to form epithelialized precursors and then adopt a more mesenchymal form. The adult podocyte maintains both these epithelial and mesenchymal characteristics – with apical-basal polarity and adherens junctions consistent with an epithelial phenotype, and expression of intermediate filament proteins and a motile and contractile cytoskeleton consistent with a mesenchymal form (Hsu, Hoffmann et al. 2008, Peti-Peterdi and Sipos 2010) The hypothesis of this project is that this delicate balance, and maintenance of these features, is controlled by *WT1* expression in the adult podocyte.

Podocytes perform a number of key functions in the glomerulus, including:

1) Provision of a size barrier to the glomerular filtrate via the slit-diaphragm, preventing the passage of albumin into the ultrafiltrate

2) Provision of a negatively charged barrier by the glycocalyx, to prevent passage of negatively charged molecules such as plasma proteins through the GFB

3) Maintenance of capillary loop architecture

4) Synthesis and maintenance of the glomerular basement membrane (GBM)

5) Production and secretion of VEGF to maintain the glomerular endothelium (Shankland 2006).

The importance of the podocyte in the glomerulus was first appreciated with the discovery that mutations in key podocyte genes are responsible for a number of congenital nephrotic syndromes, resulting in the massive loss of protein through the GFB and into the urine. Congenital Nephrotic Syndrome of the Finnish Type is caused by mutations in the major slit-diaphragm and signalling protein nephrin (*NPHS1*), and leads to untreatable neonatal nephrotic syndrome requiring early transplantation (Kestila, Lenkkeri et al. 1998). Subsequent to this, mutations in podocin (*NPHS2*) (Boute, Gribouval et al. 2000), *TRPC6* (Reiser, Polu et al. 2005, Winn, Conlon et al. 2005) and *CD2AP* (Shih, Li et al. 1999), amongst others, have been identified as causes of congenital glomerular disease.

Subsequently, podocyte dysfunction has been identified as a key mechanism behind many acquired glomerular disorders (Kriz and LeHir 2005, Shankland 2006). Podocyte injury can lead to detachment, apoptosis and dedifferentiation, which may involve an EMT. Such acquired causes of podocyte injury include autoimmune disease (membranous nephropathy, minimal change disease), infection (HIVAN), toxicity (hyperglycaemia in diabetes), mechanical stress (hypertension) and infiltration by substances such as amlyloid (Shankland 2006).

However, the key challenge in managing these diseases is that podocyte injury is progressive. Once a certain threshold of podocyte damage or loss is reached (>30%), progressive glomerular damage occurs, leading to gradual loss of renal function and the development of end stage kidney disease (Wharram, Goyal et al. 2005). It has been long established that significant

nephron loss leads to secondary damage in the remaining podocytes, due to intraglomerular hypertension as a consequence of hyperfiltration (Hostetter, Olson et al. 1981, Brenner, Meyer et al. 1982) and / or hypertrophy and reduction in podocyte density in the remaining glomeruli (Wiggins, Goyal et al. 2005) . However, it has now been definitively demonstrated that podocyte damage itself leads to direct injury of neighbouring, healthy podocytes. Using a chimeric transgenic mouse line, in which only a sub-population of podocytes expressed hCD25 (rendering them vulnerable to the immunotoxin LMB2) Ichikawa and colleagues demonstrated secondary damage to neighbouring podocytes as early as day 4 after the primary injury. The degree of this injury correlated closely with the extent of the primary injury, and minor injury (involving less that 25% of podocytes) was compatible with recovery of normal glomerular architecture. However, with more significant injury, a cascade of secondary injury occurred leading to progressive glomerular damage (Matsusaka, Sandgren et al. 2011)

The hallmark of podocyte injury is proteinuria, due to failure of the glomerular filtration barrier. A number of mechanisms are thought to contribute to the development of proteinuria. These include:

1) Foot process effacement and loss of podocyte ultrastructure
2) Abnormalities of the slit diaphragm
3) Podocyte loss

1.6.1 Foot Process Effacement

Foot process effacement is a universal response to podocyte injury, which appears to occur no matter what the primary injury (Shankland 2006). Foot process effacement describes the loss of the complex inter-digitating pattern of normal foot processes, which simplify and widen, producing fewer slit diaphragms (Inokuchi, Shirato et al. 1996, Patrakka, Lahdenkari et al. 2002). Foot process effacement involves the active reorganisation of the cytoskeleton, to retract, shorten and widen the foot processes. The degree of foot process effacement is variable amongst different proteinuric renal diseases and does not correlate with the amount of proteinuria. However, individual foot process width has been shown to directly correlate with the degree of proteinuria, confirming the importance of these changes (van den Berg, van den Bergh Weerman

et al. 2004) Effacement also leads to a changes in cell-cell contacts, with the formation of tight junctions between effaced foot processes, rather than the modified adherens junction of the slit diaphragm (Shirato 2002).

The most widely accepted theory is that foot process effacement itself and the alterations in slit diaphragm distribution account for the development of proteinuria. However, in some experimental models of proteinuria, protein leak can occur without foot process effacement (Lahdenkari, Lounatmaa et al. 2004). This may imply that the effacement is a response rather than a cause of proteinuria.

1.6.2 *Abnormalities of the slit diaphragm*

Disruption of the slit diaphragm occurs in association with foot process effacement (see above). The slit diaphragm complex also plays a critical role in signalling and regulation of the actin cytoskeleton and foot process network. Nephrin has been identified as a key regulator of podocyte signalling at the slit diaphragm, including survival (anti-apoptotic) pathways, reorganisation of the actin cytoskeleton, calcium signalling and maintenance of podocyte polarity (Welsh and Saleem 2010). Both podocin and CD2AP link nephrin to the actin cytoskeleton so are also involved in slit diaphragm signalling. Synaptopodin, which links the slit diaphragm to the actin cytoskeleton, stabilises RhoA activity to prevent development of a Cdc42/Rac1 motile phenotype in the podocyte (Greka and Mundel 2012). Given the importance of signalling from the slit diaphragm in maintaining podocyte integrity, damage to the slit diaphragm is thought to be the primary event in the podocyte response to injury (Greka and Mundel 2012).

1.6.3 *Podocyte loss*

Loss of absolute podocyte numbers, either through detachment and/or apoptosis, appears to be a key final pathway in glomerular disease. Reduced podocyte numbers are associated with a wide variety of proteinuric kidney diseases, including diabetic nephropathy, FSGS and membranous nephropathy and also with ageing (Shankland 2006). There is also a strong correlation between

podocyte loss and proteinuria, which increases as podocyte number decreases (Pagtalunan, Miller et al. 1997, Steffes, Schmidt et al. 2001, Lemley, Lafayette et al. 2002).

The main reason that podocyte loss is so harmful is that mature podocytes are quiescent, and thus unable to proliferate to replenish loss or injury. In the majority of glomerular diseases, podocytes maintain this quiescent phenotype, so are unable to proliferate adequately. However, evidence of dedifferentiation and proliferation has been found in both crescentic GN and collapsing FSGS / HIVAN (Moeller, Soofi et al. 2004, Shankland 2006).

Podocytes are able to replicate their DNA in response to injury, at least at low levels, but then upregulate CDK inhibitors such as p21 and p27, so are unable to proceed through the cell cycle.

This lack of podocyte proliferation has prompted researchers to look for a stem cell or precursor population that may be able to contribute to the podocyte pool. Evidence exists for the potential of parietal epithelial cells (PECs) to migrate onto the glomerular tuft and adopt podocyte characteristics (Appel, Kershaw et al. 2009). However, in experimental FSGS, these invading PECs have been shown to deposit extracellular matrix, contributing to the glomerular scar, so may, in fact be a patho-adaptive response to injury (Smeets, Kuppe et al. 2011)

A CD133+CD24+ progenitor cell population has also been identified at the urinary pole, which was able to regenerate both podocytes and tubular cells. The authors also demonstrated functional repair as infusion of these cells into experimental models of glomerular disease reduced proteinuria and glomerular damage (Ronconi, Sagrinati et al. 2009). These cells have also been shown to contribute to the hyperplastic lesions of collapsing glomerulopathy and crescentic glomerulonephritis, again suggesting a potential patho-adaptive mechanism. This could provide a therapeutic target (Smeets, Angelotti et al. 2009).

Thus, podocytes play a vital role in the function of the glomerulus, with a highly specialised structure and unique epithelial and mesenchymal characteristics. Abnormalities in podocyte function lead to a variety of congenital and acquired diseases emphasising their importance in renal function. This project aims to study the role of *WT1* in the podocyte in order to increase the understanding of podocyte biology and cell maintenance in the hope of identifying potential therapeutic targets that could halt or slow the progression of podocyte injury.

1.7 CURRENT KNOWLEDGE ABOUT THE ROLE OF WT1 IN THE PODOCYTE

WT1 continues to be expressed in the podocyte throughout adult life, implying it must play a role in adult podocyte maintenance. However, the role of *WT1* in adult podocytes is not well understood given the limitations of existing animal models, which are confounded by developmental effects.

Despite this, a number of *in vitro* studies have identified *WT1* as a transcriptional regulator of a number of key podocyte genes, including *nephrin, podocalyxin* and *VEGF*.

Podocalyxin is a transmembrane sialomucin, which is a constituent of the glycocalyx and maintains the glomerular charge barrier and foot process architecture. Using immortalised rat embryonic kidney cells in culture to inducibly express varying isoforms of *WT1*, Haber and colleagues demonstrated that expression of the *WT1*-KTS isoform was followed by rapid upregulation of podocalyxin, which could be immediately reversed once expression of -KTS was switched off. The same effect was not seen when using the +KTS isoform. Subsequently, conserved WT1 binding elements were identified within the podocalyxin promoter, in which WT1 binding produced a 20-30-fold increase in transcriptional activation. Podocalyxin expression follows *WT1* expression in the developing kidney, and is co-localised with WT1 in the adult, in keeping with a role for *WT1* as a direct transcriptional activator of this important podocyte gene (Palmer, Kotsianti et al. 2001).

WT1 has also been identified as a transcriptional regulator of nephrin, a signalling protein that plays a critical role in the slit diaphragm. Animal models that express altered or reduced *Wt1* are associated with a reduction in nephrin expression. Wt1 has been shown to directly transcriptionally activate nephrin *in vitro*, using an osteosarcoma cell line to inducibly overexpress the *WT1*-KTS isoform. Significant upregulation of nephrin mRNA, due to direct binding of WT1 in the nephrin promoter, was identified, which led to identification of a WT1 responsive element in the nephrin promoter, containing several repeats of a core WT1 binding sequence. The *WT1*+KTS isoform had a similar, but lesser, effect.

Nephrin has also recently been shown to be required during cardiac vessel formation. *WT1* is an essential regulator of coronary vascular development, by controlling epithelial to mesenchymal

transition of epicardially derived coronary precursors. Nephrin expression in the developing heart is temporally associated with *WT1* expression, and nephrin expression is absent from *Wt1*-knockout hearts, in keeping with a role for *Wt1* in transcriptional activation of nephrin in the heart as well as the kidney (Wagner, Morrison et al. 2011).

WT1 has also been shown to transcriptionally activate VEGF, which is normally produced by the podocyte in order to maintain the health and integrity of the adjacent glomerular endothelial cells. *In vitro* studies have demonstrated activation of the VEGF promoter by the WT1-KTS isoform, and this activation is lost when using mutant (DDS) WT1, which is unable to bind DNA effectively (Hanson, Gorman et al. 2007). Podocytes from individuals with DDS, carrying mutant *WT1*, express abnormal ratios of the stimulatory and inhibitory forms of VEGF, demonstrating *in vivo* dysregulation of VEGF expression in the context of mutant *WT1*.

Analysis of murine models carrying *Wt1* mutations have demonstrated further novel targets of *Wt1* in the podocyte, including *SceI* and *Sulf1*. *Sulf1* is an extracellular heparin sulphate 6-0 endosulfatase, which regulates the sulfation state of heparin sulphate (Ratelade, Arrondel et al. 2010) *Wt1* has been shown to transcriptionally regulate the activity of these endosulfatases, which affect VEGF signalling within the glomerulus by decreasing their bioavailability. Thus, the altered ratio of stimulatory and inhibitory forms of VEGF in DDS podocytes may be due to a combination of decreased expression and decreased bioavailability of the inhibitory VEGF165b isoform from the extra-cellular matrix (Schumacher, Schlotzer-Schrehardt et al. 2011).

Loss of *WT1* expression is a common finding in a variety of glomerular diseases. This is commonly used as a method of evaluating absolute podocyte number, yet may actually be due to loss of *WT1* expression rather than loss of cells (He, Kang et al. 2011, Toyonaga, Tsuruya et al. 2011, Tuncdemir and Ozturk 2011, Yang, Wang et al. 2012)

Some evidence of direct changes in *WT1* expression is available. *In vitro* studies have demonstrated that incubating cultured podocytes with TGFb, leads to a reduction in *WT1* expression both at the protein and mRNA level, and overexpression of *TGFb* in transgenic mice leads to reduction in *WT1* expression even before the onset of frank glomerulosclerosis. This suggests loss of *WT1* may be an early event on the progression of FSGS (Sakairi, Abe et al. 2011) In experimental sepsis, LPS-treated mice develop albuminuria, which resolves during recovery. This phenomenon is associated with loss of nuclear *WT1* expression, which relocates

to the cytoplasm, and associated loss of nephrin expression. This change in localisation of *WT1* has been suggested by the authors to lead to a 'loss of function' of WT1 as a transcriptional activator of nephrin (Kato, Mizuno et al. 2010).

In summary, *in vitro* studies have pointed to *WT1* being a key transcriptional activator of a number of important podocyte genes, and that loss of *WT1* expression may be an early event following podocyte injury. However, *in vivo* studies in the adult are required to confirm these findings, which this project aims to address.

1.8 A ROLE FOR WT1 IN ADULT TISSUE MAINTENANCE AND REGENERATION

Over recent years, there has been increased recognition of a potential role for *WT1* in tissue maintenance and regeneration (Chau and Hastie 2012). Work published during the course of this project demonstrated a number of unexpected extra-renal effects of *Wt1* deletion in adult tissue, suggesting roles for *WT1* in tissue maintenance not only in kidney, but also in pancreas, spleen, fat and bone (Chau, Brownstein et al. 2011) During development, *WT1* is expressed in mesenchymal cell populations and controls epithelial and mesenchymal transitions to form the relevant adult tissues. Preliminary evidence suggests *WT1* may also play a role in mesenchymal stem cells, providing a source of pluripotent progenitors in a variety of tissues (Chau and Hastie 2012).

A role for *WT1* has certainly been identified in cardiac regeneration. As discussed above, *WT1* plays a key role in cardiac development, where it controls EMT of epicardial cells to form coronary vascular progenitors. However, in the adult, *WT1* expression is lost in the epicardium. Interestingly, following a model of cardiac infarction, *WT1* expression is reactivated in the vascular endothelium and vascular smooth muscle cells of infarcted tissue (Wagner, Wagner et al. 2002). In global cardiac ischaemia, *WT1* expression is activated throughout the coronary vasculature of the whole heart. More recently, the regenerative potential of Wt1 positive cells in the adult heart has been demonstrated. Riley and colleagues demonstrate the existence of a small pool of Wt1 positive resident progenitor cells in adult heart, lying within the epicardium and sub-epicardium, which are activated in response to myocardial injury. Priming with thymosin ß4

generates a more rapid and enhanced response of this Wt1-positive progenitor pool, which can contribute towards replenishment of functional cardiomyocytes, and improve functional outcomes following injury (Smart, Bollini et al. 2011). However, it must be noted that subsequent work has questioned these findings, as when a more realistic clinical scenario is modelled, and thymosin ß4 is administered after myocardial injury, although there is an expansion of the Wt1+ epicardial layer and a reduction in infarct size, no evidence could be found of epicardial derived cells migrating and differentiating into cardiomyocytes. The beneficial effect of this expanded Wt1+ epicardial layer is though to be due to local paracrine effects. It has been suggested that this difference may be due to myocardial injury leading to a loss of epicardial cell plasticity (Zhou, Honor et al. 2012)

In zebrafish, which maintain the capacity to regenerate the entire nephron in the adult, Wt1-positive progenitor cells have also been identified, which are induced by nephrotoxic injury (Diep, Ma et al. 2011). These cells are able to form new functional nephrons following injury, and, most importantly, following transplantation. However, this work has not yet been replicated in mammals, which exhibit only very limited capacity for glomerular regeneration.

In the liver, stellate cells play an important role in regeneration, through secretion of growth factors that promote hepatocyte proliferation. Given the role of *WT1* in stellate cell development, and the acquisition of mesenchymal characteristics following stellate cell activation, it has also been speculated that *WT1* may play a role in liver regeneration, although such a link has yet to be proven experimentally.

1.9 CONCLUSION AND HYPOTHESIS

WT1 is an essential gene for renal development, and continues to be highly expressed in adult podocytes, where its role is not well understood. Throughout development, and potentially in some pathological processes, *WT1* plays a role in controlling epithelial-mesenchymal transitions. The podocyte itself exhibits a unique balance of epithelial and mesenchymal characteristics, which appear to be critical for its specialised function.

Thus, this project aims to analyse the role of *WT1* in the adult podocyte by answering the following questions

- Is *WT1* an essential gene in adult kidney?
- What is the role of *WT1* in the adult podocyte?
- What is the fate of *WT1* deleted cells?
- Is *WT1* loss associated with podocyte de-differentiation or a phenotypic switch into another cell type, perhaps via a process of epithelial–to-mesenchymal transition?
- Could *WT1* deletion reveal potential therapeutic targets in glomerular disease?

2 USING HUMAN WT1-MUTANT PODOCYTE CELL LINES TO ANALYSE THE ROLE OF WT1 IN THE PODOCYTE

2.1 INTRODUCTION

2.1.1 WT1 MUTATIONS IN DENYS DRASH SYNDROME

WT1 mutations in humans lead to a variety of developmental syndromes involving the kidney. Denys Drash Syndrome (DDS), the most common of these, is caused by point mutations in exons 8 & 9, encoding the zinc-finger DNA binding regions of the WT1 protein. This leads to transcription of a mutant truncated protein, which is thought to act in a dominant negative manner, as dimerization of mutant and wild-type protein prevents normal DNA binding (Little, Williamson et al. 1993, Moffett, Bruening et al. 1995). DDS causes a triad of rapidly progressive glomerulopathy, Wilms' Tumour and male pseudohermaphroditism.

The major histological lesion in DDS is diffuse mesangial sclerosis. This is difficult to explain, as differentiated mesangial cells are not thought to express *WT1* (although they arise from WT1-positive precursors). The mechanisms of mesangial involvement are not well understood, but are proposed to arise from paracrine effects from other glomerular cells (Morrison, Viney et al. 2008).

Increasing evidence points also to the existence of an abnormal podocyte phenotype in DDS, the paracrine effects of which may underlie the mesangial pathology:

1) Foot process effacement and podocyte hypertrophy and detachment are found in glomeruli of DDS patients (Niaudet and Gubler 2006)

2) *WT1* expression is severely reduced in DDS podocytes, with increased levels of proliferation associated with the lowest levels of *WT1* expression (Yang, Chen et al. 2004)

3) Overexpression of *PDGFα* and *TGFβ* (both key players in epithelial-mesenchymal transitions and in glomerular injury (Burns and Thomas 2010)) is found where *WT1* expression is low in DDS glomeruli (Yang, Chen et al. 2004).

4) DDS podocytes continue to express high levels of the stimulatory form of VEGF (VEGF165), which is usually expressed in podocyte precursors, and fail to express inhibitory VEGF165b, which is usually found in mature differentiated podocytes.

   The VEGF expression profile is more in keeping with the much earlier S-shaped body developmental stage (Schumacher, Jeruschke et al. 2007).

5) The glomerular basement membrane in DDS also resembles that of the foetal S-shaped body stage, with high levels of collagen α1 (IV) and laminin β1 and a lack of collagen α4 (IV), consistent with a delay or impairment in glomerular maturation (Schumacher, Jeruschke et al. 2007)

Therefore, further analysis of the effects of *WT1* mutations in podocytes from patients with DDS, should help to indicate the importance and possible roles of *WT1* in adult kidney. Using conditionally immortalised podocyte cell lines generated from patients with DDS allows detailed mechanistic analysis in human cells (for further discussion of conditionally immortalised podocyte cell lines see Chapter 3).

2.1.2 AIMS

The aims of the experiments described in this chapter were:

- To use conditionally immortalised podocyte cell lines generated from patients with DDS to analyse the effect of *WT1* mutations. Given the role of *WT1* in controlling the mesenchymal to epithelial transition during kidney development, this would focus on analysing the effects on the epithelial-mesenchymal balance in these podocytes.

- To compare these findings with the results of *Wt1* loss in the *Wt1*-conditional mouse, in order to help to translate these results into humans.

2.1.3 EXPERIMENTAL APPROACH

In order to analyse the effects of DDS mutations specifically on podocytes, conditionally immortalised podocyte cell lines were generated from patients with Denys Drash mutations, to be analysed in comparison to a 'wild-type' human conditionally immortalised podocyte cell line. This would allow detailed mechanistic analysis of the effects of *WT1* mutations on podocyte development and function.

These podocytes have developed under the influence of mutant *WT1*, rather than experiencing the effect of *Wt1* loss in 'normal' adult cells. The rest of this thesis investigates the role of Wt1 in the adult, using a *Wt1*-conditional mouse line to delete *Wt1* from the adult. However, they allow some comparisons to be made between the human and mouse, which would not otherwise be possible.

These cells would be analysed for expression levels of various markers of epithelial and mesenchymal characteristics and compared to both wild-type human podocytes in culture and the effects of *Wt1*-deletion in the *Wt1*-conditional mouse.

2.2 GENERATION OF HUMAN CELL LINES FROM PATIENTS WITH DDS

Wild type conditionally immortalised human podocytes (AB) were generated and cultured by the Saleem laboratory as previously described (Saleem, O'Hare et al. 2002). The mutant cell lines were derived from children with Denys Drash syndrome whose kidneys were removed for therapeutic purposes (Table 2.1). Podocytes were isolated from sieved glomeruli, grown to confluence and simultaneously transfected with the temperature sensitive SV40 (tsSV40) construct and hTERT as previously described (Saleem, O'Hare et al. 2002). After antibiotic selection, cells were subcloned.

TABLE 2.1: HUMAN PODOCYTE CELL LINES

Cell Line	**Background**
AB (control)	'Normal' podocytes isolated from a nephrectomy specimen, removed due to obstruction
DDSc24	DDS
DDSc2	DDS
DDS 3	DDS
ER	DDS
RA (control)	Isolated diffuse mesangial sclerosis (IDMS) secondary to a *PLCE1* mutation providing a positive control

2.3 DDS PODOCYTES EXHIBIT A MORE MESENCHYMAL PHENOTYPE

Culture of DDS podocytes and macroscopic phenotypic analysis was undertaken in the Saleem Laboratory in Bristol. This revealed no difference in the timing of glomerular outgrowths (podocytes) between DDS and wild-type glomeruli. After transfection and selection, macroscopically undifferentiated DDS clones were noted to have a more elongated mesenchymal morphology when subconfluent, although this became the more typical epithelial cobblestone appearance when confluent. Following differentiation, DDS clones were noted to develop an elongated fibroblastic appearance, rather than the typical flattened, arborised structure of wild type cells (Figure 2.1).

2.4 *WT1* EXPRESSION IS ALTERED IN DDS PODOCYTES

Using a *WT1*-assay that detects expression of exon transcripts 8 and 9, differing levels of *WT1* expression can be demonstrated in the different DDS clones (Figure 2.2 A). The majority of DDS mutations affect exons 8 or 9, which encode the zinc finger regions of the WT1 protein, and missense mutations can lead to a premature STOP and expression of a truncated WT1 protein (Little, Holmes et al. 1995). However, this assay does not reliably distinguish between functional or mutant WT1 so these results should be interpreted with caution. These patterns are maintained following podocyte differentiation (Figure 2.2 B). Protein analysis carried out by the Saleem laboratory using immunofluorescence and Western Blot confirmed WT1 expression at the protein level, although also could not differentiate between wild type and mutant protein (Figure 2.2 D).

However, unlike the murine cell lines (see Chapter 3), all these cells, including the wild-type (AB), demonstrated a marked downregulation of *WT1* expression following differentiation. This is a surprising result as it is in contrast to the findings in the murine cell lines used in the rest of this thesis, and other published work. This downregulation of *WT1* expression upon differentiation was also demonstrated by the Saleem laboratory, using a different assay, so appears to be robust.

Phenotypic analysis of the characteristics of these podocytes was carried out by the Saleem laboratory, and confirmed expression of nephrin (although in a disordered pattern), podocin, synaptopodin and CD2AP in these cells despite the low levels of WT1 following differentiation (Miller-Hodges E, Witherden IR *et al*, manuscript in preparation).

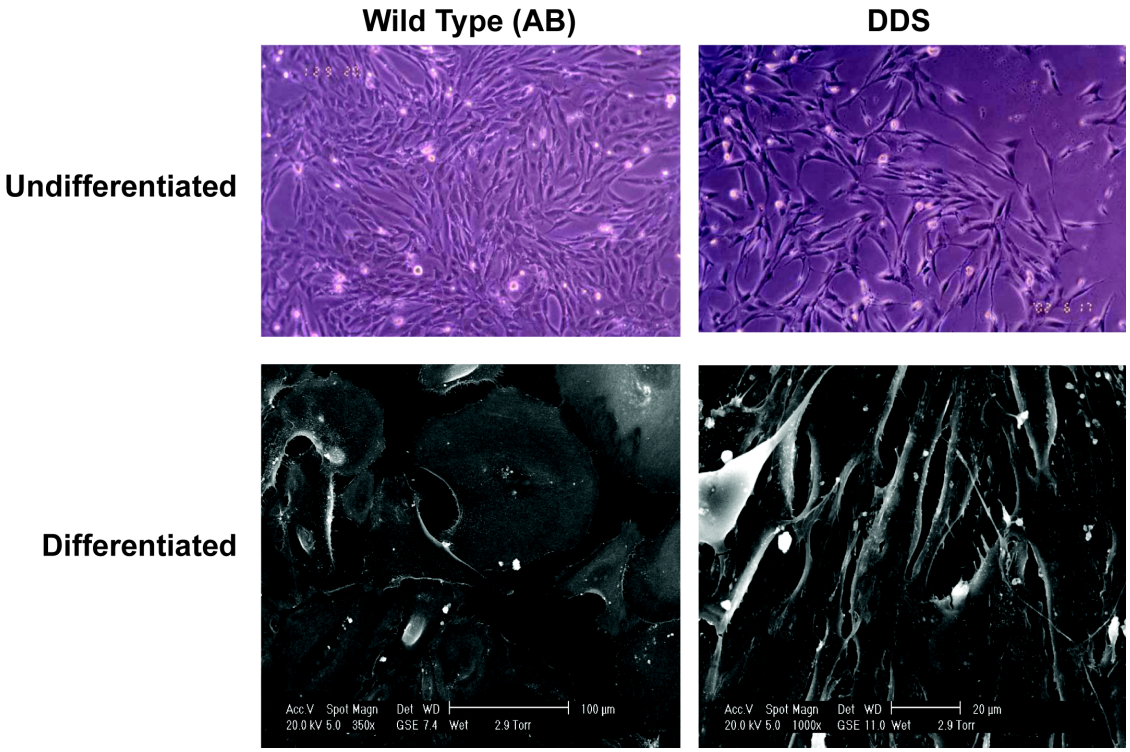

FIGURE 2.1: LIGHT MICROSCOPY OF UNDIFFERENTIATED (PROLIFERATING) AND DIFFERENTIATED 'WILD-TYPE' AND DDS HUMAN PODOCYTES

Following differentiation, DDS podocytes have a more elongated fibroblast like appearance (Images courtesy of Saleem laboratory).

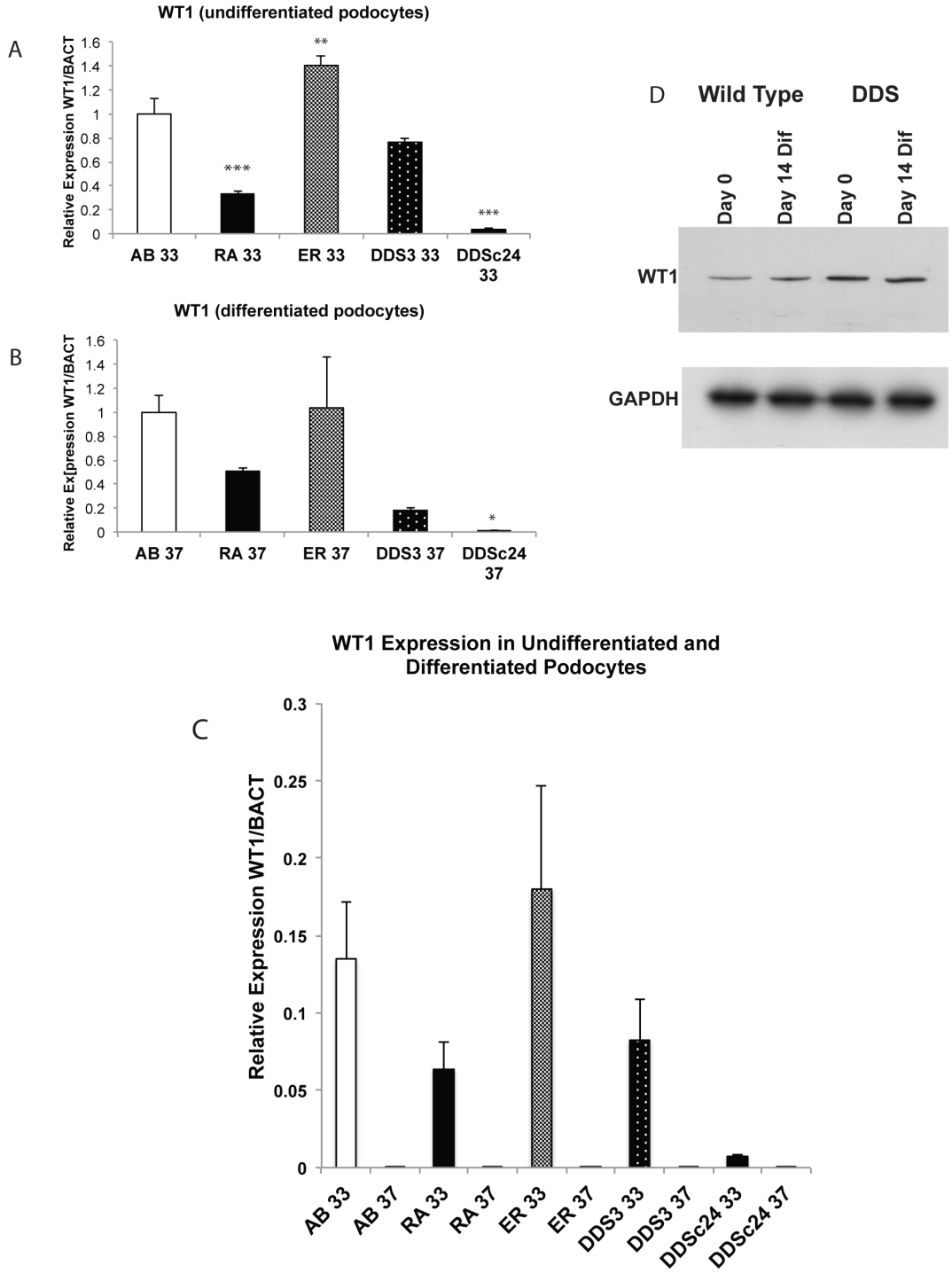

FIGURE 2.2: QUANTITATIVE RT-PCR FOR *WT1* MRNA EXPRESSION IN UNDIFFERENTIATED (33) AND DIFFERENTIATED (37) HUMAN PODOCYTES

FIGURE 2.2: QUANTITATIVE RT-PCR FOR *WT1* MRNA EXPRESSION IN UNDIFFERENTIATED AND DIFFERENTIATED HUMAN PODOCYTES

Quantitative RT-PCR for *WT1* mRNA expression (detecting transcripts of exons 8&9) in undifferentiated and differentiated human podocytes. A and B demonstrate *WT1* gene expression relative to 'wild type' (AB) in both the undifferentiated and differentiated state. C depicts the same data using actual expression levels. A) *WT1* expression in undifferentiated podocytes is most markedly reduced in DDSc24. Line RA (IDMS) also shows reduced *WT1* expression consistent with an abnormal podocyte phenotype. B) The same pattern of expression is seen following differentiation (although in the context of a PLCE1 mutation this is likely to be secondary) (* $p<0.05$; ** $p<0.01$; *** $p<0.001$ analysed using one-way ANOVA). Unlike the murine podocyte cell lines in Chapter 3 and as published in the literature, these human lines exhibit marked down-regulation of *WT1* mRNA expression following differentiation (C), although this is less apparent at the protein level (D). Western Blot courtesy of Saleem laboratory. Note that these assays do not differentiate between functional and mutant WT1 protein.

2.5 THE EPITHELIAL-MESENCHYMAL BALANCE IS DISTURBED IN DDS PODOCYTES

The epithelial-mesenchymal balance was altered to a varying degree in all DDS lines. Most significantly, the mesenchymal driver Snail was markedly upregulated in the DDS3 line when differentiated at 37 degrees (Figure 2.3 A) Snail is known to be a direct transcriptional target of *Wt1* (Martinez-Estrada, Lettice et al. 2010). Slug, another mesenchymal driver was also upregulated in some of the DDS lines, particularly DDS3 (as above) and DDSc24 (Figure 2.3 B). In line RA, in which there is no *WT1* mutation but an abnormal podocyte phenotype due to a *PlCe1* mutation leading to IDMS, Snail expression is similar to wild-type, but there is upregulation of Slug expression. TGFb, a key player in epithelial mesenchymal transitions, was also upregulated in all lines (Figure 2.3 C). One of the most notable differences was that, especially in line DDS3, which expressed the highest levels of mesenchymal drivers, there was a failure to down-regulate Snail expression following differentiation, unlike wild-type cells (Figure 2.3 D).

However, these changes were accompanied by at most modest increases in the mesenchymal markers vimentin and desmin. Very marked increases in MMP9 and in Collagen-1 were identified in clone DDS3 (Figure 2.4), the clone that expressed the highest levels of mesenchymal drivers.

When analysed separately, there is variability of the epithelial-mesenchymal phenotype amongst the different DDS lines (Figure 2.5). The most impressive phenotype is in DDS3 cells in which there is consistently elevated expression of the mesenchymal drivers Snail, Slug and TGFβ, and massive upregulation of MMP9 and Collagen 1 (Figure 2.5 C). In conjunction, this cell line expressed lower levels of the epithelial marker Zo-1, in keeping with a more mesenchymal and undifferentiated phenotype. Of note, consistently low levels of *Wnt4* expression were also demonstrated. Wnt4 is both necessary and sufficient for mesenchymal to epithelial transition during nephrogenesis, and is a direct transcriptional target of Wt1, so low levels would be predicted to affect the differentiation phenotype of podocytes (Rigby, Leitch et al. 2008).

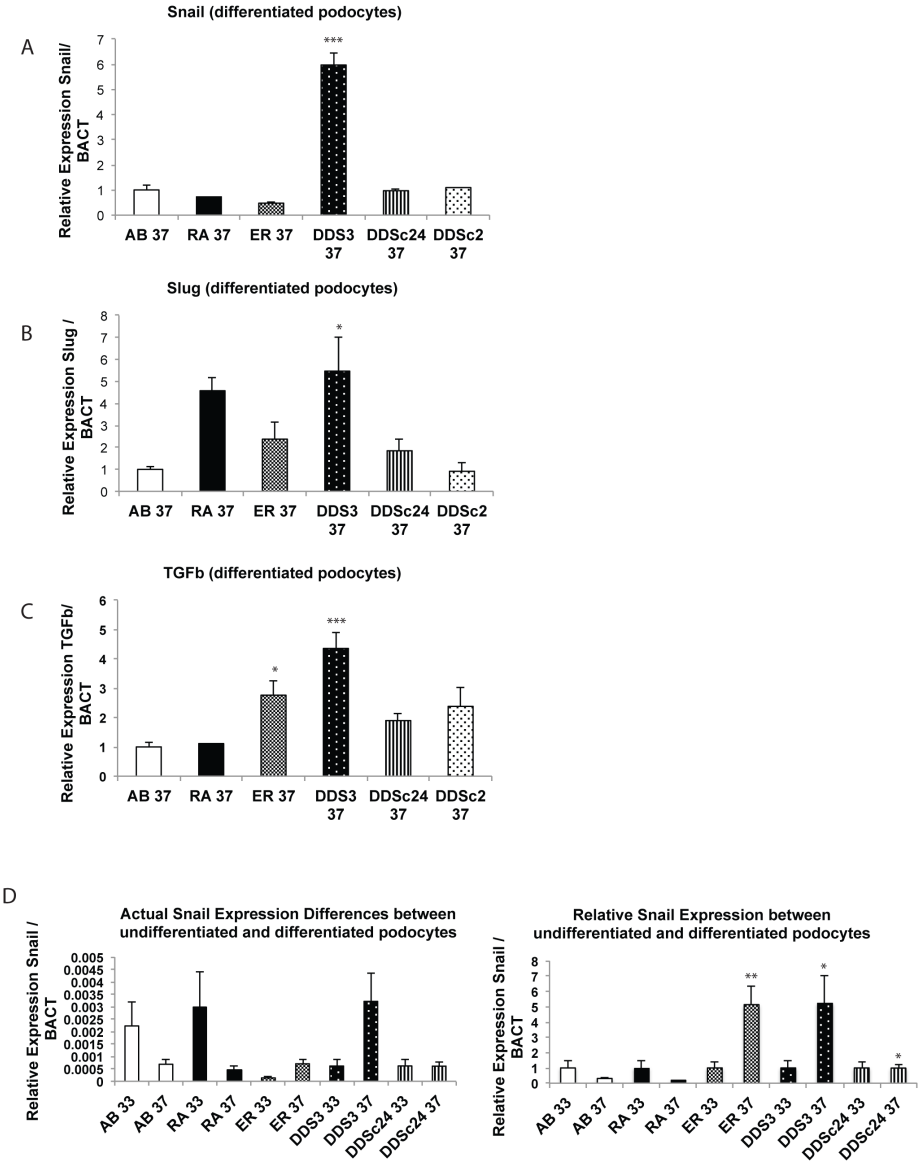

FIGURE 2.3: QUANTITATIVE RT-PCR FOR MRNA EXPRESSION OF EPITHELIAL-MESENCHYMAL DRIVERS

Expression levels represented as fold change difference from wild-type (AB). Relative Snail expression between undifferentiated and differentiated podocytes expression levels are relative to the undifferentiated state in each cell line (assigned an arbitrary level of 1). Each data point represents the mean of at least two biological replicates, analysed in triplicate, with each experiment repeated at least three times (* $p<0.05$; ** $p<0.01$; *** $p<0.001$ analysed using one-way ANOVA A,B,C and t-test D,E).

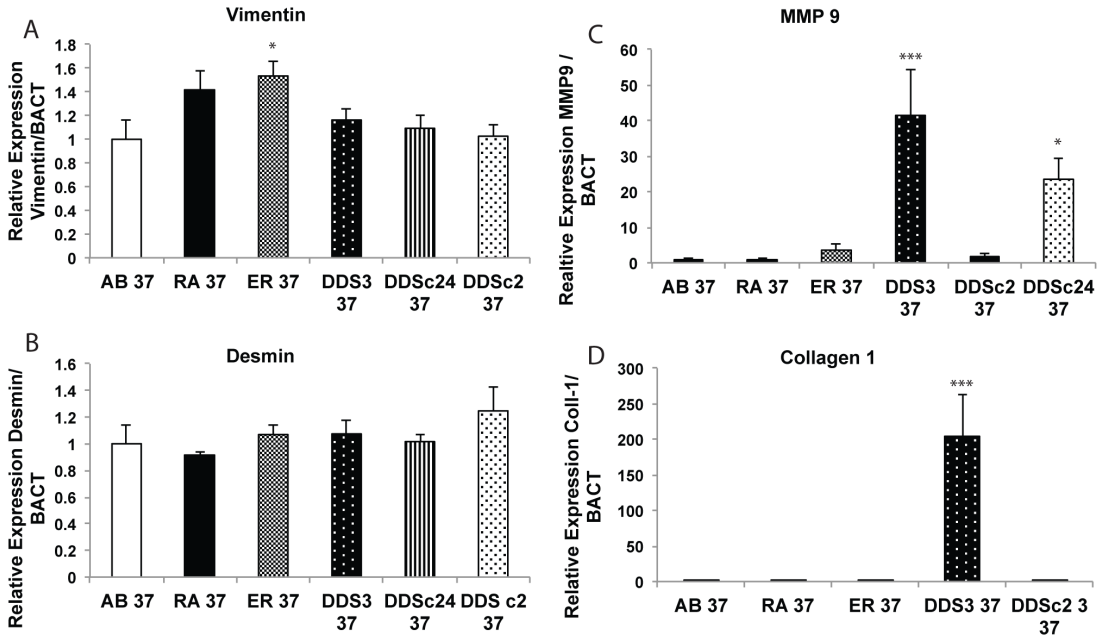

FIGURE 2.4: QUANTITATIVE RT-PCR FOR MRNA EXPRESSION OF MESENCHYMAL MARKERS

Expression levels represented as fold change difference from wild-type (AB). Each data point represents mean of at least two biological replicates, analysed in triplicate, with each experiment repeated at least three times (* $p<0.05$; **$p<0.01$; ***$p<0.001$ analysed using one-way ANOVA). Extremely high expression of MMP-9 and Collagen-1 is seen in line DDS3, which also exhibited the highest Snail, Slug and TGFβ expression.

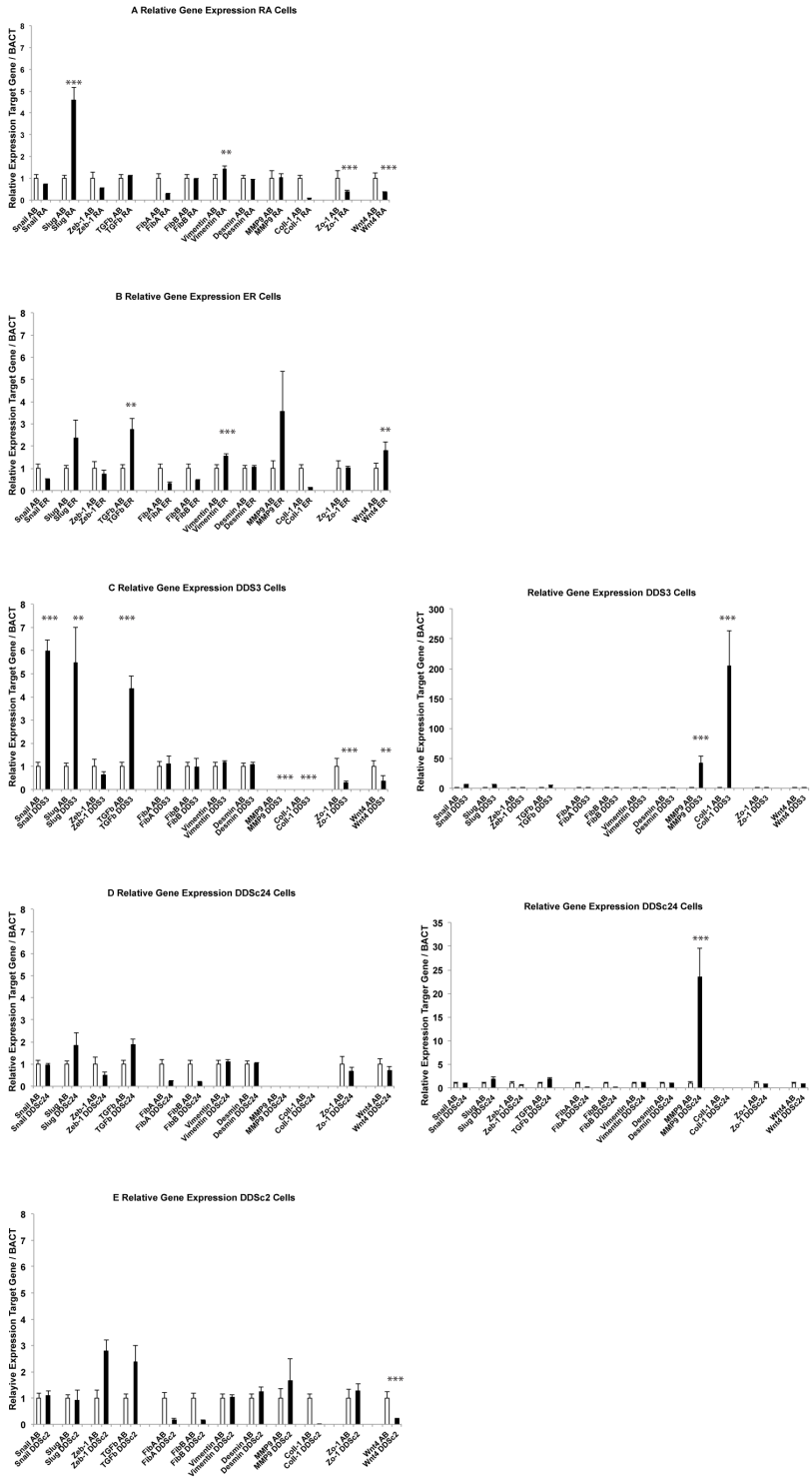

FIGURE 2.5: QUANTITATIVE RT-PCR ANALYSIS FOR MRNA EXPRESSION OF EPITHELIAL-MESENCHYMAL GENES PRESENTED ACCORDING TO CELL LINE

FIGURE 2.5: QUANTITATIVE RT-PCR ANALYSIS FOR MRNA EXPRESSION OF EPITHELIAL-MESENCHYMAL GENES PRESENTED ACCORDING TO CELL LINE (WITH THE SAME SCALE TO AID COMPARISON).

Each data point represents relevant gene expression relative to wild-type (AB) (* $p<0.05$; ** $p<0.01$; *** $p<0.001$). A) Line RA does not carry any *WT1* mutations, but is from a child with IDMS and an abnormal podocyte phenotype in the context of a PLCE1 mutation. B), C), D), E) DDS lines. Duplicate graphs to right depict outlying results (MMP-9 and Coll-1).

2.6 Conclusion: Summary of experimental findings

2.6.1 Human podocytes from patients with DDS shown downregulation of Wt1 upon differentiation

Unlike the murine cell lines used in this project and other published work, conditionally immortalised podocytes generated from human patients with DDS, and their human wild-type control, exhibit downregulation of *WT1* expression at the mRNA level after they have differentiated.

2.6.2 Human podocytes from patients with Denys Drash Syndrome exhibit variable disturbance of the epithelial-mesenchymal balance

Analysis of cell lines from patients carrying *WT1* mutations (DDS) reveals an altered epithelial-mesenchymal phenotype. This is in keeping with a role for *WT1* in podocyte differentiation and epithelial-mesenchymal characteristics. The degree of this alteration differs between cell lines. This has yet to be correlated with the mutations and phenotypic characteristics of the individual patients. Most significantly, the DDS3 cell line, exhibited a marked upregulation of the mesenchymal drivers Snail, known to be a transcriptional target of Wt1, and Slug (Martinez-Estrada, Lettice et al. 2010). However, given the variability between the differing cell lines, this has highlighted the need to interpret podocyte in vitro experimental data with caution, and ideally in the context of in vivo findings.

2.7 DISCUSSION

2.7.1 HUMAN PODOCYTES FROM PATIENTS WITH DDS SHOWN DOWNREGULATION OF WT1 UPON DIFFERENTIATION

This is a surprising finding, as both in this project using murine cell lines, and in other published work, Wt1 expression has been shown to be higher in differentiated podocytes than in proliferating cells (Miller-Hodges and Hohenstein 2012). However, as this result was replicated using a number of different assays and in a number of different hands, the results appear robust, if intriguing.

However, it must be noted that only one 'wild type' control was used in comparison to three DDS and one positive control line. Given the variation noted between the DDS lines, and the variation in 'wild type' cell lines from the same species demonstrated in Figure 3.2, it may be possible that this does not therefore truly represent the range of Wt1 expression in 'wild type' conditionally immortalised cell lines. The inclusion of further control lines would help confirm the findings that Wt1 expression levels decrease following differentiation.

Downregulation of *WT1* expression upon differentiation has been demonstrated on occasion by other investigators so this finding is not unique (Davidson, Dono et al. 2001). It is also of note that during podocyte development, the highest levels of WT1 expression are at the most epithelial S-shaped body stage, prior to full podocyte differentiation (Greka and Mundel 2012). Proliferating conditionally immortalised podocytes *in vitro* cannot fully replicate the podocyte precursors in normal development, but this observation does imply that a relative reduction in *WT1* expression also occurs as podocytes fully differentiate *in vivo*.

Wt1 expression has been found to be very variable between conditionally immortalised cell lines, with low levels in human and undetectable levels in rat cell lines (Miller-Hodges and Hohenstein 2012).

Certainly, prolonged culture of primary podocytes results in downregulation of *Wt1* expression, which may partly explain these findings. However, in this case analysis was limited to podocytes maintained at a low passage number as is widely accepted in the literature (Shankland, Pippin et al. 2007, Kabgani, Grigoleit et al. 2012).

2.7.2 *Human podocytes from patients with Denys Drash Syndrome exhibit variable disturbance of the epithelial-mesenchymal balance*

Analysis of the conditionally immortalised podocytes generated from patients with DDS demonstrates their abnormal phenotype, including with regard to alterations in the epithelial-mesenchymal balance. In conjunction with the work carried out by collaborators in Bristol, this work demonstrates the first *in vitro* analysis of human DDS podocytes, although a number of animal models have been published (Gao, Maiti et al. 2004, Ratelade, Arrondel et al. 2010).

These human podocytes do not replicate exactly the effects of *Wt1* loss in the adult, as they have developed under the influence of mutant *WT1*, both within the podocyte and throughout renal development in general. Despite this, the fact that that some alteration of the epithelial-mesenchymal balance is seen in these podocytes is consistent with the hypothesis *WT1* plays a critical role in maintaining this balance.

However, the most consistent finding amongst the DDS cell lines was their variability. It is important to note there is a great deal of variability in patients with DDS, and genotype-phenotype correlations are far from precise, with variations in glomerular pathology, and rate of disease progression (Lipska, Ranchin et al. 2014). These differences may therefore reflect other factors influencing the phenotype, such as other genetic and/or epigenetic effects However, as mentioned previously, this variability suggests analysis of further 'wild type' control lines would be useful, as this may suggest inherent differences between podocyte cell lines and demonstrates the need to interpret these results with caution, and in the context of the *in vivo* findings.

Further analysis of these lines in terms of cell motility and contractility is being undertaken in the Saleem Laboratory in order to analyse the functional effects of these changes in the epithelial-mesenchymal balance.

Interestingly, the majority of these DDS lines express only low levels of *Wnt4*. During renal development *Wnt4* expression is activated by *Wt1* (Rigby, Leitch et al. 2008) and *Wnt4* is required for mesenchymal to epithelial transition during nephrogenesis. However, in adult, differentiated kidney, *Wt1* appears to suppress *Wnt4* ((Rigby, Leitch et al. 2008) and see Chapter 4). In DDS, low levels of *Wnt4* expression, as a consequence of mutant *WT1*, would be predicted to prevent full transition through MET, halting the podocytes at an earlier developmental stage. This is consistent with published data (Ratelade, Arrondel et al. 2010).

Further analysis of these lines, to include detailed ultrastructural analysis, motility assays and protein distribution would shed light more light on the mechanistic effects of mutant *WT1*.

2.8 Concluding Remarks

Analysis and characterisation of podocyte cell lines from patients with DDS, in collaboration with the Saleem laboratory, has demonstrated the first *in vitro* model of DDS, which will serve an important role in further research, as to the mechanisms of the rapidly progressive renal failure seen in this conditions, and to shed light on to the effects of mutant *WT1* on podocyte differentiation and epithelial-mesenchymal balance.

3 GENERATING AN IN VITRO MODEL OF PODOCYTE WT1 LOSS

3.1 INTRODUCTION

3.1.1 USING CONDITIONALLY IMMORTALIZED PODOCYTE CELL LINES TO STUDY PODOCYTE BIOLOGY IN VITRO

Conditionally immortalized podocyte cell lines have been a vital tool in the study of podocyte biology and disease. Early attempts to use primary podocytes in culture were limited by their rapid de-differentiation and loss of specific morphological features such as foot processes, and the loss of key podocyte proteins such as nephrin. The generation of conditionally immortalized cell lines, which continue to proliferate in permissive conditions, and differentiate into mature podocytes in non-permissive conditions, has, in part, circumvented this problem.

Conditionally immortalised cells contain the temperature sensitive simian virus 40 (SV40) large T antigen, to allow proliferation at low (permissive) temperatures in the presence of IFN-γ, and differentiation when thermo-switched to higher temperatures with withdrawal of IFN-γ. Differentiated podocytes form flattened, arborised cells, which, in specific conditions, can express key podocyte proteins such as nephrin, synaptopodin and podocin. Both proliferating and differentiated podocytes express *Wt1*. When proliferating, podocytes exhibit a characteristic 'cobblestone' appearance, which is typical of epithelial cells in culture (Figure 3.1) (Shankland, Pippin et al. 2007).

Podocytes are cultured from isolated glomeruli (from murine or rat kidney, or from human biopsy specimens), which are separated using either sieving or magnetic sorting techniques. Podocytes can be isolated from primary culture of glomeruli, resulting in the outgrowth of cobblestone-like epithelial cells, which can then be trypsinised and subcultured to remove any residual mesangial and endothelial cells from the glomerular cores. Alternatively, isolated glomeruli are initially digested with collagenase, and passed through a 25μM cell sieve to separate the podocytes from other glomerular constituents (Shankland, Pippin et al. 2007).

Conditionally immortalised podocytes have even been established from the urine of both healthy volunteers and patients suffering from FSGS (Sakairi, Abe et al. 2010).

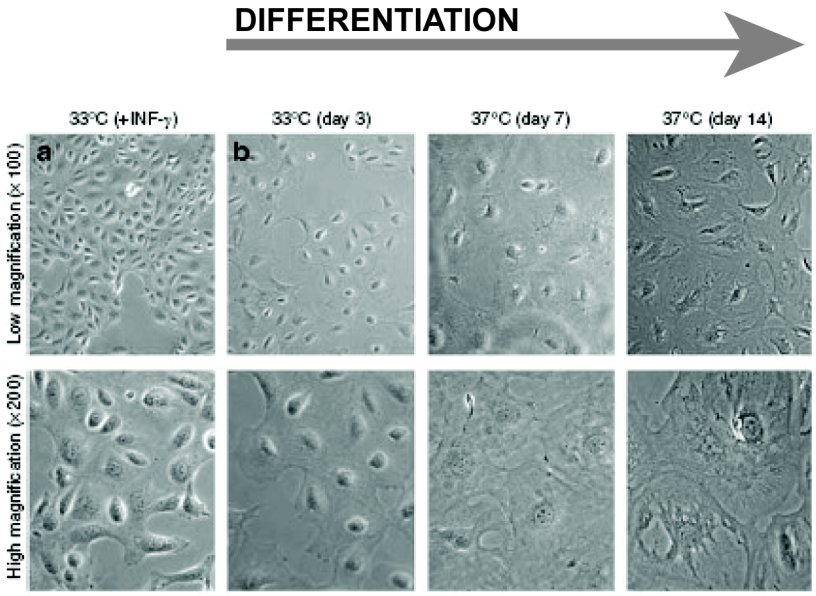

(Shankland SJ et al, 2007)

FIGURE 3.1: LIGHT MICROSCOPY OF CULTURED PODOCYTES

Light microscopy of cultured podocytes (taken from (Shankland, Pippin et al. 2007). a) At permissive temperatures (33°C) podocytes exhibit a characteristic 'cobblestone morphology' when confluent. b) Differentiating podocytes enlarge, flatten and form arborised structures.

Depending on the culture conditions, these cells have been shown to demonstrate many of the key features of podocytes, including expression of a slit diaphragm like structure between neighbouring cells (Reiser, Kriz et al. 2000, Gao, Li et al. 2007); expression of most key podocyte proteins including nephrin, podocalyxin, VEGF, podocin and synaptopodin; and quiescence when in a differentiated state (Shankland, Pippin et al. 2007). They have proved a valuable tool in dissecting some of the mechanistic aspects of podocyte behaviour, and have held particular significance in the fields of actin dynamics and cytoskeletal structure (Fuchshofer, Ullmann et al. 2011, Venkatareddy, Cook et al. 2011) and diabetic kidney disease and the effects of hyperglycaemia (Drossopoulou, Tsotakos et al. 2009, Cheng, Fan et al. 2011, Ruester, Franke et al. 2011).

3.1.2 LIMITATIONS AND DRAWBACKS OF IN VITRO PODOCYTE CULTURE SYSTEMS

Although cultured podocytes have been used widely in the published literature, they are not without their limitations. Two recent papers, published towards the end of this project, highlight the variable nature of podocytes in culture, and emphasise the importance of interpreting *in vitro* experimental findings in context. Comparison of four different conditionally immortalised podocyte cell lines (from humans, rats and mice) demonstrated significant differences between different cell lines, and between podocytes *in vivo* and those grown in culture. Culture conditions were paramount, with low densities being associated with the formation of the characteristic large, arborised cells. Analysis of specific podocyte markers found significant differences in expression of nephrin, podocin and synaptopodin mRNA and protein between different cell lines and different source organisms. Importantly, the authors detected very little nephrin expression in any of the cell lines (Figure 3.2 A, B, D), implying the formation of slit diaphragms between individual cells, a key functional feature of podocytes, must be very limited. The authors also used time-lapse photography to establish that the elongated cell processes, thought to be foot processes, were in fact dynamic lamellopodia, calling into question whether podocytes in culture truly emulate the tertiary structure of podocytes *in vivo* (Miller-Hodges and Hohenstein 2012).

Of note, varying levels of *WT1* expression were also detected. Although the murine podocyte lines analysed expressed comparable levels of *Wt1* mRNA to isolated glomeruli, the rat and human lines expressed little detectable *WT1*. Even amongst the murine lines, podocyte differentiation could be associated with very different levels of *Wt1* upregulation (Figure 3.2 C).

More recently, transgenic mouse lines have been used to isolate both podocytes and parietal epithelial cells (PECs), which had been permanently tagged with LacZ, after Cre was expressed under the control of either a PEC or podocyte specific-promoter (Kabgani, Grigoleit et al. 2012). This meant these cell types could be confidently differentiated between in culture, and revealed a number of key findings. Importantly, both podocytes and PECs expressed *Wt1*, even after six passages in primary culture. This was also confirmed *in vivo*, with faint, but detectable expression of *Wt1* in murine PECs. Wt1 is frequently used as a specific podocyte marker, especially to quantify podocyte number. This study indicates that *Wt1* expression cannot reliably differentiate between podocytes and PECs either in culture or *in vivo*. Prolonged culture of primary podocytes also resulted in downregulation of *Wt1* expression, to a level comparable with PECs, which may explain the low levels of *Wt1* expression in some conditionally immortalized lines. Synaptopodin and podoplanin expression by podocytes were found to be the most robust markers to differentiate between podocytes and PECs.

Interestingly, the authors also demonstrated the proliferation potential of cultured primary podocytes, which underwent progressive cell divisions, and were able to survive up to 35 passages in culture (although analysis of their 'podocyte characteristics' at this stage was not done). Podocytes are generally thought of as post-mitotic, terminally differentiated cells, but clearly maintain proliferative capacity when in culture.

However, despite their limitations, cultured podocytes still provide a valuable tool in studying mechanistic aspects of podocyte biology, with particular value when analyzing protein distribution and cell structure. Importantly, podocyte cell lines can limit the need for animal experiments in accordance with the 3Rs. Therefore, generating and analyzing an *in vitro* model of *Wt1* loss in podocytes was a fundamental part of this study, in order to analyse the role of *Wt1* in the podocyte.

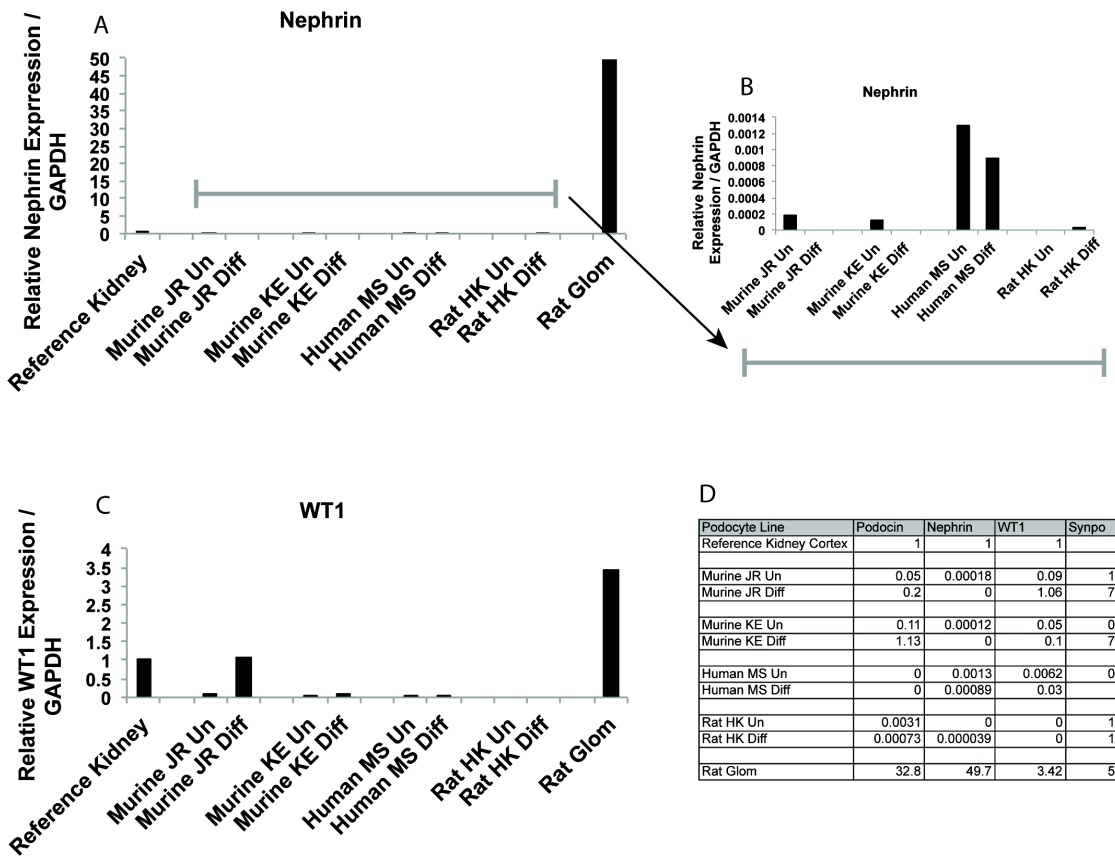

D

Podocyte Line	Podocin	Nephrin	WT1	Synpo
Reference Kidney Cortex	1	1	1	1
Murine JR Un	0.05	0.00018	0.09	1.99
Murine JR Diff	0.2	0	1.06	7.62
Murine KE Un	0.11	0.00012	0.05	0.73
Murine KE Diff	1.13	0	0.1	7.21
Human MS Un	0	0.0013	0.0062	0.09
Human MS Diff	0	0.00089	0.03	0.4
Rat HK Un	0.0031	0	0	1.65
Rat HK Diff	0.00073	0.000039	0	1.31
Rat Glom	32.8	49.7	3.42	5.87

FIGURE 3.2: EXPRESSION OF NEPHRIN AND WT1 IN DIFFERENT PODOCYTE CELL LINES (CHITTIPROL, CHEN ET AL. 2011)

Expression of Nephrin and WT1 in different podocyte cell lines (numerical data taken from (Chittiprol, Chen et al. 2011). MRNA expression was normalised to whole kidney cortex). A) Nephrin expression – all lines express low levels of nephrin in comparison to both kidney cortex and, in particular, isolated glomeruli. B) This is most apparent in the murine and rat lines, although even in the human lines, nephrin expression goes down during differentiation (data represented without controls to emphasise differences between lines) which would not be expected. C) *WT1* expression is also low in comparison to both whole kidney and glomerulus, most marked in the rat line that expresses no detectable *WT1*. D) Actual expression figures represented numerically.

3.1.3 AIMS

The aims of the experiments described in this chapter were:

- To generate a robust *in vitro* model of podocyte *Wt1* loss
- To characterize this podocyte cell line, in order to ensure it performed equivalently to other *in vitro* podocyte models
- To demonstrate significant and inducible *Wt1* loss *in vitro*
- To analyse the consequences of *Wt1* loss, particularly with regard to structural changes and protein localization

3.1.4 EXPERIMENTAL APPROACH

As other conditionally immortalized cell lines had already been generated from the *CreERWt1*$^{co/GFP}$ mouse (Martinez-Estrada, Lettice et al. 2010), the initial approach was to generate a podocyte cell line from this *in vivo* model, with the help of our collaborators in the Saleem Laboratory. This would allow *Wt1* deletion at the DNA level and direct comparison with the *in vivo* model, helping to reduce the number of animal experiments required. The GFP knock-in allele provided a surrogate marker of *Wt1* expression, and facilitated cell isolation and culture from kidney tissue. This novel line would require full analysis and characterization prior to use.

Should this line not prove suitable, *Wt1* knockdown using RNAi to stably transfect 'wild-type' conditionally immortalized podocytes would be attempted, although this would not prove as direct a comparison as the *Wt1*-deletion model above.

3.2 GENERATING A CONDITIONALLY IMMORTALIZED PODOCYTE CELL LINE FROM THE CRE ER*Wt1*$^{co/GFP}$ MOUSE

A conditionally immortalized podocyte cell line was generated from the *CreERWt1*$^{co/GFP}$ mouse by our collaborators, Prof Moin Saleem and colleagues. *Wt1*$^{GFP/+}$ mice were crossed with H-2KbtsA58 "immorto" mice carrying a temperature-sensitive simian virus 40 (SV40) large T antigen (Jat, Noble et al. 1991). These *Wt1*$^{GFP/+}$ /Immorto+ mice were mated with *CreERWt1*$^{co/co}$ mice to generate *CreERWt1*$^{co/GFP}$ / Immorto+ mice (Martinez-Estrada, Lettice et al. 2010) (Figure 3.3). The presence of the tamoxifen-inducible *Wt1* conditional allele meant the addition of tamoxifen to cell culture media would allow Cre-recombination and deletion of *Wt1*. The addition of the *Wt1-GFP* allele allowed for visualization of Wt1 expression, but did mean that these cells were compound heterozygous for *Wt1*. However, previous work suggested *Wt1*-heterozygous mice express relatively normal amounts of Wt1 protein at least in early stages (Menke, A et al. 2003) and work using the *Wt1*$^{co/GFP}$ mouse *in vivo* demonstrated normal podocyte and glomerular function up to at least 6 months of age (see Chapter 4). Also, conditionally immortalised epicardial cell lines from the same animals had proved a useful and validated tool in analyzing the role of *Wt1* in the epicardium (Martinez-Estrada, Lettice et al. 2010), implying these cells would express enough Wt1 to provide a useful *in vitro* model.

Podocytes were generated from these mice using established methods (Saleem, O'Hare et al. 2002). Cells proliferated at 33ºC in the presence of IFN-γ, and differentiated over a period of 14 days when thermo-switched to higher temperatures (38ºC) with withdrawal of IFN-γ. These cells were referred to as **Podo32.1**. In conjunction, control 'wild-type' conditionally immortalized podocytes (a kind gift from Jochen Reiser, University of Miami), referred to as **WTpodo**, were also analysed.

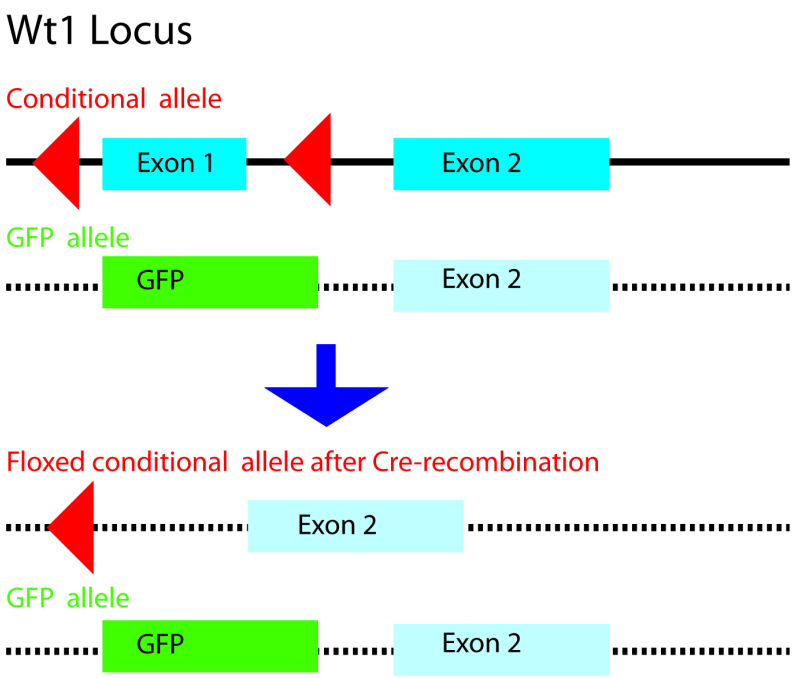

FIGURE 3.3: SCHEMATIC OF WT1$^{CO/GFP}$ MODEL

Allele one of *Wt1* contains the conditional allele with LoxP sites surrounding Exon 1. Allele two contains a knock-in GFP allele, under direct control of the *Wt1* promoter. Following Cre recombination, Exon 1 is excised so no functional Wt1 protein is transcribed yet GFP continues to be expressed in those cells where *Wt1* should be expressed.

3.3 CHARACTERISING THE CONDITIONALLY IMMORTALIZED PODOCYTE CELL LINE FROM THE CREERWT1$^{CO/GFP}$ MOUSE

3.3.1 CREERWT1$^{CO/GFP}$ CONDITIONALLY IMMORTALIZED PODOCYTES AND "WILD-TYPE" CONDITIONALLY IMMORTALIZED PODOCYTES CAN DIFFERENTIATE AND EXPRESS APPROPRIATE MARKERS OF MATURE PODOCYTES

Following fourteen days culture in differentiating conditions, both Podo32.1 (*CreERWt1$^{co/GFP}$*) and WTpodo ("wild-type") cells were analysed for morphology, and expression of appropriate podocyte markers. Proliferation was noted to reduce and finally cease in non-permissive conditions, and cells developed the characteristic flattened and arborized appearance of differentiated podocytes in culture (Figure 3.4).

Expression of podocyte markers was demonstrated at both the mRNA and/or protein level (Figures 3.5 & 3.6), to include key podocyte constituents (see Table 3.1):

TABLE 3.1: PODOCYTE MARKERS

Wt1	Transcriptional regulator
Nephrin	Slit diaphragm transmembrane receptor molecule
Podocin	Raft associated protein of the slit diaphragm
Synpatopodin	Actin-associated protein of foot process architecture
Podocalyxin	Transmembrane sialomucin involved in maintenance of the glycocalyx and glomerular charge barrier
Zo-1	Tight junction protein

Differentiation leads to an increase in gene expression of the majority of these markers, consistent with published literature (Saleem, O'Hare et al. 2002, Shankland, Pippin et al. 2007) (Figure 3.5). Although the relevant markers can be detected in both lines, stronger and more uniform expression of podocyte markers is demonstrated in the WTpodo line, both in terms of protein detected via immunofluorescence (Figure 3.7) and mRNA expression relative to kidney cortex (Figure 3.6). Notably relative nephrin expression was low in both cell lines. As discussed above, this is true of podocyte cell lines throughout the published literature, but should be taken into account when interpreting results. Some differences in morphology are also noted with a more characteristic arborized structure evident in the WTpodo line.

This analysis is limited to marker expression and not 3-dimensional structure or function.

Functional podocyte assays are published in the literature (including albumin influx assays (Li, Kang et al. 2008) and podocyte barrier capacity (Henao, Cadavid et al. 2013), but do not necessarily recapitulate the *in vivo* situation, as cell confluence has a major effect. Given these cell lines were to be used to compliment an *in vivo* model, it was decided that functional assays *in vitro* were unlikely to add much in the way of further information at this stage.

The characteristics of these cells are consistent with the published literature, indicating both these cell lines would provide a reasonable *in vitro* podocyte equivalent in order to study the effects of *Wt1* loss in an isolated cell system. It must be noted that only a small increase in *Wt1* expression is seen in the Podo32.1 cell line upon differentiation (Figure 3.5). However, as this was not dissimilar to the observed levels in other published cell lines (see above) and as both undifferentiated and differentiated cultured podocytes express *Wt1* (Figure 3.6), the decision was made to pursue further analysis of this line.

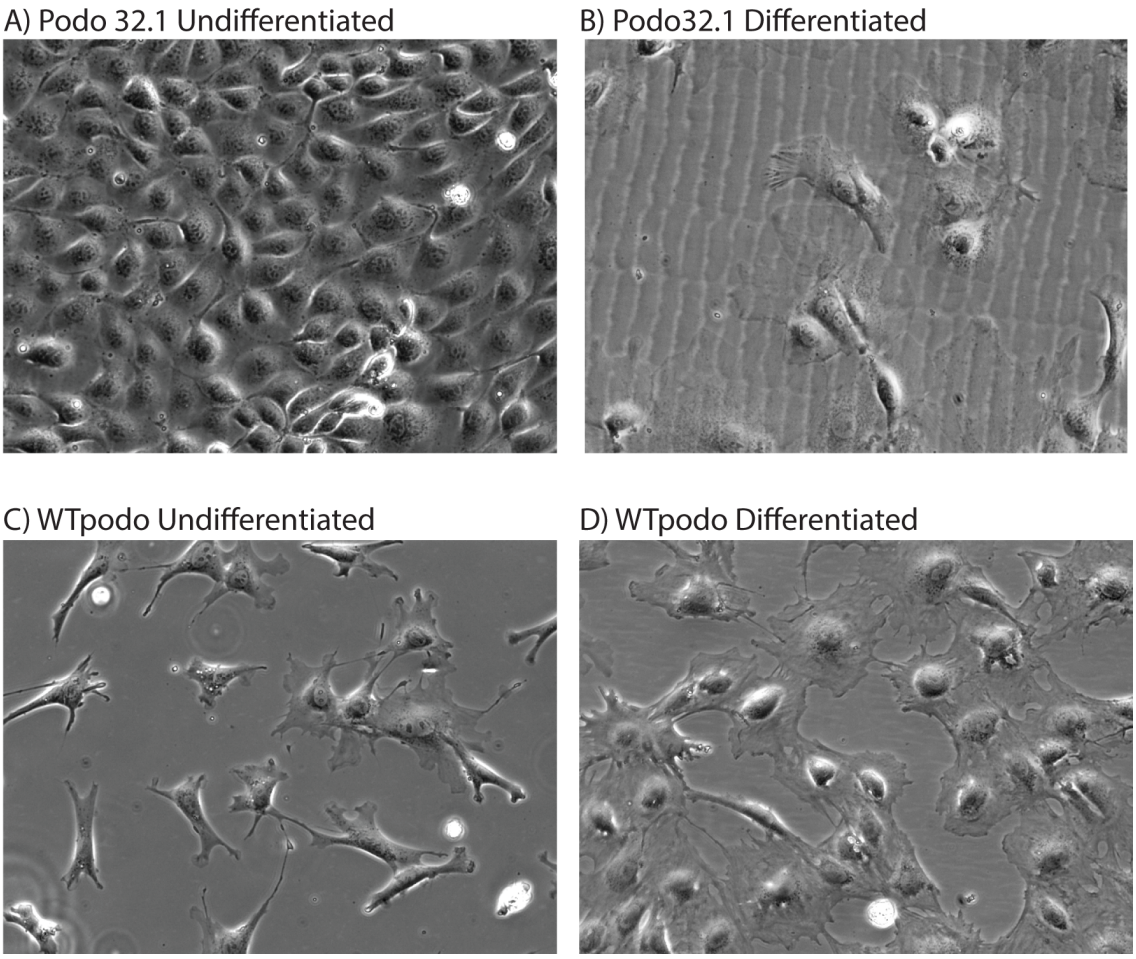

FIGURE 3.4: DIFFERENTIATION OF POD32.1 AND WTPODO CONDITIONALLY IMMORTALIZED PODOCYTES

Brightfield imaging at x100 magnification. A) Undifferentiated confluent Podo32.1 cells demonstrate typical 'cobblestone' morphology. B) Differentiated Podo32.1 cells show flattening and expansion of the cytoplasm. C) Undifferentiated WTpodo cells at low confluence. D) After differentiation, WTpodo cells take on the characteristic flattened, arborized appearance of differentiated podocytes. Following optimization of culture conditions, both cell types were grown at equivalent low confluencies in order to promote differentiation.

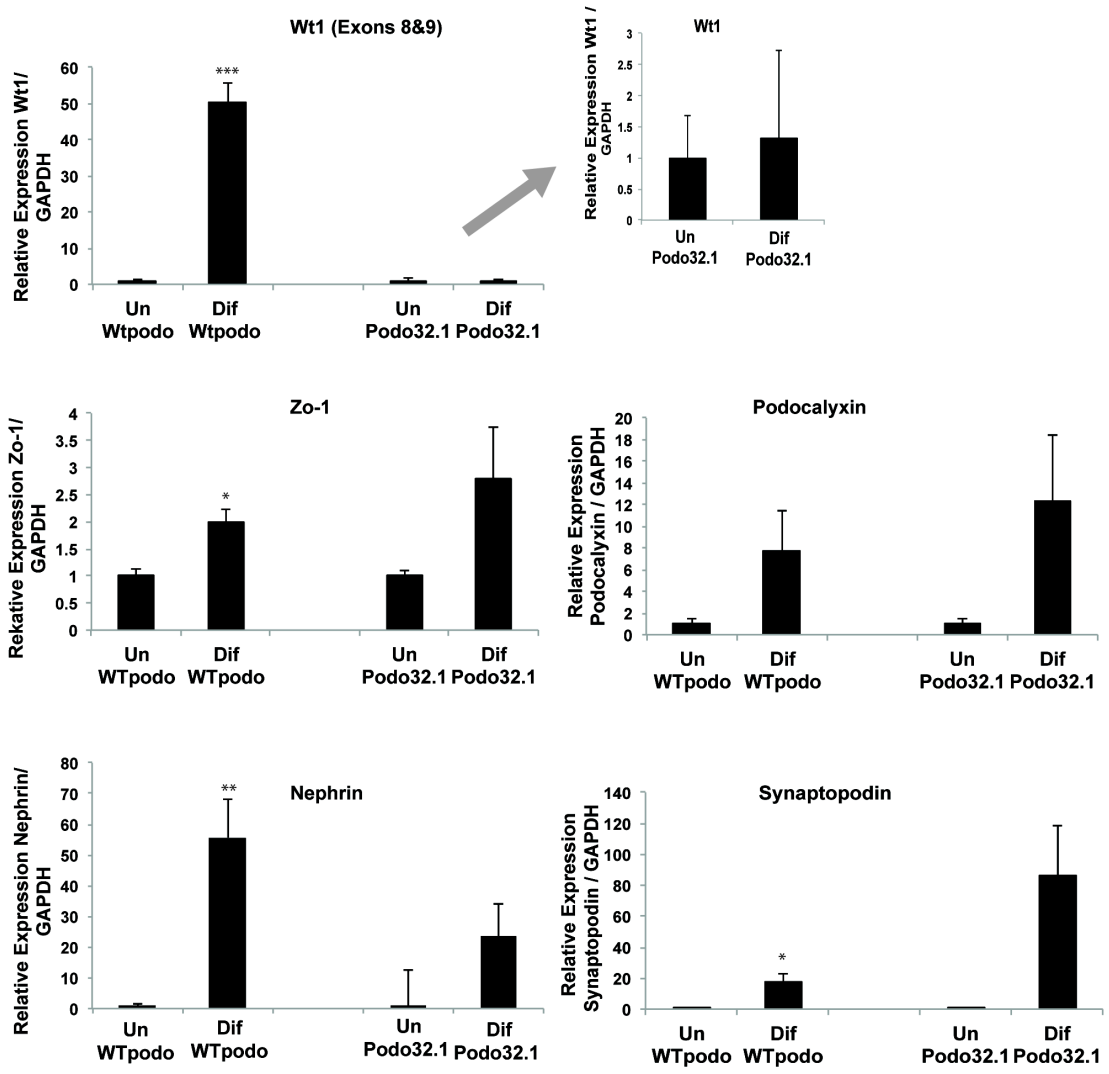

FIGURE 3.5: QUANTITATIVE PCR OF KEY PODOCYTE MARKERS IN UNDIFFERENTIATED AND DIFFERENTIATED WT PODO AND PODO 32.1 CELLS

Expressed as fold change difference between undifferentiated (Un) cells and differentiated (Dif) cells (* $p<0.05$; ** $p<0.01$; *** $p<0.001$). Undifferentiated cells were arbitrarily assigned a value of 1. Differentiation increases the expression of the major podocyte markers in both cell lines. Results represent the mean of 3 separate biological replicates, analysed in triplicate, in at least three separate experiments.

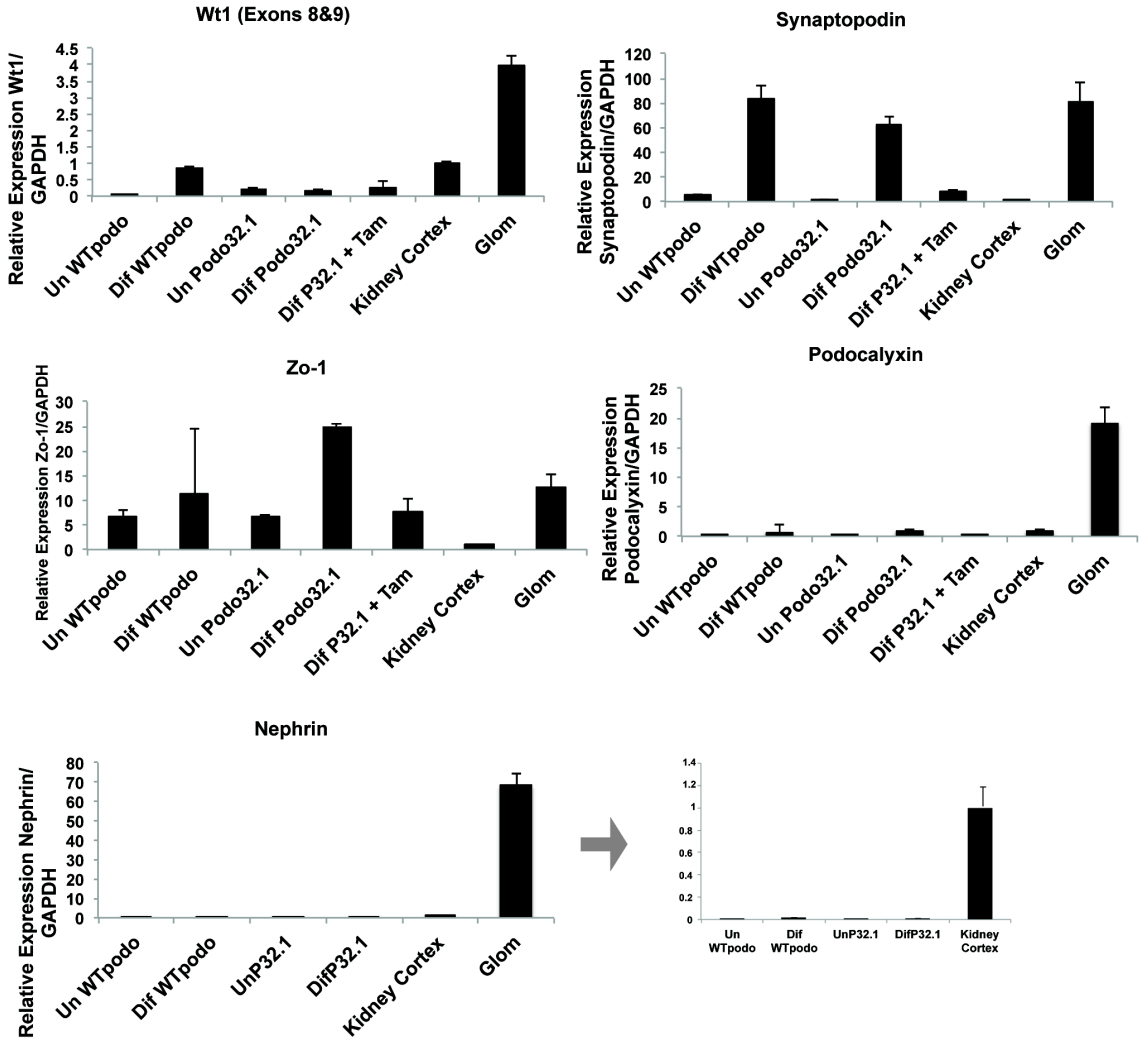

FIGURE 3.6: QUANTITATIVE PCR OF KEY PODOCYTE MARKERS IN UNDIFFERENTIATED AND DIFFERENTIATED WT PODO AND PODO 32.1 CELLS RELATIVE TO MURINE KIDNEY CORTEX AND ISOLATED GLOMERULI

Levels expressed as fold change difference in comparison to kidney cortex, arbitrarily assigned a value of 1(* $p<0.05$; ** $p<0.01$; *** $p<0.001$). Results represent means of samples analysed in triplicate. As in Chittiprol SP *et a*l (2012) levels of some major podocyte markers are very low in comparison to both kidney and glomerulus, particularly nephrin.

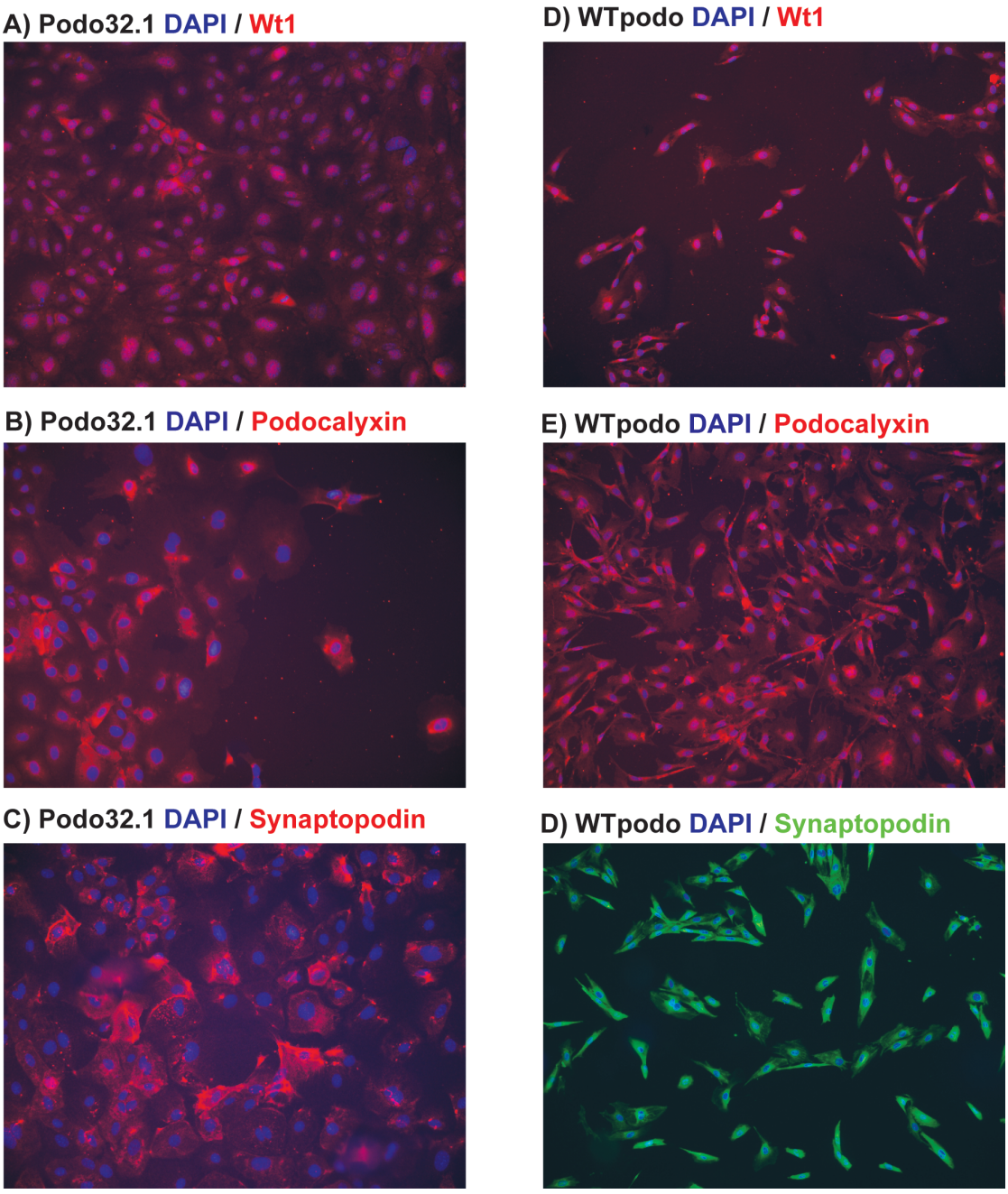

FIGURE 3.7: IMMUNOFLUORESCENCE OF DIFFERENTIATED PODOCYTES

Wide-field microscopy of immunofluorescence of differentiated podocytes (magnification x 100) Minus antibody controls were used to rule out non-specific binding of the secondary (data not shown). A) B) C) Differentiated Podo32.1 cells. D), E), F) Differentiated WTpodo cells. More consistent and intense fluorescent staining is seen in differentiated WTpodo cells.

3.3.2 *TAMOXIFEN-INDUCED CRE-RECOMBINATION CAUSES WT1 DELETION IN PODO32.1 CELLS*

A number of methods were tested to induce Cre-recombination in both undifferentiated and differentiated Podo32.1 cells, in order to optimize Cre-efficiency and minimize cell toxicity. 4OH-Tamoxifen (dissolved in ethanol) was added to culture media to delete *Wt1* and control cells were treated with vehicle (ethanol) at equivalent concentration. These methods included:

- Differentiation over 14 days in the presence of tamoxifen (1μM) (Figure 3.8 A)
- Treating with tamoxifen following differentiation (1μM for 24, 48, 72 hours) (Figure 3.8 B)
- Different doses of tamoxifen (1 μM-10μM) – cell toxicity and death occurred at 10 μM and, to a lesser degree at 5μM. Control cells were only treated with vehicle equivalent to the 1μM concentration (Figure 3.8A)

Triple primer PCR, to recognise the three possible states of the *Wt1* locus, demonstrated recombination events in all these conditions (Figure 3.8). Significant recombination occurred as early as 24 hours after tamoxifen treatment (Figure 3.8 B), although prolonged treatment over 14 days appeared to result in almost total recombination, and complete loss of the conditional allele (Figure 3.8A)

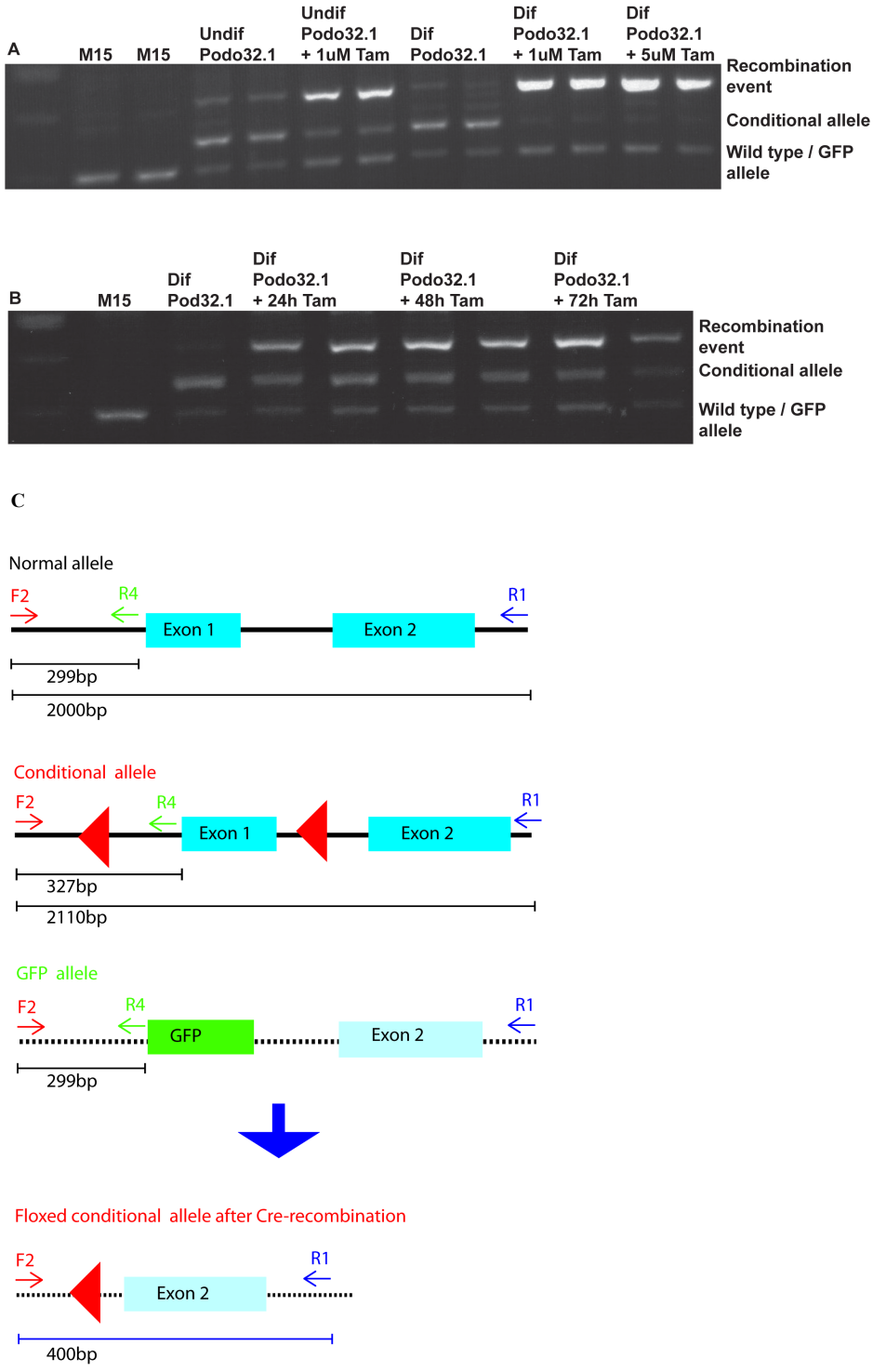

FIGURE 3.8: TRIPLE PRIMER PCR TO DEMONSTRATE CRE-RECOMBINATION AND *WT1*-LOSS AT THE DNA LEVEL

FIGURE 3.8: TRIPLE PRIMER PCR TO DEMONSTRATE CRE-RECOMBINATION AND *WT1*-LOSS AT THE DNA LEVEL

A) Recombination efficiency using different doses of tamoxifen over 14 days. Although this is not a formal quantitative PCR assay, almost complete loss of the conditional allele can be seen in differentiated Podo32.1 cells using doses of both 1μM and 5μM tamoxifen. A faint band to show recombination events exists in the control (vehicle treated) cells, consistent with low level of Cre-activity in the absence of tamoxifen, ("leaky Cre-activity"). B) Recombination efficiency using 1μM tamoxifen for 24, 48 or 72 hours following full differentiation. Significant recombination occurs as early as 24 hours. Double lanes represent duplicate biological replicates (1 flask per lane). C) Schematic of triple-primer PCR to show 400bp band following recombination and loss of exon 1.

3.3.3 No macroscopic phenotype is evident following tamoxifen-mediated Cre-recombination

Despite evidence of *Wt1* deletion at the DNA level, no macroscopic phenotype was evident in *Wt1*-deleted cells. Cells treated with tamoxifen (at 1μM concentration) in permissive conditions continued to proliferate normally and look healthy. At 5μM tamoxifen there was excess cell death, presumably due to toxicity, as all cells died at 10μM tamoxifen (Figure 3.9). However, the remaining cells appeared to differentiate normally. Cells treated either during or after differentiation also appeared healthy with no overt phenotype.

3.3.4 Evidence of significant Wt1 loss at either the mRNA or protein level cannot be demonstrated.

Quantitative RT-PCR was used to analyse *Wt1* gene expression following tamoxifen-mediated Cre recombination and *Wt1* deletion. However, in all conditions tested, no significant reduction in *Wt1* gene expression could be demonstrated (Figure 3.10). Difficulties were encountered in establishing a reliable anti-Wt1 antibody for Western Blot, but, in keeping with the gene expression data, no loss of Wt1 at the protein level in recombined cells could be demonstrated either (Figure 3.11). This is in direct contrast to the *in vivo* situation, where *Wt1* deletion leads to profound loss of *Wt1* gene and protein expression (Figure 3.12)

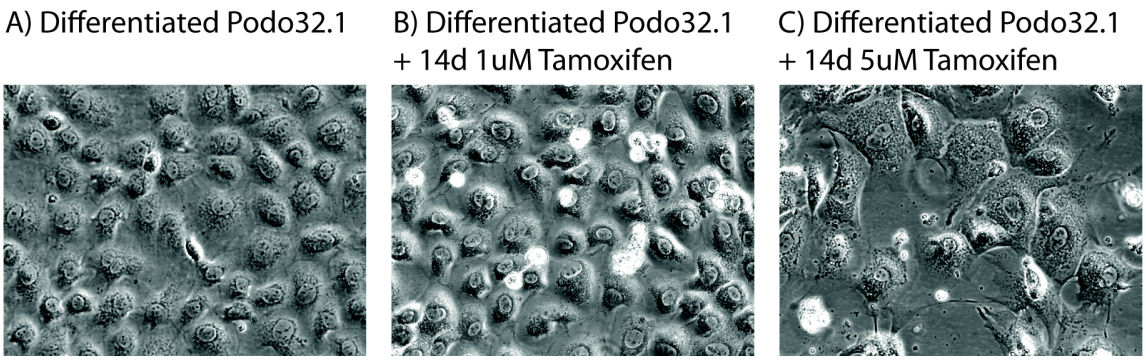

FIGURE 3.9: DIFFERENTIATED PODOCYTES FOLLOWING WT1-DELETION

Brightfield microscopy of differentiated Podo32.1 cells (x100 magnification). A) Differentiated Podo32.1 cells at relatively high confluence (so arborisation / cytoplasmic spreading is limited. B) Podo32.1 cells differentiated over 14 days in 1μM tamoxifen – cell density remains equivalent to untreated cells and cells differentiate normally. C) Podo32.1 cells differentiated over 14 days in 5μM tamoxifen. At higher concentrations of tamoxifen some cell toxicity occurs so cell density is reduced. However, the remaining cells appear to differentiate normally

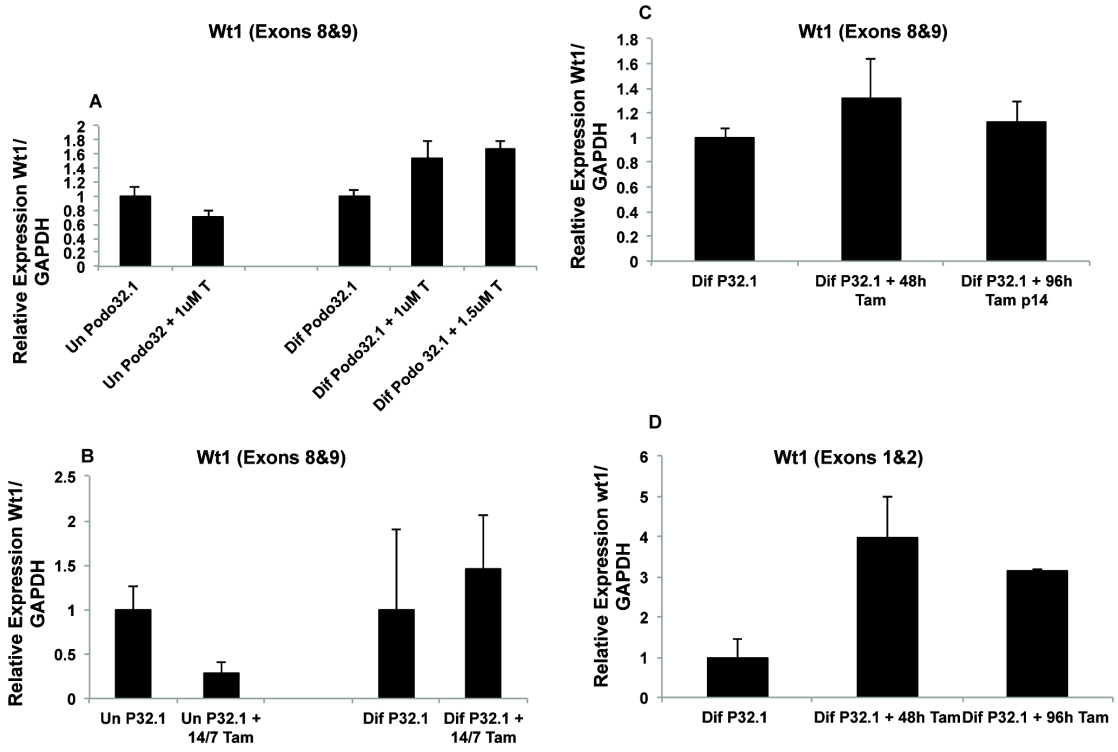

FIGURE 3.10: QUANTITATIVE RT-PCR FOR *WT1* EXPRESSION IN "WT1-DELETED" CELLS

Quantitative RT-PCR for *Wt1* expression (assay detecting exons 8 and 9 or exons 1 and 2 as detailed) following tamoxifen induced Cre-recombination. A) Podo 32.1 cells treated with tamoxifen or vehicle at different doses over a period of 14 days (differentiated cells were differentiated in the presence of tamoxifen). All cells died in 10µM Tamoxifen and insufficient RNA could be extracted from cells differentiated in 5µM Tamoxifen. B) Podo32.1 cells treated with 1µM tamoxifen for 14 days. Some reduction in *Wt1* expression is seen in undifferentiated cells, but this does not reach statistical significance. C) Tamoxifen treatment (1µM) to differentiated cells for differing time periods. D) Specific *Wt1* assay to detect exons 1 and 2 (exon 1 is deleted following Cre recombination). Conditions as per (C). Each graph represents mean of each experiment repeated in triplicate.

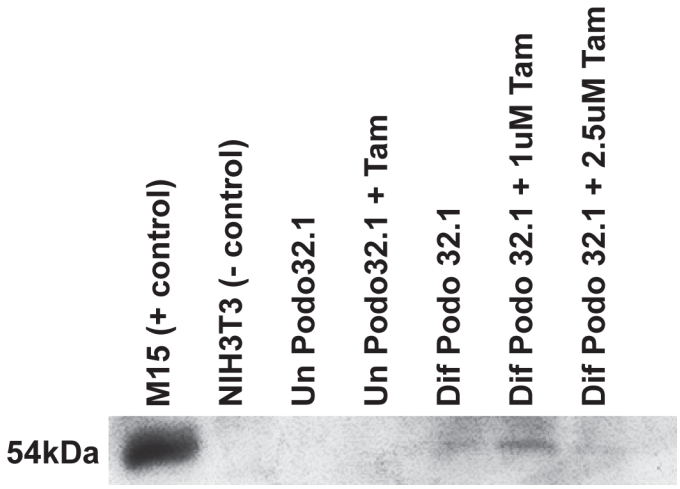

FIGURE 3.11: WESTERN BLOT FOR WT1

Western blot for Wt1 using Santa-Cruz C19 antibody. A reliable Wt1 antibody was not available for these experiments, so this blot represents the best example of multiple attempts. Podo32.1 cells were treated over 14 days with tamoxifen or vehicle and harvested for protein extraction. 30μg protein was loaded into each lane. Given the poor quality of this blot it was not re-probed at the time with a loading control. However, this was the best example blot available despite multiple repeats, due to poor quality of a new antibody batch. Despite this, it does indicate the low / undetectable level of Wt1 expression in undifferentiated Podo32.1 cells and no loss of Wt1 expression in differentiated Podo 32.1 cells following tamoxifen treatment, in keeping with the other experimental findings.

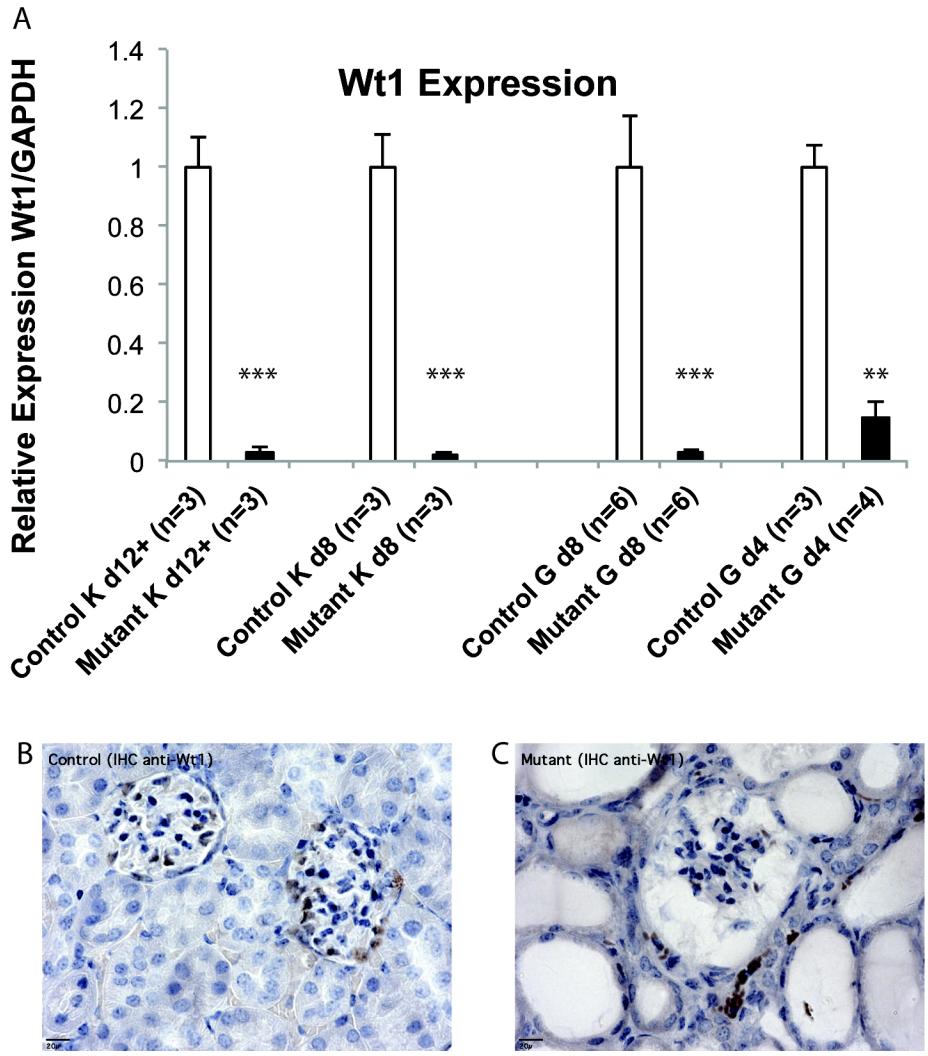

FIGURE 3.12: WT1 DELETION IN VIVO

A) Massive reduction in *Wt1* gene expression follows *Wt1* deletion (K=kidney cortex, G=isolated glomeruli) as demonstrated by Q-RT-PCR, represented as fold change difference in comparison to control (assigned value of 1). This occurs as early as day 4 after the start tamoxifen treatment (* $p<0.05$; **$p<0.01$; ***$p<0.001$) Each experiment was analysed in triplicate and repeated at least twice. B) Cre-negative $Wt1^{co/co}$ control littermates exhibit normal Wt1 IHC staining of glomerular podocytes. C) Following *Wt1* deletion, virtually no Wt1 protein can be detected in mutant animals (day 12). Some background DAB staining (extracellular) can be seen (for further information and control staining see Figure 4.11).

3.3.5 *Wt1*-DELETION DOES NOT CAUSE CELL DEATH OR DETATCHMENT

Given the clear evidence of Cre-mediated recombination at the DNA level, and the demonstrable loss of Wt1 *in vivo* and in other cell-based systems generated from this model (Martinez-Estrada, Lettice et al. 2010, Chau, Brownstein et al. 2011), it was entirely unexpected that no differences in gene or protein expression could be detected.

Cell death and detachment of *Wt1*-deleted cells could partly explain the aberrant RNA and protein findings, as detached cells would be washed away and therefore not be included in the analysis. As these methods are quantitative, the results would vary more significantly than the qualitative PCR assay for recombination, which would still detect any remaining *Wt1*-deleted cells and generate a band. However, when observed during differentiating culture conditions, tamoxifen treated (*Wt1* deleted) cells did not appear to reduce in number, or undergo excess cell death.

Therefore, in order to assess for certain whether excess *Wt1*-deleted cells were being lost from the culture, tamoxifen and vehicle treated cell cultures were analysed for the degree of apoptosis, and under time-lapse imaging to detect and quantify levels of cell death and detachment.

Analysis of levels of apoptosis using a commercially available Caspase-Glo 3/7 Assay to measure activated caspase 3 and 7 revealed only small differences in apoptosis between *Wt1*-deleted (tamoxifen treated) and vehicle treated cells (Figure 3.13). At maximal fluorescence intensity (i.e. maximal caspase activity - at one hour) there is no significant difference between tamoxifen and vehicle treated cells, indicating an excess of apoptosis in response to tamoxifen treatment and/or *Wt1*-deletion could not explain these results.

Given the marked excess in apoptosis in differentiated podocytes as compared to M15 (embryonic metanephric mesenchyme) cells, these results should be interpreted with caution. In order for the assay to work, the podocytes had to be passaged when already differentiated to ensure equivalent densities were plated. This may lead to an excess of apoptosis, in comparison to the proliferating M15 cells.

Timelapse imaging of differentiating cells was used in conjunction to analyse levels of cell detachment in tamoxifen treated / *Wt1*-deleted cells (Figure 3.13 B). Only a few cells per microscopic field dethatched during the course of differentiation, and there was no difference between control and *Wt1*-deleted Podo32.1 cells. No toxic effect of tamoxifen at 1μM concentration was noted on differentiating WTpodo cells, indicating any effect seen would be due to *Wt1*-deletion.

Thus loss of *Wt1*-deleted cells from the pool of cells analysed could not explain the inability to detect a reduction in *Wt1* expression following Cre-recombination at the mRNA or protein level.

A

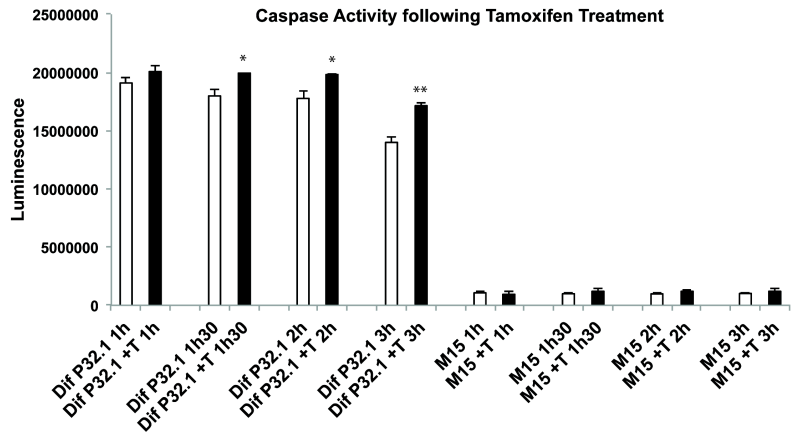

B

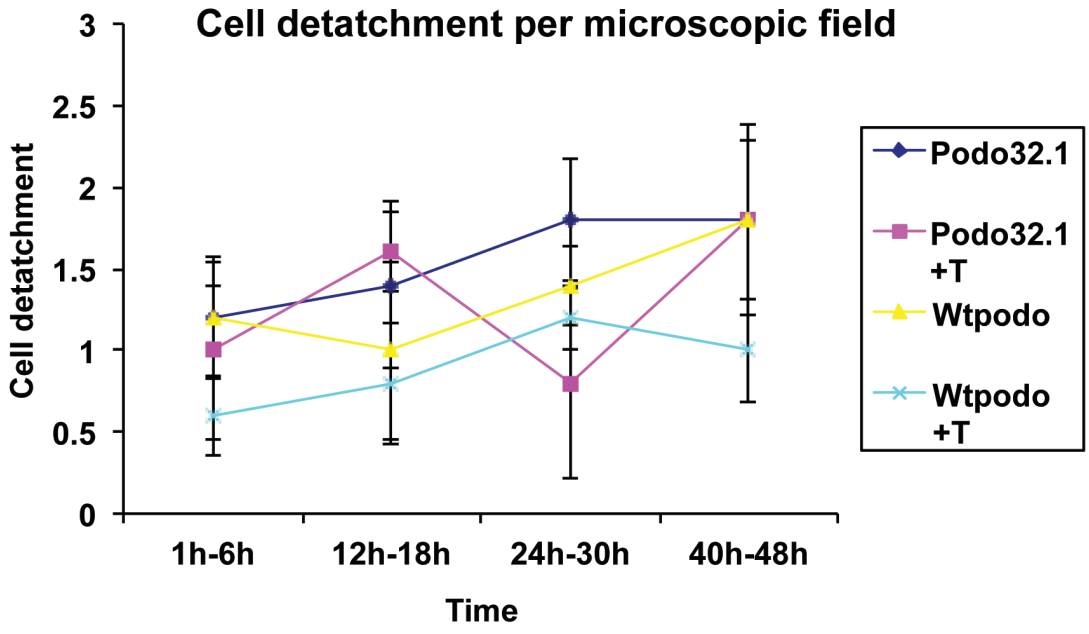

FIGURE 3.13: *WT1*-DELETION DOES NOT CAUSE CELL DEATH OR DETACHMENT

FIGURE 3.13: *WT1*-DELETION DOES NOT CAUSE CELL DEATH OR DETACHMENT

A) Caspase 3/7 apoptosis assay. Caspase activity is proportional to luminescence intensity (y-axis). At maximum fluorescence intensity (1hr) there is no significant difference in caspase activity between tamoxifen treated (*Wt1*-deleted) and vehicle treated Podo32.1 cells. Tamoxifen and vehicle treatment does not affect caspase activity (apoptosis) in M15 cells. A significant excess of apoptosis is seen in differentiated podocytes in comparison to actively proliferating M15 cells (* $p<0.05$; ** $p<0.01$; *** $p<0.001$). **B**) Level of cell detachment during differentiation. Time-lapse photography of differentiating cell cultures was used to count the number of cell deaths / detachments occurring during differentiation. Each point represents mean number of cell detachments for 5 microscopic positions at each time point. (Error bars = +/-SEM). Levels of cell detachment are low, with no difference between tamoxifen and vehicle treated (control) cells. Thus a high level of cell loss would not explain the failure to detect a difference in *Wt1* expression following tamoxifen treatment.

3.3.6 *Wt1*$^{CO/GFP}$ *conditionally immortalised cells express only low levels of Wt1*

As discussed earlier, both proliferating and differentiated podocytes in culture express *Wt1*. However, when compared to a positive control of whole kidney extract, differentiated Podo32.1 cells expressed relatively low levels of *Wt1 (*Figure 3.14*)*. These cells represent a clonal population of podocytes, so one would expect much higher levels of *Wt1* than kidney cortex (in which podocytes make up only a fraction of cells). The WTpodo cell line appears to express higher relative and actual levels of *Wt1* when differentiated, more in keeping with the levels expected. It may be, perhaps as a consequence of the compound heterozygosity in an isolated cell system, that Podo32.1 cells only express very low levels of *Wt1*. This would be in contrast to the in vivo situation, as markedly reduced levels of Wt1 protein are not seen in the *Wt1*-heterozygous mouse.

Some evidence of low-level Cre-activity in the absence of tamoxifen-induction was also noted (see Figure 3.8) which may have led to a global reduction in *Wt1* expression over serial passages (although podocytes were only used up to passage 18 for analysis).

Given these baseline low levels, I was not able to detect differences in *Wt1* expression between control and tamoxifen treated cells. Importantly, when examined microscopically and by FACS analysis, these cells do not express detectable GFP. The GFP allele faithfully expresses GFP under control of the *Wt1* promoter, so this would be in keeping with negligible expression of *Wt1* from these cells (Figure 3.15), rather than loss of the remaining Wt1 conditional allele due to low-level, "leaky" Cre-recombination. This could also explain the low levels of podocyte markers in the Podo32.1 cells when differentiated, particularly nephrin, a known Wt1 target (Figure 3.5). Following discussion with our collaborators at the Saleem laboratory, when these cells were first generated, detectable GFP expression was visualised microscopically (Moin Saleem, personal communication). This loss of GFP expression reflects loss of Wt1 expression, which could imply cell transformation had occurred (Shankland, Pippin et al. 2007).

However, as mentioned above, in work published subsequent to these experiments, it appears that conditionally immortalised podocyte cell lines can express variable and very low levels of *WT1*. Presumably as a consequence of this many of these lines also express very low levels of nephrin (Steege, Fahling et al. 2008). This work also demonstrated that in primary cultures of podocytes *Wt1* expression decreases over time, which is another explanation for this presumed loss of Wt1 expression over time.

Given the inability to demonstrate Wt1 loss using *CreERWt1*$^{co/GFP}$ conditionally immortalised podocytes, these cells were not suitable for use for further analysis of the effects of Wt1 loss *in vitro*.

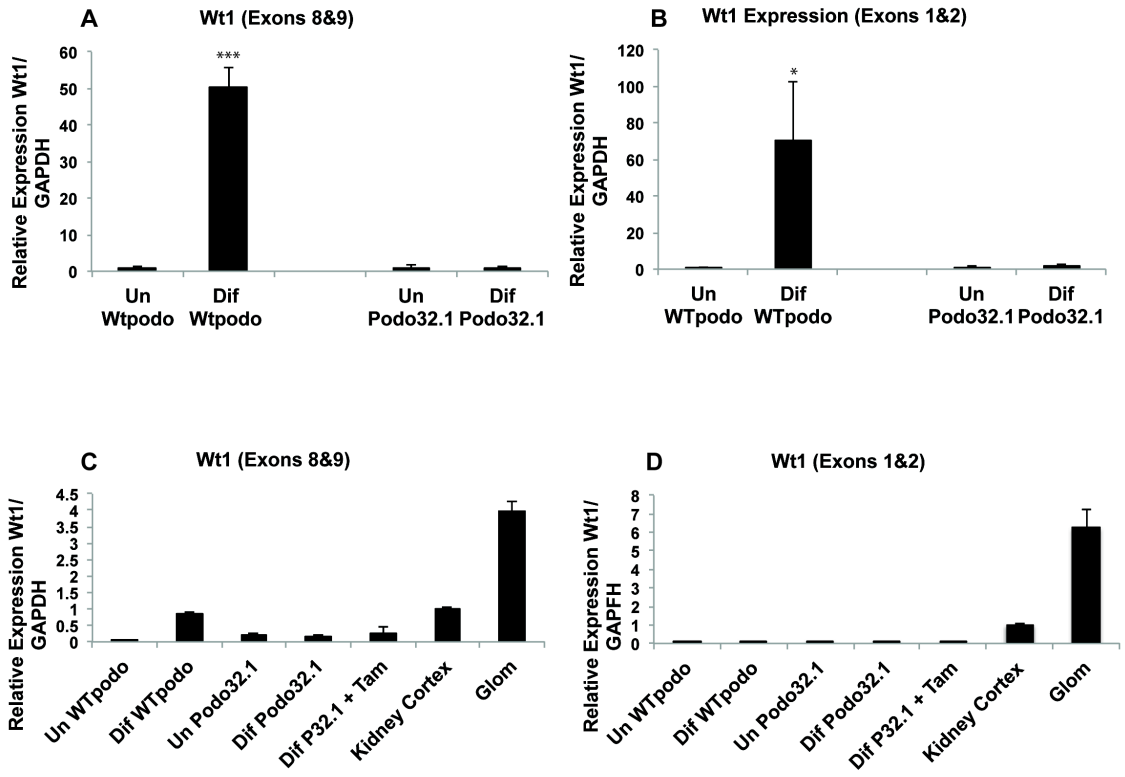

FIGURE 3.14: QUANTITATIVE RT-PCR FOR *WT1* MRNA EXPRESSION

A) and B) Two different assays for *Wt1* expression to detect either Exons 7&8 (all isoforms - as shown in Figure 3.5) or Exons 1&2 (Exon one is excised following Cre-recombination). *Wt1* expression in differentiated cells is represented as fold change difference from undifferentiated cells, arbitrarily assigned a value of 1 (* $p<0.05$; ** $p<0.01$; *** $p<0.001$). Using both assays, there is little upregulation of *Wt1* expression in the Podo 32.1 cell line when differentiated. C) and D) *Wt1* expression relative to kidney cortex. Again Podo32.1 cells express relatively little *Wt1* in comparison to differentiated WTpodo cells, and both express far less *Wt1* than would be expected in comparison to whole kidney or isolated glomeruli.

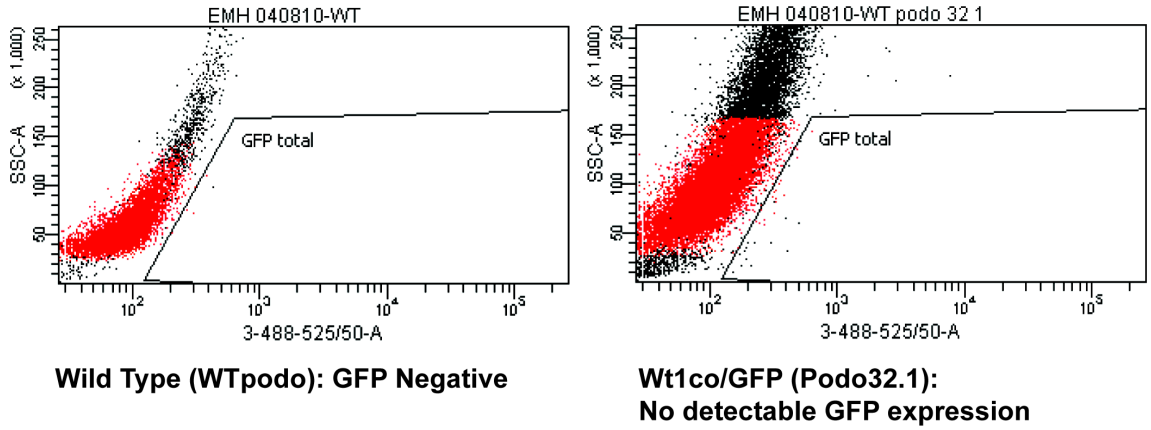

FIGURE 3.15: FACS ANALYSIS FOR GFP EXPRESSION IN *CREERWT1*$^{CO/GFP}$ PODOCYTES

WTpodo cells are GFP negative as expected. However, no GFP expression can be detected in Podo32.1 cells either, which should express GFP when and where *Wt1* is being expressed.

3.4 Alternative Methods to achieve Wt1 loss in podocytes in vitro: Achieving Stable Wt1 knockdown using RNAi in cultured podocytes

3.4.1 Introduction

As the *Wt1*$^{co/GFP}$ (Podo32.1) cell line did not provide a useable *in vitro* model of *Wt1* loss, alternative methods had to be sought. RNA interference would allow conditional *Wt1* knockdown in differentiated podocytes and has already been used as an effective method of *Wt1* knockdown in a number of scenarios:

1) *Wt1* knockdown in both M15 cells and *ex vivo* embryonic kidney organ culture, which achieved up to 80% protein repression. Non-specific RNAi did not affect Wt1 expression, implying no general toxic effect of the siRNA technique (Davies, Ladomery et al. 2004)

2) RNAi mediated *Wt1* knockdown in M15 cells using transient siRNA transfection to achieve 53-80% knockdown efficiency at the mRNA level (Ratelade, Arrondel et al. 2010)

In order to achieve stable *Wt1* knockdown in podocytes, lentiviral mediated RNAi was used to achieve maximum transfection efficiency (Moin Saleem, personal communication).

3.4.2 Using the Thermo Scientific Open Biosystems Expression Arrest GIPZ Lentiviral shRNAmir kit to knockdown Wt1 in podocytes.

This commercially available kit used a pGIPZ lentiviral vector in order to achieve RNA interference of *Wt1*. Three *Wt1* knockdown constructs were used, Wt1-17, Wt1-46 and Wt1-52, which were all predicted to bind in exons 3 and 4, and thus would knock down all relevant *Wt1* isoforms. Control constructs consisted of a negative control non-silencing construct (N-S) and two positive control off-target constructs (GAPDH and EG5). This vector contained a short hairpin RNA construct, to express the human microRNA-30 transcript, which included a Drosha processing site to increase knockdown efficiency. GFP expression and puromycin resistance allowed dual selection of effectively transduced cells (Figure 3.16).

Transfection and viral production of control and *Wt1* constructs was performed in HEK293 cells. Transduction of target cells with both control and *Wt1* constructs was carried out in both permissive and differentiated 'wild-type' podocytes (*WTpodo*) and M15 cells. After transduction with viral stock, cells were exposed to puromycin selection for one week and then FACS sorted for GFP expression, as a surrogate marker of shRNA expression.

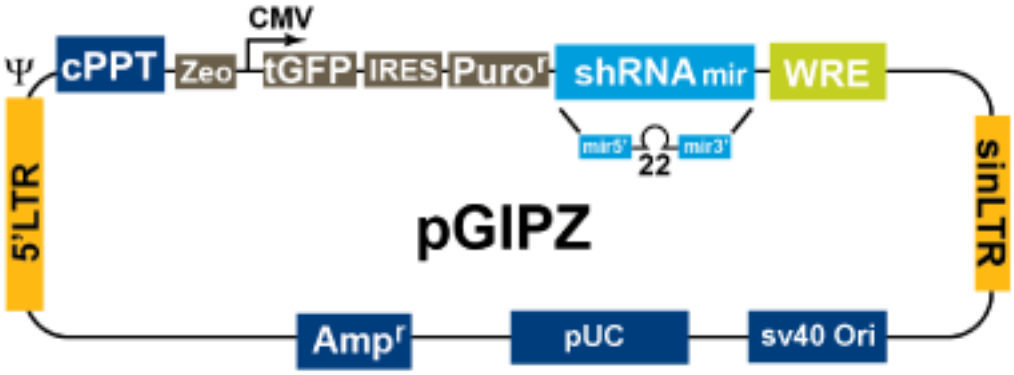

FIGURE 3.16: PGIPZ LENTIVIRAL SHRNA EXPRESSION VECTOR

Clockwise from top left: cPPT - Central Polypurine Tract to help translocate vector into the nucleus of non-dividing cells; Zeo – bacterial zeomycin selectable marker; CMV promoter; turboGFP – to track shRNA expression; Puro – mammalian selctable marker; shRNAmir – short hairpin RNA construct; WRE – to enhance stability and translation of shRNA transcripts; SIN-LTR – 3' self-inactivating long terminal repeat; pUC – origin of replication for high copy replication and maintenance in E.coli; Amp – ampicillin resistance; 5'LTR – 5' long terminal repeat.

3.4.3 Efficient transduction of both undifferentiated and differentiated podocytes is achieved using the pGIPZ Lentiviral Vector

Following selection on puromycin for one week, cells were trypsinised and the single cell suspension FACS sorted for GFP expression.

In undifferentiated (dividing) cells the vast majority of cells were GFP positive (i.e. they were all expressing shRNA). The top 10% of GFP expressing cells (i.e. with the highest shRNA expression) were sorted and grown. (Figure 3.17). Lentiviral transduction was slightly less efficient in differentiated (non-dividing) cells although there was still a significant GFP positive population. As these terminally differentiated cells could not be expanded, the top 25% of GFP positive cells were selected for analysis (Figure 3.18).

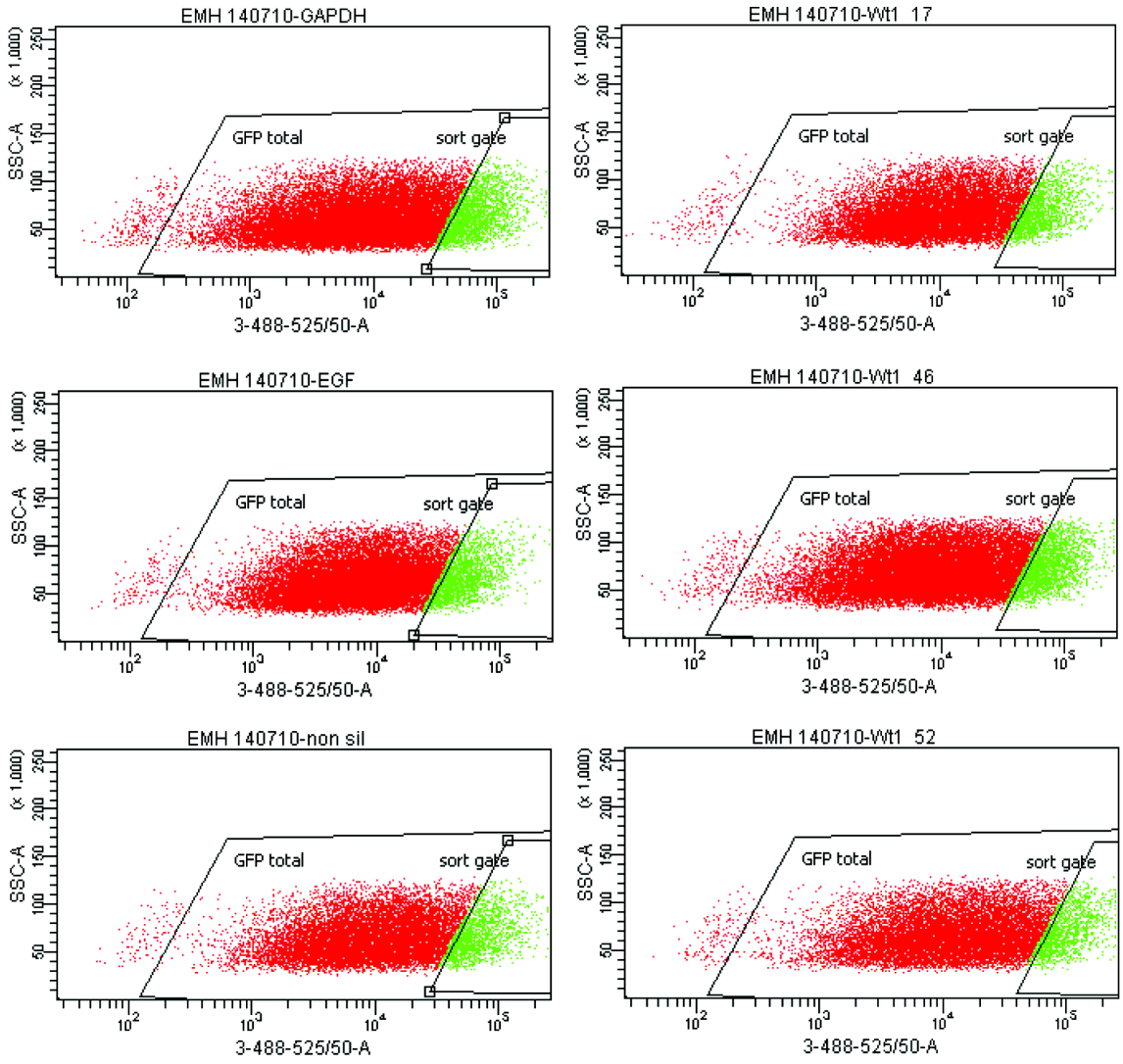

FIGURE 3.17: FACS SORT FOR GFP EXPRESSION OF UNDIFFERENTIATED WTPODO CELLS TRANSDUCED WITH THE DIFFERENT LENTIVIRAL VECTORS

Majority of cells are GFP positive and top 10% GFP expressing cells were sorted to expand for analysis (shown in green). A repeat experiment yielded similar results.

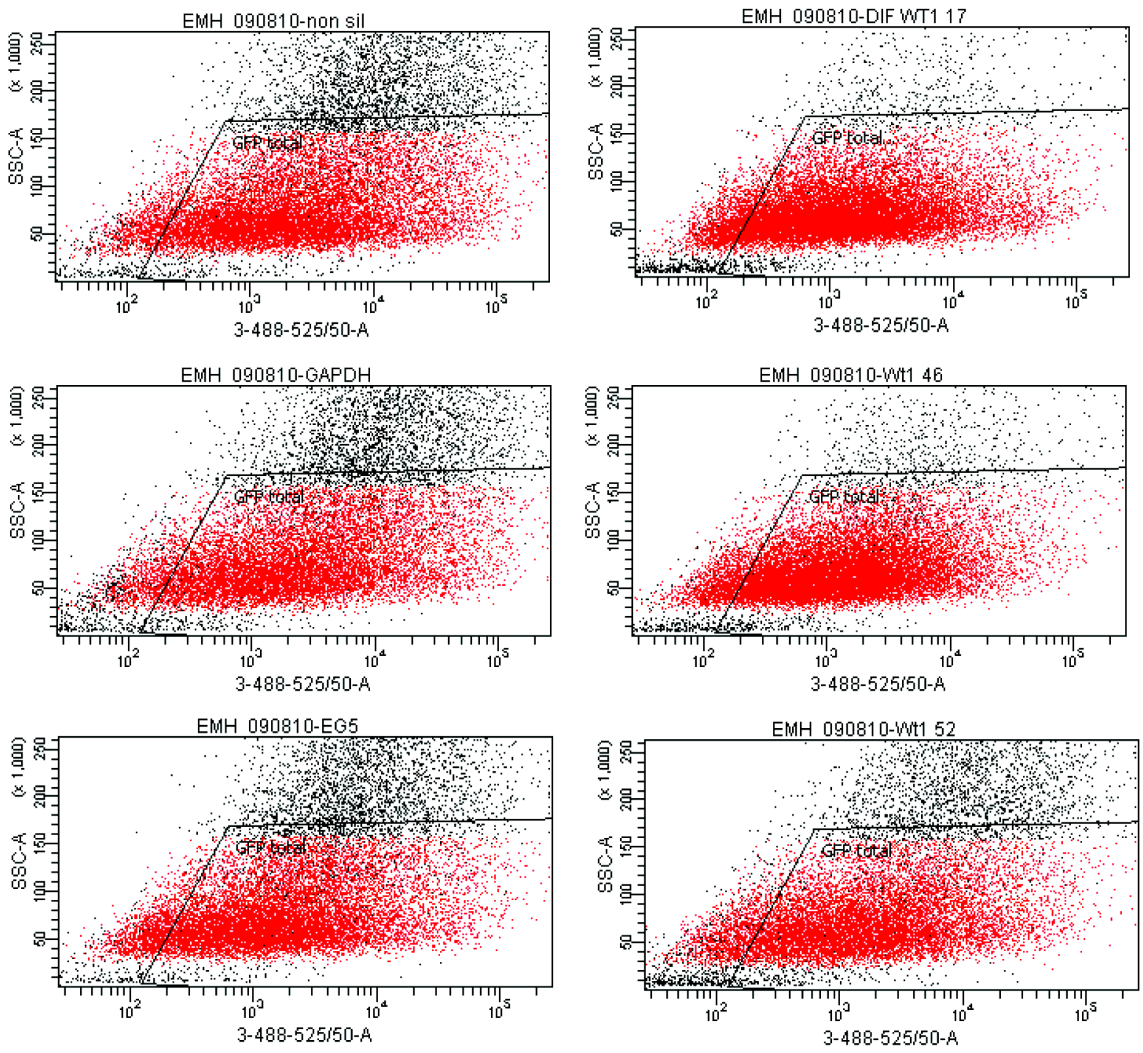

FIGURE 3.18: FACS SORT FOR GFP EXPRESSION OF DIFFERENTIATED WTPODO CELLS TRANSDUCED WITH THE DIFFERENT LENTIVIRAL VECTORS

Majority of cells are GFP positive and top 25% GFP expressing cells were sorted and collected for RNA extraction and analysis. Two repeat transduction experiments yielded similar results.

3.4.4 *WT1 KNOCKDOWN CANNOT BE DETECTED IN UNDIFFERENTIATED CELLS*

Initial analysis for mRNA expression by quantitative PCR indicated non-significant knockdown of *Wt1* in transduced cells (Figure 3.19). Beta-Actin was used as the reference gene, as GAPDH knockdown was the off-target positive control so could not be used as a reference. However, similar reductions in *Wt1* expression could be seen in cells transduced with the control constructs. Despite repeating the whole experiment, including transfection and packaging of the viral constructs and re-transducing new podocytes, this unexpected pattern persisted.

When interrogating the results in detail it appeared that given the very low level of *Wt1* expression in the undifferentiated WTpodo cells, the *Wt1* QPCR assay (detecting exons 8 and 9) was not sensitive enough to detect a difference between the cDNA sample and the negative control (minus-reverse transcriptase) (Figure 3.20). Therefore, although GFP and puromycin expression indicated successful transduction with lentivirus and expression of shRNA, it was impossible to demonstrate this directly or quantitatively in terms of knockdown of *Wt1* gene transcription in the undifferentiated state.

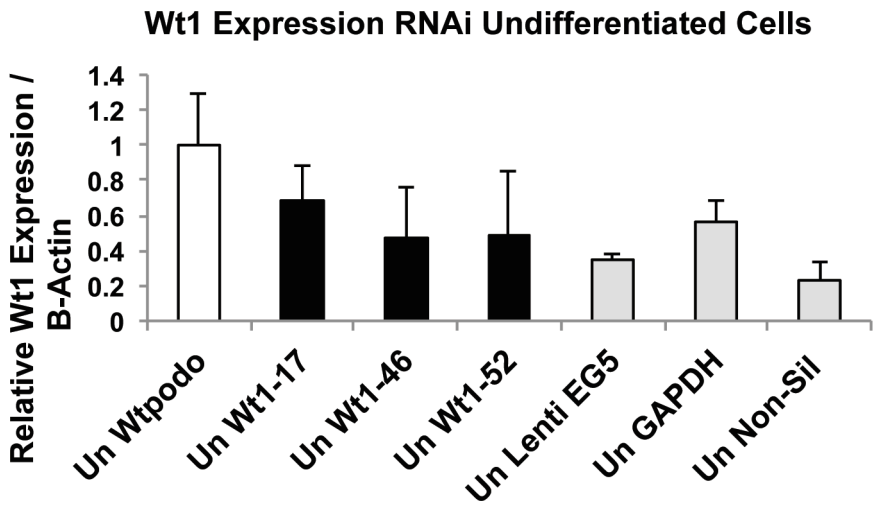

FIGURE 3.19: REPRESENTATIVE QPCR ASSAY FOR WT1 EXPRESSION (ASSAY DETECTING EXONS 8&9) IN UNDIFFERENTIATED CELLS FOLLOWING LENTIVIRAL TRANSDUCTION IN THE UNDIFFERENTIATED (PROLIFERATING) STATE

Results represented as fold change in expression from untreated cells (arbitrarily assigned a value of 1). Results depict mean values of two biological replicates per sample, with each sample analysed in triplicate.

A Undifferentiated

Un WTpodo

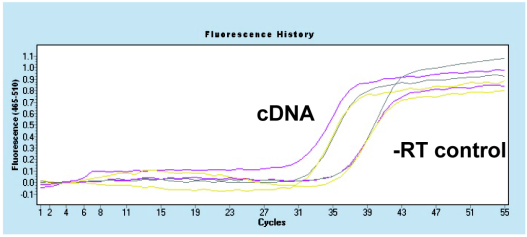

Un WTpodo Wt1-46

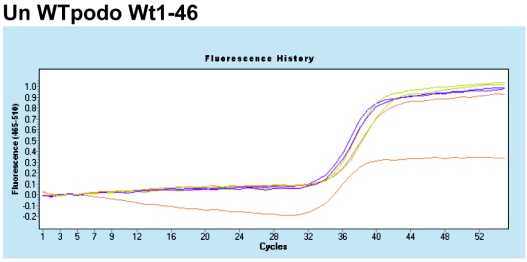

Un WTpodo Wt1-52

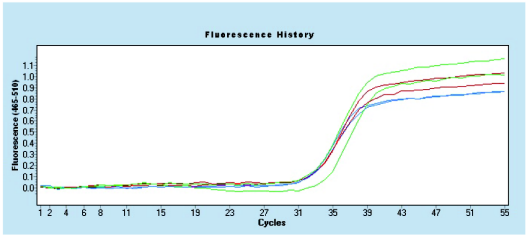

B Differentiated

Dif WTpodo

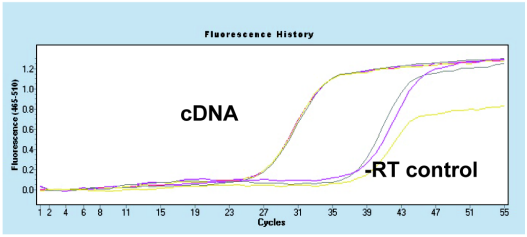

Dif WTpodo Wt1-46

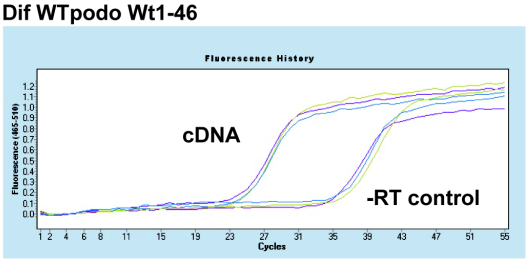

Dif WTpodo Wt1-52

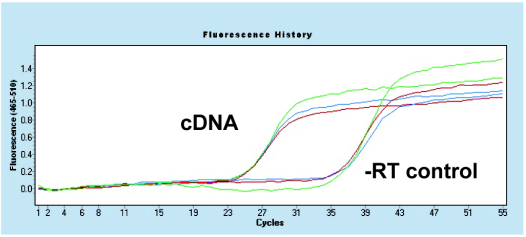

C M15

M15

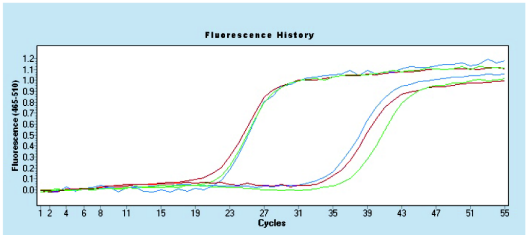

FIGURE 3.20 AMPLIFICATION CURVES FOR Q-RT-PCR WT1 ASSAY OF UNDIFFERENTIATED WTPODO CDNA

FIGURE 3.20: AMPLIFICATION CURVES FOR Q-RT-PCR WT1 ASSAY OF UNDIFFERENTIATED WTPODO CDNA

A) In undifferentiated cells, particularly following siRNA there is no significant difference between the cDNA sample and –reverse transcriptase control sample (equivalent to genomic DNA contamination) so significant mRNA expression is not detected. However, in differentiated (B) and M15 (C) cells, the clear difference between cDNA and –RT control is apparent.

As previously demonstrated, effective lentiviral transduction was also demonstrated in differentiated cells, as the cells expressed both GFP and puromycin resistance. Differentiated WTpodo cells express significant levels of *Wt1* so any knockdown should have been detectable. However, all siRNA treated cells seemed to demonstrate increased levels of Wt1 expression at the mRNA level in comparison with untreated cells. (Figure 3.21) These results were entirely unexpected and possibly reflected an alteration in phenotype as a consequence of the numerous passages required in order to ensure efficient viral transduction, once cells were already differentiated.

However, the same vector had also been used to knockdown *Wt1* in M15 cells. These cells express a very high level of *Wt1*. This proved the pGIPZ vectors effectively reduced *Wt1* mRNA expression. However, some effect was also seen in the positive control siRNA constructs, meaning the effects of *Wt1* knockdown could not be differentiated confidently from a general siRNA effect (Figure 3.22). Therefore *Wt1* knockdown could be achieved, but to definitely prove the effects detected were only due to Wt1 loss, new control constructs were needed.

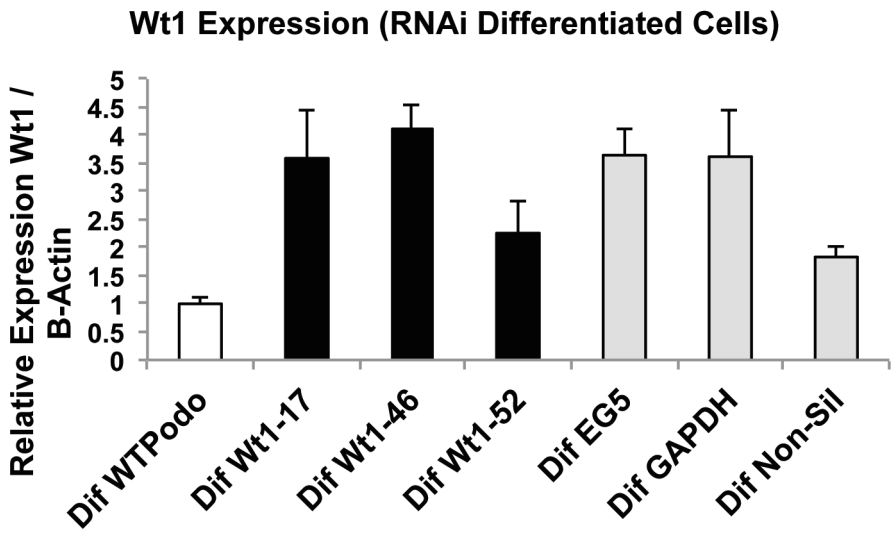

FIGURE 3.21: Q-RT-PCR FOR WT1 EXPRESSION FOLLOWING RNAI TO DIFFERENTIATED CELLS

Data bars represent means of relative expression changes as compared to untreated WTpodo cells (assigned a value of 1) of three separate biological replicates (each analysed in triplicate). In differentiated cells the lentiviral siRNA method appears to increase Wt1 expression (at the RNA level) for all constructs, implying a methodological problem or confounding effect.

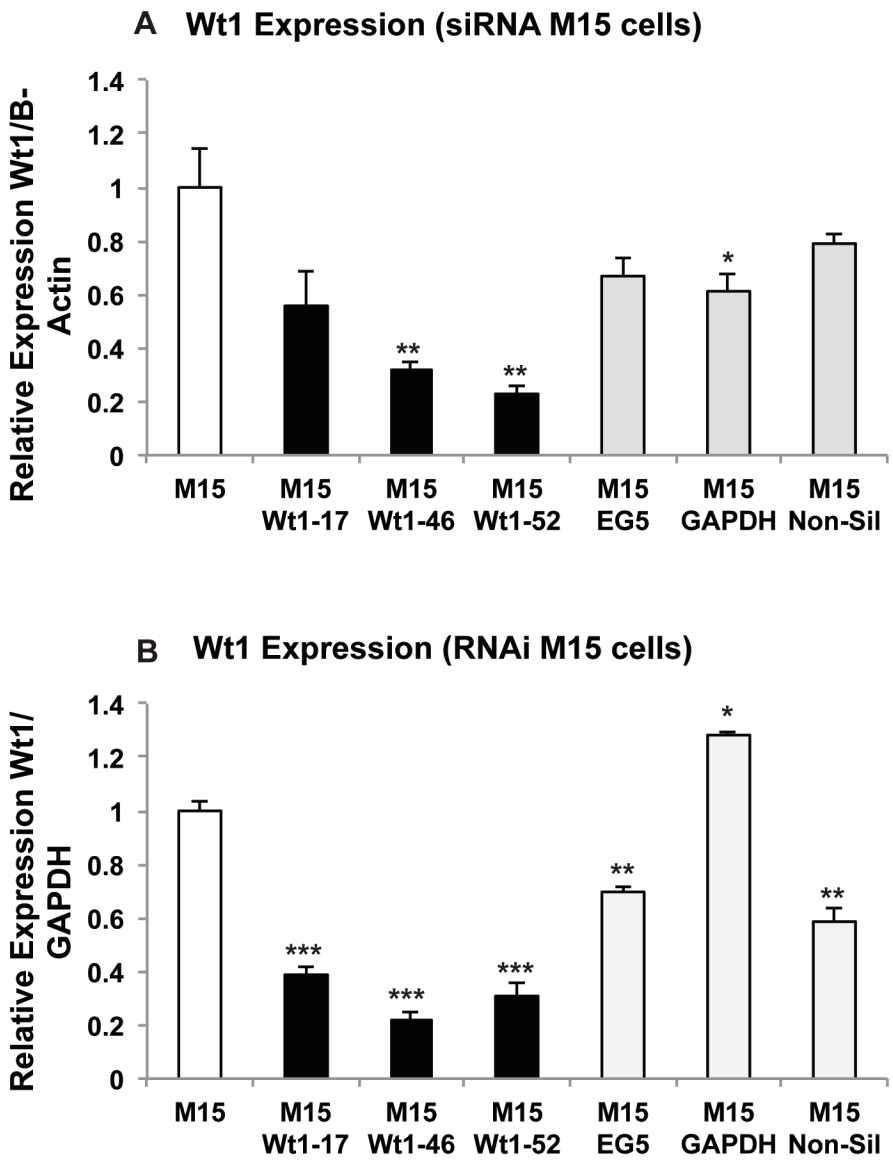

FIGURE 3.22: Q-RT-PCR FOR WT1 EXPRESSION FOLLOWING LENTIVIRALLY MEDIATED RNAI TO M15 CELLS

A) Wt1 expression relative to B-Actin reference: all constructs produce a degree of Wt1 knockdown, which is also significant in the positive GAPDH control. B) Wt1 expression relative to GAPDH reference – although the GAPDH positive control must be ignored, this assay also shows significant knockdown in the other two control constructs. Data bars represent mean Wt1 expression relative to untreated cells. Each experiment was repeated in triplicate (* $p<0.05$; ** $p<0.01$; *** $p<0.001$).

3.4.5 *Putative Wt1-knockdown podocytes are unable to differentiate.*

Although *Wt1* knockdown at the mRNA level could not be demonstrated directly in undifferentiated podocytes, the fact that these cells strongly expressed GFP and were puromycin resistant proved they were effectively expressing shRNA (GFP expression and expression of the shRNA were directly linked in this construct – see Figure 3.16). Extrapolating from the results in M15 cells, in which *Wt1* knockdown was clearly demonstrated, would imply these podocytes would exhibit significant and demonstrable *Wt1* knockdown when differentiated and during differentiation.

In order to test this, equal numbers of cells were plated and thermo-switched to promote differentiation. However, putative *Wt1*-knockdown cells were unable to differentiate. Cells transduced with the non-silencing construct, and wild-type cells, appeared to differentiate normally, with a slowing and cessation of proliferation, enlargement of the cell body, flattening of the cytoplasm and arborisation. In contrast, the cells transduced with the *Wt1*-knockdown constructs demonstrated a clear phenotype after only a few days of differentiation. Rather than flatten and arborize, they remained small and shrunken and underwent cell death and detachment (Figure 3.23).

Following 14 days of differentiation, significantly fewer putative *Wt1*-knockdown cells survived (Figure 3.23 E). After harvesting and extracting RNA from the remaining cells they were analysed for levels of *Wt1* expression (Figure 3.24). Unfortunately, these results again do not demonstrate a loss of *Wt1* in the putative knockdown cells. This may be due to a number of reasons. Firstly, RNA analysis of dead or dying cells is unlikely to be accurate, although too few cells remained for accurate analysis of protein expression. Collecting detached cells from the media was unlikely to address this issue, as these cells would be dead and mRNA expression would not be detectable. Secondly, it is likely the cells that survived had the highest levels of *Wt1* expression so would not be representative of the population as a whole. Ideally protein analysis would be used to verify a loss of Wt1 protein expression, however, as discussed earlier no robust Wt1 antibody was available for Western Blot.

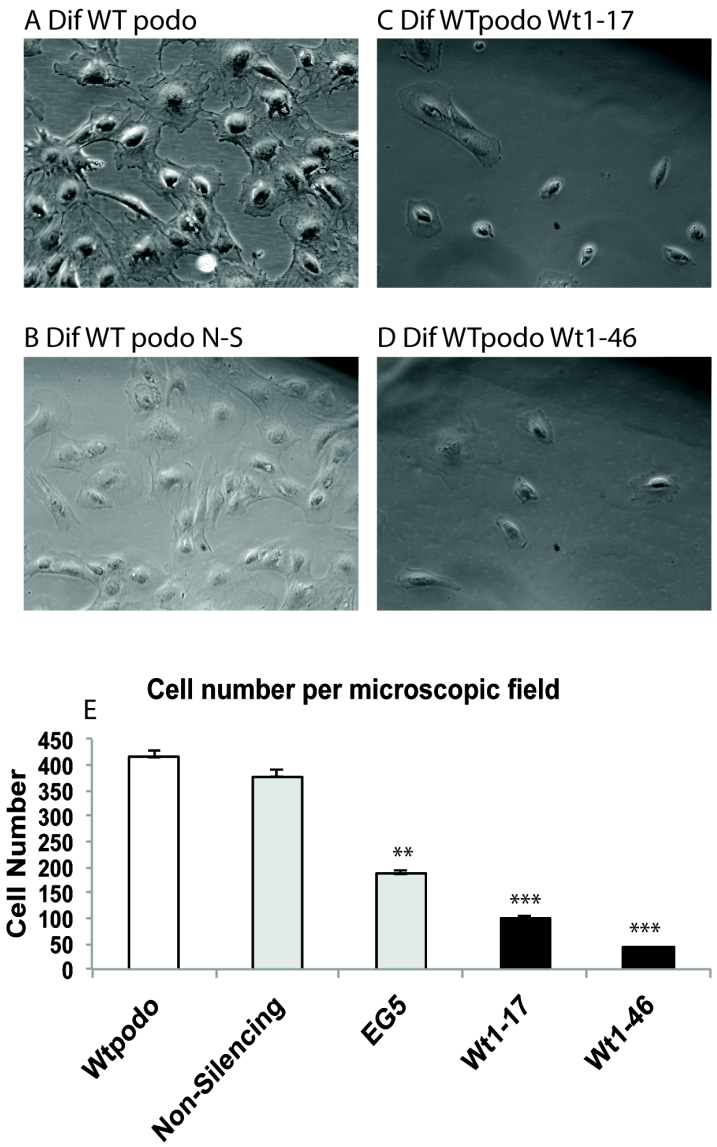

FIGURE 3.23: PUTATIVE *WT1*-KNOCKDOWN CELLS ARE UNABLE TO DIFFERENTIATE

Brightfield imaging of WTpodo cells in culture (magnification x 100). A) & B) Untreated cells and non-silencing siRNA differentiate normally, with flattening, cytoplasmic spreading and arborisation. C) & D) Cells transduced with Wt1 knockdown constructs are unable to differentiate, and detach and die. Images taken on day 9 of differentiation, as too few cells remained at day 14. E) Cell number per x10 magnification microscopic field D14 differentiation. Mean of 10 cell counts per sample (* $p<0.05$; **$p<0.01$; ***$p<0.001$).

Although this phenotype cannot be wholly proven to be as a consequence of *Wt1* knockdown, it is clear these cells are effectively transduced with the lentiviral construct and that in other cell types this leads to effective *Wt1* knockdown. This would imply this phenotype may be explained by Wt1 loss. Certainly, as discussed elsewhere in this thesis, *in vivo* and *ex vivo*, *Wt1* is required for normal podocyte differentiation, which would be in keeping with this result.

However, given the aberrant *Wt1* expression in the positive control cells it was important to repeat this experiment with proper controls that did not significantly affect *Wt1* expression in order to validate these results.

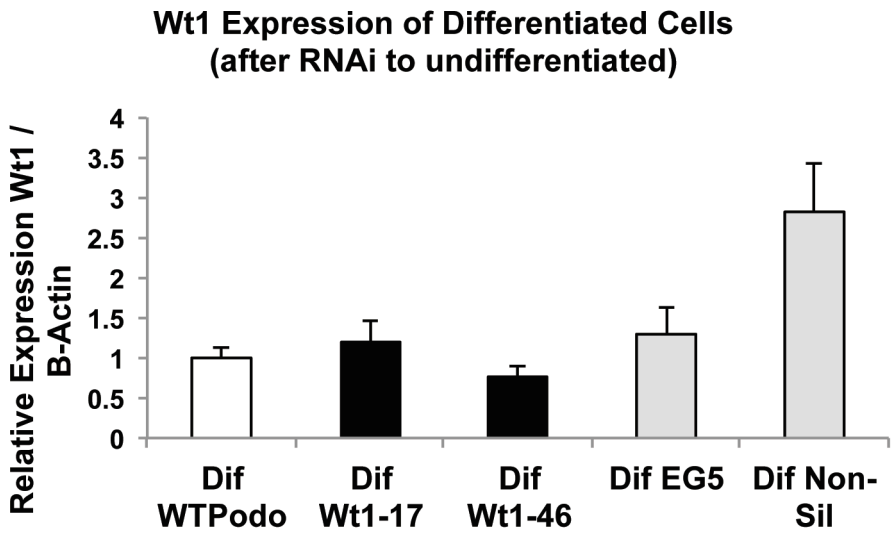

FIGURE 3.24: Q-RT-PCR FOR *WT1* MRNA EXPRESSION FOLLOWING WT1 KNOCKDOWN IN UNDIFFERENTIATED CELLS, WHICH WERE THEN DIFFERENTIATED OVER A PERIOD OF 14 DAYS

Graph represents means of relative expression changes compared to untreated WTpodo cells (arbitrarily assigned a value of 1) of three separate biological replicates of differentiation (each analysed in triplicate). Unfortunately contamination occurred in the cells transduced with Wt1-52 and GAPDH constructs so they could not be analysed. No significant loss of *Wt1* expression is demonstrated.

3.4.6 USING PREVIOUSLY ESTABLISHED WT1-KNOCKDOWN AND CONTROLS IN THE PGIPZ VECTOR TO VALIDATE RESULTS

A quality of the pGIPZ system was the ability to replace the short hairpin RNA construct with an alternative sequence. Transient and effective knockdown of *Wt1* had previously been achieved by the lab using other systems using Wt1 (Wt1-1600) and LacZ control constructs (Rigby, Leitch et al. 2008). Importantly the LacZ control did not affect Wt1 expression, unlike the pGIPZ control vectors.

The Wt1-17, -46 and -52 constructs were replaced by these established constructs by my colleague, Mara Artibani. Correct integration of the construct was verified using restriction digests.

An optimised lentiviral packaging and transduction method was used to test these new constructs on both M15 cells and podocytes (Cockrell, Ma et al. 2006). . In brief, SODK3 packaging cells were used to express trans-lentiviral packaging proteins and GFP from a Tet-off (tTA) system. Following removal of doxycycline from culture media, the cells expressed packaging proteins and GFP, so could be FACS sorted. This would select for the highest expressers of packaging proteins. Activated (GFP positive) cells, were transfected with the lentiviral construct using FuGENE® HD Transfection Reagent. Viral containing supernatant was harvested after 72 hours, for transduction of target cells, using polybrene. Transduced target cells were selected on puromycin for at least one week, before FACS sorting for GFP expression (surrogate marker of shRNA expression), and the top 10% GFP expressing cells (equivalent to maximal expression of shRNA) selected and grown on.

Given the technical demands of podocyte culture, the system was first tested and optimised in M15 cells.

3.4.7 OPTIMISING THE SYSTEM IN M15 CELLS

3.4.7.1 Effective transduction of M15 cells with lentivirus

Following viral transduction and 2 weeks selection on puromycin, M15 cells were FACS sorted for GFP expression (marker of lentiviral expression). FACS analysis revealed efficient transduction of the vast majority of cells and the top 10% were sorted and grown on (Figure 3.25).

3.4.7.2 Effective Wt1 knockdown is achieved in M15 cells

The optimised pGIPZ Wt1-1600 construct achieved 70% reduction in Wt1 expression at the mRNA level in M15 cells (Figure 3.26).

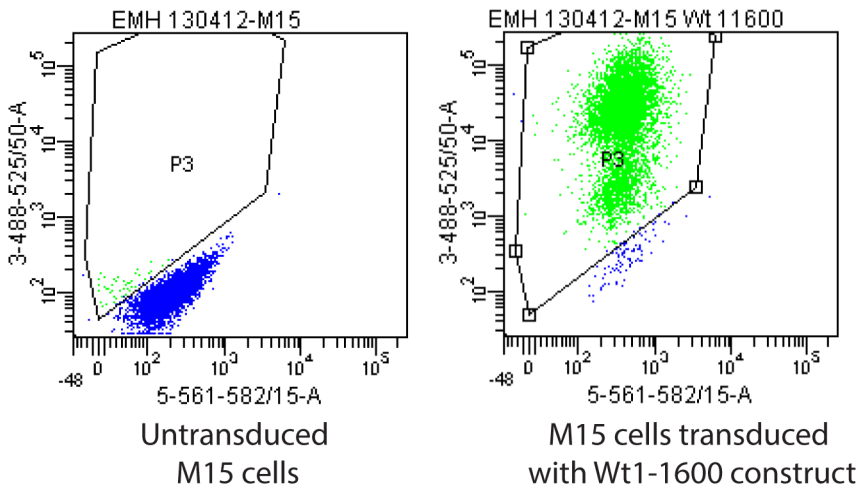

FIGURE 3.25: FACS ANALYSIS FOR GFP EXPRESSION IN TRANSDUCED M15 CELLS

Representative FACS sort for GFP expression of M15 cells transduced with the Wt1-1600 construct. Majority of cells are GFP positive and top 10% GFP expressing cells were sorted to expand for analysis (shown in green).

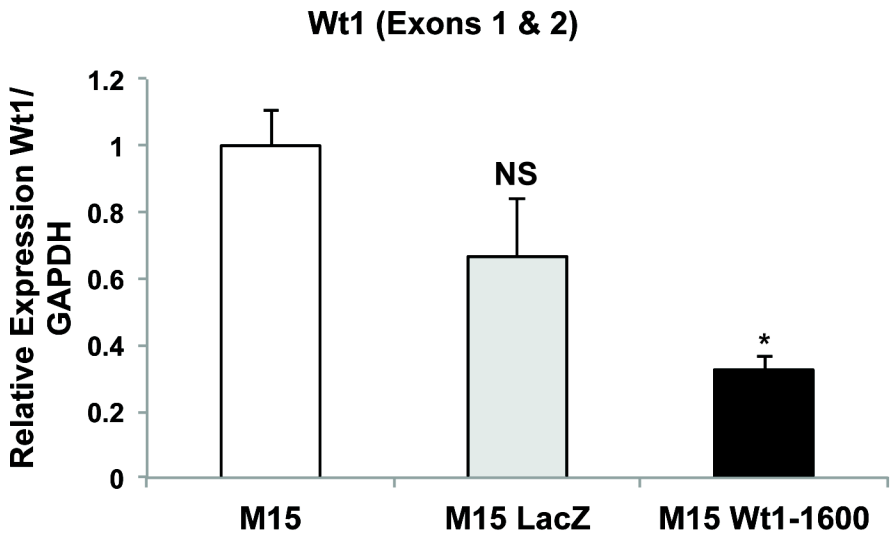

FIGURE 3.26: Q-RT-PCR FOR WT1 MRNA EXPRESSION IN M15 CELLS

Non-significant reduction in Wt1 expression is seen with the LacZ control. A 70% knockdown efficiency (at the mRNA level) is demonstrated with the Wt1 (Wt1-1600) construct (* $p<0.05$; **$p<0.01$; ***$p<0.001$). Graphs represent mean expression (relative to untransduced cells) of two separate biological replicates, each analysed in triplicate.

3.4.8 *Effective Wt1 knockdown is achieved in conditionally immortalised podocytes*

Using the optimised system, undifferentiated podocytes were efficiently transduced with lentivirus. Following viral transduction and 2 weeks selection on puromycin, FACS analysis for GFP expression (as a surrogate marker of shRNA expression) revealed efficient transduction of the majority of cells. The top 10% of GFP-expressing cells were sorted and grown on (Figure 3.27).

Using a different and more sensitive assay (detecting exons 1 and 2) allowed accurately detection of *Wt1* mRNA expression in undifferentiated cells. Therefore, *Wt*1 knockdown could be demonstrated even in undifferentiated cells, consistent with that found in M15 cells (Figure 3.28).

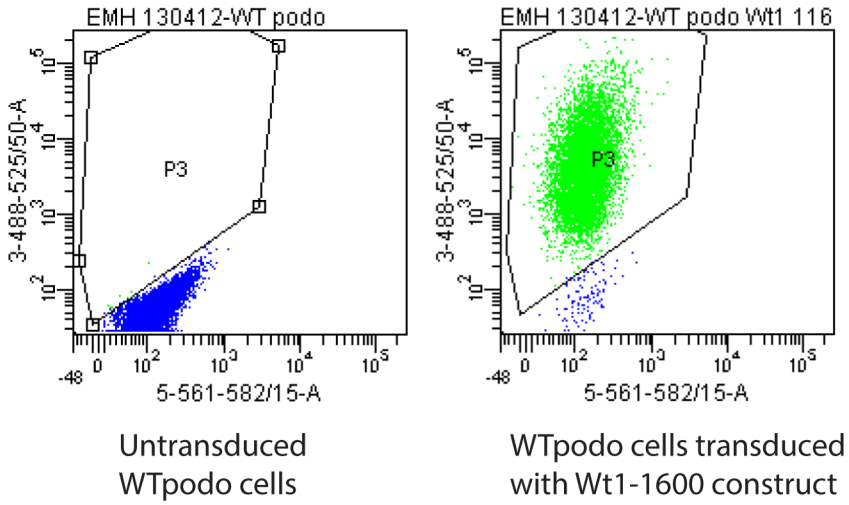

FIGURE 3.27: FACS ANALYSIS FOR GFP EXPRESSION IN TRANSDUCED PODOCYTES

Representative FACS sort for GFP expression of undifferentiated WTpodo cells transduced with the different lentiviral vectors. Majority of cells are GFP positive and top 10% GFP expressing cells were sorted to expand for analysis (shown in green).

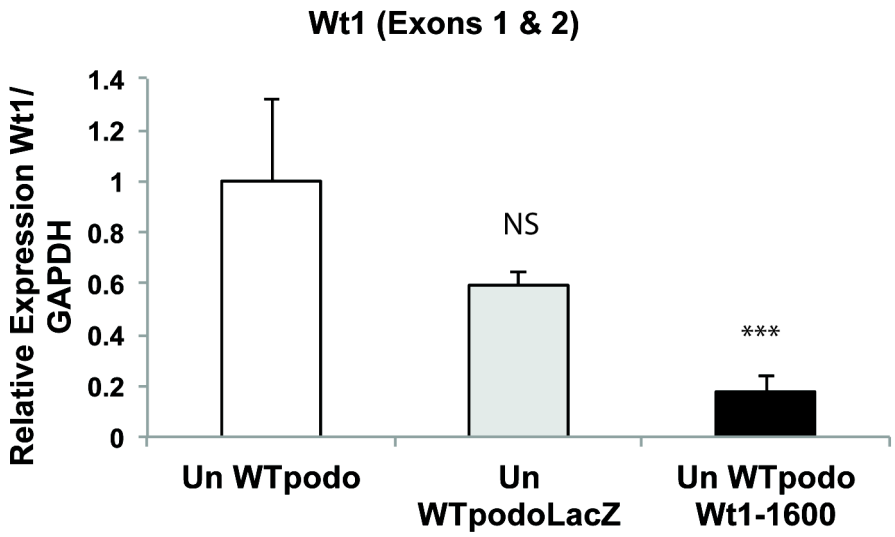

FIGURE 3.28: Q-RT-PCR FOR *WT1* MRNA EXPRESSION IN UNDIFFERENTIATED WTPODO CELLS

Non-significant reduction in *Wt1* expression is seen with the LacZ control. An 80% knockdown efficiency (at the mRNA level) is demonstrated with the Wt1 (Wt1-1600) construct (* $p<0.05$; ** $p<0.01$; *** $p<0.001$). Graphs represent mean expression (relative to untransduced cells) of two biological replicates, each analysed in triplicate.

3.4.9 *WT1 IS REQUIRED FOR DIFFERENTIATION OF CONDITIONALLY IMMORTALISED PODOCYTES IN CULTURE*

Although efficient lentiviral transduction is possible in differentiated cells, this is a difficult system to use as the population cannot be expanded, and the process of transduction requires multiple passages and prolonged culture of terminally differentiated cells, which may encourage phenotypic alterations, senescence and cell death.

Therefore, the best system to study the effects of *Wt1* knockdown in vitro appeared to be stable transduction of undifferentiated conditionally immortalised podocytes, which could proliferate to expand the population and be maintained in culture, yet be differentiated when required.

However, when *Wt1* knockdown podocytes were plated at equivalent density and differentiated over a period of 14 days, they were unable to differentiate. As previously, a marked phenotype was demonstrated in *Wt1* knockdown cells, with failure of normal differentiation cell death and detachment (Figure 3.29).

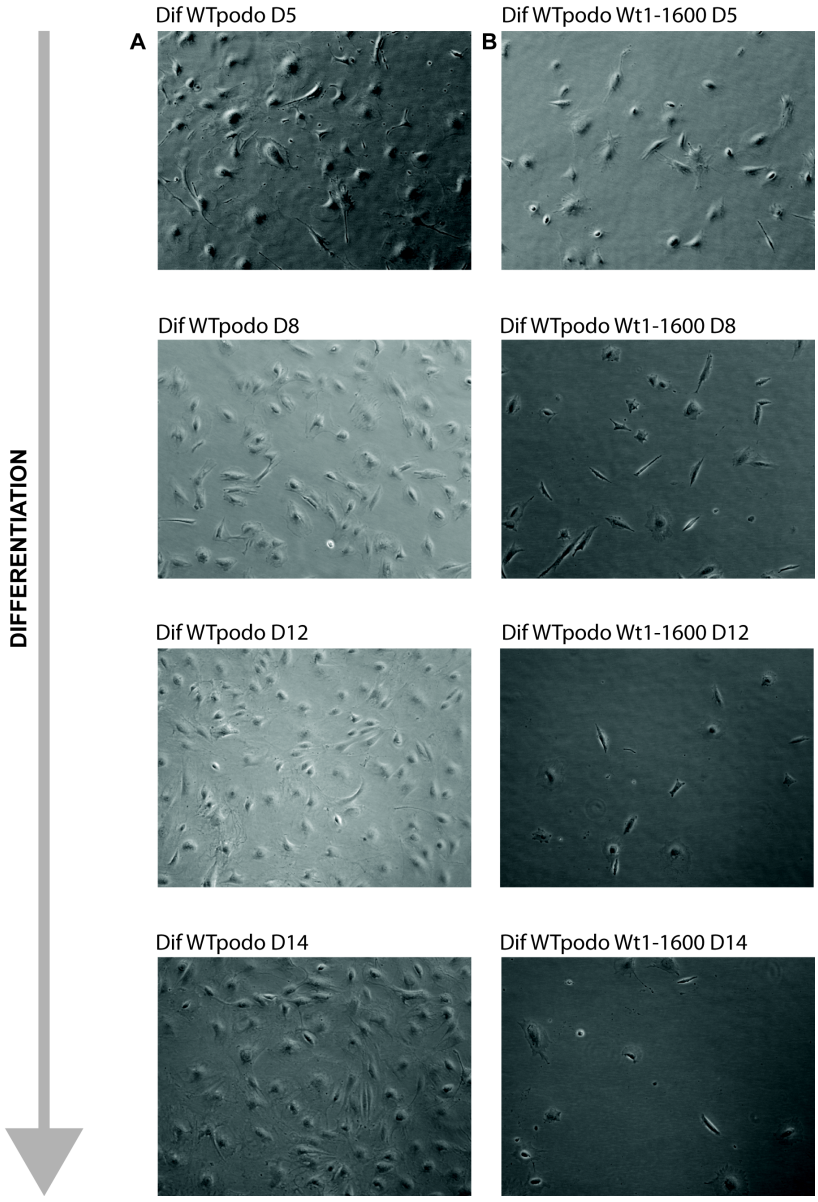

FIGURE 3.29" WT1 KNOCKDOWN PODOCYTES ARE UNABLE TO DIFFERENTIATE

Brightfield images of differentiating Wt1-knockdown podocytes (magnification x100). A) Untreated differentiating WTpodo cells differentiate normally. B) After siRNA mediated Wt1-knockdown in the undifferentiated state, WTpodo Wt1-1600 cells cannot differentiate. They become small, shrunken and detach and die resulting in marked cell loss.

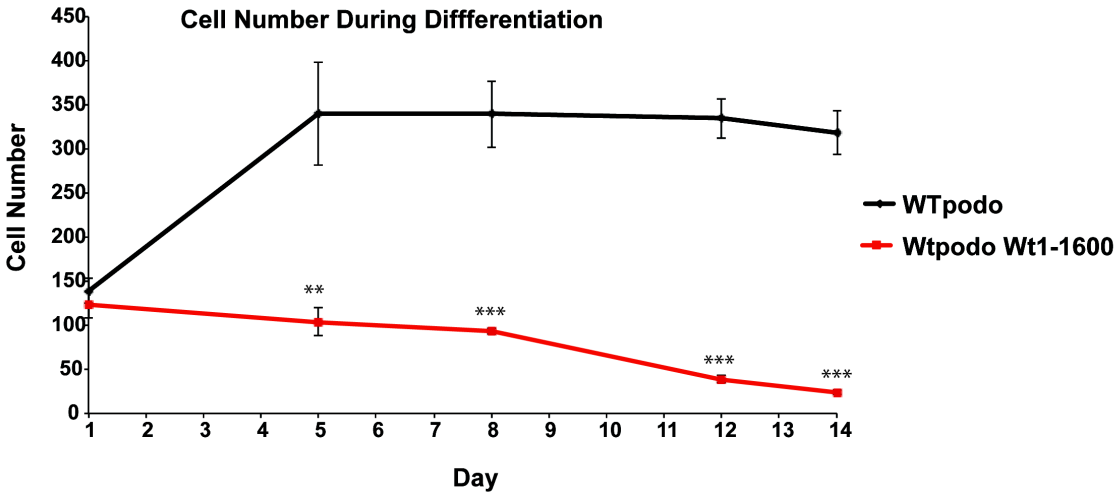

FIGURE 3.30: CELL DEATH OCCURS IN DIFFERENTIATING WT1-KNOCKDOWN PODOCYTES

Cell count per x10 magnification microscopic field over 14 days of differentiation. Each point represents mean of 10 fields of view across two biological replicates (two flasks of differentiating cells) counted (error bars +-SEM * $p<0.05$; ** $p<0.01$; *** $p<0.001$). From as early as day 5, significantly fewer *Wt1* knockdown cells survive, and by day 14 very few remain.

Quantification of these results reveals a significant reduction in cell number as early as day 5 of differentiation (Figure 3.30). By day 14 virtually no Wt1 knockdown cells remain, consistent with the results demonstrated using the original Wt1-17, Wt1-46 and Wt1-52 constructs (see Figure 3.23).

Unfortunately, no control (LacZ) siRNA is available for comparison in this experiment as all replicates of this culture became contaminated (presumably introduced during FACS sorting) so all differentiation replicates were unusable. The whole differentiation experiment could not be repeated within the time available. This means that it is possible the effects on differentiation may be due to RNAi and not a specific Wt1-related effect. Although the effects of two independent *Wt1* knockdown experiments are consistent, and this fits with the published literature, the LacZ siRNA control would be required to unequivocally prove this is not just an siRNA effect. It must be noted, that in the original siRNA experiment, no effect was seen using the Non-Silencing siRNA control (Figure 3.23), implying the lentiviral transduction itself is unlikely to affect differentiation, and although an effect was seen using the EG5 control, it had been demonstrated that this construct also affected *Wt1* expression, which could explain this finding (Figure 3.22).

Thus *Wt1* knockdown conditionally immortalised podocytes are unable to differentiate, and undergo cell death and detachment. This demonstrates a clear phenotype in the context of *Wt1* loss, but unfortunately does not lend itself well to further analysis.

3.5 Conclusion: Summary of experimental findings

3.5.1 CreERWt1$^{co/GFP}$ conditionally immortalised podocytes do not provide a robust model to study the effects of Wt1 loss in podocytes in vitro

Podo32.1 cells (CreER*Wt1*$^{co/GFP}$) appear able to differentiate and become quiescent, and express some key podocyte markers at low levels. However, they only express very low levels of *Wt1*, so the effects of genetic deletion cannot be detected, and this may explain why podocyte markers, particularly nephrin, are only detected at a reduced level in this system.

3.5.2 RNAi can be used to stably knock down Wt1 in podocytes in vitro

Lentiviral mediated RNAi is an effective and flexible method of *Wt1* knockdown. Although possible in differentiated cells, stable transduction of undifferentiated cells allows expansion of the *Wt1* knockdown population to facilitate further analysis.

3.5.3 Wt1 is necessary for differentiation of podocytes in culture

Using a number of independent *Wt1*-knockdown constructs, and lentiviral protocols, *Wt1*-knockdown cells are unable to differentiate in culture, with significant cell loss detected as early as day 5.

3.6 DISCUSSION

3.6.1 CREERWT1$^{CO/GFP}$ CONDITIONALLY IMMORTALISED PODOCYTES DO NOT PROVIDE A ROBUST MODEL TO STUDY THE EFFECTS OF WT1 LOSS IN PODOCYTES IN VITRO

Genetic methods of *Wt1* deletion have not been possible, as the Podo32.1 cell line generated from the CreER*Wt1*$^{co/GFP}$ mouse did not provide a robust model to study the effects of *Wt1* loss *in vitro*. Although this would have been the ideal system to complement the *in vivo* model, thorough analysis revealed it did not recapitulate the *in vivo* situation. This line expressed only low levels of *Wt1*. Most importantly, changes in *Wt1* expression levels following genetic deletion could not be detected. This could have been for a number of reasons:

1) As a consequence of compound heterozygosity in an isolated cell system

   Although *Wt1*-heterozgosity *in vivo* has not been shown to markedly affect the amount of Wt1 protein (see earlier), these cells were cultured in isolation, which may have affected the normal or compensatory levels of *Wt1* expression.

2) As a consequence of low level Cre-activity in the absence of tamoxifen induction.

   As demonstrated earlier, there was evidence of Cre-recombination events and therefore *Wt1*-deletion occurring at the DNA level, even in control (vehicle treated) cells. This may account for a reduction in *Wt1* expression across the population. However, this assay also clearly demonstrates the persisting presence of the conditional allele, so this effect can only be partial.

3) Due to reduced *Wt1* expression in culture

   As previously discussed, prolonged culture of primary podocytes results in a reduction in *Wt1* expression. Although the number of passages was limited to less than 20, this may have affected the levels of *Wt1* expression in the Podo32.1 cells, especially in the context of compound heterozygosity and low-level, 'leaky' Cre-recombination. Evidence supporting this is demonstrated by the loss

of GFP expression in culture, which was noted to be present microscopically when the cell line was generated.

As discussed earlier, the use of conditionally immortalised podocytes in culture offers a useful tool to dissect the mechanisms of podocyte biology. However, a number of limitations exist in this system, and it is debatable how closely the behaviour of podocytes in culture recapitulates the complex interactions and glomerular 'cross-talk' *in vivo*. Nevertheless, when used in combination with the *in vivo* model, a robust *in vitro* model of *Wt1* loss in podocytes would have provided a valuable complementary tool to analyse the mechanistic consequences and effects of *Wt1* loss, as well as helping to limit the number of animal experiments.

No analysis of the functional consequences of these findings was undertaken, as podocytes in culture exhibit only partially the functions of podocytes *in vivo*. Albumin influx assays have been used to analyse the effectiveness of podocytes as part of the glomerular filtration barrier (Li, Kang et al. 2008, Herman-Edelstein, Thomas et al. 2011). However, given that podocytes should not reach confluency when differentiating (Shankland, Pippin et al. 2007) these methods are probably artificial, and were unlikely to add further useful information given the complementary *in vivo* system.

3.6.2 RNAi can be used to stably knock down Wt1 in podocytes in vitro and Wt1 is necessary for differentiation of podocytes in culture

Wt1 can be knocked down in podocytes using siRNA, which offered an alternative *in vitro* model of *Wt1* loss, especially as stably transduced cells can be produced. Using different *Wt1* knockdown constructs, these cells all exhibited the same phenotype, and were unable to differentiate in culture. In both murine podocyte cell lines analysed, as well as in previously published work, *Wt1* expression increases with differentiation, and *in vivo*, the differentiated adult podocyte continues to express high levels of *Wt1 (Miller-Hodges and Hohenstein 2012)*. As discussed earlier, *WT1* mutations lead to human diseases such as DDS in which the podocytes are abnormal. This finding supports the assumption that *Wt1* is critical for podocyte differentiation, which has not yet been demonstrated conclusively *in vivo*.

A limitation of this work is the lack of a conclusive control to demonstrate the effects of differentiation are purely as a consequence of *Wt1* loss. No general siRNA effect could be seen in the Non-Silencing control, which supports the conclusion that this effect is due to loss of *Wt1*. Although the consistency of this data in two entirely separate scenarios offers validation, ideally repetition of the differentiation experiments to include the positive LacZ control would be undertaken.

Rescue experiments to replace Wt1 and conclusively demonstrate this phenotype was due to *Wt1* loss would be extremely difficult given the complexity of *Wt1* isoform expression and the lack of available data regarding the relative expression of the different isoforms during kidney development and in adult podocytes,. A further challenge would be the fact that Wt1 effects appear to be extremely dose-sensitive. Heterozygous mice express up to 95% of wild type Wt1 RNA levels yet develop glomerulosclerosis at 6 months of age and rescue of the Wt1-null phenotype using a Yeast Artificial Chromosome containing the human WT1 gene lead to different effects (crescentic glomerulonephritis versus mesangial sclerosis) depending on gene dosage (Guo, Menke et al. 2002).

As *Wt1* knockdown cells cannot differentiate, their analysis can only be limited, as it is only in the differentiated state that they are thought to most closely resemble actual podocytes (Shankland, Pippin et al. 2007). As demonstrated, lentiviral siRNA can also be used in differentiated cells, but the transduction method appears to affect the phenotype of these

quiescent, differentiated cells, which should not be maintained for prolonged periods in culture. Differentiated cells cannot be maintained or expanded in culture so their use is also limited.

Therefore, using an inducible lentiviral vector, which can be used to transduce undifferentiated cells to provide a stable population, yet can then be induced once cells have differentiated, provides the ideal solution to this problem. The Thermo Scientific TRIPZ shRNAmir construct allows tightly regulatable RNAi in cell systems, and shRNA expression can be induced by tetracycline over a period of 48-72 hours. Cloning of the Wt1-1600 and LacZ control constructs into the TRIPZ vector has been undertaken by my colleague, Mara Artibani. These inducible constructs would provide a stable means of *Wt1* knockdown in podocytes that have already differentiated, facilitating detailed mechanistic analysis of the consequences of *Wt1* loss, most importantly in terms of regulation of key podocyte genes, and alterations of cell architecture, especially with regard to the epithelial-mesenchymal characteristics of the cells.

3.7 Concluding Remarks

These experiments have had only partial success in generating an in vitro model of *Wt1* loss as the *CreER*Wt1$^{co/GFP}$ line did not behave as expected. However, successful lentiviral mediated RNAi to knock down *Wt1* was achieved, confirming the need for *Wt1* for successful podocyte differentiation in culture.

Development of this methodology, using an inducible shRNA construct, will allow more detailed analysis of this phenotype, especially with regard to the effects of Wt1 loss on the expression of key podocyte proteins, on cell structure and on the epithelial-mesenchymal balance.

4 *Wt1* IS CRITICAL FOR GLOMERULAR FUNCTION IN ADULT KIDNEY

4.1 INTRODUCTION

WT1 plays an essential role in renal development, where it controls the process of mesenchymal to epithelial transition that forms the nephron. This is at least in part through transcriptional regulation of *Wnt4* (Stark, Vainio et al. 1994, Kispert, Vainio et al. 1998, Davies, Ladomery et al. 2004, Rigby, Leitch et al. 2008). Indeed, the eponymous Wilms' Tumour, in which *WT1* mutations account for 15-20% of cases, is thought to arise from a failure of normal differentiation during kidney development. (Coppes-Zantinga and Coppes 1999). *WT1* mutations also cause a number of developmental syndromes affecting the kidney, including Denys-Drash Syndrome, which leads to diffuse mesangial sclerosis and abnormal podocyte function and Frasier Syndrome, which usually causes FSGS.

In adult life the main site of *WT1* expression is the podocyte, where its role is not well understood. Models to study the role of *WT1* in adult podocytes have been limited, due to the renal agenesis phenotype and embryonic lethality of the *Wt1*-null mouse (Kreidberg, Sariola et al. 1993). The *Wt1*-heterozygote mouse exhibits a seemingly normal phenotype at birth and during early life, with no evidence of glomerular dysfunction, but develops albuminuria and glomerulosclerosis as it ages. 80% of *Wt1*-heterozygotes develop severe glomerulosclerosis by 400 days old (Menke, A et al. 2003). This implies a continuing role for *Wt1* in the adult kidney, but cannot exclude the development of glomerulosclerosis as a consequence of an undetected developmental effect. A number of animal models of Denys-Drash Syndrome, carrying human DDS *Wt1* mutations, are also available. These exhibit similar phenotypes to the human disease and confirm the significance of *Wt1* mutations in the development of this condition. However, as with the actual human syndrome, the renal phenotype has also been affected by abnormal *Wt1* expression throughout development as well as in the adult kidney.

Therefore, this project, which utilised a *Wt1*-conditional mouse in order to delete *Wt1* only in adult tissue, would offer a unique opportunity to analyse the role of *Wt1* solely in adult kidney, whilst avoiding any confounding developmental effects.

4.2 AIMS

The aims of the experiments described in this chapter were:

- To delete *Wt1* from fully differentiated adult podocytes *in vivo*
- To analyse the effects of *Wt1* deletion on podocytes, and any consequences on other cells of the kidney
- To compare the effects of *Wt1* deletion with other causes of podocyte injury
- To draw conclusions as to the specific role of *Wt1* in the differentiated podocyte, particularly with regard to the epithelial-mesenchymal balance

4.3 EXPERIMENTAL APPROACH

The tamoxifen-inducible *Wt1*-conditional mouse had already been generated in the laboratory and was available for further analysis of the renal phenotype (Martinez-Estrada, Lettice et al. 2010). Preliminary analysis of the effects of *Wt1*-deletion had already been carried out and was published during the course of this project (Chau, Brownstein et al. 2011). This had used a relatively high dose of tamoxifen (4mg/40g body weight for 5 days IP) in comparison to other work in the literature (Hayashi and McMahon 2002, Wang, Wang et al. 2010). Using this high dose of tamoxifen resulted in phenotypes in multiple tissues, including fat, bone, blood and pancreas, as well as kidney. The mice were rendered moribund by 7-10 days so had to be euthanased for humane reasons. This rapid and severe phenotype was therefore poorly amenable to detailed analysis.

Consequently, a 'low-dose' experimental protocol was devised, in which mice would be injected with tamoxifen at 1mg/40g, initially for 5 days. This would reduce the number of Cre-recombination events, with the aim of ameliorating the phenotype (Hayashi and McMahon

2002). As this dosing regimen had not been tested before, this model would be optimized prior to use (Figure 4.1).

CreER+Wt1$^{co/co}$ mutant mice were paired with *CreER-Wt1*$^{co/co}$ sex-matched, litter-mate controls. Both control and mutant mice would be injected with tamoxifen, to ensure any resulting phenotype was not a consequence of tamoxifen toxicity. Animals aged between 16 and 24 weeks were used.

Full characterisation of the clinical phenotype over time would be undertaken, focused on the renal consequences of *Wt1*-deletion. Although other work in the lab had demonstrated a variety of extra-renal effects in this mouse model, the high level of *Wt1* expression in the kidney, and the known consequences of *Wt1*-deletion and/or mutations on renal development, made it seemed unlikely these would be significantly influenced by the extra-renal phenotypes.

However, this project also included the generation of an inducible podocyte-specific Cre line, containing a podocyte specific reporter (Podocin-GFP-CreERT2: see Chapter 5). By crossing this model with the *Wt1*-conditional mouse, *Wt1* deletion would be limited to the podocyte avoiding any extra-renal effects (Figure 4.2). In conjunction, generation of an in vitro model of *Wt1* loss would facilitate detailed and mechanistic analysis of the role of *Wt1* in the podocyte, with the aim of confirming the *in vivo* findings.

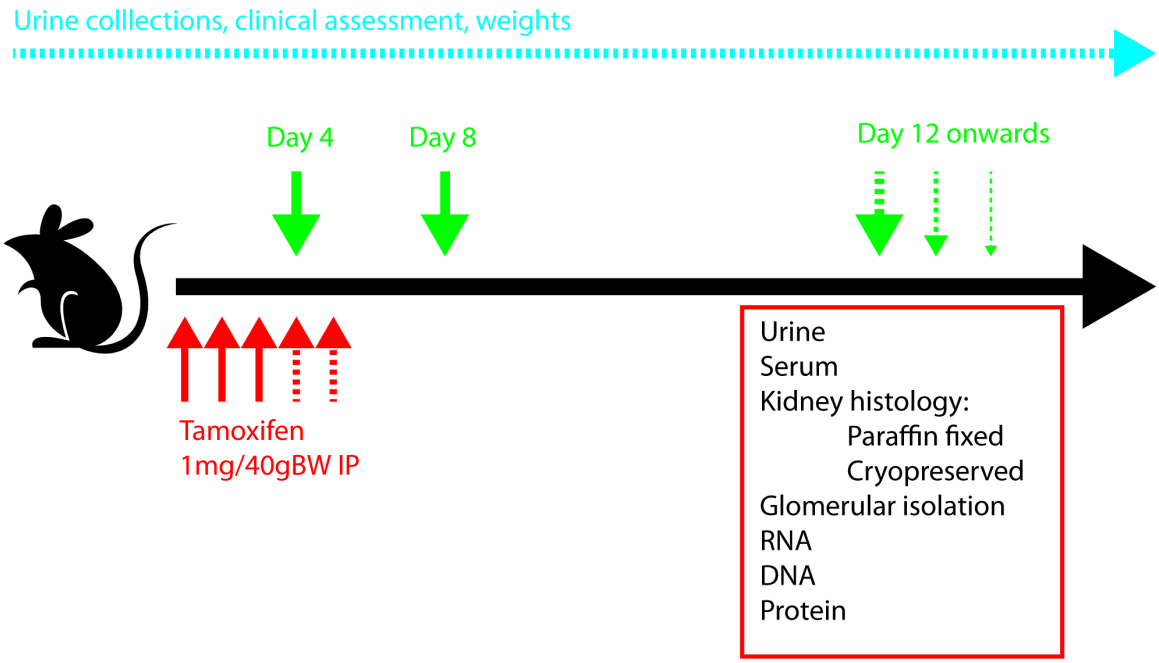

FIGURE 4.1: EXPERIMENTAL TIMELINE

Mutant and control mice would be injected with tamoxifen 1mg/40g BW as depicted. Initial analysis would follow mice until they required culling for humane reasons (day 12+). Analysis of subsequent experimental groups would be at fixed time points, depending on the disease-free survival analysis. Mice would be inspected daily for signs of distress and urine collected throughout the experimental time-course. After mice were sacrificed, serum and tissue would be collected as detailed.

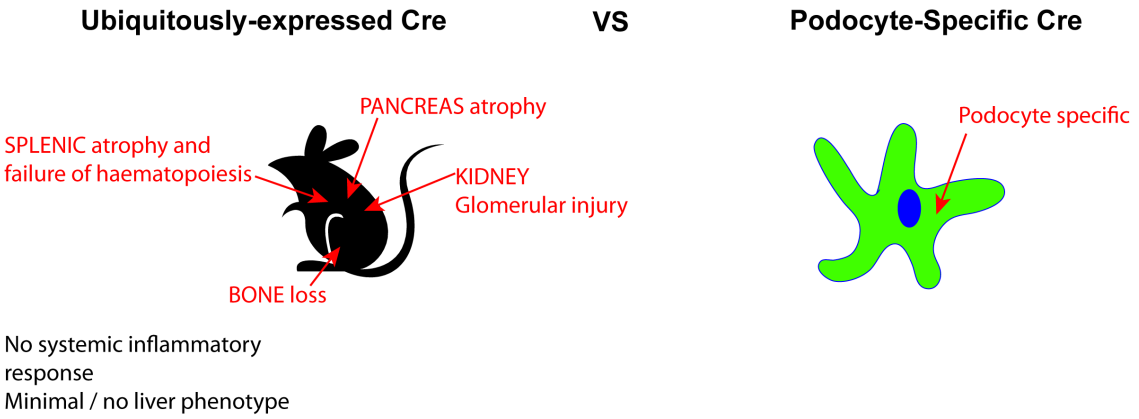

FIGURE 4.2: UBIQUITOUSLY-EXPRESSED VS PODOCYTE-SPECIFIC CRE LINES

Cartoon comparing the existing *Wt1*-conditional model using a ubiquitously expressed Cre, which exhibited extra-renal effects when injected with high doses of tamoxifen, with a podocyte-specific Cre in which *Wt1*-deletion would be limited to the podocyte

In addition to the tamoxifen-inducible *Wt1*-conditional mouse, other models would be used (Figure 4.3). The *CreERWt1*$^{co/GFP}$ mouse carries one conditional allele and one allele containing a GFP-knock-in into exon one of *Wt1* (Hosen, Shirakata et al. 2007). This faithfully expresses GFP at the sites of active *Wt1* expression. This model would facilitate identification of podocytes, which would continue to be labeled with GFP after *Wt1* deletion. However, this model expresses GFP in a dynamic fashion, as expression depends on *Wt1*-promoter activity, so would be 'switched off' if *Wt1* gene expression stopped. Stability of the GFP protein would mean this switch would not be instantaneous. It must also be noted that this is not a tagged GFP protein so produces no functional *Wt1* and is not specifically localized within the cell. As a consequence of the GFP knock-in, these animals would be compound heterozygotes for *Wt1*. However, previous work suggests that *Wt1*-heterozygote or compound heterozygote animals continue to express sufficient *Wt1*-protein and are free of renal disease until 6 months of age (Menke, A et al. 2003, Martinez-Estrada, Lettice et al. 2010).

In order to control for any effects due to 'Cre-toxicity' (Loonstra, Vooijs et al. 2001) separate controls were also generated which were Cre positive but with no conditional allele: *CreERWt1*$^{+/+}$. Both Cre-positive and Cre-negative (wild-type) age and sex matched littermates were analysed separately, to ensure Cre-recombinase activity did not account for the observed phenotype.

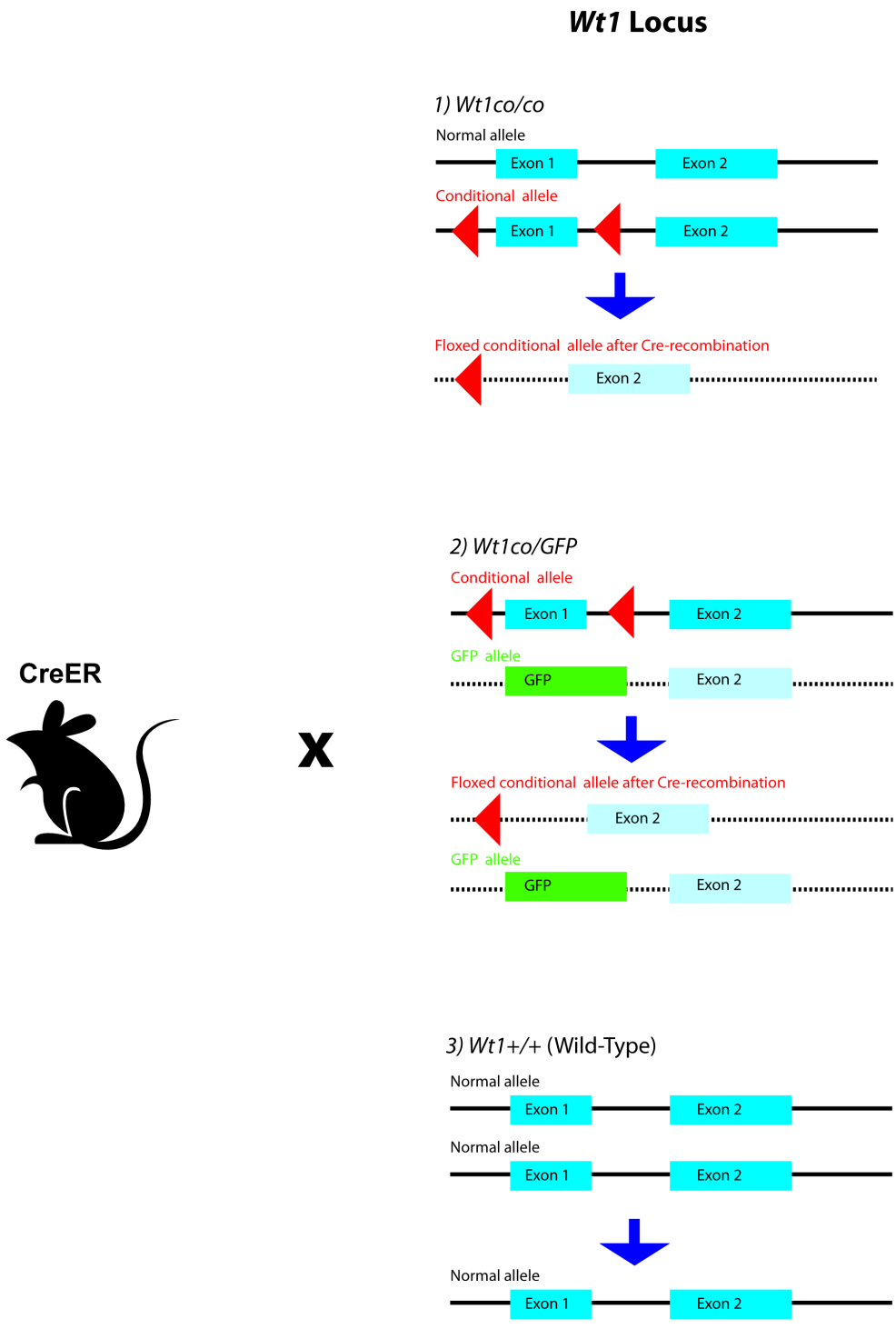

FIGURE 4.3 MOUSE MODELS USED IN THE ANALYSIS OF WT1 DELETION IN THE ADULT

Figure 4.3: Mouse models used in the analysis of Wt1 deletion in the adult

1) *CreERWt1*$^{co/co}$: Exon one of both alleles is flanked by two LoxP sites, facilitating homozygous deletion of *Wt1* following Cre-recombination. 2) *CreERWt1*$^{co/GFP}$: One *Wt1* allele contains the conditional allele and the other a GFP knock-in allele. This allows expression of GFP at sites of active *Wt1* expression. Following Cre-recombination, *Wt1* is deleted from the conditional allele, although GFP expression can continue if *Wt1* promoter activity continues. 3) *CreERWt1*$^{+/+}$ (wild-type): Control line to ensure no effect of Cre-toxicity. Contains normal *Wt1* alleles so Cre-activity should exert no effect.

A number of podocyte-injury models have already been published which result in varying degrees of glomerular damage and albuminuria (Wharram, Goyal et al. 2005, Mollet, Ratelade et al. 2009, Matsusaka, Sandgren et al. 2011). Analysis of the renal phenotype in these models has included serum and urinalysis, renal histology and the changes in expression of key podocyte proteins. Similar methods would be used in order to analyse the renal consequences of *Wt1* deletion in the adult. These would include:

- Survival
- Clinical phenotype: Renal function (in terms of serum urea and creatinine), serum albumin, oedema
- Function of the glomerular filtration barrier: albuminuria
- Histological damage
- Loss of podocyte proteins
- Loss / detachment of podocytes
- Changes in the epithelial-mesenchymal balance in podocytes

When describing the experimental results the following terminology will be used:

CONTROL – Cre-negative $Wt1^{co/co}$ or $Wt1^{co/GFP}$

MUTANT – Cre-positive $Wt1^{co/co}$ or $Wt1^{co/GFP}$

Cre+ CONTROL – Cre-positive $Wt1^{+/+}$

Wild type CONTROL – Cre-negative $Wt1^{+/+}$

UNINJECTED - Cre-positive $Wt1^{co/co}$ or $Wt1^{co/GFP}$ not injected with tamoxifen

4.4 OPTIMIZING THE ANALYSIS OF *WT1*-DELETED KIDNEYS

In order to analyse the effects of *Wt1* deletion, a number of approaches would be used.

RNA, DNA and protein extraction from whole kidney cortex was quick and straightforward, and provided plentiful experimental material. Despite the fact that podocytes only contribute a small proportion of the kidney tissue, Quantitative RT-PCR would provide a sensitive enough tool to detect any differences between control and mutant animals (Heid, Stevens et al. 1996).

In order to control for any effects in other renal cell types, analysis of isolated podocytes was required to ensure the experimental findings reflected the effects in podocytes themselves. The main methods of podocyte isolation are glomerular sieving or using magnetic beads (Dynabeads) to isolate de-capsulated glomeruli, highly enriched for podocytes (Takemoto, Asker et al. 2002, Shankland, Pippin et al. 2007).

Unfortunately, previous attempts in the lab to introduce the Dynabead system technique did not prove robust or successful, so glomerular sieving was utilized. This provided a tissue sample highly enriched for podocytes. Microscopic inspection of the sieved sample demonstrated the presence of glomeruli, and analysis of podocyte marker expression using quantitative RT-PCR demonstrated these specimens were highly enriched for podocytes in comparison to whole kidney cortex (Figure 4.4). However, this method was lengthy and provided only limited experimental tissue (e.g. 1-2µg RNA), so both kidneys from each experimental animal needed to be used to generate sufficient sample material. Animal numbers were limited during the time frame of this project, given that separate histological specimens also needed to be acquired. When attempting to follow animals until later time points, some died unexpectedly, meaning that RNA extraction was not possible so these could not be analysed at all. This has limited the n-numbers at each time point.

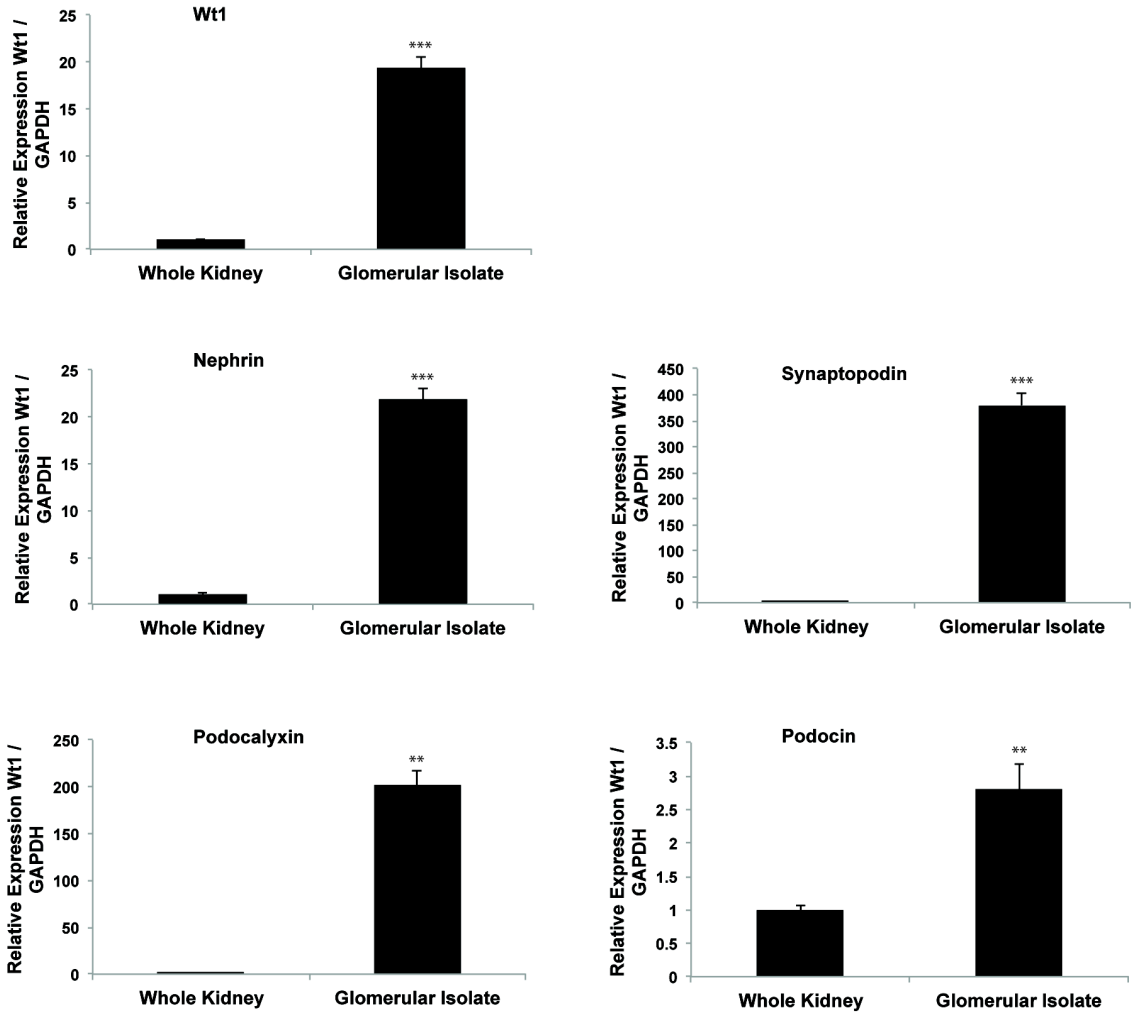

FIGURE 4.4: QUANTITATIVE RT-PCR OF MRNA EXPRESSION OF MAJOR PODOCYTE GENES IN KIDNEY CORTEX AND ISOLATED GLOMERULI.

RNA was extracted from kidney cortex and isolated glomeruli from wild-type (CD1) animals. Significantly increased expression is seen in seen in the glomerular isolates in comparison to whole kidney, confirming that the podocyte population was highly enriched. Data points represent fold-change difference to kidney cortex (arbitrarily assigned a value of 1). (* $p<0.05$; ** $p<0.01$; *** $p<0.001$).

FACS has also been used to specifically isolate fluorescently labeled podocytes to allow analysis of a pure podocyte population (Sison, Eremina et al. 2010). Using the *CreERWt1*$^{co/GFP}$ model, all Wt1-expressing podocytes are labeled with GFP. This would facilitate isolation of a pure GFP-positive podocyte population for analysis. A number of methods of tissue lysis and cell sorting were tried (see Materials and Methods), in order to attempt to generate a single cell suspension for FACS, but these were unsuccessful, with few or no fluorescent cells identified. This was perhaps due to podocyte damage occurring during the lengthy protocols or during the tissue lysis required to generate a single cell suspension.

Towards the end of the project a new protocol, adapted from Susan Quaggin's laboratory was tried which successfully isolated GFP-positive podocytes (Welsh, Hale et al. 2010). However, only a few thousand podocyte cells could be isolated from a single animal, limiting the amount of tissue available for analysis. The results using this method do not form part of this thesis, as it was used on too few samples in the time available. However, this will be used for future work to specifically analyse *Wt1*-deleted podocytes in isolation.

4.5 USING A LOW DOSE TAMOXIFEN PROTOCOL TO DELETE *WT1* IN THE *CREERWT1*$^{co/co}$ MODEL

As discussed above, a novel protocol using a low-dose of tamoxifen, in order to reduce the number of Cre-recombination events to attempt to ameliorate the severe phenotype, was used.

A dose-response to tamoxifen had previously been demonstrated in the literature (Hayashi and McMahon 2002). In order to confirm this effect specifically in the kidney, this was tested *in vivo* using the CreER line crossed with a *Rosa26R*$^{YFP/YFP}$ reporter (*CreERR26R*$^{YFP/YFP}$) (Srinivas, Watanabe et al. 2001). Cre-recombination would result in permanent expression of YFP in cells in which Cre had been active, which could then be quantified.

CreERR26R$^{YFP/YFP}$ mice were injected with tamoxifen at either 4mg/40g bodyweight or 1mg/40g bodyweight for 5 days and sacrificed on day 14. Kidneys were fixed and analysed for YFP expression (using an anti-GFP antibody). No ill effects were noted in either the Cre-positive or Cre-negative animals.

Analysis of the differing tamoxifen dosing regimens confirmed a reduced level of Cre-recombination (i.e. Cre was active in a lower percentage of cells with the lower dose) although significant levels were still achieved (Figure 4.5). An average of 98% of glomerular cells in the 4mg model stained positive for GFP, compared with 65% in the 1mg model.

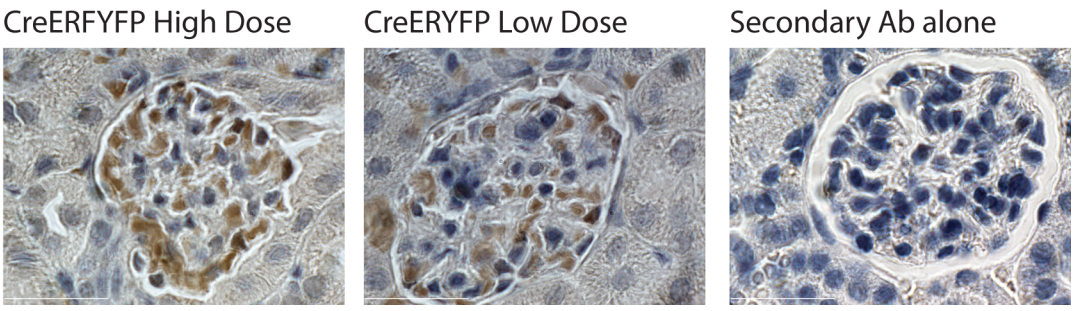

FIGURE 4.5: TESTING THE EFFICIENCY OF CRE-RECOMBINATION IN THE KIDNEY USING DIFFERENT DOSES OF TAMOXIFEN

A) IHC for YFP expression: The majority of cells in the high dose animals were YFP positive (calculated by counting YFP positive area per dapi-stained cell nucleus), with a Cre-recombination efficiency of 98% (Range 88-100%. YFP positive cells / Total cells per glomerulus. N=2). B) IHC for YFP expression: fewer cells in the low dose animals were YFP positive, with Cre-recombination efficiency of 65% (Range 48-83%. YFP positive cells / Total cells per glomerulus. N=2). Mosaic Cre-recombination was achieved by reducing the tamoxifen dose.

Initial analysis was carried out in parallel with a pilot experiment in which *CreERWt1*$^{co/co}$ mice were injected with the low-dose protocol (tamoxifen 1mg/40g bodyweight for 5 days) and followed until they deteriorated.

The initial pilot group of mice injected with the low dose tamoxifen regimen, over 5 days, survived more than a month. At which point they became hunched, oedematous and unwell, so had to be euthanased for humane reasons. However, the next group of animals became unwell as early as day 12 (Figure 4.6). This was more typical of subsequent experiments and the prolonged survival of the original group was never repeated. In order to try and analyse the phenotype over time the dose was cut still further.

The same dosing protocol was also used with *CreERWt1*$^{co/GFP}$ mice, whose phenotype appeared even more severe as they became oedematous and moribund as early as day 8. This experiment was carried out in metabolic cages.

In both cases control (*CreER-Wt1*$^{co/co}$ and *CreER-Wt1*$^{co/GFP}$) littermates exhibited no ill-effects and remained completely healthy.

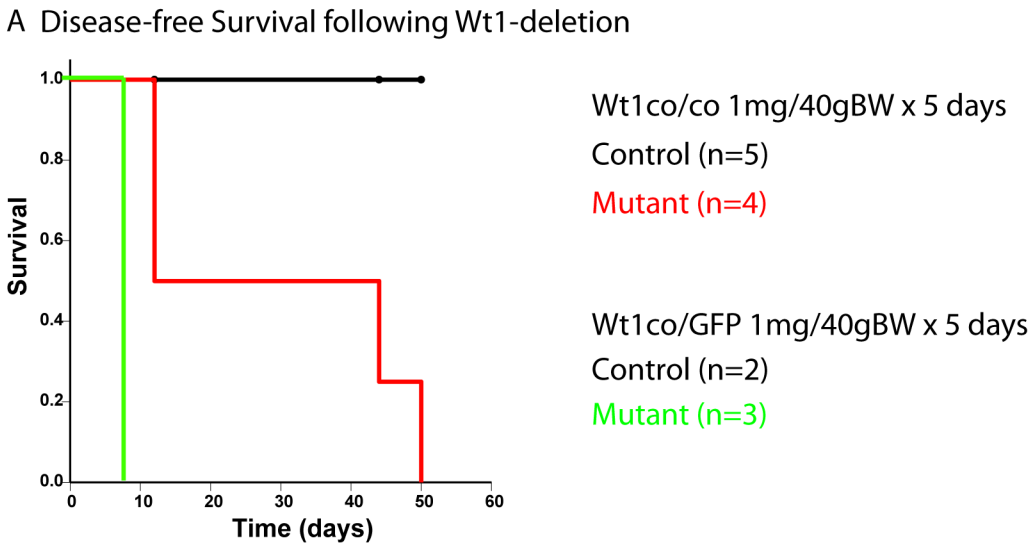

FIGURE 4.6: DISEASE-FREE SURVIVAL FOLLOWING WT1 DELETION, USING TAMOXIFEN AT 1MG/40G BODYWEIGHT FOR 5 DAYS, IN *CREERWT1*$^{CO/CO}$ AND *CREERWT1*$^{CO/GFP}$ MICE

Both control (*CreER-Wt1*$^{co/co}$ or *Wt1*$^{co/GFP}$) and mutant (*CreER+Wt1*$^{co/co}$ or $^{co/GFP}$) mice were injected with tamoxifen at 1mg/40g bodyweight for 5 days and followed until they had to be euthanased for humane reasons. Mean disease-free survival of *Wt1*$^{co/co}$ mutant animals was 29.5 days (range 12-50 days), and 8 days in *Wt1*$^{co/GFP}$ animals. A) In the initial pilot experiment (control n=3, mutant n=2) mutant mice survived up to day 50 (mutant male d50, mutant female d44), and control mice remained healthy. However, in the next cohort (control n=2; mutant n=2) the mutant animals became unwell on day 12 requiring euthanasia. These mice were kept in metabolic cages, which may have exacerbated the phenotype (see later). *CreERWt1*$^{co/GFP}$ mice required euthanasia even earlier on day 8. Again, these mice were housed in metabolic cages.

4.5.1 Using a very low dose tamoxifen protocol to delete *Wt1* in the *CreER Wt1*$^{co/co}$ model

As both dose and dosing schedule had been shown to affect the efficiency of Cre-recombination (Hayashi and McMahon 2002) the tamoxifen dosing schedule was reduced further to three days (1mg/40g bodyweight x 3 days) in order to try and promote survival, to allow more detailed analysis of the phenotype (Figure 4.7).

As before, *CreERWt1*$^{co/co}$ mice were injected with the very low dose regimen (1mg/40g bodyweight x 3 days) and followed until they became unwell. These mice survived between 15 and 23 days (Mean 19 days) and so this dosing regime was continued for all future experiments to minimize tamoxifen toxicity, injection load and maximize survival to allow detailed analysis.

However, in order to ensure all mice were analysed fully, and to limit the total number of mice required, the animals were initially sacrificed at 4 days and then 8 days post-tamoxifen treatment, to complement the data generated from the 'survival' experiments.

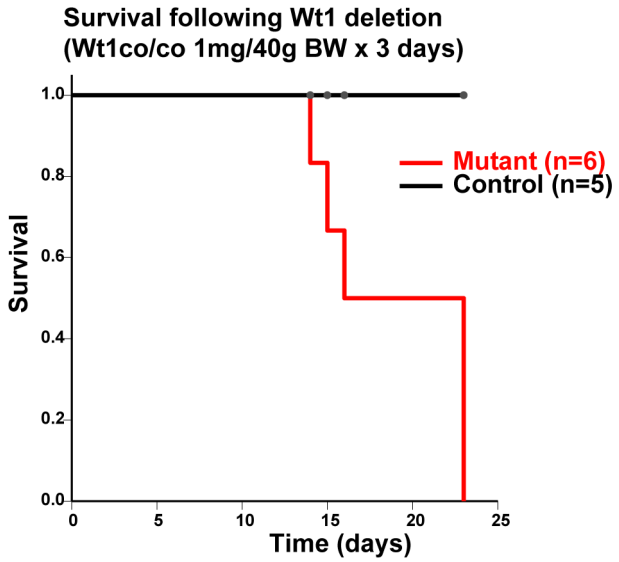

FIGURE 4.7: DISEASE-FREE SURVIVAL FOLLOWING *WT1* DELETION USING TAMOXIFEN AT 1MG/40G BODYWEIGHT FOR 3 DAYS

Both control (*CreER-Wt1*$^{co/co}$ or *Wt1*$^{co/GFP}$) and mutant (*CreER+Wt1*$^{co/co}$ or *Wt1*$^{co/GFP}$) mice were injected with tamoxifen at 1mg/40g bodyweight for 3 days and followed until they had to be euthanased for humane reasons. Mean survival of *Wt1*$^{co/co}$ mutant animals was 29.5 days (range 12-50 days), and 8 days in *Wt1*$^{co/GFP}$ animals.

4.6 CLINICAL CONSEQUENCES OF *WT1* DELETION

4.6.1 EARLY DEATH

As discussed above, *Wt1* deletion in *CreERWt1*$^{co/co}$ and *CreERWt1*$^{co/GFP}$ mice led to their rapid and early death. These mice were euthanased for humane reasons when they became significantly unwell but a few animals became unwell over the weekend, when daily inspection was limited, and actually died spontaneously, confirming the phenotype was not recoverable. Although the initial pilot experiment demonstrated prolonged (over 1 month) survival using the 5-day low dose protocol, further animals did not survive beyond day 12. When tamoxifen injections were limited to three days mean survival was 19 days (range 15-23). *CreERWt1*$^{co/GFP}$ mice were affected more severely, and became very unwell by day 8. Due to limited availability of these animals, all were therefore culled at that stage in further experiments.

Clinically the mice deteriorated very quickly. They were inspected daily to ensure no unnecessary suffering and euthanased as soon as they exhibited significant signs of distress. A modified distress score was used to objectively assess clinical deterioration (Figure 4.8 A). However, given the confounding effect of the peripheral oedema, body weight was not used as a clinical parameter (Ullman-Cullere and Foltz 1999, Hawkins 2002). A higher score demonstrated clinical deterioration.

Parameter	Animal ID	Score
Appearance	Normal	0
	General Lack of Grooming	1
	Piloerection, fresh ocular & nasal discharges	2
	Piloerection, hunched up	3
	Above and eyes half closed	4
Natural Behaviour	Normal	0
	Minor Changes	1
	Less mobile & isolated, but alert	2
	Restless or very still, not alert	3
Hydration status	Normal	0
	Abnormal skin pinch test	5
	Ascites	5
Clinical signs	Normal Respiratory rate & pattern	0
	Slight changes, increased rate only	1
	Increased rate with abdominal breathing	2
	Decreased rate with abdominal breathing	3
	Marked abdominal breathing and cyanosis	4
Provoked behaviour	Normal	0
	Minor depression or exaggerated response	1
	Moderate change in expected behaviour	2
	Very weak and precomatose	3
	Total	0-19
		Day:

A

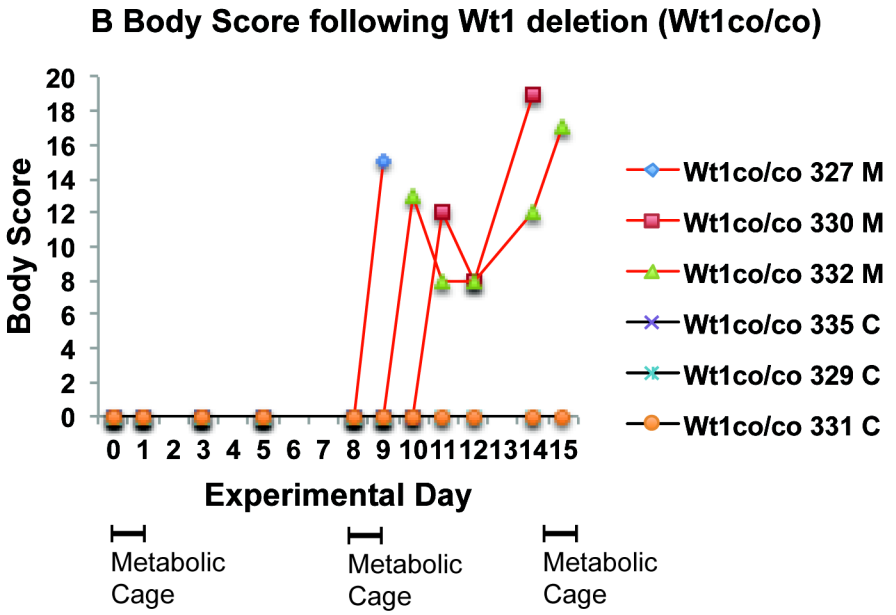
B Body Score following Wt1 deletion (Wt1co/co)
Body Score
20
18
16
14
12
10
8
6
4
2
0
0 1 2 3 4 5 6 7 8 9 10 11 12 13 14 15
Experimental Day
Wt1co/co 327 M
Wt1co/co 330 M
Wt1co/co 332 M
Wt1co/co 335 C
Wt1co/co 329 C
Wt1co/co 331 C
Metabolic Cage
Metabolic Cage
Metabolic Cage

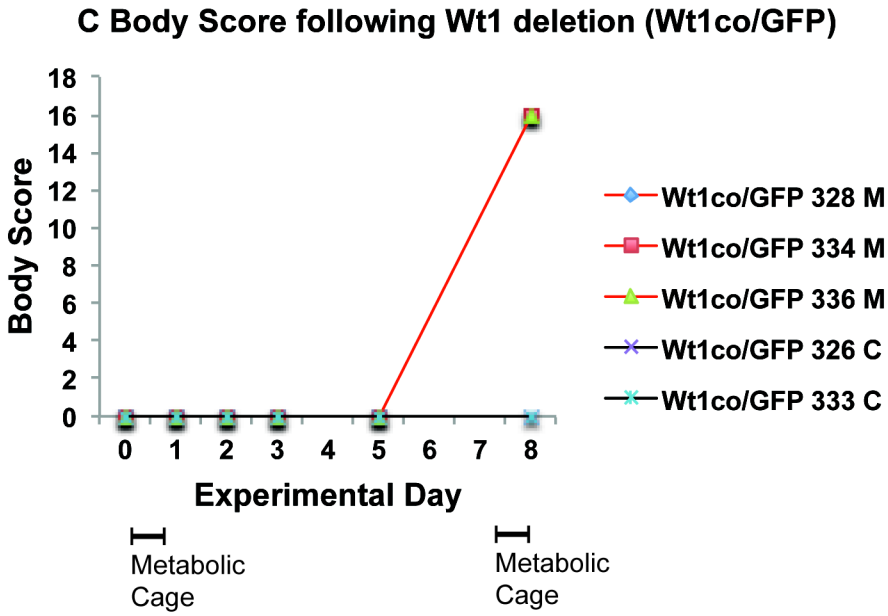
C Body Score following Wt1 deletion (Wt1co/GFP)
Body Score
18
16
14
12
10
8
6
4
2
0
0 1 2 3 4 5 6 7 8
Experimental Day
Wt1co/GFP 328 M
Wt1co/GFP 334 M
Wt1co/GFP 336 M
Wt1co/GFP 326 C
Wt1co/GFP 333 C
Metabolic Cage
Metabolic Cage

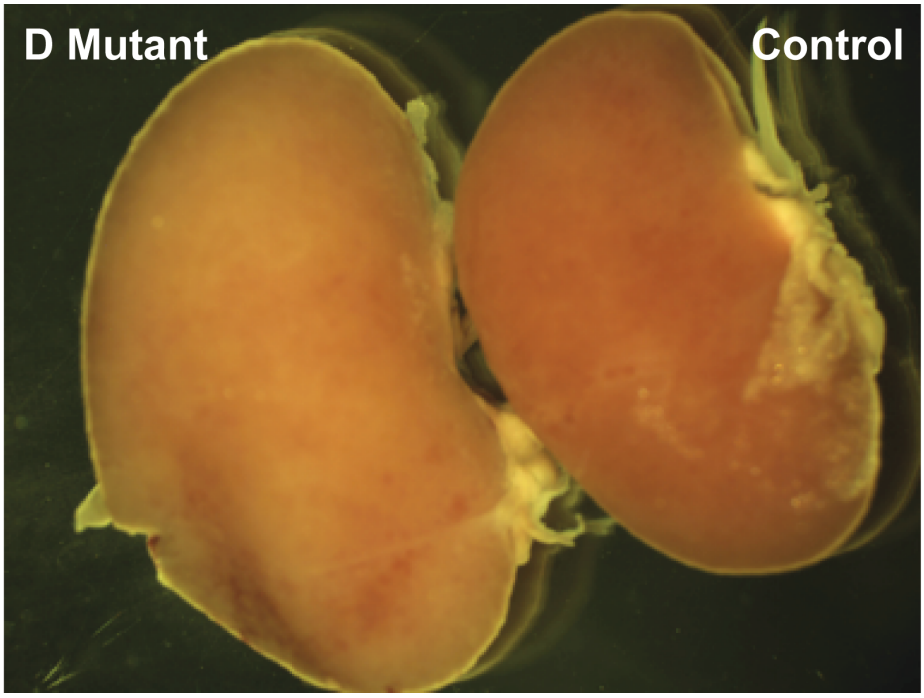

FIGURE 4.8: ASSESSING HEALTH / DISTRESS USING A MODIFIED BODY SCORE & MACROSCOPIC FINDINGS

A) Body score was analysed at least every other day using a modified body score template. B) In mutant (M) *Wt1*$^{co/co}$ animals a rapid deterioration in body score occurred after day 8, although this was followed by some improvement in health status. This deterioration coincided with using the metabolic cage for 24 hours for urine collection, despite prior habituation. A further deterioration was seen at day 14, again in the context of the metabolic cage, although at this point the animals were euthanased for humane reasons. C) Mutant (M) *Wt1*$^{co/GFP}$ animals exhibited a rapid deterioration in body score on day 8, following use of the metabolic cage. They were subsequently euthanased for humane reasons. D) Macroscopic appearance of mutant and control kidneys

These data appeared to indicate a detrimental effect from the use of metabolic cages on mutant animals, perhaps due to a stress effect (despite prior habituation) (Lee, Webb et al. 2004). Further analysis of this effect was not possible within the constraints of this project, but, as urine collection using the metabolic cage was subject to contamination by food and droppings (despite the use of cages in which waste should have been separated) it was decided to use spontaneous voiding in order to collect urine for analysis, and abandon the use of metabolic cages. Given the time constraints, further survival analysis without using the metabolic cages was not formally undertaken to ensure all experimental tissue could be utilized efficiently.

Clinically mutant mice became less active, hunched and developed flank oedema. At necroscopy, free fluid (ascites) was apparent in the abdominal cavity of all mutant animals. However, as discussed earlier, the degree was difficult to quantify, as the additional weight due to fluid retention was probably counteracted by actual lean mass loss. The kidneys of mutant mice were enlarged, pale and oedematous (Figure 4.8 D). Control littermates remained healthy, as did both Cre+ and Cre- $Wt1^{+/+}$ mice analysed separately.

4.6.2 *Wt1* DELETED MICE DEVELOP SEVERE ALBUMINURIA AND SERUM HYPOALBUMINAEMIA

Spontaneously voided urine was collected, stored at -20°C and analysed in control-matched batches using a commercial Microalbumin Kit (Olympus Diagnostics Ltd, Watford, UK) adapted for use on a Cobas Fara centrifugal analyser (Roche Diagnostics Ltd, Welwyn Garden City, UK), by Forbes Howie, Chief Biomedical Scientist at the Edinburgh University Clinical Biochemistry Section. Analysis of urinary albumin and albumin/creatinine ratio (ACR) revealed significant albuminuria by experimental day 8 (Figure 4.9).

When comparing the actual ACR amounts, a small but significant difference was also noted between the Cre-negative control and Cre-positive mutant $Wt1^{co/co}$ and $Wt1^{co/GFP}$ animals even at baseline (day 0). This was much less than the increase caused by *Wt1* deletion. No significant difference was detected between the Cre-negative $Wt1^{co/co}$ and $Wt1^{co/GFP}$ control animals at baseline or following tamoxifen injection.

The albuminuria was accompanied by profound serum hypoalbuminaemia, consistent with severe nephrosis (Figure 4.10 A). At day 8, all three of the hypoalbuminaemic mutant serum samples were lipaemic, consistent with the hyperlipidaemia seen in human nephrotic syndrome, thought due in part to reductions in lipoprotein lipase and tissue lipoprotein receptors (Wang, Shearer et al. 2012)

At this relatively early time point, only mild changes were seen in the serum urea and creatinine levels (Figure 4.10 B & C), with a significant but small increase in serum urea concentration in mutant animals on day 4, which had increased further by day 8. These results come from animals sacrificed at specified time points, in order to ensure full and comparable analysis between experimental groups. Therefore, they were not yet exhibiting the extreme phenotype observed in mice followed for the survival studies. Serum analysis from later time points would be expected to demonstrate the development of renal failure, although these experiments could not be repeated within the timeframe of this project.

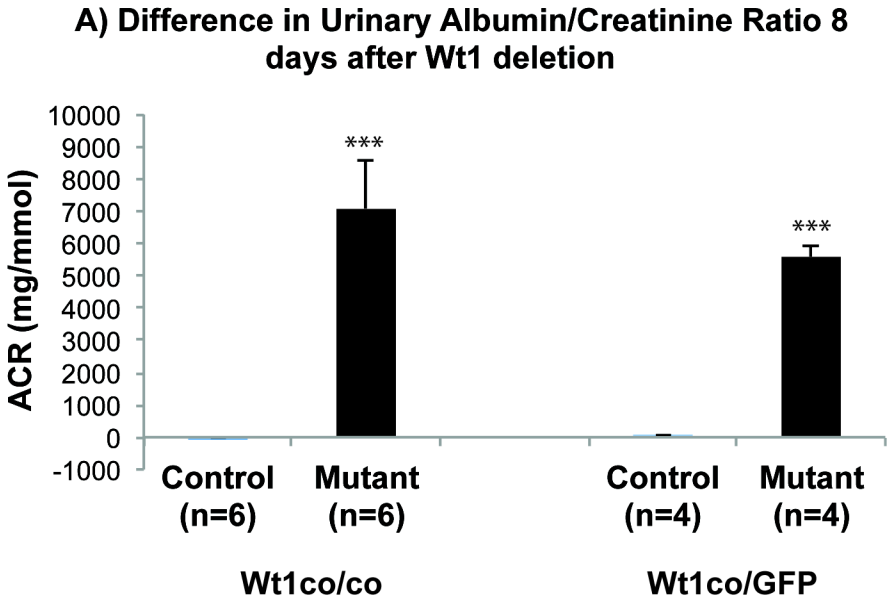
A) Difference in Urinary Albumin/Creatinine Ratio 8 days after Wt1 deletion
ACR (mg/mmol)
10000
9000
8000
7000
6000
5000
4000
3000
2000
1000
0
-1000
***
***
Control (n=6)
Mutant (n=6)
Control (n=4)
Mutant (n=4)
Wt1co/co
Wt1co/GFP

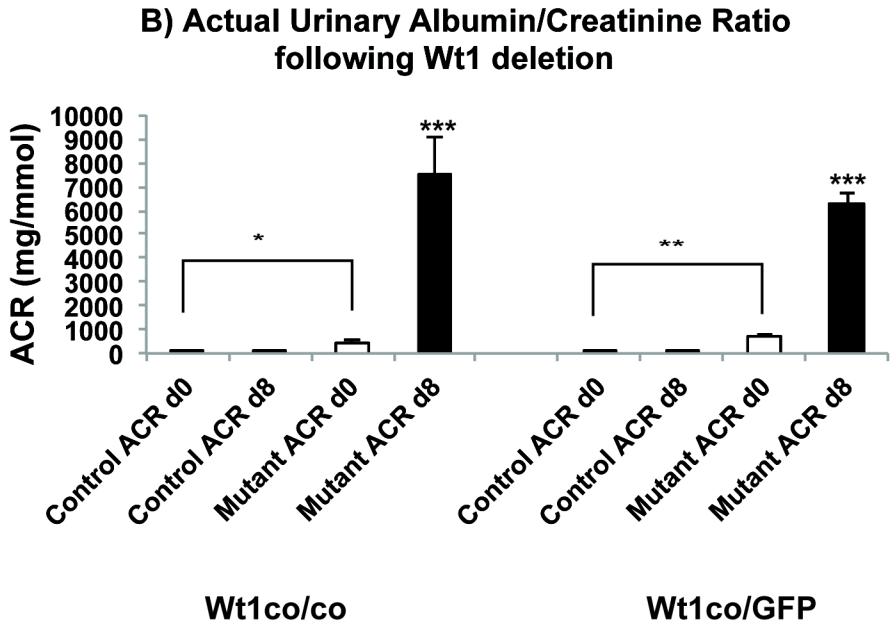
B) Actual Urinary Albumin/Creatinine Ratio following Wt1 deletion
ACR (mg/mmol)
10000
9000
8000
7000
6000
5000
4000
3000
2000
1000
0
*
**
***
***
Control ACR d0
Control ACR d8
Mutant ACR d0
Mutant ACR d8
Control ACR d0
Control ACR d8
Mutant ACR d0
Mutant ACR d8
Wt1co/co
Wt1co/GFP

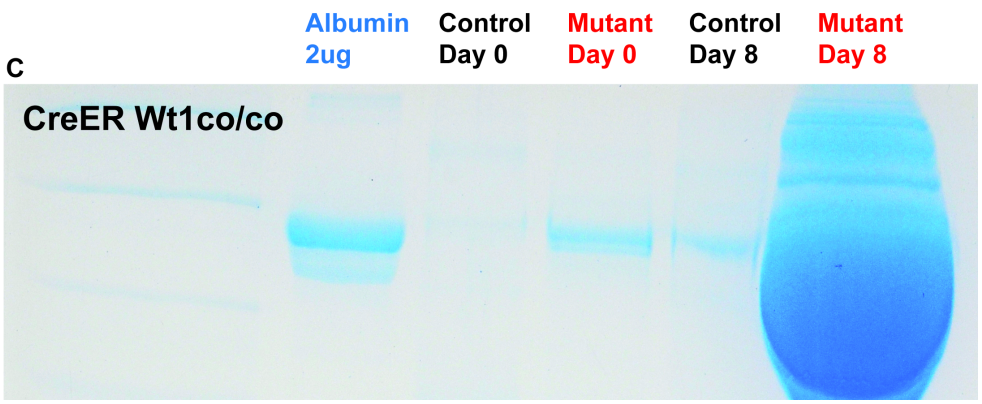

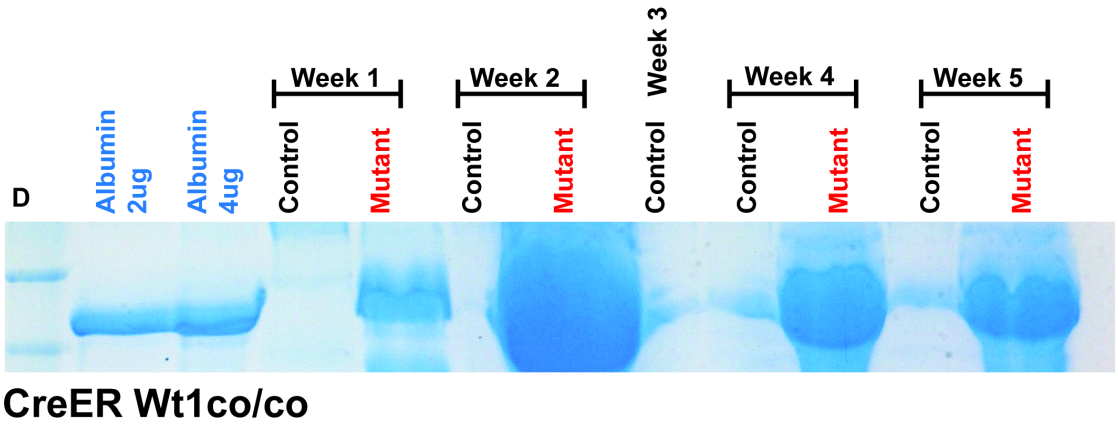

FIGURE 4.9: ALBUMIN CREATININE RATIO FOLLOWING TAMOXIFEN TREATMENT TO DELETE *WT1*

Figure 4.9: Albumin Creatinine Ratio following tamoxifen treatment to delete *Wt1*

Albumin/Creatinine Ratio was used for an accurate measure of albuminuria, by controlling for urine concentration. A) Difference in ACR between day 0 and day 8 after tamoxifen injection. A huge and highly significant increase in ACR can be seen in both $Wt1^{co/co}$ and $Wt1^{co/GFP}$ mutant animals. B) Actual ACR on day 0 and day 8 following tamoxifen injections, in $Wt1^{co/co}$ and $Wt1^{co/GFP}$ animals. Again, a highly significant increase in ACR is seen in both mutant models. Some differences are also seen at baseline (prior to tamoxifen injection) between Cre-negative and Cre-positive matched littermates. This just reaches significance in the $Wt1^{co/co}$ model and is more significant in the $Wt1^{co/GFP}$ model. No significant difference was found between Cre-negative $Wt1^{co/co}$ and $Wt1^{co/GFP}$ controls, indicating the compound heterozygosity of the $Wt1^{co/GFP}$ animals does not in itself predispose to the development of albuminuria at this early stage. (* $p<0.05$; ** $p<0.01$; *** $p<0.001$) C) Coomassie blue staining of *CreERWt1*$^{co/co}$ control and mutant mouse urine at experimental day 0 and day 8 (injected with 1mg/40gBW x 3 days). Mutant animals develop severe albuminuria by day 8. D) Coomassie Blue staining of CreER $Wt1^{co/co}$ control and mutant mouse urine from the longest surviving animals injected with tamoxifen 1mg/40gBW x 5 days.

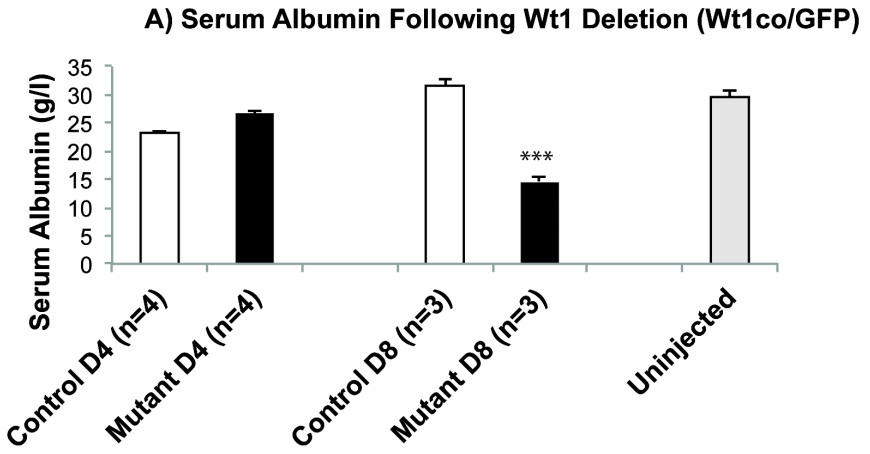
A) Serum Albumin Following Wt1 Deletion (Wt1co/GFP)
Serum Albumin (g/l)
35
30
25
20
15
10
5
0
***
Control D4 (n=4)
Mutant D4 (n=4)
Control D8 (n=3)
Mutant D8 (n=3)
Uninjected

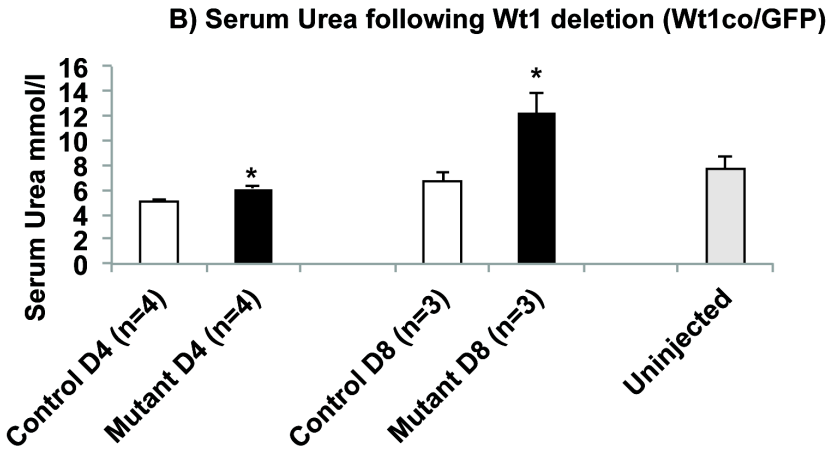
B) Serum Urea following Wt1 deletion (Wt1co/GFP)
Serum Urea mmol/l
16
14
12
10
8
6
4
2
0
*
*
Control D4 (n=4)
Mutant D4 (n=4)
Control D8 (n=3)
Mutant D8 (n=3)
Uninjected

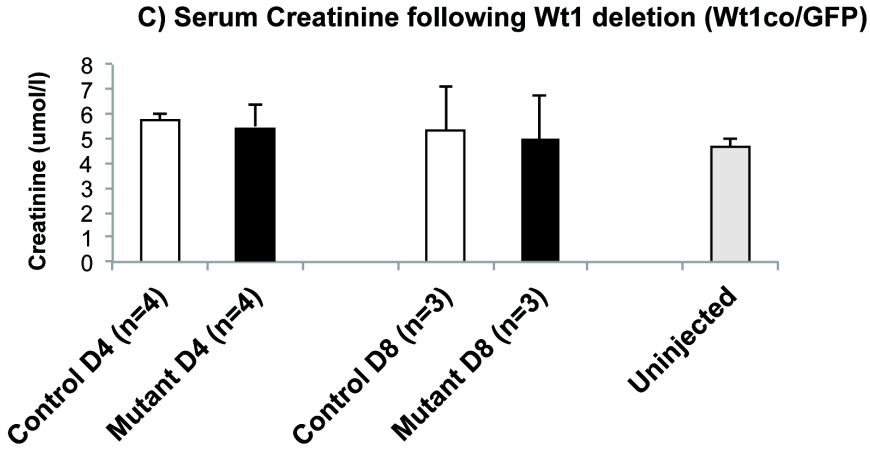
C) Serum Creatinine following Wt1 deletion (Wt1co/GFP)
Creatinine (umol/l)
8
7
6
5
4
3
2
1
0
Control D4 (n=4)
Mutant D4 (n=4)
Control D8 (n=3)
Mutant D8 (n=3)
Uninjected

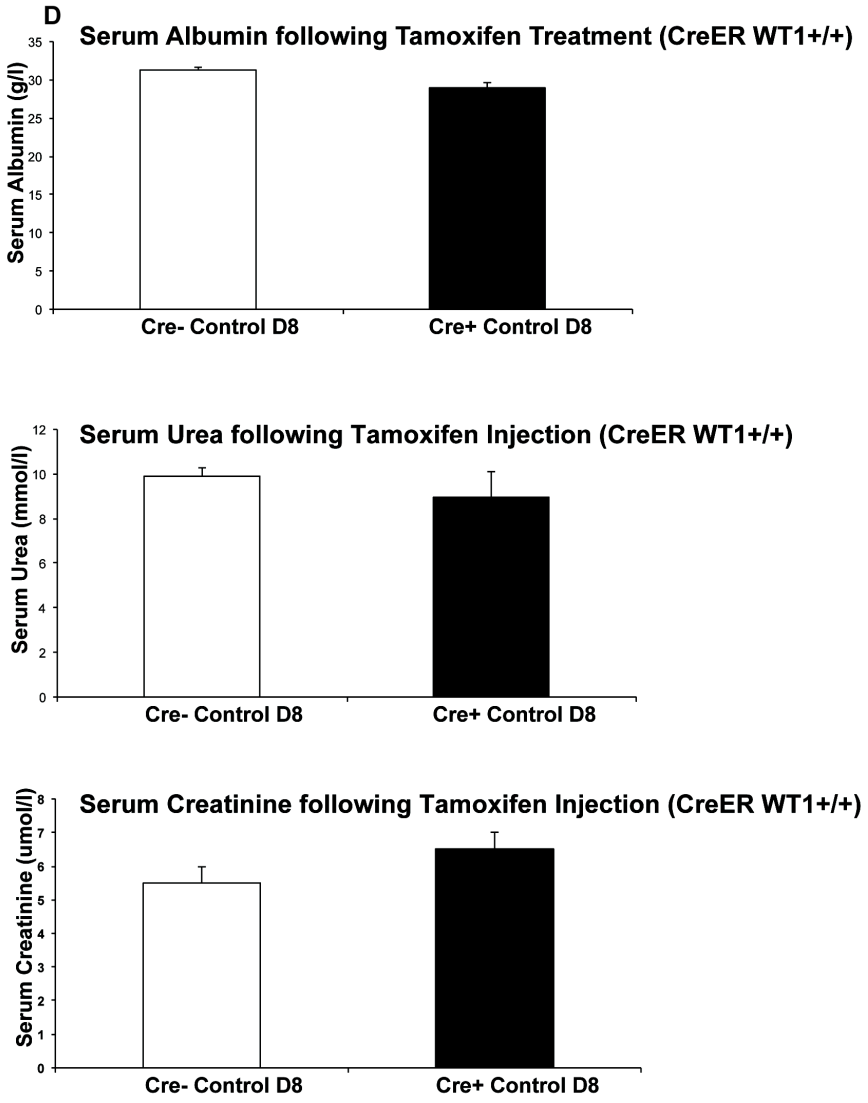

FIGURE 4.10: SERUM ALBUMIN, UREA AND CREATININE FOLLOWING WT1 DELETION

FIGURE 4.10: SERUM ALBUMIN, UREA AND CREATININE FOLLOWING WT1 DELETION IN CREER *WT1*$^{CO/GFP}$ MICE (TAMOXIFEN 1MG/40G BW X 3 DAYS).

Serum samples were obtained using cardiac puncture immediately following euthanasia by CO2 inhalation. A) Serum Albumin: no difference is seen between control and mutant animals by day 4. By day 8, mutant mice exhibit significant hypoalbuminaemia. B) Serum Urea: a small but significant increase in serum urea is seen by day 4, which increases by day 8 in mutant animals. C) Serum Creatinine: no difference is seen between control and mutant animals in by experimental day 8. D) Serum albumin, urea and creatinine levels in Cre-positive and Cre-negative wild-type control mice following tamoxifen injection. No Cre-toxicity effect is demonstrated. (* $p<0.05$; ** $p<0.01$; *** $p<0.001$)

4.7 TAMOXIFEN-INDUCED CRE-RECOMBINATION LEADS TO *WT1*-DELETION AND SIGNIFICANT *WT1*-LOSS.

Although the *Wt1*-conditional model had already been used successfully in combination with an epicardial-Cre line, to achieve epicardial-specific Wt1-loss, it was important to confirm that *Wt1* deletion, and subsequent loss of Wt1 gene and protein expression was occurring within the kidney (Martinez-Estrada, Lettice et al. 2010). Triple primer PCR confirmed recombination events were occurring at the DNA level (in DNA isolated from kidney cortex), with resultant loss of the conditional allele following tamoxifen treatment (Figure 4.11 A). As expected this was associated with a significant loss of *Wt1* gene expression, as early as day 4 from the start of tamoxifen treatment (Figure 4.11 B). At day 4, quantitative RT-PCR for RNA demonstrated *Wt1* gene expression in mutant glomeruli was only 15% of control, dropping to 2% by day 8 in both isolated glomeruli and kidney cortex. Analysis of Wt1 protein expression using immunohistochemistry confirmed loss of Wt1 staining in the glomerulus (Figure 4.11 C & D).

It is interesting to note, that although there is increased Wt1 loss over time, there appears to be limited / undetectable differences between mice injected with 3 days or 5 days of tamoxifen. In figure 4.11 D, the mice taken at day 12 were injected with 5 days tamoxifen, but fit the ongoing pattern of increasing Wt1 loss over time. Unfortunately no direct comparison could be made between Wt1 protein loss according to the tamoxifen dosing regimen, as the tissues were harvested at earlier pre-specified time points in the animals injected with only 3 days of tamoxifen. When comparing dosing regimens using a YFP-reporter line (see above), Cre-recombination efficiency did appear to be dose dependent.

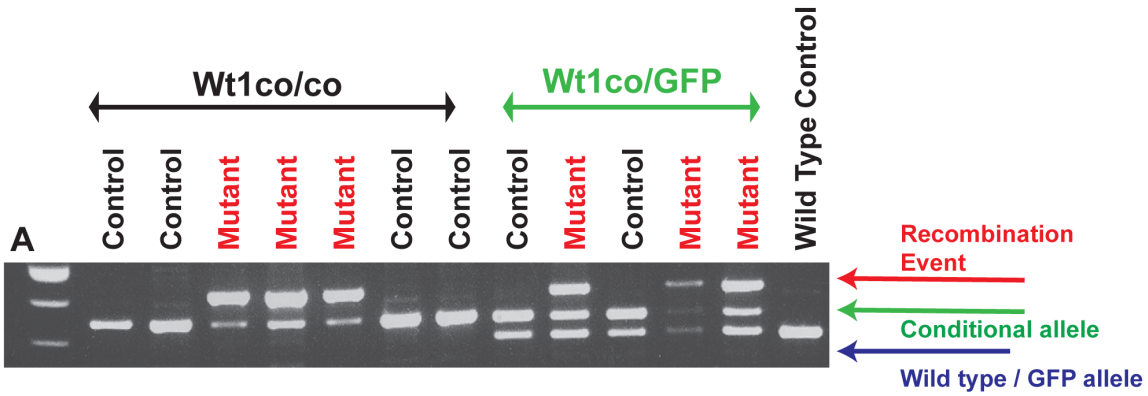
A
Wt1co/co
Wt1co/GFP
Control
Control
Mutant
Mutant
Mutant
Control
Control
Control
Mutant
Control
Mutant
Mutant
Wild Type Control
Recombination Event
Conditional allele
Wild type / GFP allele

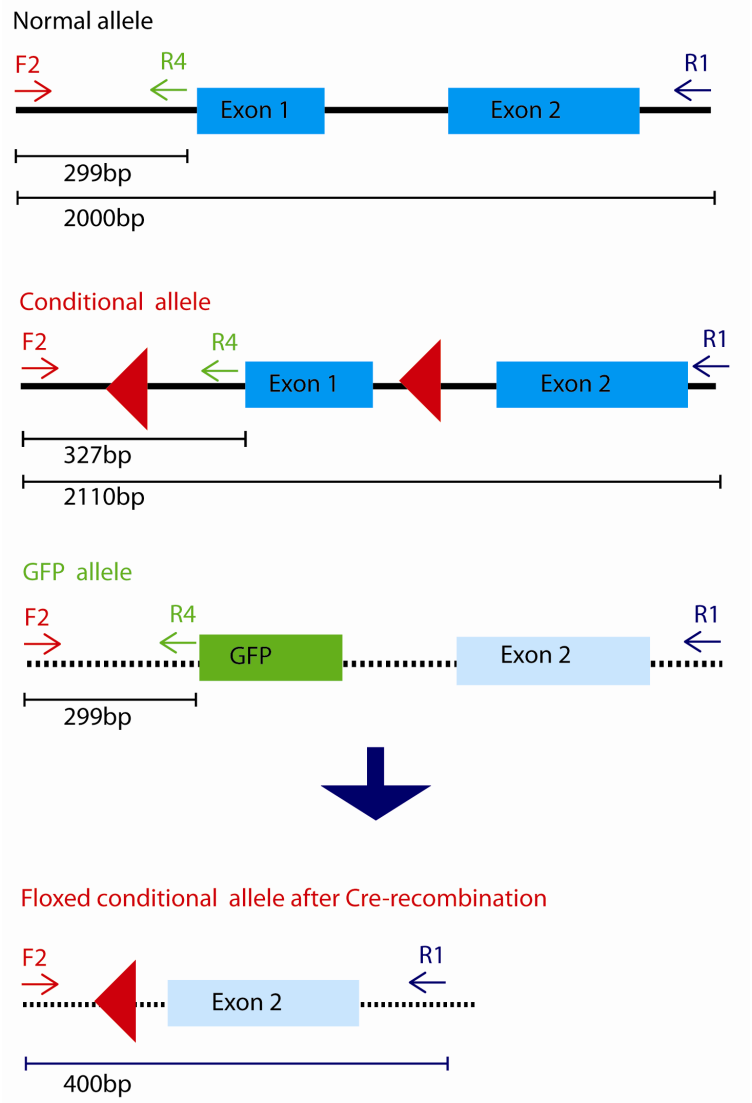
Normal allele
F2
R4
R1
Exon 1
Exon 2
299bp
2000bp
Conditional allele
F2
R4
R1
Exon 1
Exon 2
327bp
2110bp
GFP allele
F2
R4
R1
GFP
Exon 2
299bp
Floxed conditional allele after Cre-recombination
F2
R1
Exon 2
400bp

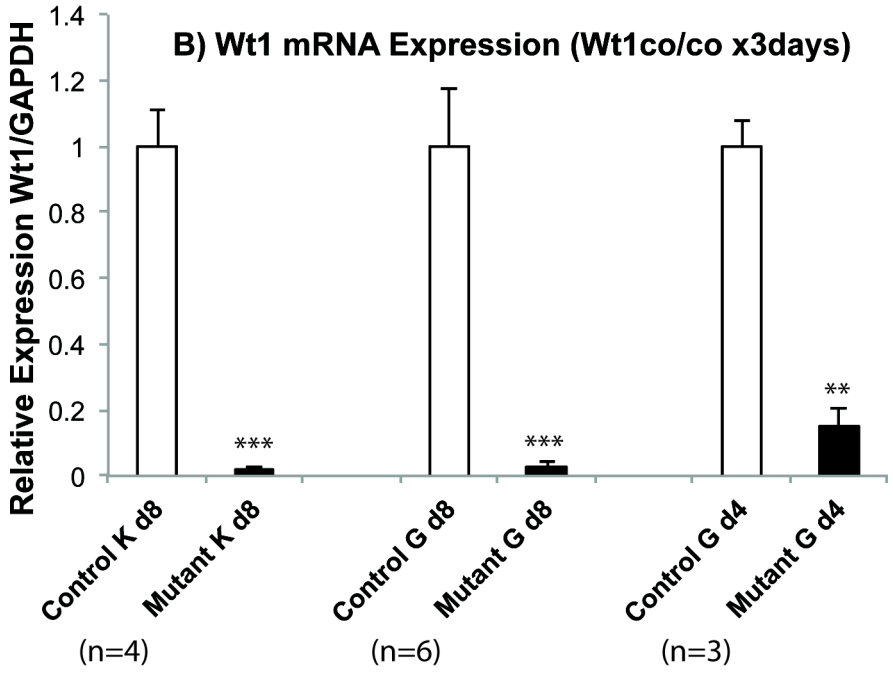
B) Wt1 mRNA Expression (Wt1co/co x3days)
Relative Expression Wt1/GAPDH
1.4
1.2
1
0.8
0.6
0.4
0.2
0
***
***
**
Control K d8
Mutant K d8
Control G d8
Mutant G d8
Control G d4
Mutant G d4
(n=4)
(n=6)
(n=3)

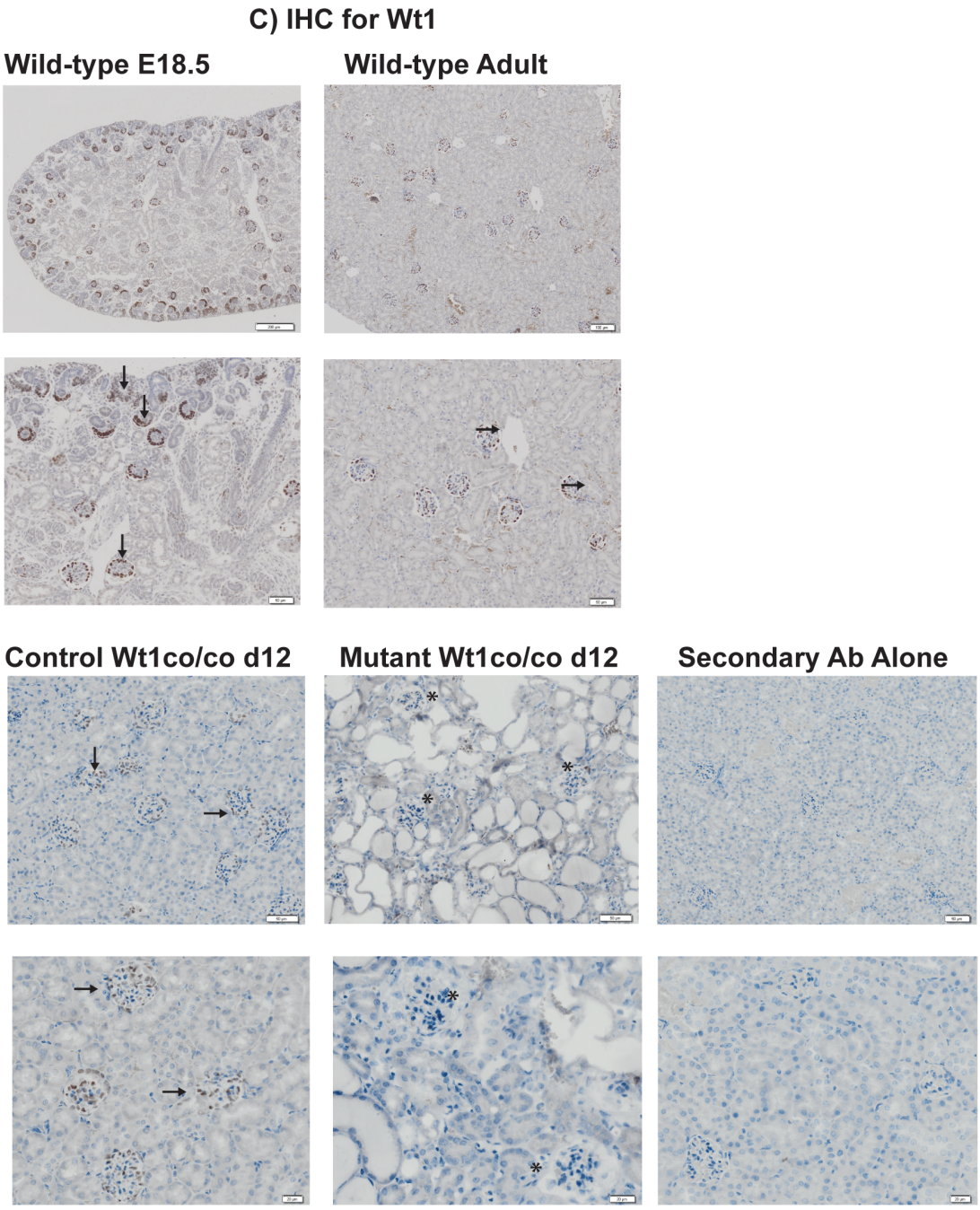
C) IHC for Wt1
Wild-type E18.5
Wild-type Adult
Control Wt1co/co d12
Mutant Wt1co/co d12
Secondary Ab Alone

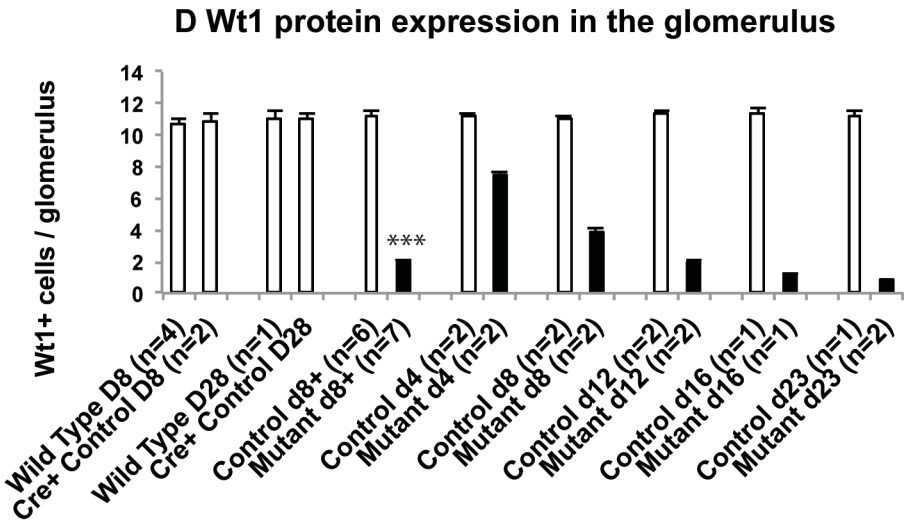

FIGURE 4.11: WT1 LOSS FOLLOWING CRE-RECOMBINATION

A) Triple primer PCR demonstrates Cre recombination at the DNA level, with recombination events only occurring in the Cre-positive mutant animals. Cartoon schematic explains the method. B) Quantitative RT-PCR for *Wt1* (detecting exons 1 and 2, expressed in all relevant isoforms. Exon one is deleted following Cre-recombination) demonstrating significant reduction of *Wt1* mRNA expression following *Wt1*-deletion (* $p<0.05$; ** $p<0.01$; *** $p<0.001$). G = Glomerular isolate, K = Kidney cortex. C) Wt1 protein is lost from the glomerulus following tamoxifen treatment of Cre-positive mutant animals. In control littermates Wt1-positive nuclei can be seen clearly, mainly at the periphery of the glomerulus (arrows). However, in mutant animals almost all Wt1 nuclear staining is gone (asterisks). No staining is detected using a minus primary antibody control. D) Quantification of immunohistochemistry demonstrating a reduction in the number of Wt1 positive nuclei per glomerulus across 50 randomly sampled glomeruli. Cre+ and Cre- control animals exhibit normal Wt1 staining, indication no effect of Cre-toxicity on Wt1 expression.

4.8 *Wt1* DELETION CAUSES SEVERE GLOMERULAR INJURY.

Histological analysis of *Wt1*-conditional mice revealed significant glomerular injury following *Wt1* deletion. Control and Cre+ control animals did not exhibit such changes. This analysis was carried out with the help of James Bailey, comparative pathologist, QMRI.

The main histological features were (Figure 4.12):

1) Severe podocyte injury with vacuolation
2) Severe injury and vacuolation of parietal epithelial cells
3) Loss of glomerular capillary architecture
4) Marked enlargement of Bowman's Capsule
5) Accumulation of protein casts in tubules and Bowman's Space
6) Tubular ectasia and vacuolation of tubular epithelial cells, with intact basement membrane
7) Cellular debris in tubular lumen
8) Only mild interstitial inflammation

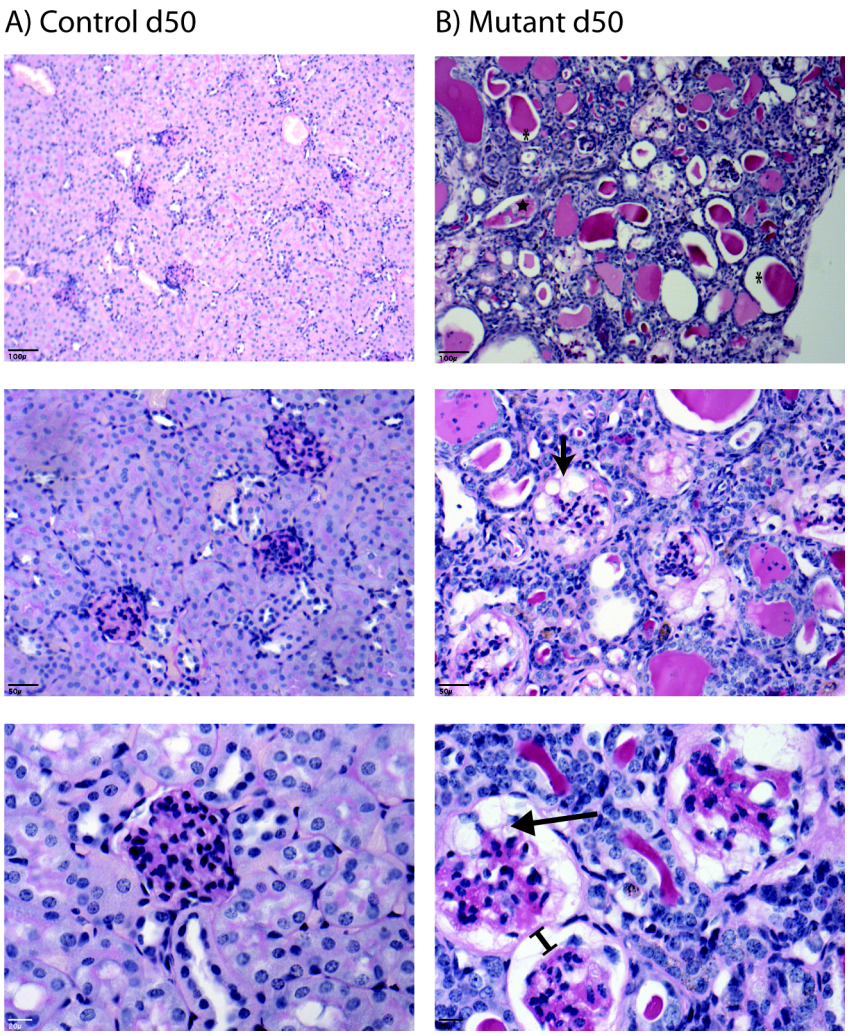

FIGURE 4.12: HISTOLOGICAL CHANGES FOLLOWING *WT1* DELETION

A) Control animals have normal cortical histology. B) Mutant (Wt1 deleted) animals exhibit severe glomerular injury, most notably vacuolation and injury to both podocytes (straight arrowhead) and parietal epithelial cells (curved arrowhead); enlargement of Bowman's Space (marked); intra-luminal protein casts and tubular ectasia (*) and cellular debris within the tubular lumen (star).

As mice had been sacrificed at a number of time points, the evolution of these changes could be followed chronologically. At day 4, just over half of glomeruli in mutant mice exhibit some form of glomerular damage (Figure 4.13 A). However, this damage is only mild, with an average histological damage score of only 1 (0-25%) (Figure 4.13 B). The number of affected glomeruli increases over time, as does the severity of damage (Figure 4.13 A & B). Over time, there is increased interstitial fibrosis, and an increase of the mild interstitial inflammatory infiltrate. Glomerulosclerosis and increased matrix deposition is evident both within the glomerulus and interstitium (Figure 4.13 C & D).

Immunohistochemistry for the macrophage marker F4/80 did not demonstrate an excess of interstitial macrophages in Wt1-deleted glomeruli (Figure 4.13 E).

Analysis of the apoptosis marker activated Caspase 3 and the proliferation marker Phospho-Histone H3 did not reveal an excess of apoptosis or proliferation in *Wt1*-deleted glomeruli (Figure 4.14). The occasional apoptotic cell was identified in both control and mutant animals, with a significant increase in apoptotic cells in *Wt1*-deleted animals after 12 days (Figure 4.14 A: Cre+ Control 0.8±0.79, "wild-type" 0.9±0.74, Control D4 0.75±0.63, Mutant D4 0.8±0.67, Control D12+ 0.9±0.8, Mutant D12+ 5.2±1.31 per x20 cortical field). However, these were almost entirely tubular, with only very occasional apoptotic cells identified in the glomeruli. Heavy albuminuria is a recognized cause of tubular epithelial cell apoptosis, so this is likely to be a secondary phenomenon to the albuminuria caused by *Wt1*-deletion (Ohse, Inagi et al. 2006).

Increased proliferation was noted in the cortex of *Wt1*-deleted kidneys after day 12, but again, this was limited to the tubules, and is likely to be a regenerative response to tubular injury (Figure 4.14 B). Occasional mitotic cells could be identified lining Bowman's Capsule, consistent with proliferation parietal epithelial cells. However, within the constraints of the analysis performed, no significant increase in these cells was identified in the *Wt1*-deleted animals.

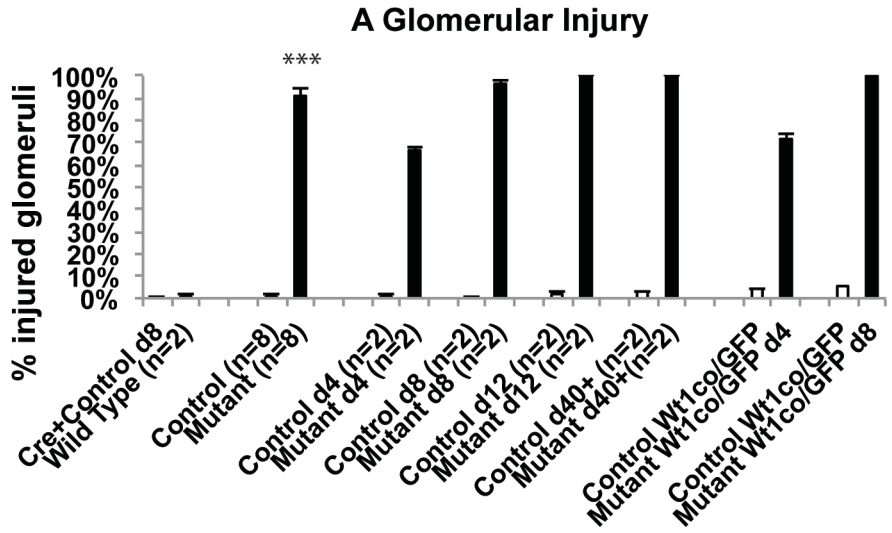
A Glomerular Injury
% injured glomeruli
100%
90%
80%
70%
60%
50%
40%
30%
20%
10%
0%
***
Cre+Control d8 (n=2)
Wild Type (n=2)
Control (n=8)
Mutant (n=8)
Control d4 (n=2)
Mutant d4 (n=2)
Control d8 (n=2)
Mutant d8 (n=2)
Control d12 (n=2)
Mutant d12 (n=2)
Control d40+ (n=2)
Mutant d40+(n=2)
Control Wt1co/GFP
Mutant Wt1co/GFP d4
Control Wt1co/GFP
Mutant Wt1co/GFP d8

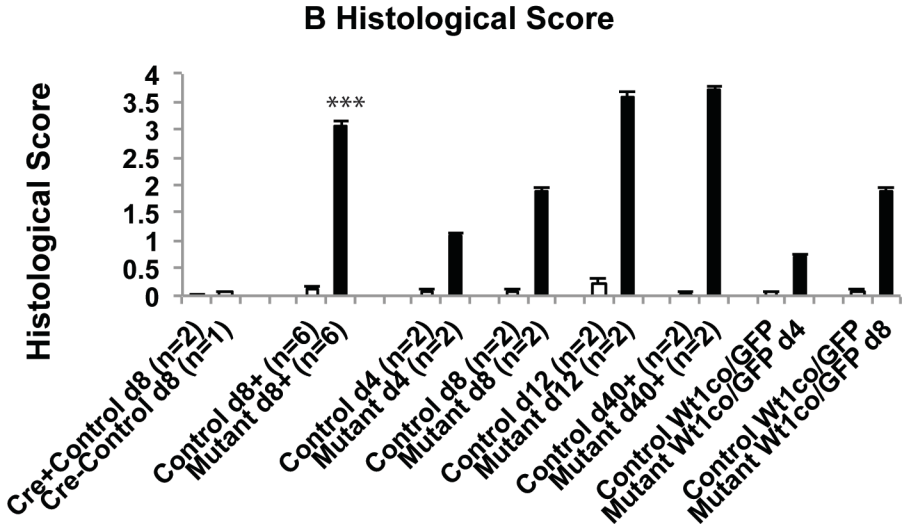
B Histological Score
Histological Score
4
3.5
3
2.5
2
1.5
1
0.5
0
***
Cre+Control d8 (n=2)
Cre-Control d8 (n=1)
Control d8+ (n=6)
Mutant d8+ (n=6)
Control d4 (n=2)
Mutant d4 (n=2)
Control d8 (n=2)
Mutant d8 (n=2)
Control d12 (n=2)
Mutant d12 (n=2)
Control d40+ (n=2)
Mutant d40+ (n=2)
Control Wt1co/GFP
Mutant Wt1co/GFP d4
Control Wt1co/GFP
Mutant Wt1co/GFP d8

C

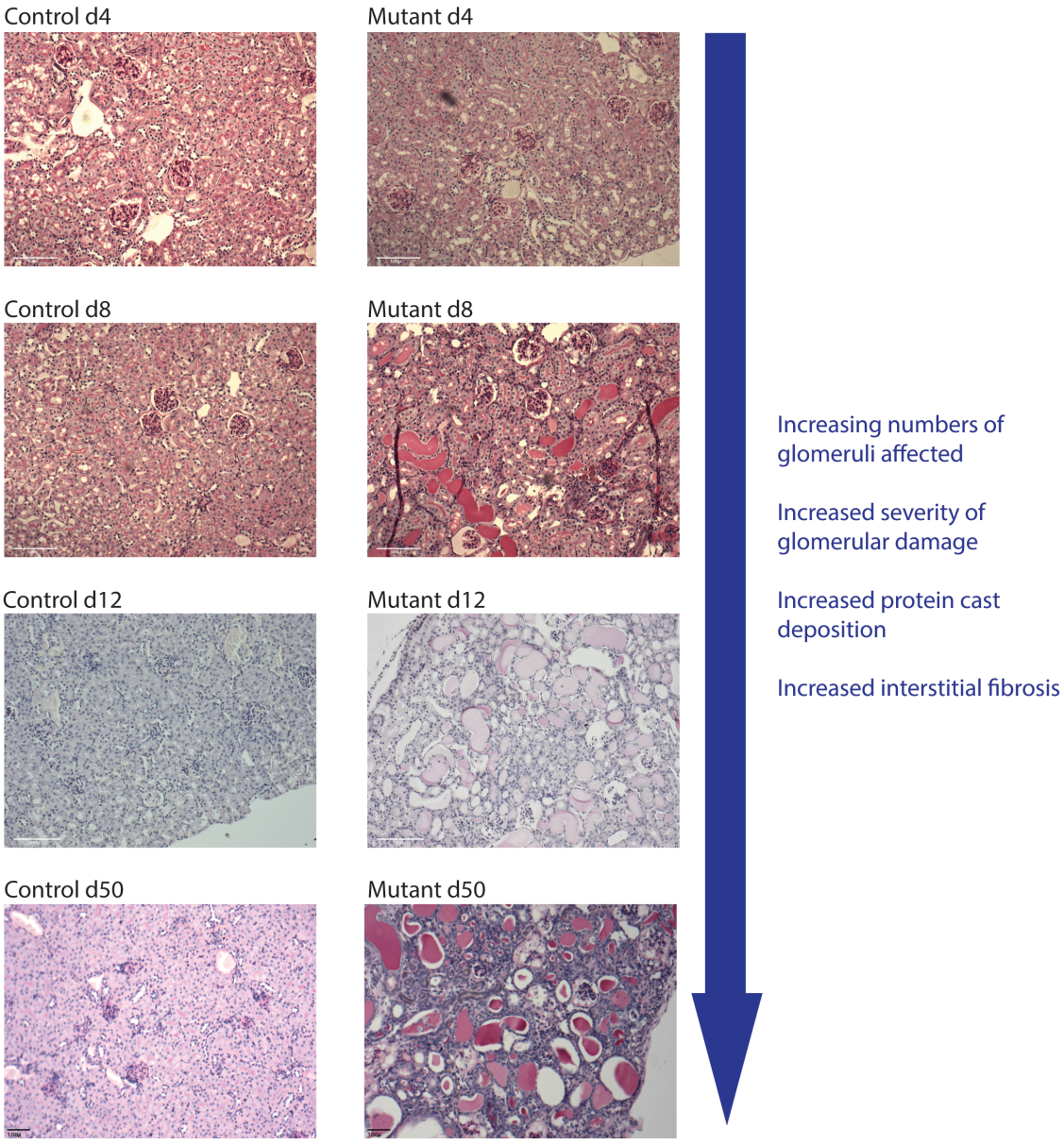
Control d4
Mutant d4
Control d8
Mutant d8
Control d12
Mutant d12
Control d50
Mutant d50
Increasing numbers of glomeruli affected
Increased severity of glomerular damage
Increased protein cast deposition
Increased interstitial fibrosis

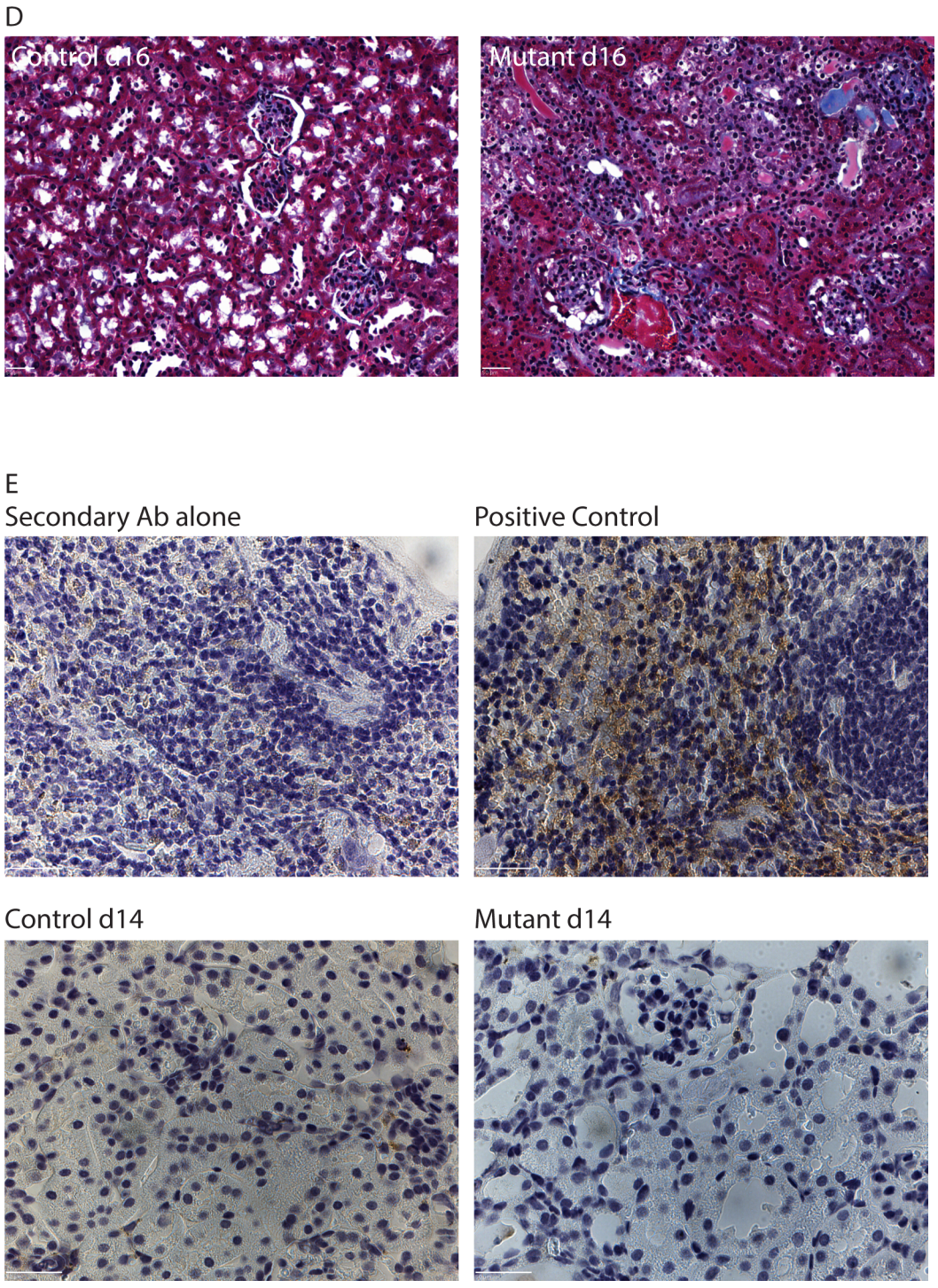

FIGURE 4.13: GLOMERULAR INJURY FOLLOWING WT1-DELETION

FIGURE 4.13: GLOMERULAR INJURY FOLLOWING WT1-DELETION

PAS staining of paraffin embedded kidney cortex. A) The proportion of affected glomeruli was quantified by examining 30 randomly selected x10 microscopic fields of kidney cortex. B) A modified histological scoring method (Suzuki, Matsusaka et al. 2009) was used to semi-quantify the degree of glomerular damage across 30 randomly selected glomeruli examined at x40 magnification (Score 0 = no damage, 1 = 0-25% glomerular volume, 2 = 25-50%. 3 = 50-75%, 4 = 75-100%). C) PAS staining of histological changes over time. D) Masson Trichome staining of kidney cortex demonstrating increased interstitial scarring in mutant animals. E) IHC for the macrophage marker F4/80: no macrophage infiltrate is seen in mutant animals.

A

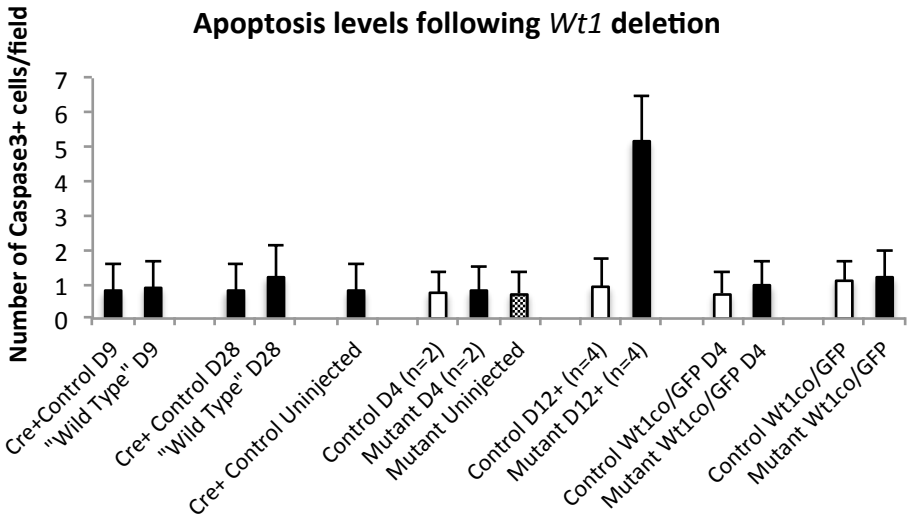

B

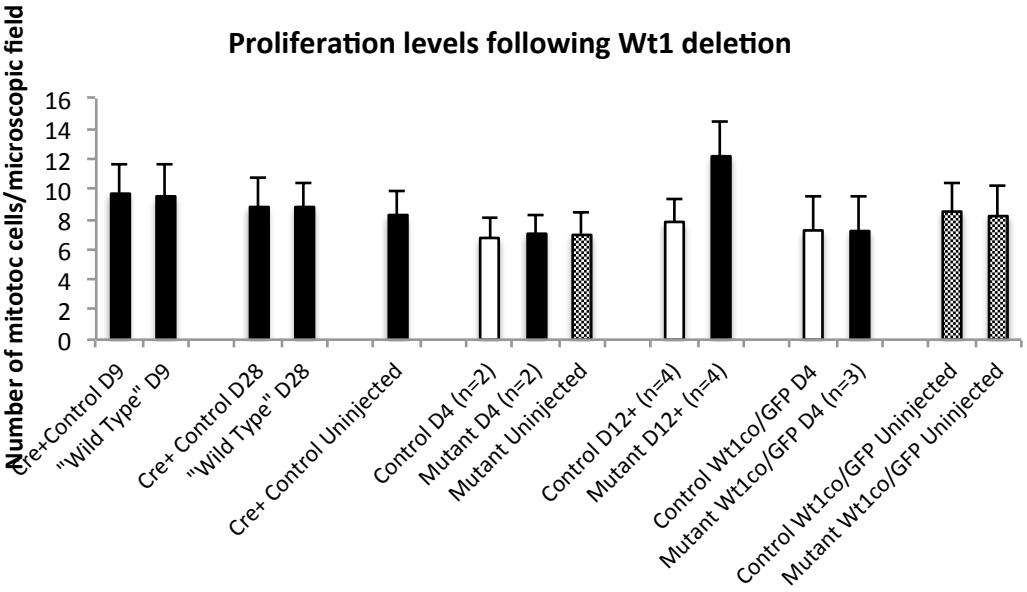

FIGURE 4.14: APOPTOSIS AND PROLIFERATION FOLLOWING WTI-DELETION

FIGURE 4.14: APOPTOSIS AND PROLIFERATION FOLLOWING *WT1*-DELETION

A) Apoptosis was quantified using immunohistochemistry for cleaved Caspase 3. The number of Caspase 3+ apoptotic cells per x20 cortical field was quantified in 20 randomly selected cortical fields in 3 serial sections. Biological replicate n-numbers are shown. A significant increase in apoptosis was identified in Wt1-deleted animals after day 12, but this was limited to the tubules. B) Proliferation was quantified using immunohistochemistry for Phospho-histone H3. The number of Phospho-histone H3+ mitotic cells per x20 cortical field was quantified in 20 randomly selected cortical fields in 3 serial sections. Biological replicate n-numbers are shown. An increase in proliferation was demonstrated in Wt1-deleted animals after day 12, but again, this was limited to the tubules and not the glomeruli.

4.8.1 THERE IS NO EVIDENCE OF SIGNIFICANT NEPHRON LOSS IN *WT1*-DELETED GLOMERULI

The progressive nature of glomerular disease remains a major obstacle in the management of chronic kidney disease. The mechanisms of this progression are not well understood, but once a critical threshold of damage, no matter what the primary cause, is reached, either per glomerulus, or per kidney, then progressive damage occurs, with an increasing number of glomeruli becoming sclerotic over time. This leads to downstream loss of renal tubules, and the accumulation of interstitial fibrosis.

However, in the longest surviving *Wt1*-deleted mice glomerular numbers were similar in both control and mutant animals (Figure 4.15), suggesting that despite the profound glomerular damage there was no evidence of total glomerular sclerosis and resultant nephron loss. Although as the longest surviving animals only survived 6 weeks from *Wt1*-deletion, analysis may have been too early to detect an effect, which, in other models of podocyte injury, usually occurs after six to eight weeks (Mollet, Ratelade et al. 2009, Fukuda, Wickman et al. 2012). Despite the absence of detectable nephron loss, tubular damage is evident in *Wt1*-deleted kidneys, with increased matrix deposition and interstitial fibrosis.

.

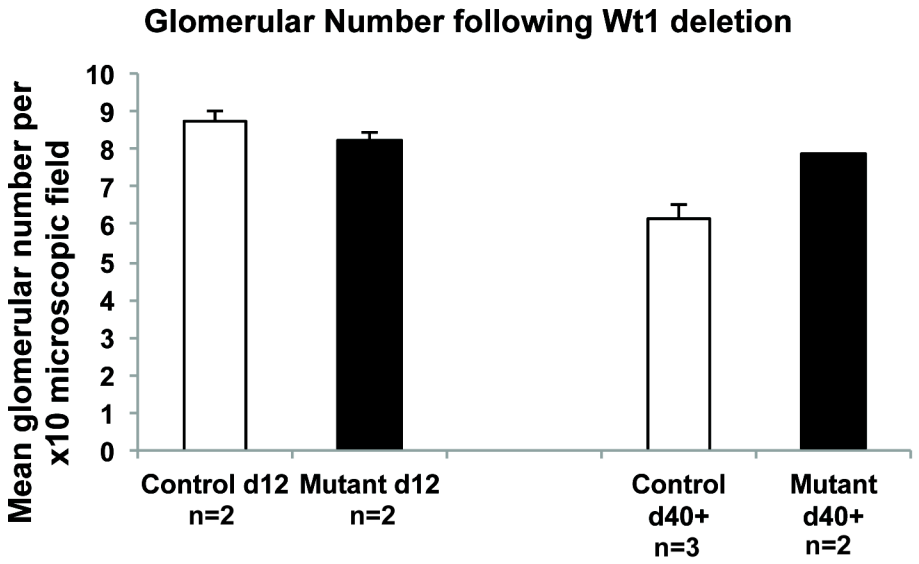

FIGURE 4.15: TOTAL GLOMERULAR NUMBER FOLLOWING *WT1*-DELETION

The total number of glomeruli per x10 magnification randomly chosen microscopic field were counted (30 different microscopic fields). No difference is seen between control and mutant mice at either day 12 or day 40. This analysis was not extended to the earlier time points, as the time-scale would be too short to expect any detectable reduction in glomerular number.

4.9 *Wt1* DELETION LEADS TO THE LOSS OF MAJOR PODOCYTE PROTEINS

Loss of expression of key podocyte proteins is associated with podocyte injury and/or depletion. As discussed above, *Wt1* is thought to be transcriptional activator of a number of key podocyte genes, including nephrin (*NPHS1*) and podocalyxin (*PODXL*). Following *Wt1* deletion, kidney cortex and/or isolated glomeruli were analysed for expression of key podocyte genes (Figure 4.16 A, B, C), and kidney sections analysed immunhistochemically for expression of these proteins Figure 4.16 D). Loss of these markers would indicate either loss of actual podocytes or loss of podocyte characteristics in damaged cells.

Marked down-regulation of major podocyte markers is seen following *Wt1* deletion, using quantitative RT-PCR for analysis of mRNA expression. Nephrin is a key component of the podocyte slit diaphragm and is essential for maintenance of the glomerular filtration barrier (Welsh and Saleem 2010). Nephrin expression is reduced dramatically following *Wt1* deletion, with mutant animals expressing only 1-2% of control levels. This can be seen in both isolated glomeruli and whole kidney cortex. This dramatic reduction is maintained even to the later time points. Such significant loss of nephrin would lead to loss of slit diaphragm architecture and failure of the glomerular filtration barrier. This is in keeping with the massive albuminuria seen following *Wt1* deletion. Unfortunately these results could not be verified at the protein level, as although a number of anti-nephrin antibodies were tried, none provided robust or reliable immunodetection.

This loss of nephrin expression following *Wt1*-deletion is in keeping with the previously published findings that nephrin is transcriptionally activated by *Wt1* (Wagner, Wagner et al. 2004). However, nephrin loss is a common finding in many examples of podocyte injury as a consequence of loss of slit diaphragm structures. Both these mechanisms may explain this finding.

Podocalyxin is another transcriptional target of Wt1 and is a trans-membrane sialomucin involved in maintenance of the glycocalyx and glomerular charge barrier. A small (approximately 20%) reduction in podocalyxin expression is seen by experimental day 8, which reaches significance in analysis of whole kidney cortex. However, at later time points (after day

12) an 88% reduction in podocalyxin expression in kidney cortex is seen in mutant animals. This is in keeping with the immunohistochemical data demonstrating significant loss of podocalyxin from the glomerulus (Figure 4.16 D).

Podocin is another constituent of the slit diaphragm, but is not known to be a direct transcriptional target of Wt1. Podocin expression is reduced by 90% in mutant glomeruli as early as day 8, and by 99% in mutant kidney cortex at later stages (after day 12). Immunofluorescence analysis of glomerular podocin protein expression reveals marked loss of podocin staining in mutant glomeruli, with loss of the normal linear capillary loop pattern, and a stippled, granular distribution in mutant glomeruli. Cre+ controls are unaffected (Figure 4.16 E). In *Wt1*$^{co/GFP}$ controls, podocin staining colocalises with GFP expression from GFP positive podocytes, although in mutant animals, podocin staining is again lost, and becomes dispersed and granular (Figure 4.16 F).

Synaptopodin is an actin-associated protein, associated with maintaining the architecture of the foot processes. A small, but not significant reduction in glomerular synaptopodin expression is seen in mutant glomeruli at day 8 (although biological replicate numbers are small). However, in kidney cortex at day 8 and after day 12, there is no detectable loss of synaptopodin expression. Synaptopodin protein expression in mutant glomeruli confirms these finding with only minimal loss of staining in mutant glomeruli at days 8 and 23. Interestingly, foci of brightly stained cells are also seen, which merit further investigation.

Zo-1 is a tight junction protein of the podocyte and expression levels in analysis of both *Wt1*-deleted glomeruli or kidney cortex do not reveal a change in overall gene expression between control and mutant animals.

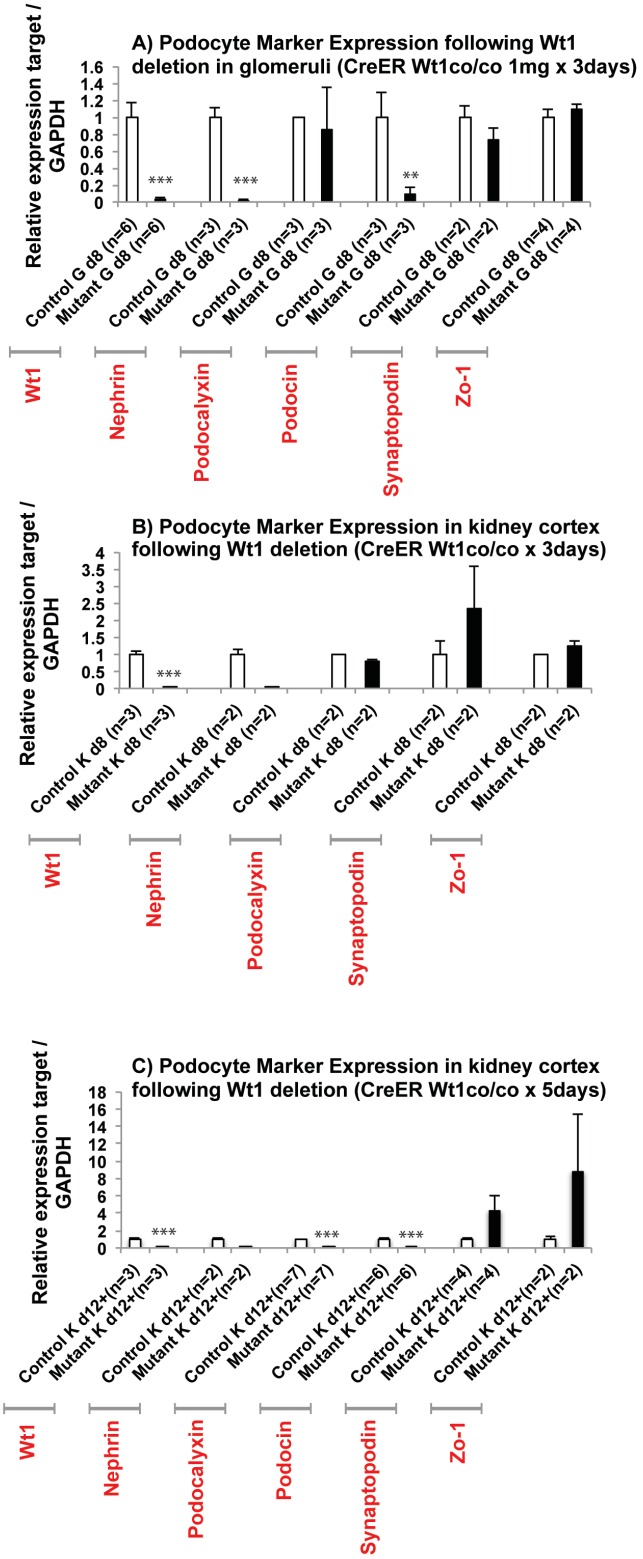
A) Podocyte Marker Expression following Wt1 deletion in glomeruli (CreER Wt1co/co 1mg x 3days)
Relative expression target / GAPDH
1.6
1.4
1.2
1
0.8
0.6
0.4
0.2
0
***
***
**
Control G d8 (n=6)
Mutant G d8 (n=6)
Control G d8 (n=3)
Mutant G d8 (n=3)
Control G d8 (n=3)
Mutant G d8 (n=3)
Control G d8 (n=3)
Mutant G d8 (n=3)
Control G d8 (n=2)
Mutant G d8 (n=2)
Control G d8 (n=4)
Mutant G d8 (n=4)
Wt1
Nephrin
Podocalyxin
Podocin
Synaptopodin
Zo-1
B) Podocyte Marker Expression in kidney cortex following Wt1 deletion (CreER Wt1co/co x 3days)
Relative expression target / GAPDH
4
3.5
3
2.5
2
1.5
1
0.5
0
***
Control K d8 (n=3)
Mutant K d8 (n=3)
Control K d8 (n=2)
Mutant K d8 (n=2)
Control K d8 (n=2)
Mutant K d8 (n=2)
Control K d8 (n=2)
Mutant K d8 (n=2)
Control K d8 (n=2)
Mutant K d8 (n=2)
Wt1
Nephrin
Podocalyxin
Synaptopodin
Zo-1
C) Podocyte Marker Expression in kidney cortex following Wt1 deletion (CreER Wt1co/co x 5days)
Relative expression target / GAPDH
18
16
14
12
10
8
6
4
2
0
***
***
***
Control K d12+(n=3)
Mutant K d12+(n=3)
Control K d12+(n=2)
Mutant K d12+(n=2)
Control K d12+(n=7)
Mutant d12+(n=7)
Conrol K d12+(n=6)
Mutant K d12+(n=6)
Control K d12+(n=4)
Mutant K d12+(n=4)
Control K d12+(n=2)
Mutant K d12+(n=2)
Wt1
Nephrin
Podocalyxin
Podocin
Synaptopodin
Zo-1

D

Control d44: anti-Podocalyxin

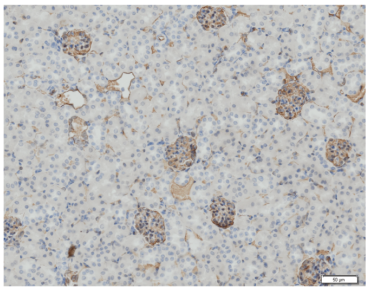

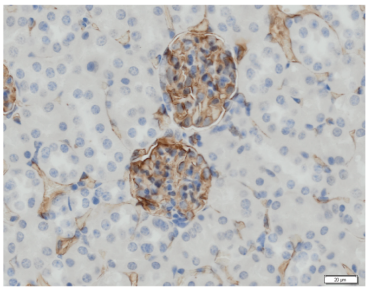

Secondary Ab alone

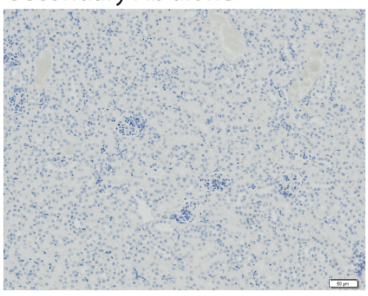

Mutant d44: anti-Podocalyxin

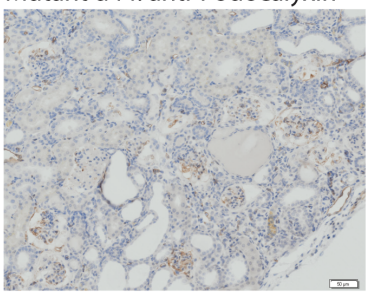

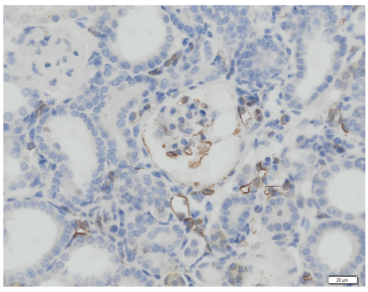

Control d12: anti-Podocalyxin

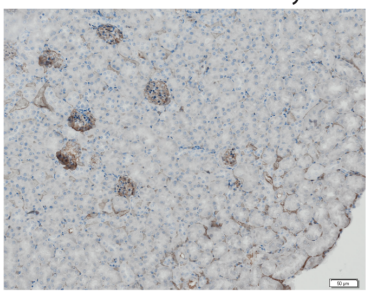

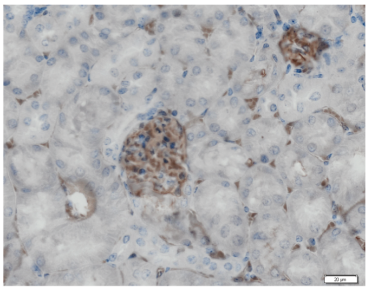

Secondary Ab alone

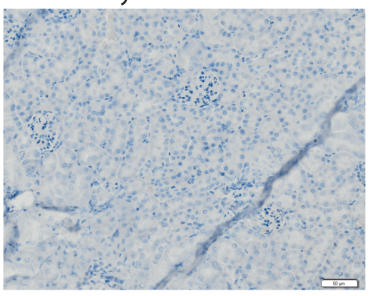

Mutant d12: anti-Podocalyxin

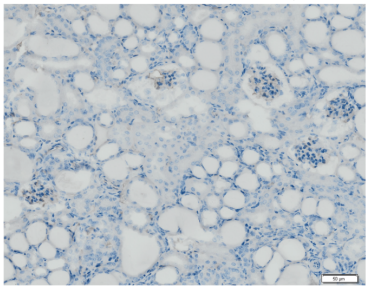

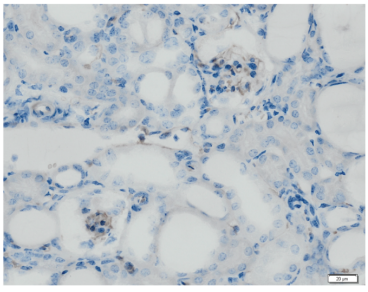

E

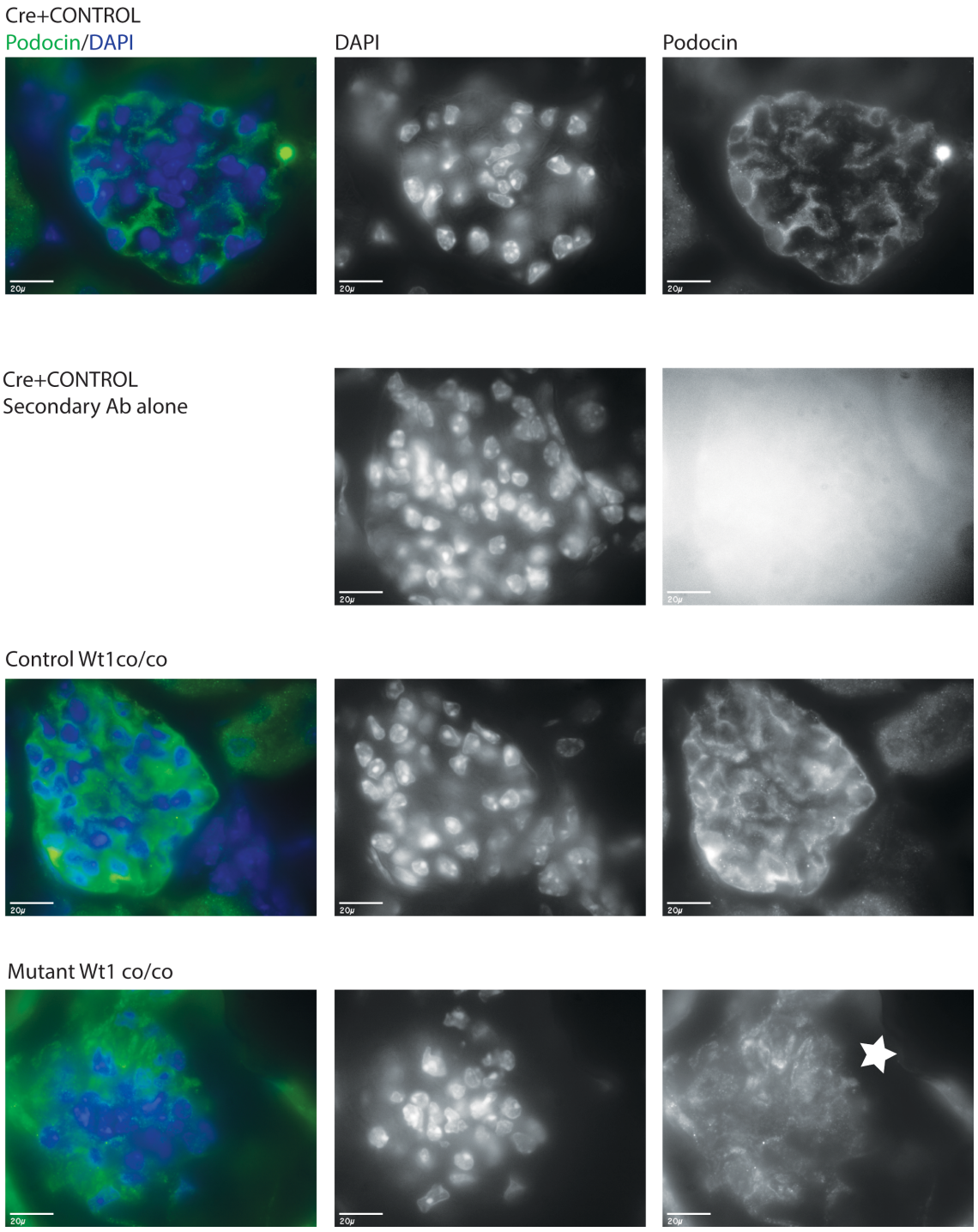
Cre+CONTROL
Podocin/DAPI
DAPI
Podocin
Cre+CONTROL
Secondary Ab alone
Control Wt1co/co
Mutant Wt1 co/co
20μ

F

Control Wt1co/GFP

Podocin/GFP | Podocin | GFP

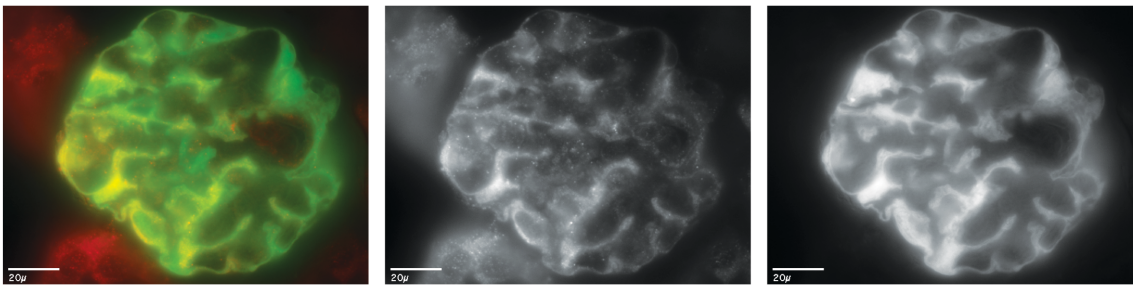

Mutant Wt1co/GFP

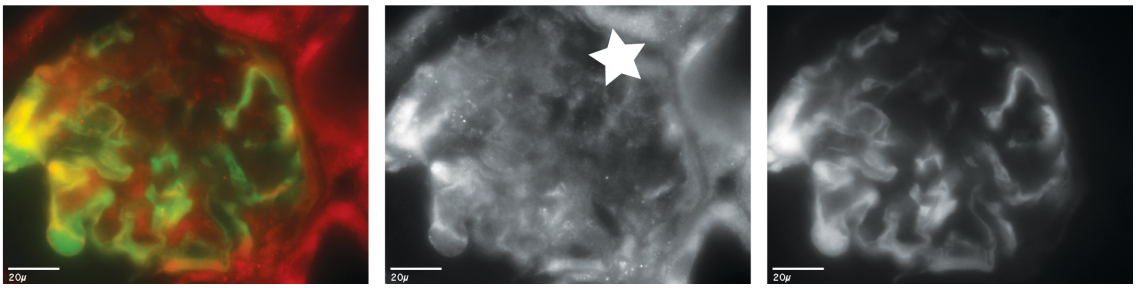

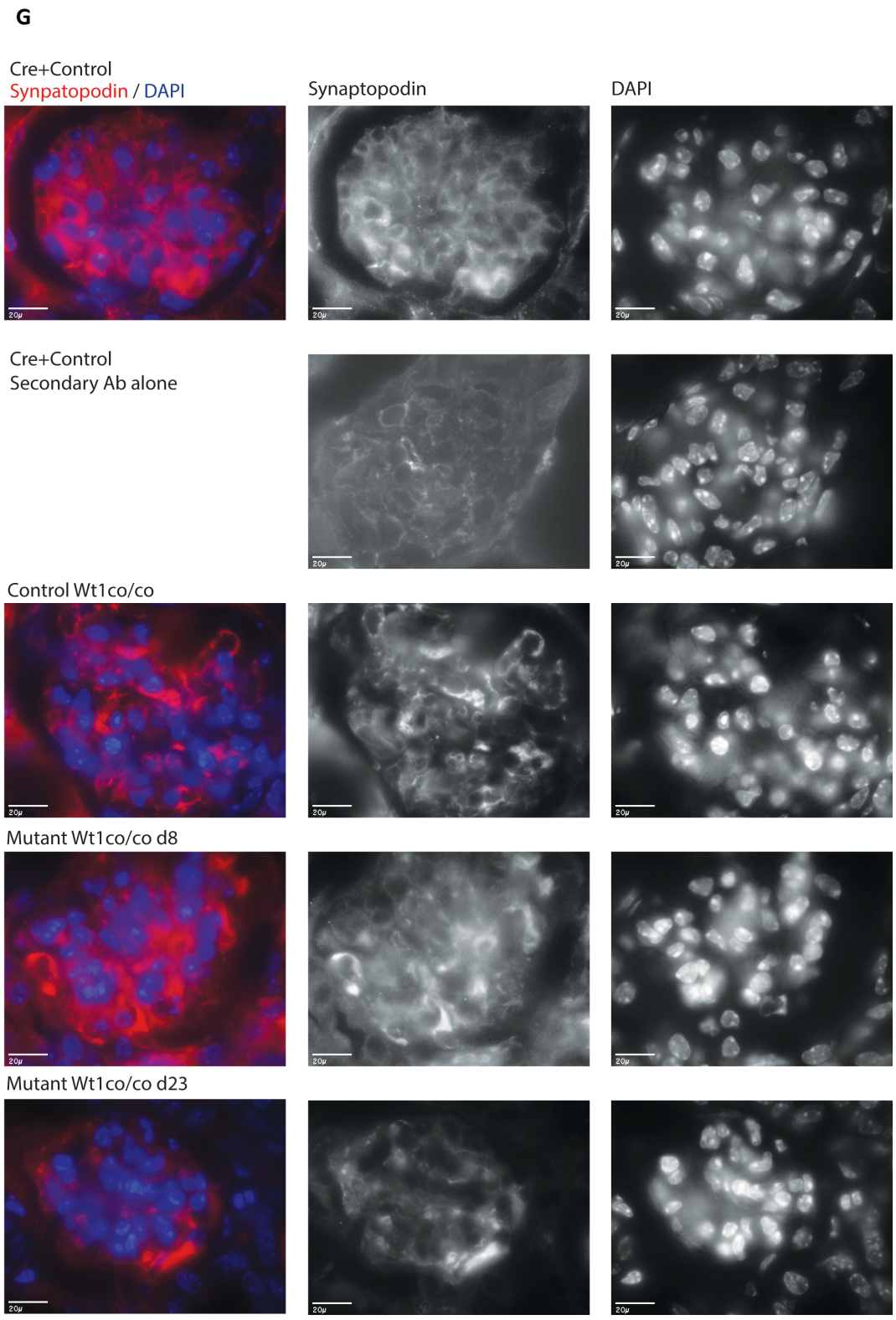

FIGURE 4.16: PODOCYTE MARKER EXPRESSION FOLLOWING *WT1* DELETION

FIGURE 4.16: PODOCYTE MARKER EXPRESSION FOLLOWING WT1 DELETION

A, B, C) Quantitative RT-PCR for mRNA expression following *Wt1*-deletion. N-numbers represent biological replicates. Each experiment was performed in triplicate. Data points represent means of fold-change difference from control (assigned value of 1). Error bars represent S.E.M. A) Podocyte marker expression in **isolated glomeruli** following *Wt1* deletion (CreER $Wt1^{co/co}$ 1mg/40gBW x 3 days). B) Podocyte marker expression in **kidney cortex** following *Wt1* deletion (CreER $Wt1^{co/co}$ 1mg/40gBW x **3** days). C) Podocyte marker expression in **kidney cortex** following *Wt1* deletion (CreER $Wt1^{co/co}$ 1mg/40gBW x **5** days). (* $p<0.05$; ** $p<0.01$; *** $p<0.001$ analysed using students T-test, non-parametric data analysed using M.U.W.) D) IHC for podocalyxin. Control animals exhibit strong staining throughout the glomerulus. This is mostly lost in *Wt1*-deleted mutant animals. E) IF for podocin: Control and Cre+control animals demonstrate normal linear staining delineating the capillary loop architecture. Mutant animals show loss of fluorescence, which becomes granular and poorly demarcated (star). F) IF for podocin in CreER $Wt1^{co/GFP}$ animals: Podocin co-localises with GFP (Wt1) expression in the podocyte. Again, there is loss of fluorescence and the linear staining pattern in mutant animals (star). G) IF for synaptopodin expression. Mutant animals display only subtle loss of staining in the glomerulus at both early and later time stages. Foci of brightly stained cells can also be seen following *Wt1* loss.

4.10 *Wt1* DELETION DOES NOT LEAD TO SIGNIFICANT PODOCYTE LOSS OR DETATCHMENT.

The dramatic loss of podocyte-specific proteins seen in *Wt1* deleted glomeruli could be explained by death and detachment of *Wt1* deleted podocytes. Therefore it was important to assess whether podocytes were being lost from Wt1-deleted glomeruli. Given the degree of glomerular injury, histological identification of podocytes was very difficult. Traditionally, the standard method of estimating podocyte number has been by counting the number of Wt1-positive cells per glomerulus (He, Kang et al. 2011, Toyonaga, Tsuruya et al. 2011, Tuncdemir and Ozturk 2011). Clearly, this method was unsuitable in this model of *Wt1* deletion. Therefore, the CreER$Wt1^{co/GFP}$ model was utilized. This model has been well-characterised and faithfully recapitulates *Wt1*-expression *in vivo* (Hosen, Shirakata et al. 2007, Martinez-Estrada, Lettice et al. 2010). *Wt1* is deleted from the conditional allele while GFP expression was maintained at sites of active *Wt1* promoter activity. As this model is dynamic, GFP expression would be lost (influenced by the inherent stability of the GFP protein within the cell) if *Wt1*-promoter activity was absent. However, it offered a useful surrogate measure of the presence or loss of previously Wt1-positive cells from the glomerulus following *Wt1*-deletion.

4.10.1 CreERWt1$^{co/GFP}$ MICE EXHIBIT STRONG GFP EXPRESSION IN THE RENAL PODOCYTES.

Endogenous GFP expression can be easily visualized on cryosections of CreER $Wt1^{co/GFP}$ kidney. As the GFP is a knock-in construct the protein is not specifically localized within the cell (the majority of Wt1 is nuclear) so the GFP protein can be seen throughout the podocyte, delineating the podocyte foot processes. In Cre-negative $Wt1^{co/GFP}$ controls or uninjected Cre-positive $Wt1^{co/GFP}$ animals, strong and consistent GFP expression is seen throughout the glomerulus and is seen in every glomerulus (Figure 4.17 A).

Following *Wt1* deletion, there is only partial loss of GFP expression from the glomerulus, demonstrating that few GFP-expressing podocytes have been lost. This indicates that the profound loss of podocyte markers is not simply a consequence of podocyte detachment (Figure 4.17 B, C & D).

As the *Wt1*$^{co/GFP}$ model only survived up to day 8, this analysis is early, so it is possible that *Wt1*-deleted podocytes would eventually detach. However, even at this early time point, significant loss of podocyte markers was demonstrated, despite the majority of podocytes remaining present on the glomerulus. Therefore, it appears, there is a definite loss of expression distinct from a simple loss of cells.

A) Control d8

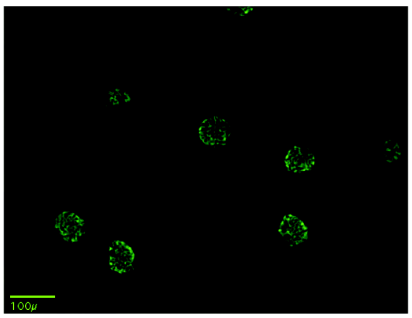

Normal glomerular fluorescence

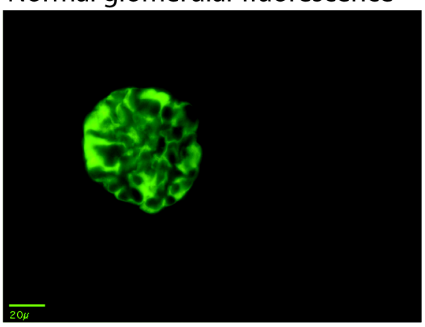

B) Mutant d8

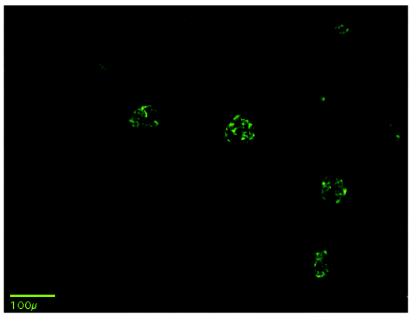

1) Normal glomerular fluorescence

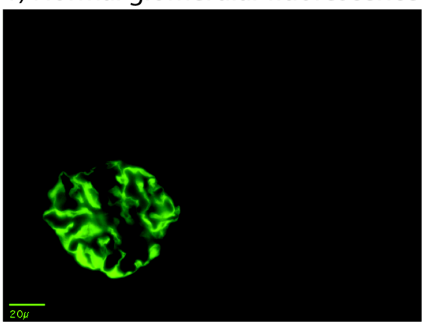

2) 25-50% fluorescence lost

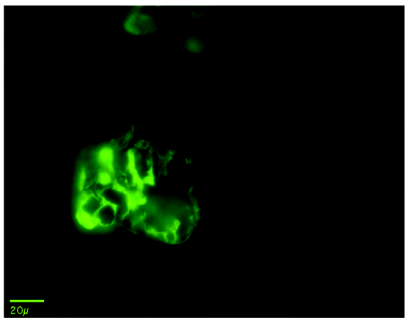

3) 50-75% fluorescence lost

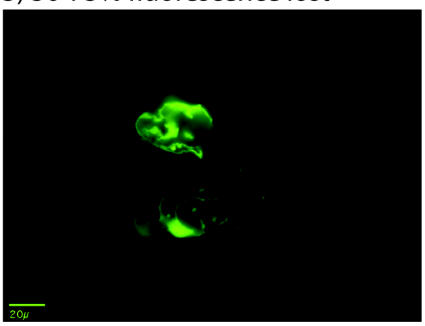

4) 75-100% fluorescence lost

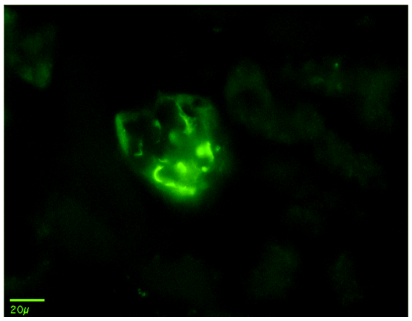

5) Differently affected glomeruli

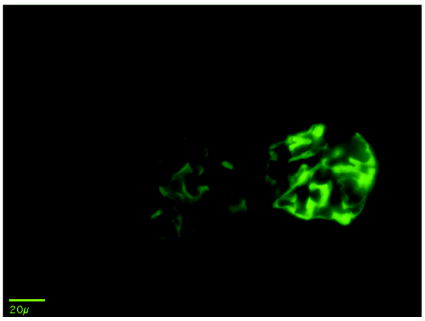

C) Control d4

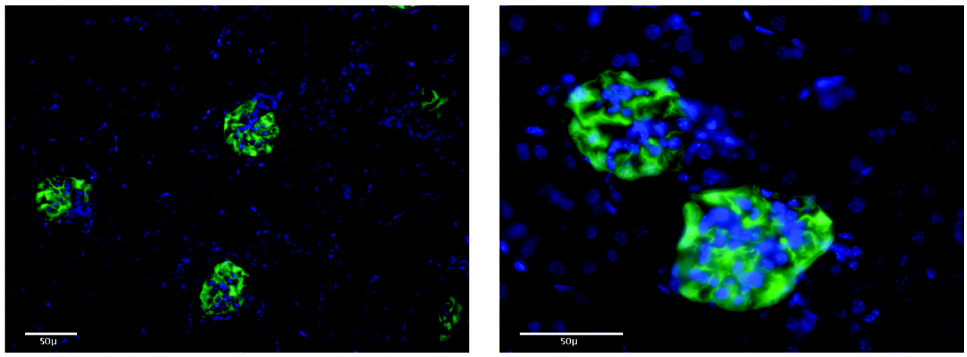

Mutant d4

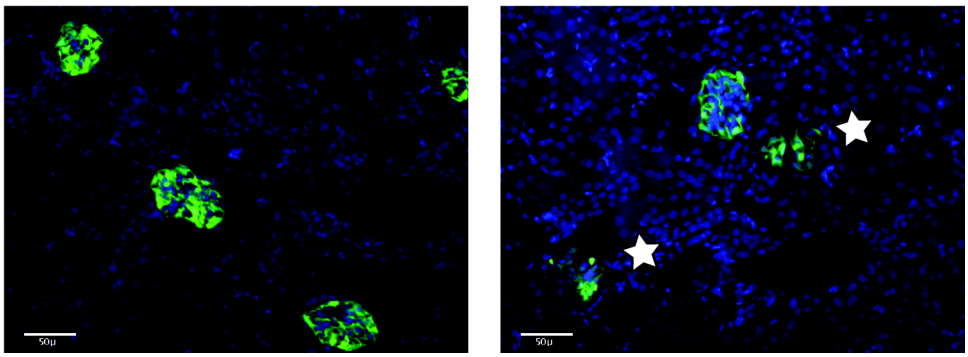

D

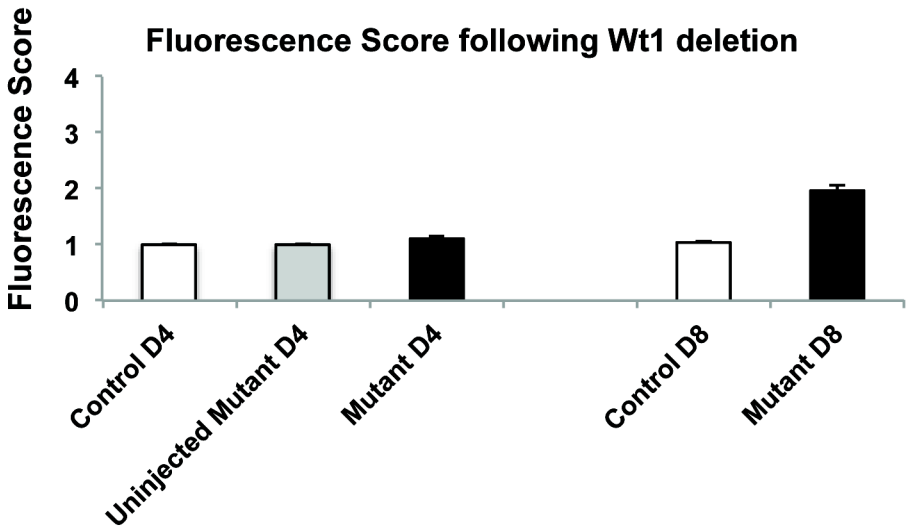

FIGURE 4.17: USING THE *WT1*$^{CO/GFP}$ MOUSE TO ESTIMATE PODOCYTE LOSS FOLLOWING *WT1* DELETION

A) Endogenous fluorescence in CreER *Wt1*$^{co/GFP}$ mice. In control animals all glomeruli exhibit uniform linear fluorescence consistent with the podocytes enveloping the glomerular capillaries. B) Loss of fluorescence following *Wt1* deletion (day 8). In the x10 magnification some glomeruli exhibit normal fluorescence, but others show patchy areas where fluorescence has been lost. A degree of podocyte loss will lead to denuded areas where no fluorescent podocytes remain. Glomeruli were scored visually according to the size of the area in which fluorescence had been lost (1 = 0-25% loss; 2 = 25-50% loss; 3 = 50-75% loss; 4 = 75-100% loss). C) At day 4 little difference is seen between control and mutant animals. By day 8 most mutant animals had lost up to 25-50% of the fluorescent area. D) Quantification of fluorescence score across 50 glomeruli per animal. At day 4 little difference is seen between control and mutant animals. However by day 8 most mutant animals had lost up to 25-50% of the fluorescent area, although some glomeruli remained normal (C star).

4.11 *Wt1* LOSS AFFECTS THE EPITHELIAL TO MESENCHYMAL BALANCE IN ADULT KIDNEY

A key theme of this project was to investigate the role of *Wt1* in maintaining the unique epithelial-mesenchymal characteristics of adult podocytes. *Wt1* is known to play a direct role in controlling mesenchymal to epithelial transition during kidney development and in controlling the opposite process, epithelial to mesenchymal transition, during heart development, via direct transcriptional regulation of E-cadherin and Snail (Davies, Ladomery et al. 2004, Rigby, Leitch et al. 2008, Martinez-Estrada, Lettice et al. 2010).

Therefore it was hypothesized that *Wt1*-loss would lead to a change in the epithelial-mesenchymal balance in podocytes, thus affecting their specialized function.

Initial analysis of the expression of key epithelial and mesenchymal genes revealed interesting findings following *Wt1* deletion. In *Wt1*-deleted glomeruli there was a rapid and early increase in the expression of the key mesenchymal drivers, Snail, Slug and Zeb-1 (Figure 4.18 A). This was followed by an increase in expression of the mesenchymal markers vimentin, desmin and fibronectin (Figure 4.18 B), which had occurred by day 8. Most intriguingly, in this early analysis, there was no detectable loss of expression of the epithelial markers P-cadherin and Zo-1 (Figure 4.18 C). This was initially detected on analysis of whole kidney cortex, so was interpreted to be an off-target effect due to the massive glomerular injury. However, as demonstrated in figure 4.18, the same pattern was also demonstrated in isolated glomeruli.

Marker expression alone represents only one aspect of the epithelial-mesenchymal characteristics of a cell type. Although not possible within the time frame of this project, ultrastructural analysis following *Wt1* deletion is now being undertaken, using scanning electron microscopy to analyse cell-cell junctions and the degree of foot process effacement. Although these studies are ongoing, preliminary analysis of *Wt1*-deletion using the high-dose tamoxifen model does reveal substantial foot process effacement, indicating alteration of the specialized tight junctions (the slit diaphragms) between podocytes (Chau, Brownstein et al. 2011). As nephrin is a key constituent of the slit diaphragm, and nephrin expression decreases dramatically following *Wt1* deletion, it is likely that the slit diaphragms (adherens junctions) are lost in keeping with an alteration of the specialized epithelial-mesenchymal balance. Further evidence

to support this would be the development of massive albuminuria, demonstrating a failure of the glomerular filtration barrier.

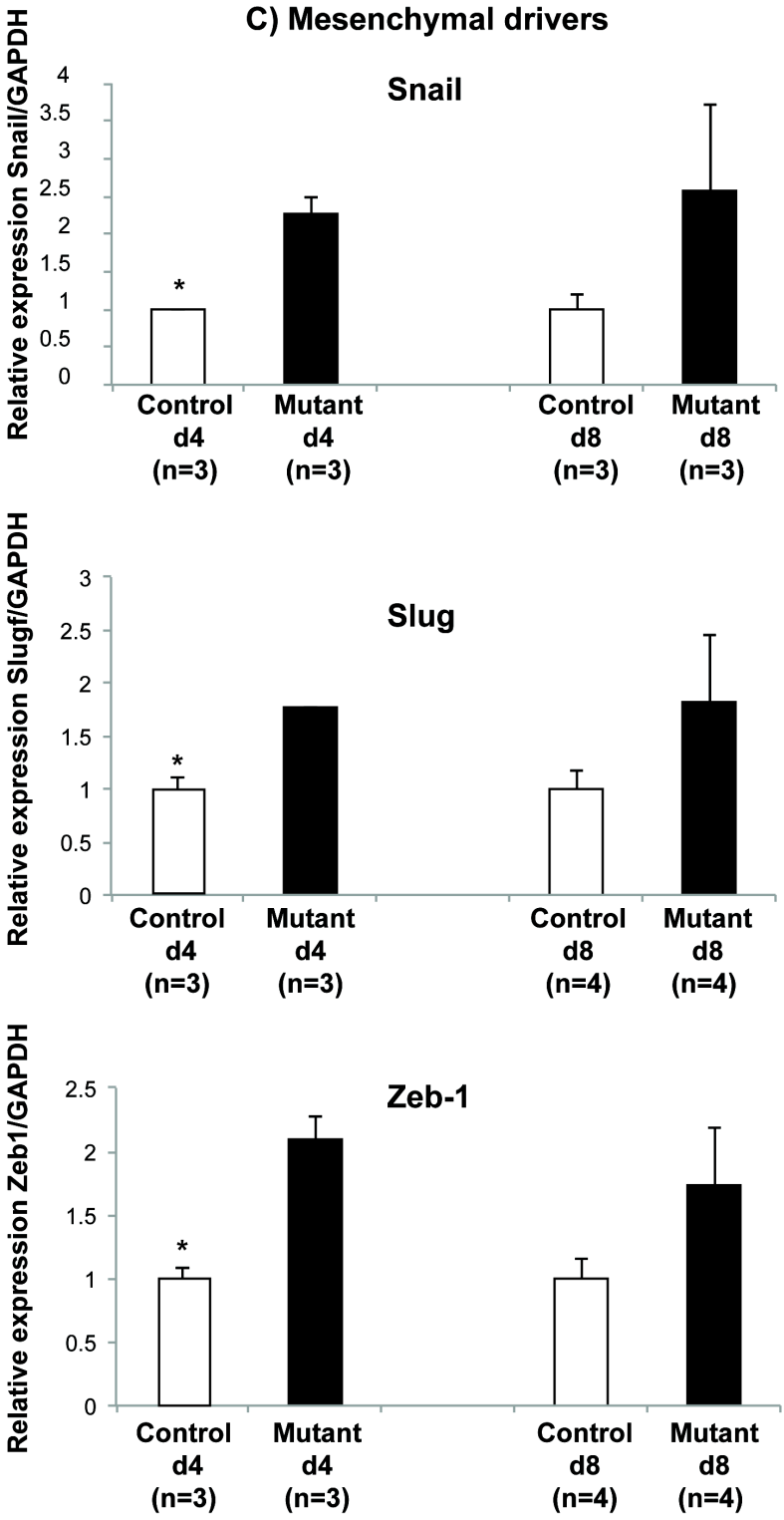
C) Mesenchymal drivers
Snail
Relative expression Snail/GAPDH
4
3.5
3
2.5
2
1.5
1
0.5
0
*
Control d4 (n=3)
Mutant d4 (n=3)
Control d8 (n=3)
Mutant d8 (n=3)
Slug
Relative expression Slugf/GAPDH
3
2.5
2
1.5
1
0.5
0
*
Control d4 (n=3)
Mutant d4 (n=3)
Control d8 (n=4)
Mutant d8 (n=4)
Zeb-1
Relative expression Zeb1/GAPDH
2.5
2
1.5
1
0.5
0
*
Control d4 (n=3)
Mutant d4 (n=3)
Control d8 (n=4)
Mutant d8 (n=4)

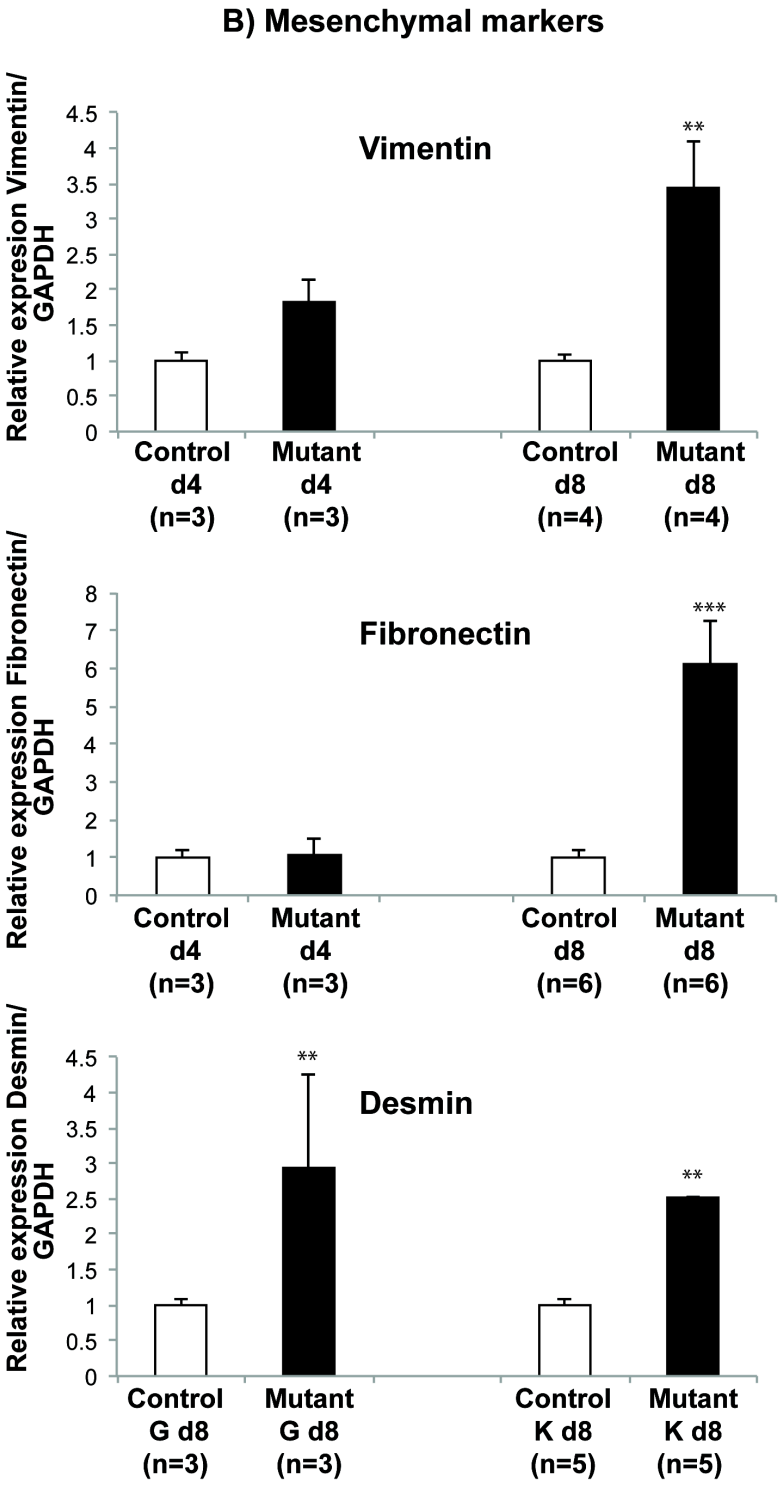
B) Mesenchymal markers
Relative expresion Vimentin/ GAPDH
Vimentin
**
4.5
4
3.5
3
2.5
2
1.5
1
0.5
0
Control d4 (n=3)
Mutant d4 (n=3)
Control d8 (n=4)
Mutant d8 (n=4)
Relative expression Fibronectin/ GAPDH
Fibronectin
***
8
7
6
5
4
3
2
1
0
Control d4 (n=3)
Mutant d4 (n=3)
Control d8 (n=6)
Mutant d8 (n=6)
Relative expression Desmin/ GAPDH
Desmin
**
**
4.5
4
3.5
3
2.5
2
1.5
1
0.5
0
Control G d8 (n=3)
Mutant G d8 (n=3)
Control K d8 (n=5)
Mutant K d8 (n=5)

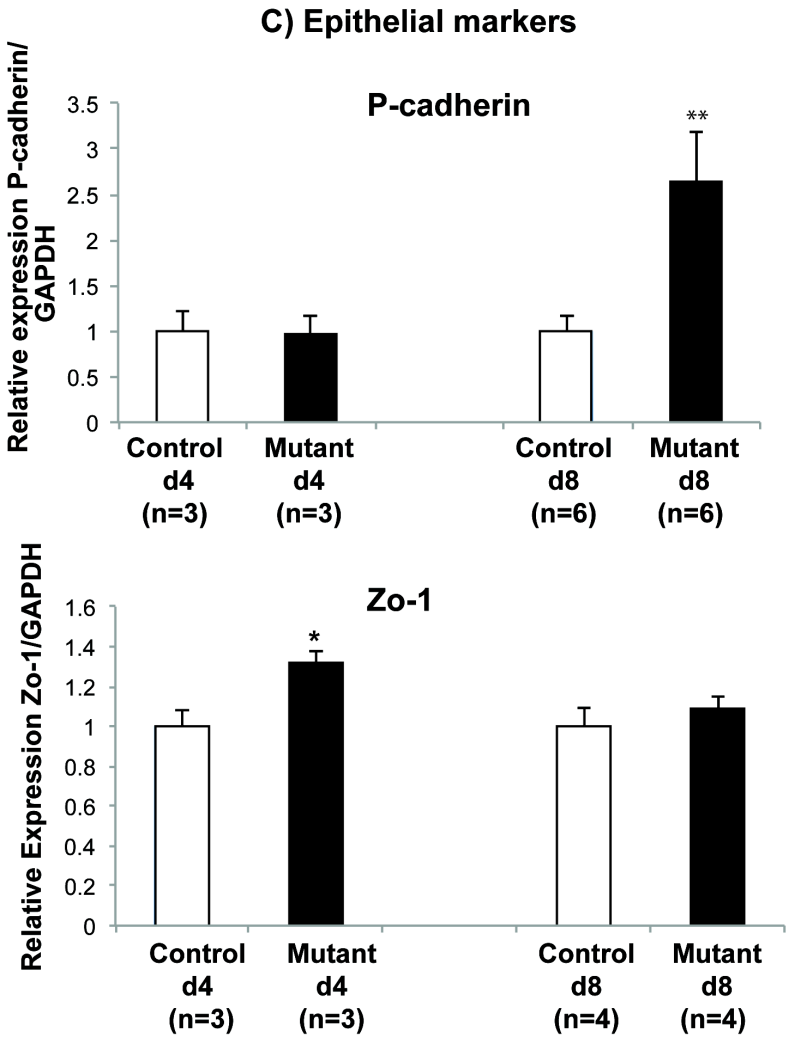

FIGURE 4.18: QUANTITATIVE RT-PCR FOR MRNA EXPRESSION OF KEY EPITHELIAL AND MESENCHYMAL MARKERS IN WT1 DELETED GLOMERULI

A) Mesenchymal drivers such as Snail, Slug and Zeb-1 increase early after *Wt1* deletion, with significant increases detected as early as day 4. B) By day 8 mesenchymal markers such as fibronectin, desmin and vimentin also increase. C) However, no resultant loss of epithelial markers is seen.

4.12 WT1-DELETION LEADS TO RE-EXPRESSION OF WNT4, CONSISTENT WITH EARLIER DEVELOPMENTAL PATHWAYS

Given the importance of *Wt1* during renal development, it was decided to analyse *Wt1*-deleted kidneys for evidence of re-expression of developmental pathways. During nephrogenesis, Wt1 controls mesenchymal to epithelial transition of the developing nephron, via regulation of *Wnt4*. *Wnt4* is expressed throughout the MET stage of renal development, but not in adult kidney. However, in *Wt1*-deleted kidneys a 6-fold increase in *Wnt4* expression is found as early as day 8 (Figure 4.19). This would be in keeping with the previous data that *Wt1* plays a repressive role with regard to *Wnt4* expression in adult kidney.

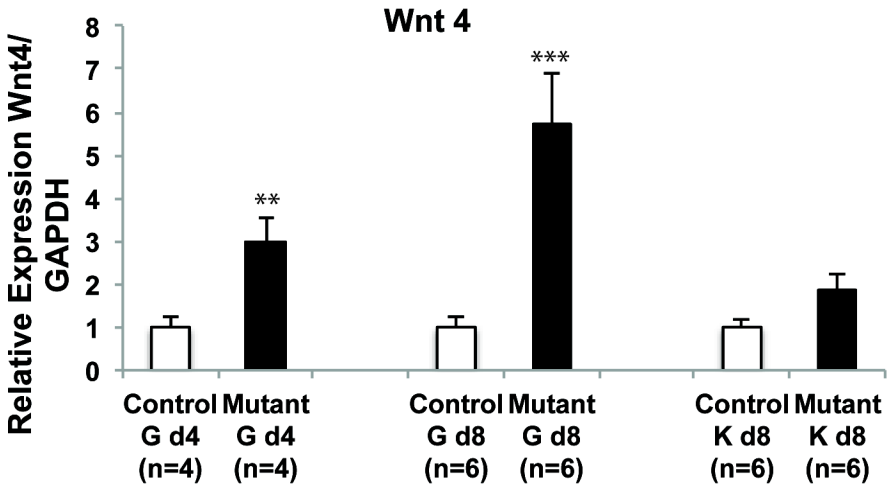

FIGURE 4.19: QUANTITATIVE RT-PCR FOR MRNA EXPRESSION OF WNT4 IN WT1 DELETED GLOMERULI.

4.13 SUMMARY OF FINDINGS

This project has demonstrated the essential role of *Wt1* in adult kidney, which, before the start of this project had not been conclusively proven.

Wt1-deletion in the adult mouse leads to

1) Early death
2) Oedema, massive albuminuria and hypoalbuminaemia, consistent with severe nephrotic syndrome, indicating failure of the glomerular filtration barrier
3) Severe damage to podocytes and parietal epithelial cells
4) Loss of key podocyte markers
5) Dysregulation of the epithelial-mesenchymal balance in podocytes
6) Upregulation of Wnt4 and other developmental pathways

4.14 DISCUSSION

4.14.1 OVERVIEW OF ANALYSIS

The CreER $Wt1^{co/co}$ model provided an inducible and conditional model of *Wt1* deletion, allowing analysis of the consequences of *Wt1* loss in the adult, whilst avoiding any confounding developmental phenotypes.

This model was already available at the start of the project, so formed the basis of analysis of the renal phenotype. However, it must be highlighted that the use of the ubiquitously expressed Cre-recombinase meant that *Wt1* deletion was not limited solely to the podocyte. During the course of this project, a preliminary analysis of the consequences of whole-body *Wt1* deletion has been published (Chau, Brownstein et al. 2011). As discussed earlier, this revealed some interesting and surprising extra-renal effects. The existence of such extra-renal effects may have consequences for the renal phenotype analysed, hence, the requirement for generating a podocyte specific model of *Wt1* deletion (see Chapter 5). However, this model used a higher dose of tamoxifen to achieve almost complete recombination, ensuring *Wt1* was deleted everywhere. Using a lower dose of tamoxifen as in this project led to mosaic recombination events and ameliorated the phenotype. It is also important to highlight that none of the extra-renal effects noted in the high-dose model would be predicted to directly affect the podocyte. Most notably, there was no evidence of any systemic inflammatory response, which may have influenced the renal phenotype.

Optimising the analysis of the renal phenotype proved challenging, and meant the number of biological replicates in each experimental group was limited, and a number of different time points and dosing regimens were analysed, with only few animals per group. The relevant dosing regimens and time of sacrifice are detailed for each experiment, but as, discussed below, little difference in *Wt1* loss is seen between the 5-day and 3-day dosing regimens, so the findings are discussed in combination. Having now optimized the protocol, a further analysis at 10 or 12 days would be useful, which would be predicted to demonstrate the development of frank renal failure.

Analysis of whole kidney cortex was quick and straightforward and provided abundant sample material. However, although quantitative RT-PCR was sensitive enough to detect differences between control and mutant animals, any differences would include the effect on other renal cell-types, presumably secondary effects. Therefore analysis of a pure or enriched podocyte population was required. Glomerular isolation provided tissue samples highly enriched for podocytes, to allow sensitive detection of any differences between control and *Wt1*-deleted animals. However, this protocol produced only tiny samples, so histological analysis could not be carried out on the same animals, limiting the numbers of experimental animals still further. As whole glomeruli were isolated, analysis also unfortunately included mesangial cells and endothelial cells, so the results would not cleanly reflect the effects of *Wt1*deletion specifically on podocytes. As *Wt1*is not expressed by either endothelial cells or mesangial cells, these should not experience any direct effects from the consequences of *Wt1* deletion, although they may have been affected by the adjacent podocyte injury (Wharram, Goyal et al. 2005, Mollet, Ratelade et al. 2009).

FACS isolation of fluorescently-labelled podocytes allows specific isolation and analysis of a pure podocyte population. However, finding a usable method, which provided sufficient sample material for adequate analysis, was not possible during the time-frame of this project. Subsequently, as a workable new protocol has now been optimised, this will be used for future analysis of *Wt1*-deleted podocytes. In combination with novel approaches to analyse small amounts of experimental tissue e.g. RNeasy Micro Kit (Qiagen 74004) or Fluidigm single-cell analysis (Citri, Pang et al. 2012) , specific analysis of Wt1-deleted podocytes should be possible.

4.14.2 WHY DIDN'T REDUCING THE TAMOXIFEN DOSE ALWAYS SIGNIFICANTLY IMPROVE SURVIVAL?

In the initial pilot experiment, the mutant mice receiving 1mg/40g BW tamoxifen for 5 days survived over a month. This result was never achieved with subsequent experiments and the tamoxifen dose had to be cut still further to 3 days. This resulted in only small effects on prolonging survival.

Assessment of Cre-recombinase efficiency using an YFP-reporter demonstrated a dose-dependent reduction in the number of Cre-recombination events, in keeping with the published literature (Hayashi and McMahon 2002). However, even at the lowest doses of tamoxifen, there was still a dramatic reduction in *Wt1* gene and protein expression.

The CreER $Wt1^{co/co}$ mice were originally in a mixed background, but were being serially inbred onto a C57/BL6 background to maintain the line and reduce genetic heterogeneity. This may have exacerbated the phenotype in later generations and contributed to the sensitivity to tamoxifen. If further time had been available, analysis of a further range of dosing schedules, using both a reporter and analysed in terms of *Wt1*-loss and disease-free survival, would have been useful.

The phenotype was even more marked in the $CreERWt1^{co/GFP}$ animals. As a consequence of the GFP knock-in allele these mice are compound heterozygote for *Wt1*. This does not seem to significantly affect renal development or renal function in early adult life but would mean only one Cre-recombination event was required per cell to completely delete *Wt1* from the kidney. It is also possible that this compound heterozygosity lead to altered *Wt1* expression during development so $CreERWt1^{co/GFP}$ podocytes and associated glomerular cells were already abnormal and therefore more susceptible to both primary and secondary damage. However, any glomerular abnormalities prior to *Wt1* deletion were not detectable histologically or immunohistochemically.

It has recently been shown conclusively that podocyte damage affecting only a limited number of podocytes also causes damage to other cells within the glomerulus (Matsusaka, Sandgren et al. 2011). Chimeric mice, in which only a subpopulation of podocytes expressed hCD25 (the receptor for the immunotoxin LMB2), were treated with intravenous immunotoxin LMB2. This

caused toxin-mediated injury only to the hCD25+ podocyte population. However, the authors also found that secondary injury, to podocytes that were not susceptible to LMB2, occurred as early as day 4 after the primary toxin injury. The degree of this damage correlated closely with the proportion of podocytes damaged by the primary injury. This and other studies, suggest a threshold of injury (e.g. <25% of total podocytes), which, if broached, results in progressive damage (Wharram, Goyal et al. 2005).

Although the CreER*Wt1*$^{co/co}$ mice were analysed early after the initial injury (*Wt1* deletion) it is still possible that secondary injury to other podocytes was already occurring, contributing to the severe phenotype. If this were the case, in order to abrogate it, *Wt1*deletion would have to be limited to a very small number of podocytes (e.g. less than 25%), which would make analysis of the direct consequences of *Wt1*deletion very difficult. Therefore, given the aims of this project, it was better to maintain a significant degree of *Wt1* loss and analyse the phenotype early, to focus on the primary effects of *Wt1* loss.

4.14.3 WHY DID THE MICE DIE?

As discussed, *Wt1* deletion led to early death in adult mice. However, analysis of renal filtration function (in terms of serum urea and creatinine) revealed only a small rise in urea by day 8. This in itself cannot explain why the animals died (or were so close to death). However, this result is artificial, as the 8 day time point was chosen to precede any clinical deterioration to ensure all experimental material could be harvested and analysed. Therefore, it pre-empted the significant clinical deterioration seen in the survival analyses. Unfortunately, serum analyses were not possible during these initial pilot experiments in which animals were followed until death or until they required euthanasia.

In work carried out and published by Chau *et al*, documenting the preliminary analysis of the renal affects of *Wt1* deletion using the high-dose tamoxifen regime (4mg/40g bodyweight x 5 days), a similar pattern is seen, with early maintenance of glomerular filtration function, yet with a rise in serum urea and creatinine by day 10. Numbers were too small for this to be significant in terms of creatinine. Therefore, in these experiments, although renal failure was not detected at day 8, it is likely this, in combination with the severe oedema, accounted for the clinical deterioration and death in these animals at later stages. Importantly, the animals were sacrificed

for humane reasons, so the presence of significant oedema, with its effects on mobility and respiration, meant they had to be sacrificed to avoid unnecessary suffering. Macroscopically, on inspection at necropsy, the hearts, lungs and liver looked normal, and on more detailed analysis by Chau and Brownstein, both lungs and heart were normal, so were unlikely to contribute to the early death (Chau, Brownstein et al. 2011). This is of particular importance given the known roles of *Wt1* in cardiac development, thus implying *Wt1* deletion may have affected the heart in the adult.

4.14.4 *Wt1* deletion causes significant albuminuria and hypoalbuminaemia, consistent with failure of the glomerular filtration barrier

Wt1-deleted mice develop profound albuminuria and serum hypo-albuminaemia consistent with failure of the glomerular filtration barrier. Protein leak is the hallmark of podocyte damage (Kriz and LeHir 2005), so this finding is consistent with *Wt1*deletion leading to a rapid podocyte injury and failure of podocyte and glomerular filtration barrier function. No such effect was seen in the Cre-positive control mice injected with tamoxifen, so this was not due to a tamoxifen or Cre-toxicity effect.

It must be noted that mutant animals had more albuminuria even at baseline, most evident in the $Wt1^{co/GFP}$ line. This is probably due to a low degree of 'leaky' Cre-recombination, even without the presence of tamoxifen (Hayashi and McMahon 2002). No difference was detected between the Cre-negative $Wt1^{co/co}$ and Cre-negative $Wt1^{co/GFP}$ control animals, indicating that there was no effect from the compound *Wt1*-heterozygosity in early adult life (although glomerulosclerosis has been shown to develop in Wt1-heterozygotes in later life (Menke, A et al. 2003)).

The existence of albuminuria at baseline indicates there must be a low level of glomerular damage causing the protein leak. As there is no difference between serum albumin and serum urea and creatinine in Cre-negative and Cre-positive animals even at day 4, and in uninjected Cre-positive animals, it is unlikely this degree of glomerular damage is significant. Certainly, there is little evidence of damage histologically, although, as in human Minimal Change Disease, histological analysis can miss podocyte lesions such as foot process effacement. Analysis of podocyte ultrastructure using scanning electron microscopy will help clarify whether there is any

evidence of pre-existing podocyte damage before tamoxifen–induced Cre-recombination and *Wt1*-deletion.

A degree of pre-existing glomerular damage should be taken into account, as pre-existing damage would increase the vulnerability of mutant kidney to further injury, caused by the *Wt1*deletion. Ideally, comparing the vulnerability of Cre-negative and Cre-positive animals prior to *Wt1* deletion, to other models of glomerular injury (e.g. Adriamycin-nephropathy, passive Heymann nephritis) would help clarify the degree of pre-existing damage, as histology and IHC may not be sensitive enough (Ohse, Vaughan et al. 2010).

However, as the consequence of 'leaky' Cre-recombination is, in fact, low-level *Wt1*-deletion, this does not detract from the phenotype observed, and actually supports the conclusion that *Wt1* is essential for adult podocyte function. The only possible confounding effect could be a slight exacerbation of the damage caused by widespread Wt1 deletion, if this occurred on an already vulnerable kidney.

4.14.5 Altering the tamoxifen dose did not appear to alter the degree of Wt1 loss.

As discussed above, there appears to be limited / undetectable differences in *Wt1* loss between mice injected with 3 days or 5 days of tamoxifen. However, when comparing dosing regimens using a YFP-reporter line (see above), Cre-recombination efficiency did appear to be dose dependent. This could be explained in that *Wt1*-deletion may have simply been more efficient than expression of the YFP reporter. Alternatively, as mentioned previously, there is significant evidence that a) podocyte injury damages other podocytes and b) podocyte damage itself is associated with *Wt1* loss, although whether this is due to cell loss or a reduction in *Wt1* expression from remaining cells remains to be elucidated.

4.14.6 *Wt1* deletion in the kidney leads to both podocyte and PEC damage and tubular injury

Significant damage to both podocytes and parietal cells is seen following *Wt1* deletion. Traditionally, only podocytes are thought to express *Wt1*. Counting the number of Wt1-positive cells is an established method for estimating podocyte number. However, accumulating evidence demonstrates that *Wt1* is also expressed by some parietal epithelial cells, especially those situated at the border between Bowman's capsule and the glomerular tuft, which have been termed 'parietal podocytes' by some authors (Ohse, Vaughan et al. 2010, Kabgani, Grigoleit et al. 2012). Therefore, this damage may be due to a direct effect of *Wt1* deletion in PECs, or could be as a paracrine consequence of the podocyte damage. Using the podocyte-specific model of *Wt1* loss would differentiate between the relative contributions of these two potential mechanisms.

The importance of parietal epithelial cells in glomerular injury and in glomerular regeneration is of increasing interest (Appel, Kershaw et al. 2009, Ohse, Pippin et al. 2009, Smeets, Angelotti et al. 2009), and *Wt1* may play a key role in the plasticity of these cells, especially in terms of migration onto the glomerular tuft to regenerate podocytes (Appel, Kershaw et al. 2009, Swetha, Chandra et al. 2011). The role of *Wt1* in PECs is not well understood, nor the significance of Wt1 expression at the in these 'parietal podocytes'. Further analysis using *in vitro* models of parietal epithelial cells (Ohse, Pippin et al. 2008) or PEC-specific Cre lines (Kabgani, Grigoleit et al. 2012) in combination with the *Wt1*-conditional model would help to shed light on this.

Although there was no evidence of nephron loss during the period analysed, over time, *Wt1*-deleted kidneys did develop features of matrix deposition and interstitial fibrosis, with tubular damage. This is likely to be due to the accumulation of protein casts and direct tubular toxicity due to the heavy albuminuria. A number of studies have documented the toxic effects of albuminuria on tubular epithelial cells, via a number of mechanisms, including oxidative stress and induction of apoptosis (Donadelli, Zanchi et al. 2003, Erkan, Devarajan et al. 2005, Ohse, Inagi et al. 2006, Shalamanova, McArdle et al. 2007) .

However, many of these studies rely on toxin-mediated glomerular damage, which, by definition, is not podocyte-specific. A recent study using targeted podocyte injury using a transgenic mouse line expressing the diphtheria-toxin receptor on podocytes revealed that low-

level podocyte damage (<20%) with resultant transient albuminuria, leads to adaptive responses, including a proliferative response in tubular epithelial cells, and resolution of the proteinuria without tubular damage. This indicates albuminuria per se is not sufficient to cause tubular damage. This situation is similar to that seen in human Minimal Change Disease, where heavy albuminuria can occur without detectable tubular injury. The authors found that tubular injury correlated with the degree of persistent glomerular injury (e.g. occurring after >40% podocyte damage) rather than albuminuria in isolation. They proposed that other serum factors within the ultrafiltrate, released as a consequence of glomerular injury, rather than the albumin itself, are responsible for causing the tubular injury in this scenario, adding further complexity to the accumulating evidence for 'cross-talk between cells of the glomerulus and nephron (Guo, Marlier et al. 2012). However, the animals in this model only experience transient albuminuria, so this cannot prove that prolonged exposure to urinary albumin may exert a toxic effect. Certainly in human chronic kidney disease, reduction of proteinuria is associated with slowing progression of renal disease (Halbesma, Kuiken et al. 2006, 2007) in keeping with a role for direct tubular toxicity over time. However, as renin-angiotensin blockade is the method of choice for reducing proteinuria, which has direct effects on the podocyte itself, the reduction of proteinuria may not be the main mechanism behind this effect (Macconi, Sangalli et al. 2009, Moeller 2010, Fukuda, Wickman et al. 2012).

Therefore, the increasing tubular injury and interstitial fibrosis subsequent to *Wt1*-deletion is likely to be a consequence of sustained glomerular damage and persistent proteinuria. At later time points, the cellular debris seen in some tubular lumens (which themselves maintain an intact tubular basement membrane) implies cell loss from higher up the nephron, i.e. from the glomerulus itself. This is further evidence of the severe degree of sustained glomerular damage following *Wt1* deletion.

4.14.7 Why does Wt1-deletion lead to loss of podocyte specific proteins?

Mice deleted for *Wt1* demonstrate significant loss of many major podocyte specific proteins. Both nephrin and podocalyxin are known to be direct transcriptional targets of Wt1, so loss of *Wt1* expression is likely to cause downregulation of their expression. However, other podocyte proteins such as podocin and synaptopodin are also lost. Loss of podocyte marker expression is seen in both models of podocyte injury (Mollet, Ratelade et al. 2009, Macary, Rossert et al. 2010) and in human glomerular diseases (Shankland 2006, Greka and Mundel 2012). These

effects appear to be a generic response to injury. However, as discussed later, Wt1 loss results in far more severe phenotype than other podocyte injury models, which may imply it plays an upstream role in podocyte differentiation. Although WT1 has not been shown to directly transcriptionally regulate podocin, it is interesting to note that the other site of podocin expression is the Sertoli cell of the testis, another site of adult Wt1 expression. As discussed earlier, these specialized cells maintain both epithelial and mesenchymal characteristics, have a specialized blood/testis barrier and are critical for germ cell differentiation, echoing some of the specialised features of podocytes (Relle, Cash et al. 2011)

Podocyte apoptosis and detachment are also important mechanisms of glomerular injury, so it was important to try and establish whether the profound loss of podocyte markers was simply due to rapid loss of cells. Using the *CreERWt1*$^{co/GFP}$ mouse to trace the early fate of *Wt1*-deleted cells, it appears that although there is some loss of fluorescent area (i.e. loss of fluorescently labelled podocytes - 25-50% by day 8) this did not appear enough to explain the significant changes in podocyte marker expression, particularly in terms of the profound nephrin loss (nephrin expression in mutant Wt1-deleted animals was only 1-2% of control). Most notably, some glomeruli did not exhibit any loss of fluorescence at day 8, even though histologically, all glomeruli exhibited signs of podocyte injury by this stage. Fluorescence was analysed using a visual scoring method, blinded between samples. Objective measurements of fluorescence using imaging programmes e.g. IPlab to measure fluorescence intensity proved impossible to standardize between samples, due to saturation of pixels in different images.

Given the dynamic nature of GFP expression in these mice, another explanation for this finding could be loss of *Wt1* promoter activity in *Wt1* deleted cells, corresponding to a phenotypic switch following *Wt1*-deletion.

The loss of podocyte markers following *Wt1* deletion is therefore likely to be due to a combination of loss of expression and some loss of cells.

Isolation of a pure podocyte population using FACS would allow for analysis of the *Wt1*-deletion phenotype specifically within the podocytes. As the *CreERWt1*$^{co/GFP}$ mouse expresses GFP in a dynamic fashion, i.e. whenever there is *Wt1* promoter activity, this means that, if cells that used to be podocytes undergo any kind of phenotypic change and stop expressing Wt1, and therefore expressing GFP they would be excluded from analysis. As these time points are early,

this loss of fluorescence, given the stability of the GFP protein, is unlikely to have a major effect. However, a more robust method of isolating a pure podocyte population in which *Wt1* had been deleted would be to use a triple transgenic in which there was a Cre-activated reporter (e.g. YFP), such as the $Wt1^{CreERT2/co}$ $R26R^{YFP/YFP}$ model discussed in Chapter 5.

4.14.8 *Wt1 loss affects the epithelial to mesenchymal balance in adult kidney*

Wt1 has a role in controlling both the epithelial to mesenchymal transition and its reverse, mesenchymal to epithelial transition, in development, so it was hypothesized that *Wt1* loss would affect the unique epithelial and mesenchymal characteristics of podocytes. Preliminary analysis of this, at the expression level, demonstrates an increase in key mesenchymal drivers, including Snail, a known Wt1 target, and increased mesenchymal markers, in response to *Wt1* loss. Interestingly, this is not accompanied by a loss of epithelial markers, notable *P-cadherin* and *Zo-1*, so these early changes do not represent a 'classical' EMT. Instead, this is in keeping with a transitional stage, perhaps consistent with an earlier developmental form, as has been seen in published in vitro work (Herman-Edelstein, Thomas et al. 2011). As podocytes exhibit both epithelial and mesenchymal characteristics, it would be artificial to try and categorise them as either epithelial or mesenchymal so a 'classical EMT' would not be expected. This data, however, would support a role for *Wt1* in maintaining this specialized balance.

The role of epithelial to mesenchymal transition in disease has been the subject of intense study over recent years, and has been described as a pathological mechanism in both renal interstitial fibrosis, through EMT of tubular epithelial cells (Liu , Ivanova, Butt et al. 2008) and even in podocytes themselves (Li, Kang et al. 2008). However, this has become an increasingly controversial issue, with elegant lineage tracing experiments revealing a key role for renal pericytes, rather than an EMT of tubular epithelial cells, as the source of myofibroblasts to produce matrix and fibrosis (Humphreys, Lin et al. 2010).

A criticism of earlier work analyzing pathological EMT within the kidney has been the reliance on marker expression (Zeisberg and Duffield 2010). Therefore, in order to confirm this phenotype in *Wt1*-deleted cells, ultrastructural analysis needs to be undertaken. This would reveal any changes in the tight junctions or adherens junctions, and any subsequent loss of cell

polarity and organization, which is necessary for cells to undergo an EMT (Chau and Hastie 2012). The analysis of *in vitro* models of *Wt1* loss would also add mechanistic information as to the changes in podocyte structure and function in response to *Wt1* deletion, especially in terms of motility (Welsh, Hale et al. 2010) and protein distribution (Miller-Hodges E, Witherden IR *et al*, manuscript in preparation). However, as podocytes in culture only partly recapitulate the *in vivo* situation, especially in terms of forming slit diaphragms, the analysis of tight junction formation would be limited in this scenario, so *in vivo* ultrastructural analysis would be superior.

4.14.9 Wt1 loss leads to re-expression of Wnt 4.

In the developing kidney, detailed analysis using ChIP, has demonstrated that the processes of EMT in cardiac development and MET in kidney development are controlled by *Wt1,* through influencing the chromatin conformation at the *Wnt4* locus. In kidney development, *Wt1* maintains chromatin at the *Wnt4* locus in an active state and promotes *Wnt4* expression via recruitment of the co-activators Cbp and p300. Additional data suggests a temporal effect of *Wt1* on *Wnt4* expression. At later stages of development, *Wt1* may switch to a repressing mode (Rigby, Leitch et al. 2008). This is confirmed here in adult kidney, where *Wt1* loss results in reactivation of *Wnt4* at the gene expression level.

A number of studies have demonstrated the importance of canonical Wnt / beta-catenin signalling in renal development (Stark, Vainio et al. 1994, Carroll, Park et al. 2005, Merkel, Karner et al. 2007, Schmidt-Ott and Barasch 2008)**.** Final completion of the MET process to form the differentiated nephron, appears to rely upon non-canonical Wnt-signalling, through the Calcium/NFAT pathway, downstream of Wnt4 (Burn, Webb et al. 2011).

Although critical for renal development, Wnt/beta-catenin signaling is effectively silenced in adult, differentiated kidney. Reactivation of the Wnt signaling pathway occurs in response to certain models of renal injury (Surendran, McCaul et al. 2002, He, Dai et al. 2009). More recently it has been shown that Wnt/beta-catenin signaling is reactivated in podocytes of human and animal models of glomerular disease. Overexpression of *Wnt1* exacerbates podocyte injury whereas blockade of Wnt signaling, either pharmacologically, or genetically, is protective in animal models of glomerular disease (Dai, Stolz et al. 2009). This re-activation of Wnt4

expression following *Wt1* deletion may, therefore, reflect either a generic response to injury or a *Wt1*-specific response. Further analysis is required to differentiate between these effects (see final discussion).

4.14.10 How does Wt1 deletion compare with other genetic models of podocyte injury?

A number of podocyte injury models have been published, exhibiting a variety of phenotypes and severity.

Podocin is a critical component of the slit diaphragm and Podocin (*NPHS2*) mutations lead to steroid resistant nephrotic syndrome (Machuca, Benoit et al. 2010) and can also predispose to FSGS (McKenzie, Hendrickson et al. 2007). A mouse model in which podocin is conditionally inactivated in adult podocytes most closely resembles the phenotype seen in *Wt1*-deleted mice, with albuminuria, hyperlipidaemia and FSGS developing at 4 weeks, leading to renal failure (Mollet, Ratelade et al. 2009). Histologically, FSGS and matrix accumulation is seen in at least 30% of glomeruli at 4 weeks, with pseudocrescent formation, tubular dilatation and protein casts. By 9 weeks, global sclerosis and interstitial fibrosis is seen. Similar levels of Cre-recombination (70%) are recorded, with about 50% loss of podocin expression at 1 week, and almost complete absence of podocin by 4 weeks. This is similar to the *Wt1* loss in this project.

However, a striking difference between these two models is the rapid onset and severity of the *Wt1* deletion phenotype, which develops massive proteinuria after only one week, and can lead to early death in only a week or two. In contrast, *NPHS2* (podocin) inactivation did not lead to detectable albuminuria until after 2 weeks, and animals survived an average of 11 weeks. Histological changes were also seen much earlier following *Wt1* deletion.

Nephrin mutations in humans cause severe congenital nephrotic syndrome (Kestila, Lenkkeri et al. 1998). Conventional nephrin knockout in mice leads to early perinatal mortality. This can be partially rescued by transgenic expression of a rat nephrin transgene, although mice still develop proteinuria and kidney abnormalities. However, no conditional nephrin knockout has yet been published so this model cannot be directly compared with the conditional *Wt1* mouse.

A transgenic line expressing nitroreductase under control of the podocin promoter, allows podocyte specific toxic injury. This results in transient proteinuria, histological damage, including podocyte vacuolation, hypercellularity and collapse of the glomerular tuft and progressive interstitial fibrosis. There is loss of podocyte markers, similar to the phenotype observed after *Wt1* deletion (Macary, Rossert et al. 2010). The mice analysed exhibited prolonged survival and recovery of the proteinuria, but, nearly 50% of experimental animals died within the first 3 days of the experiment so were not analysed. Whether these represent the more severe end of the phenotypic spectrum, more similar to that seen after *Wt1* deletion remains speculative.

Therefore, although similar phenotypic consequences are seen in other models of podocyte injury, none seem to be as severe as *Wt1* deletion. Conditional models of podocyte gene deletion do, however, remain limited. The severity of the *Wt1*-deletion phenotype may be due to increased efficiency of the transgene, although Cre-recombination events appear to be similar, and tamoxifen doses were reduced. Alternatively, it may be due to *Wt1* playing a fundamental upstream role in podocyte differentiation and function, leading to profound effects following *Wt1* loss. However, the mechanisms behind this remain to be elucidated (see final discussion).

4.15 Concluding Remarks

Conditional deletion of *Wt1* in the adult mouse has confirmed the essential role of *Wt1* in adult kidney, which was not proven before the start of this project

Wt1 loss leads to severe podocyte injury, failure of the glomerular filtration barrier, loss of key podocyte proteins and alteration of the epithelial-mesenchymal balance in podocytes. This phenotype appears more severe than that seen in other published models of podocyte injury.

Although challenges optimising the model means that numbers are small, techniques have now been developed to facilitate analysis specifically of *Wt1* deleted podocytes, in order to confirm these findings, and elucidate the mechanisms underlying them.

5 GENERATING A PODOCYTE SPECIFIC IN VIVO MODEL OF WT1-LOSS

5.1 INTRODUCTION

5.1.1 WT1 EXPRESSION IN THE ADULT

WT1 was thought to be expressed in a very restricted pattern in the adult: the renal podocyte, the mesothelial layer surrounding the visceral organs (Walker, Rutten et al. 1994), approximately 1% of bone marrow cells (Hosen, Shirakata et al. 2007) and in the sertoli cells of the testes and granulosa cells of the ovary (Pelletier, Schalling et al. 1991, Armstrong, Pritchard-Jones et al. 1993, Rao, Pham et al. 2006).

However, during the course of this project, it was demonstrated that following whole-body *Wt1* deletion in adult mice, multiple organ failure develops rapidly (Chau, Brownstein et al. 2011). This phenotype appears far more dramatic than this restricted *Wt1* expression pattern would suggest, implying that *Wt1* expression and function in the adult is far more widespread than previously thought.

The mechanisms underlying this phenotype remain to be elucidated in detail, but potential processes have been suggested (Chau, Brownstein et al. 2011). The observed phenotypes and involved organ systems include:

1) RENAL: Severe podocyte damage, albuminuria and renal failure

   Assumed to be a consequence of a vital function of *Wt1* in renal podocytes.

2) FAT: Significant fat loss

   Hypothesized to be an effect of *Wt1* on adipocyte homeostasis, as *Wt1*-GFP expressing cells have been identified in the stromal vascular portion of fat pads.

3) MUSCULOSKELETAL: Significant bone loss

Thought to result from increased osteoclast activity caused by local factors released from mesenchymal stromal cells and haematopoietic stem cells. The marked loss of *IGF-1* expression following *Wt1* deletion may also play a role, as mice mutant for both *IGF-1* and its binding protein subunit ALS (Acid Labile Subunit) also demonstrate severe bone thinning reminiscent of the phenotype following *Wt1* deletion (Yakar, Rosen et al. 2002).

4) HAEMATOLOGICAL: Failure of erythropoiesis

Thought to be due to a critical role of *Wt1* in erythrocyte precursors.

5) HAEMATOLOGICAL: Splenic atrophy

Caused by diminished extramedullary haematopoiesis in the red pulp compartments and reduced rates of proliferation in the mutant spleen

6) ENDOCRINE: Atrophy of exocrine pancreas

As this is not associated with a demonstrable rise in serum amylase, this does not appear to be a typical pancreatitis. It may be due to activation of pancreatic stellate cells, which may, as in the liver, arise from a precursor population of Wt1-positive mesothelial cells (Ijpenberg, Perez-Pomares et al. 2007),

Thus, deletion of *Wt1* using a ubiquitously expressed Cre causes more widespread effects than would be predicted. In order to study specifically the role of *Wt1* in the podocyte, a podocyte specific Cre would be required to eliminate the extra-renal manifestations of *Wt1*-loss.

5.1.2 *LIMITING WT1 DELETION TO THE KIDNEY*

Wt1 deletion using the ubiquitously expressed Cre does result in a number of extra-renal effects. It is important to note, however, that there is no evidence of a systemic inflammatory response in this model, which, if present, may have had a marked effect on the renal phenotype, and potentially cause immune-mediated podocyte injury and/or renal failure as part of a multi-organ failure or systemic inflammatory response (Chau, Brownstein et al. 2011).

In practice, these extra-renal effects are unlikely to affect the direct podocyte injury, but could theoretically influence the renal phenotype.

Therefore, in order to properly analyse both the renal-specific and podocyte-specific effects of *Wt1* loss it was important to create a model in which *Wt1* deletion was limited to the podocyte. This would remove any confounding extra-renal effects and also clarify that the observed extra-renal phenotypes were not secondary effects of the profound nephrosis or renal failure. At the time of starting this project a number of transgenic lines were available which had been used to express Cre within the podocyte. These included:

1) A Nephrin-Cre (Neph-Cre) mouse expressing Cre-recombinase under the control of the murine Nephrin (*NPHS1*) promoter (Wang, Wang et al. 2010). When crossed with Z/EG reporter lines, podocyte specific Cre-recombination was demonstrated, with GFP expression detected indirectly in podocytes, using an anti-GFP antibody (Eremina, Wong et al. 2002). These lines have been used subsequently by a number of other groups in order to achieve podocyte-specific gene alteration in vivo: 1) to activate Notch in developing podocytes (Waters, Wu et al. 2008); 2) to delete the VEGF Receptor-2 from podocytes (Sison, Eremina et al. 2010); and 3) to overexpress Laminin beta-1 to rescue a mouse model of Pierson Syndrome (Suh, Jarad et al. 2011), amongst others. However, as this model is not inducible, *Wt1* would have been deleted from the start of *Nephrin* expression in the mature podocyte (as early as E13.5) and not just in the adult.

2) A transgenic line expressing a tamoxifen-inducible Cre-recombinase under the control of a CMV enhanced chicken βactin promoter. When crossed with a reporter line Z/AP, hAP expression was detectable in skeletal and heart muscle tissue, in a tamoxifen-dose dependent manner, as well as in renal podocytes, in which Cre-recombination efficiency was thought to reach 60-90% (Bugeon, Danou et al. 2003). Obviously, given the extra-renal Cre-recombinase activity, this line would not clarify the podocyte specific effects of *Wt1*-deletion cleanly.

3) A doxycycline-inducible Podocin-Cre transgenic mouse line, using Cre-recombinase under control of the rtTA-M2 transcription factor, with the rtTA-M2 gene under control of a 2.5kb fragment of the Podocin *(NPHS2*) promoter, in a single transgene construct (JRC-CRE). Transgenic animals were crossed with a Z/AP reporter line and Cre-recombination was induced by doxycycline administration through drinking water, from age 8-10 weeks for 14 consecutive days. Expression of Cre-recombinase protein was

demonstrated in glomerular podocytes, with alkaline phosphatase expression limited to the podocytes. This demonstrated both functional and specific Cre-recombinase activity in podocytes (Juhila, Roozendaal et al. 2006).

This model offered both inducible and podocyte specific Cre-recombinase activity, however, as a key aim of this project was a direct comparison with the tamoxifen-inducible ubiquitously expressed Cre, the ideal model would be a tamoxifen-inducible podocyte-specific Cre line. Non-inducible Cre lines would have initiated Cre recombination as soon as podocytes differentiated, so would not be comparable with the effect of mass *Wt1* deletion in adult podocytes that had developed normally. The doxycycline-inducible podocyte-specific Cre was already available, but, to make a direct comparison, a tamoxifen–inducible Cre would be more comparable, as tamoxifen itself can exert some toxic effects (Higashi, Ikawa et al. 2009).

5.2 AIMS

The aims of the experiments described in this chapter were

- To generate a tamoxifen-inducible, podocyte-specific Cre transgenic mouse, which would express Cre under the control of tamoxifen and the Podocin (*NPHS2*) promoter.
- To characterize this transgenic line and confirm podocyte-specific Cre-recombination by crossing with a reporter strain
- To cross with the $Wt1^{co/co}$ line in order to generate an inducible podocyte-specific model of *Wt1*-deletion
- To analyse the effects of podocyte-specific *Wt1*-deletion and compare with the effects using the ubiquitously expressed Cre.

5.3 EXPERIMENTAL APPROACH

The tamoxifen-inducible, podocyte-specific Cre transgenic mouse would be generated using a GFP-CreERT2 fusion construct (McMahon, Aronow et al. 2008) under the control of the Podocin promoter. This would label Podocin-expressing cells with GFP as well as providing inducible Cre activity (Figure 5.1).

Genetic recombination events to allow definitive lineage tracing have been used since the 1990s, and the use of fluorescent proteins as markers avoids the need for tissue fixation prior to analysis (Mao, Fujiwara et al. 1999, Kretzschmar and Watt 2012). Similar to the concept used by Hans Clevers in his seminal work on LGR5 cells in the intestine, for example, this promoter-reporter construct would elegantly allow identification and tracing of all podocytes (labelled with GFP), and, if crossed with a different coloured reporter line, all podocytes in which Cre had been active (Barker, van Es et al. 2007). This would facilitate specific analysis of *Wt1*-deleted podocytes and their fate, and crucially, could identify whether any level of podocyte regeneration occurred following *Wt1*-mediated glomerular injury.

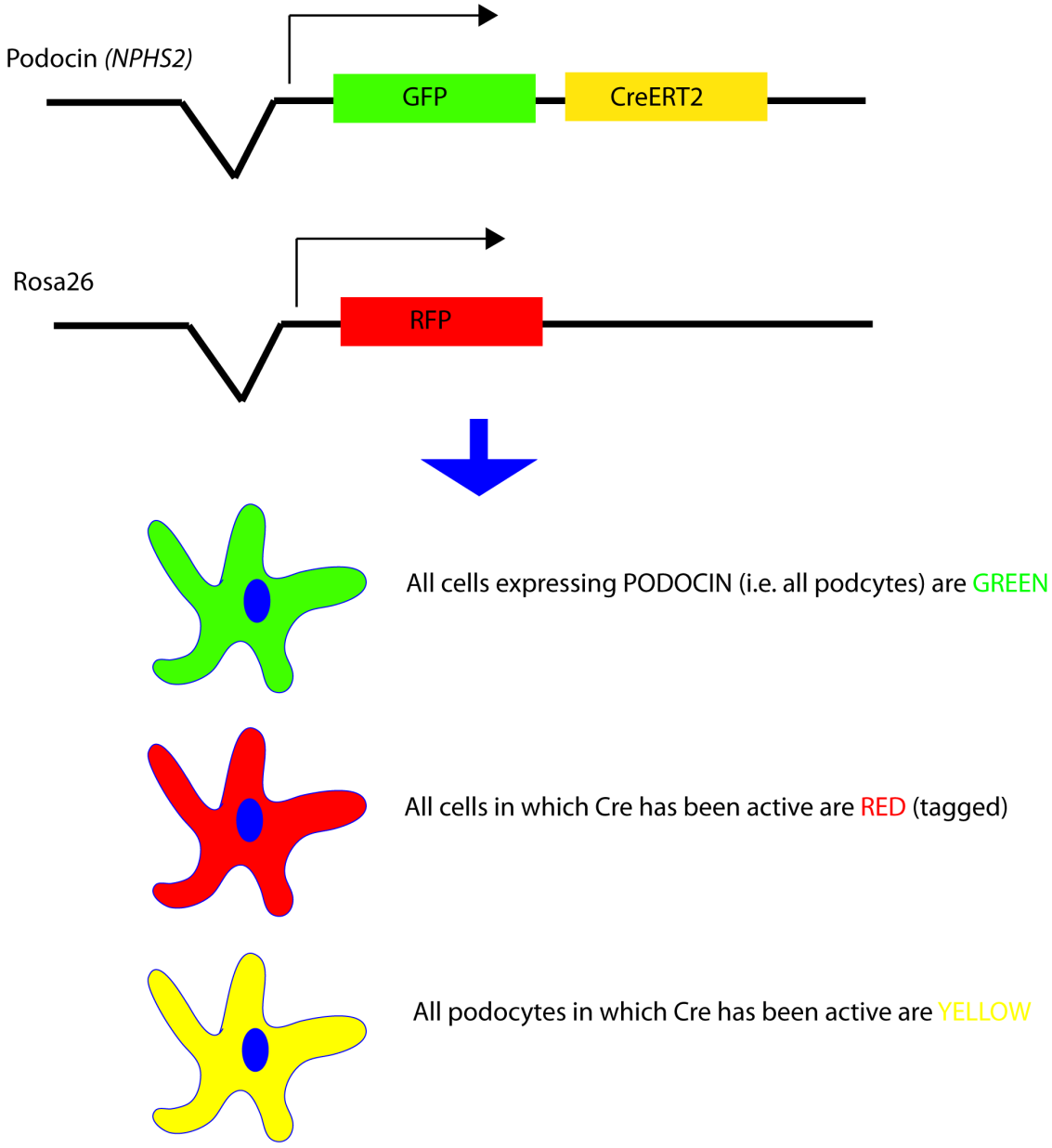

FIGURE 5.1: SCHEMATIC OF *PODOCIN*-GFP-CREERT2 TRANSGENIC LINE

Figure 5.1: Schematic of *Podocin*-GFP-CreERT2 transgenic line

The *Podocin*-GFP-CreERT2 fusion construct both labels podocytes with GFP and provides inducible Cre activity to mediate podocyte specific *Wt1*-deletion when crossed with the *Wt1*$^{co/co}$ line. If crossed with a further reporter line (e.g expressing RFP) the fate of those podocytes in which Cre has been active, and therefore *Wt1* has been deleted, can be specifically traced.

Podocin is a lipid-raft associated protein, which is only expressed in podocytes. It is associated with the slit diaphragm where it has been shown to recruit nephrin. Podocin was originally identified as a cause of steroid resistant nephrotic syndrome in childhood, where mutations account for up to 10-26% cases of childhood steroid resistant nephrotic syndrome (Ruf, Lichtenberger et al. 2004). Previous work has demonstrated heterozygous Podocin-deficient mice remain viable (Philippe, Weber et al. 2008) and the doxycycline inducible Podocin-Cre mice mentioned previously were shown to have no deleterious renal phenotypes (Juhila, Roozendaal et al. 2006). This made it an ideal candidate promoter for generating a podocyte specific GFP-Cre.

5.3.1 *Using Gateway Recombineering to generate a BAC transgenic mouse*

BAC recombineering offered an efficient method of in vivo genetic engineering, avoiding the limitations of traditional cloning techniques, such as the need for specific restriction sites encompassing the gene of interest. Recombineering utilises the bacteriophage lambda site-specific recombination pathway. Short sequences of phage DNA, which correspond with the bacterial DNA, allow precise recombination into the genome. These site-specific recombination events are reversible, so DNA can be excised following integration, leaving the original sequence. This allows faster, more flexible and more efficient cloning in order to produce the desired construct (Sharan, Thomason et al. 2009).

Gateway recombination cloning technology (Invitrogen Gateway® Multisite Cloning) uses the bacteriophage lambda site specific recombination pathway in E.coli, in which site specific recombination occurs via corresponding att sequences (Tsvetanova, Peng et al. 2012). The bacterial attB sequence corresponds with a complementary phage attP sequence, allowing site-specific recombination of phage DNA into the bacterial genome. The recombined attB and attP sites then become attL and attR sequences (Left and Right respectively). These can revert to the original sequences following excision of the phage DNA. The att sequences rely upon a unique 7bp core sequence that reduces cross reactivity between them.

The Gateway system utilizes this phenomenon, in which an *in vitro* recombination reaction occurs between two attB sites on one DNA sequences and two attP sites on a second DNA

sequence: the BP reaction. As with bacteriophage lambda, the recombined sequences are termed attL and attR respectively. These, reversible, reactions form the basis of gateway cloning.

This system allowed rapid, specific and flexible cloning to create the Podocin-GFP-CreERT2 construct. The completed construct would be used to generate transgenic animals using a number of techniques:

1) Direct micro-injection of BAC DNA into the pronucleus of fertilised mouse oocytes

   This would facilitate rapid and efficient integration of target DNA, but can be limited by positional effects and so would require screening of a number of transgenic lines (Rossant, Nutter et al. 2011).

2) Direct injection of BAC DNA into ES cells

   To allow rapid integration and pre-screening of ES clones prior to generation of transgenic animals (Van Keuren, Gavrilina et al. 2009).

3) Targeted integration into ES cells

   To allow site-specific recombination of the Podocin-GFP-CreERT2 construct into the Podocin locus, thus avoiding any positional or copy-number effects. This method, however, would take much longer than the previous methods described (Adams and van der Weyden 2008).

5.4 GENERATING THE GATEWAY CONSTRUCT

Gateway multisite cloning technology requires a series of simple steps in order to generate a construct (Figure 5.2):

1) Constructing an Entry Clone

    I) Amplification of target DNA sequence

    II) Recombination into Gateway Donor Vector

2) Constructing an Expression Clone

    I) Recombination of Entry Clone into Destination Vector (containing relevant backbone)

An existing expression clone generated in the lab (referred to in this thesis as GFP-Cre-IRES-puro-BAC) formed the basis of constructing the new expression clone (Figure 5.3) (Dolt, Lawrence et al. 2013) . This original expression clone contained a GFP-Cre cassette, but in order to generate an inducible podocyte-specific Cre, this cassette needed to be replaced with the GFP-CreERT2 construct, a kind gift from Andy McMahon (Kobayashi, Valerius et al. 2008).

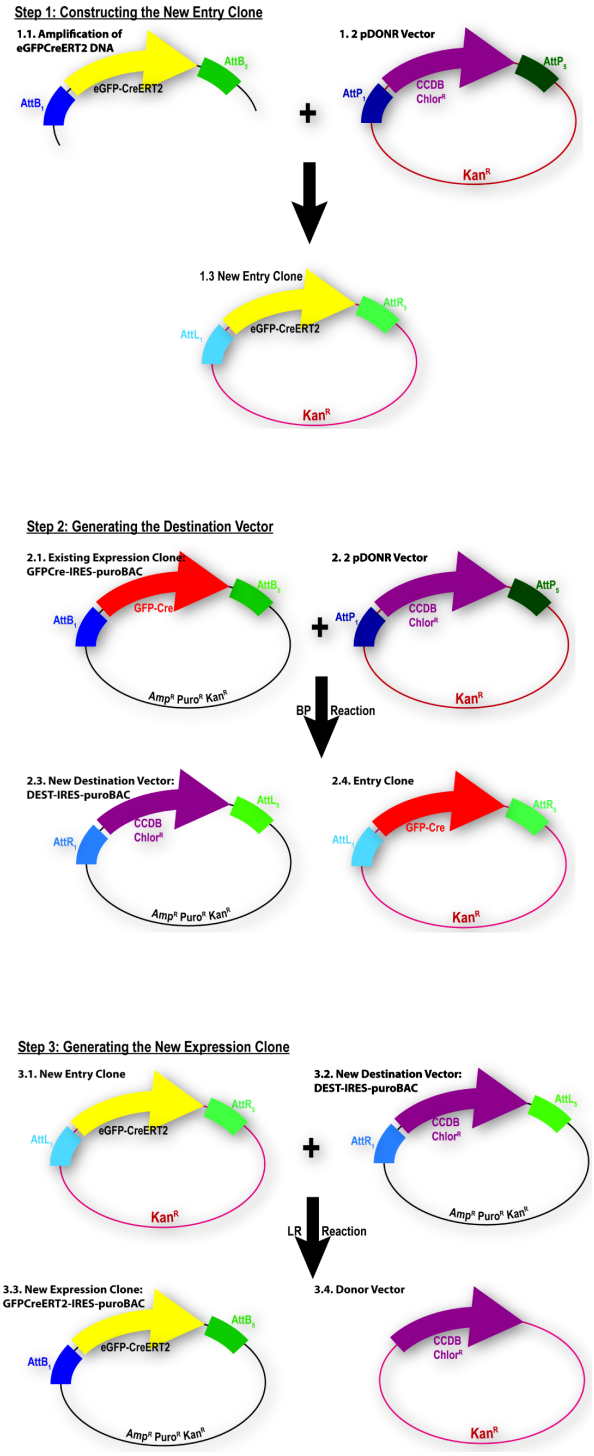

FIGURE 5.2: SCHEMATIC ILLUSTRATING THE STEPS TO GENERATE THE PODOCIN-GFP-CREERT2 EXPRESSION CLONE

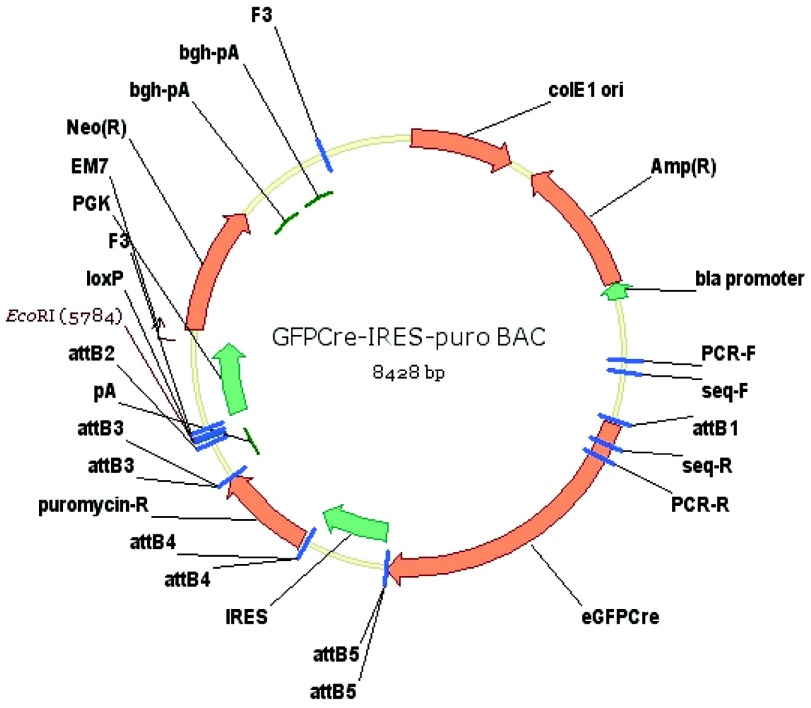

FIGURE 5.3: THE EXISTING EXPRESSION CLONE: GFP-CRE-IRES-PURO-BAC, CONTAINING A GFP-CRE CASSETTE

5.4.1 Step 1: Constructing the Entry Clone

The GFP-CreERT2 construct was amplified using PCR primers containing attB1 and AttB5R sites to facilitate homologous recombination between the PCR product and homologous sequences in the pDONR221 P1-P5r vector (Invitrogen Multisite Gateway Pro) (Figure 5.4 A).

A BP reaction between the gateway pDONR221 P1-P5r vector and the purified GFP-CreERT2 PCR product generated the new entry clone, which would be used to modify the existing expression clone (Figure 5.2 Step 1).

This reaction mixture was used to transform chemically competent "one shot" bacteria. Several thousand colonies were obtained and 16 clones selected for automated mini-prep and sequencing. Clones A1, B1 and H1 were 100% accurate, with correct inclusion of the GFP-CreERT2 construct. **Entry Clone A1** was selected for further use.

5.4.2 Step 2: Regenerating the Destination Vector

A BP reaction between the existing GFP-Cre-IRES-puro-BAC expression clone (containing all 5 Multisite Gateway fragments) and the pDONR 221 P1-P5r Vector changed the expression clone back into a destination vector (Figure 5.2 Step 2).

Following transformation of ccdB competent DB3.1 bacteria, an *Eco*RI restriction digest of mini-prepped DNA was used to confirm correct replacement of the GFP-Cre segment. Clones A1, B2 and E5 digested correctly, and clone A1 (Destination Vector A1) was chosen for further experiments (Figure 5.4 B)

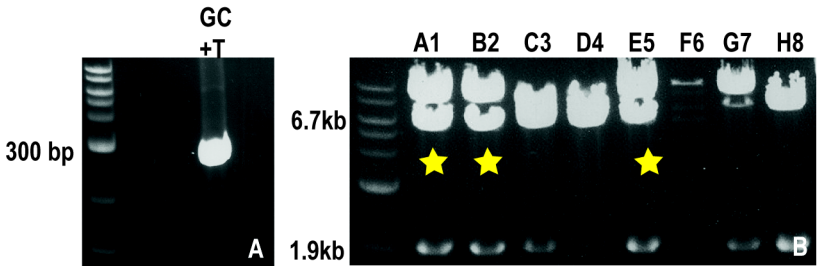

FIGURE 5.4: CONSTRUCTING THE ENTRY CLONE

A) PCR amplified GFPCreERT2 cassette (GC = GC mix, T = Template). B) EcoR1 restriction digest of the destination vector. Correct digest pattern (1.9kb and 6.7kb band) indicated by stars.

5.4.3 STEP 3: GENERATING THE NEW EXPRESSION CLONE

To generate the new GFP-CreERT2-containing expression clone, an LR reaction was performed between the new destination vector (DEST-IRES-puro-BAC) and the new entry clone A1 (containing the GFP-CreERT2 construct) (Figure 5.2 Step 3).

The reaction mix was used to transform DH5α Library Efficient bacteria. Restriction digests were used to confirm correct integration. However, none of the three colonies obtained demonstrated correct integration.

Despite multiple cloning attempts, no correctly integrated colonies grew. This was also found to be the case by my colleague, Karamjit Singh-Dolt, who was attempting to use the same gateway vector backbone to generate a *Six2*-driven GFP-Cre-IRES-puro transgenic mouse and also, by reinserting MKate2 into the same backbone, to generate a Nanog-driven mKate2-Cre-IRES-puro transgenic line (Dolt, Lawrence et al. 2013). The destination vector was found to be unstable at the multiple cloning site, preventing correct recombination of the novel constructs.

However, by altering the order of the restriction sites at the multiple cloning site, growing the transformed bacteria at 30º and using Stbl2 chemically competent cells specifically designed for unstable inserts, this problem was overcome. The new destination vector, generated by Dr Singh-Dolt was used to generate the new expression clone (Figure 5.5).

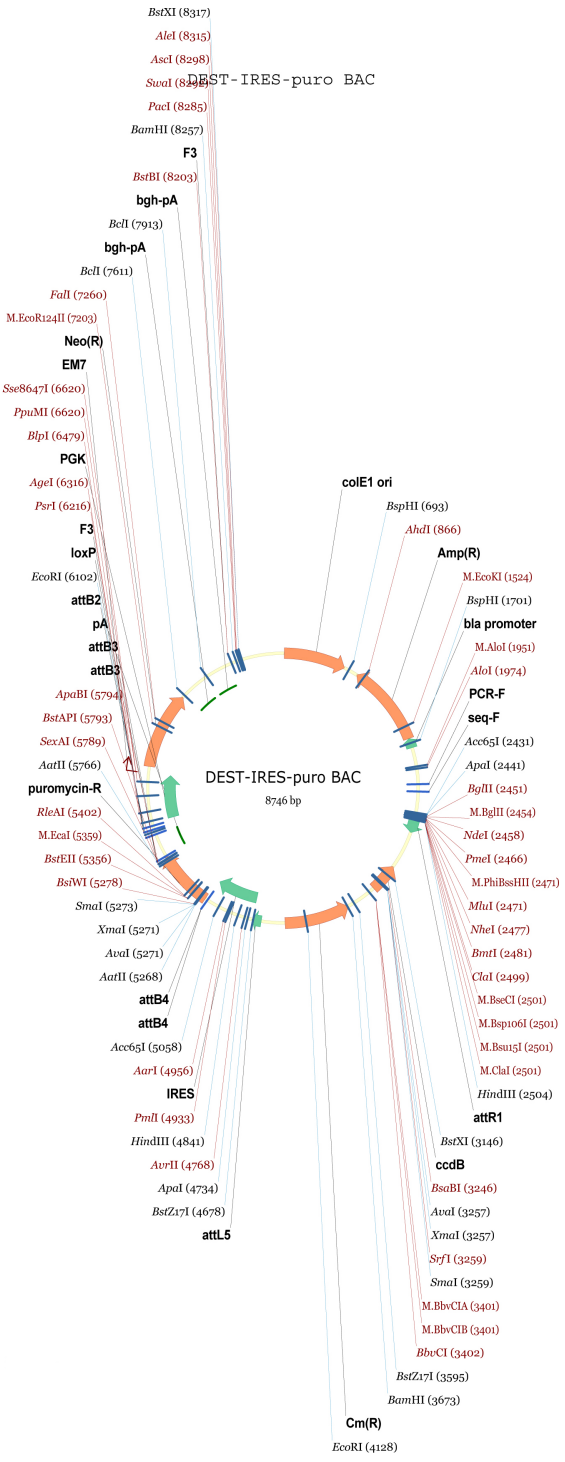

FIGURE 5.5: MODIFIED DESTINATION VECTOR, WITH ALTERED MULTIPLE CLONING SITE

5.4.4 Step 3: Generating the new Expression Clone #2

As before, in order to generate the GFP-CreERT2 containing expression clone, an LR reaction between the new and stabilized destination vector (DEST-IRES-puro-BAC) and the entry clone A1 (containing the eGFP-CreERT2 construct) was performed. The reaction mixture was used to transform Stbl2 chemically competent bacteria, grown at 30°C. Restriction digests confirmed correct integration (Figure 5.6). Clone C demonstrated the predicted digestion pattern so was selected for use.

The presence of the unique restriction sites in the multiple cloning sites, required for integration into the podocin BAC, were verified using restriction digests to generate a single linearised construct at 9.3kb (Figure 5.6 D, E, F, G).

This confirmed correct integration of the GFP-CreERT2 construct into the destination vector, therefore generating the desired Gateway expression clone.

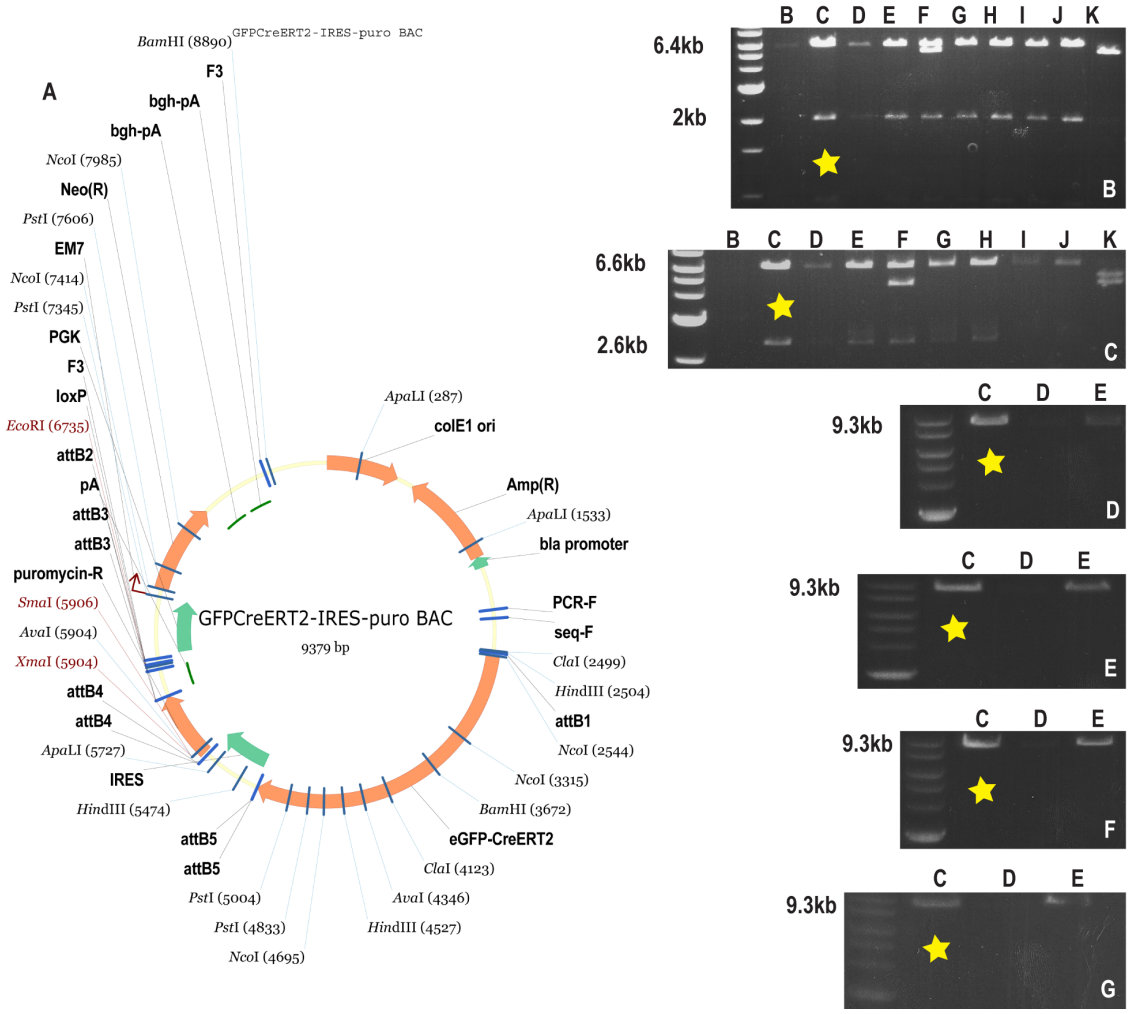

FIGURE 5.6: COMPLETED GFP-CREERT2-IRES-PURO CONSTRUCT

A) Restriction digest map: GFP-CreERT2-IRES-puroBAC; B) *Hin*dIII restriction digest (predicted bands 0.9kb, 2kb and 6.4kb); C) *Pst*I restriction digest (predicted bands at 0.1kb, 2.6kb and 6.6kb); D) *Pac*I restriction digest; E) *Asc*I restriction digest; F) *Sal*I restriction digest; G) *Nde*I restriction digest (predicted single 9.3kb bands). Correct digestion patterns in Clone C are indicated by star.

5.5 Recombineering the GFP-CreERT2-IRES-puro-BAC Expression Clone into the Podocin BAC

5.5.1 Amplifying the Recombineering Arms

Podocin BAC BMQ 417-H15 (Geneservice) was used as the template for amplification of the short homologous arms for the recombineering reaction. Individual BAC clones were mini-prepped and an arbitrary *Hin*dIII restriction digest was used to confirm the clones were identical (Figure 5.7 A). The Podocin (*NPHS2*) promoter region was amplified using PCR primers designed to amplify regions 200-300nt upstream and downstream of the endogenous start site in the murine Podocin sequence (Figure 5.7 B and 5.8). These primers were designed to contain appropriate restriction sites to facilitate incorporation into the template Podocin BAC.

Unfortunately, the recombineering arms failed to amplify, despite optimising PCR conditions and trying alternative Taq polymerases. A further *Hin*dIII restriction digest confirmed that BAC DNA was present, but the presence of the Podocin sequence could not be demonstrated, even using previously verified primers (Mollet, Ratelade et al. 2009). This indicated the BMQ 417-H15 BAC did not actually contain the Podocin sequence.

A new Podocin BAC (RP23-387A22 – Geneservice) was purchased and used as template. As before, a number of clones were mini-prepped and digested with arbitrary restriction enzymes in order to ensure they were identical.

The 5'arm amplified correctly, giving a 312bp PCR product. However, the 3' arm generated an extended 600bp product rather that the 213nt predicted despite optimization of PCR conditions (Figure 5.9 A). It was sequenced and compared to the genomic podocin sequence using BLAST. This revealed that the Pac1-F primer was binding to a similar sequence upstream of the start site, generating the longer product. The 3' arm primers were redesigned to bind within intron 1, and generated the expected product (Figure 5.9 B & C).

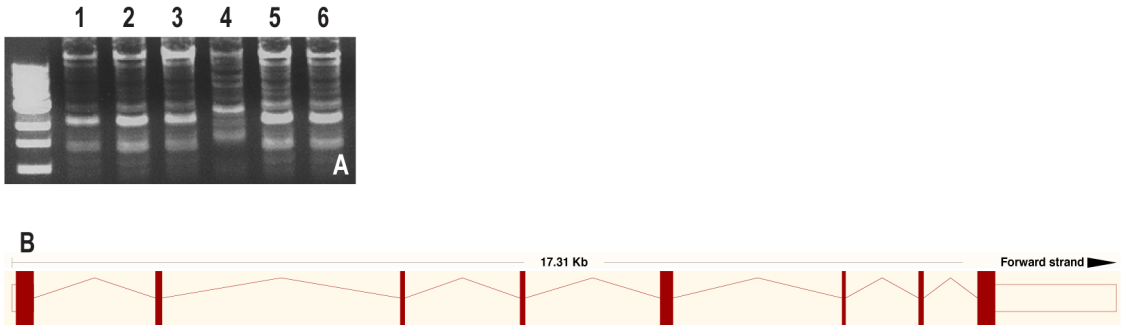

FIGURE 5.7: PODOCIN BAC

A) *Hind*III digest of *Podocin* BAC BMQ 417-H15. All clones are identical apart from 4, which was discarded. B) Podocin transcript summary. The construct was designed to recombineer into the Podocin promoter sequence, disrupting exon 1.

NPHS2 (Podocin)

Taagaaagcatggaaacaggacctgggaaagaaagtgaacctttctaaacacagaaagcagacccccctagtgcagtgtgttctgtctcaagcactgttag
ccacctaagcagagcctgctgtggtctttctcaaagcaaccgggtgcgggtgcactggcaccaagaatctcccattcaggtcctctgagagcattgcatcc
tgtctattttagaggtatgttggcaccatccagacccaagaaggaacagcaatttggttaggtgtgggtatggccacctcaggccccgccctccgcacctcc
ctccagacagcaaggtccttagggccttggggtcgctccccatcggctcagaaagctGGGGCTGCGACTCTGCCAGCAGCTGG
CTCCGGGGTTGCACCGCTGCATTGAGA**ATG**GACAGCAGGGCGCGGAGCTCTTCCCGAGAGG
CCCACGGGAGAAGTAGCAGGTCCTCCTCTAGGGATGACAAGAAGGCAAAGGCCGGGAGGGG
CAGCAGAGGCCGCGCACGTCCGGATGCTGGAGCAGAGCGGCAGAGCACCGGGCGGACAGCG
ACCCGAGGGGAGCCCCGAGCTCCCGCTGCCACCGCCACCGTAGTGGACGTGACGAGGTTCGG
GGCCCTGGTGAGGAGGGCACGGAAGTGGTGGCGCTGCTGGAGAGCGAGCGACCAGAGGAAG

Nphs2 5 NdeI/F: gcgcCATATGcacctaagcagagcctgc

Nphs2 5 SalI/R: gcgcGTCGACTCTCAATGCAGCGGTGCA

Length: 312 nt

Nphs2 3 PacI/F: gcgcTTAATTAAGACAGCAGGGCGCGGA

Nphs2 3 AscI/R: tataGGCGCGCCAACCTCGTCCACGTCCAC

Length: 213 nt

FIGURE 5.8: DESIGNING THE PRIMERS FOR AMPLIFICATION OF THE RECOMBINEERING ARMS

Each primer contains unique restriction sites for integration into the template Podocin BAC (colour coded)

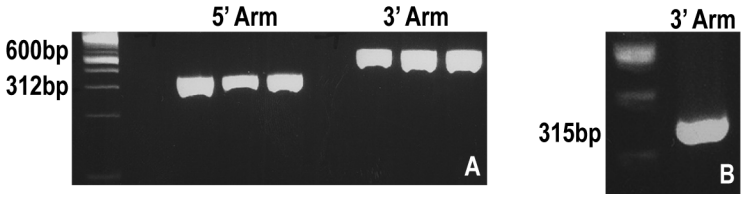

C Nhps2 (Podocin)

Taagaaagcatggaaacaggacctgggaaagaaagtgaacctttctaaacacagaaagcagacccccctagtgcagtgtgttctgtctcaagcactgttag
ccacctaagcagagcctgctgtggtctttctcaaagcaaccgggtgcgggtgcactggcaccaagaatctcccattcaggtcctctgagagcattgcatcc
tgtctattttagaggtatgttggcaccatccagacccaagaaggaacagcaatttggttaggtgtgggtatggccacctcaggccccgccctccgcacctcc
ctccagacagcaaggtccttagggccttggggtcgctccccatcggctcagaaagctGGGGCTGCGACTCTGCCAGCAGCTGG
CTCCGGGGTTGCACCGCTGCATTGAGA**ATG**GACAGCAGGGCGCGGAGCTCTTCCCGAGAGG
CCCACGGGAGAAGTAGCAGGTCCTCCTCTAGGGATGACAAGAAGGCAAAGGCCGGGAGGGG
CAGCAGAGGCCGCGCACGTCCGGATGCTGGAGCAGAGCGGCAGAGCACCGGGCGGACAGCG
ACCCGAGGGGAGCCCCGAGCTCCCGCTGCCACCGCCACCGTAGTGGACGTGACGAGGTTCGG
GGCCCTGGTGAGGAGGGCACGGAAGTGGTGGCGCTGCTGGAGAGCGAGCGACCAGAGGAAG
gtatggaaggtagatcccacgagaaggtgtggagggtaggcgcgagatgtcagacaagtgcagtgagttgccaggcttgtggtgggaccatggtgggg
aggagaaggcacgagctacgcagttacttagtgatggagatcaaagtgcatcagctgaaatacaaatagcaacatcagctaatactttgtcccaagccacc
aatgaagttggaagagagagttgtttaggaccgggttcaacatgcaattatggtcatggacctgtggacacagcactttatatgatggctctaagcaacaac
cttgtgcctcctcttccctcgtccttgccaatcagtcttaagcctaagactattttaacctttctttggaat

Nphs2 5 NdeI/F: gcgcCATATGcacctaagcagagcctgc

Nphs2 5 SalI/R: gcgcGTCGACTCTCAATGCAGCGGTGCA Length: 312nt

~~Nphs2 3 PacI/F: *gcgcTTAATTAA*GACAGCAGGGCGCGGA~~

~~Nphs2 3 AscI/R: *tata*GGCGCGCC*AACCTCGTCCACGTCCAC* Length: 213nt~~

Nphs2 3 PacI/F: gcgcTTAATTAAtggaaggtagatcccacgag

Nphs2 3 AscI/R: tataGGCGCGCCggaagaggaggcacaaggtt Length: 315nt

FIGURE 5.9: DESIGNING THE RECOMBINEERING ARMS

Figure 5.9: Designing the recombineering arms

Each primer contains unique restriction sites for integration into the template Podocin BAC (colour coded). A) PCR amplification of 5' and 3' recombineering arms. Three lanes for each represent different PCR conditions. 5' Arm gives 312bp expected product. However, the 3' Arm generates aberrant ~600bp product rather than the 213nt expected; B) The redesigned 3' recombineering arm primers generate the expected 315bp product. C) Murine Podocin promoter sequence showing redesigned 3' recombineering arm primers

5.5.2 Cloning the 5' Recombineering Arm into the GFP-CreERT2-IRES-puro-BAC (GCT2iP) vector

The 5' recombineering arm was amplified from the RP23 Podocin BAC using the Fast Start High Fidelity PCR System (Figure 5.10 A).

Serial restriction digests were used to prepare the vector and recombineering arm for ligation, to cut at the respective *Nde*I and *Sal*I sites. The restriction enzyme was inactivated and the digested vector and the recombineering arm ligated. The ligated construct used to transform Stbl2 competent cells.

Only 2 colonies grew, and these were mini-prepped and digested to confirm integration of the 5'arm. A double digest using *Nde*I/*Sal*I confirmed the presence of the 5' arm in Clone C (Figure 5.10 B). Further restriction digests were performed using *Nde*I/*Xho*I to confirming integration of the 5' recombineering arm in clones GCT2iP5' B & C (Figure 5.10 C).

5.5.3 Cloning the 3' Recombineering Arm into the GFP-CreERT2-IRES-puro-BAC (GCT2iP 5') vector

The same protocol was followed to integrate the 3' recombineering arm. The GFP-CreERT2-IRES-puro-BAC containing the 5' arm (GCT2iP-5') was digested with both *Asc*I and *Pac*I, and ligated overnight with the purified 3' recombineering arm. The ligated construct was used to transform Stbl2 competent cells. The 2 colonies that grew (A & B), were digested to check for integration (Figure 5.11 A, B, C, D). Clone B was correct – referred to as GCT2iP-5'3'. This construct was then used to recombineer into the Podocin BAC.

5.5.4 *Electroporation of BAC DNA into EL350 cells*

Maxi-prepped BAC DNA was used to transform EL350 cells (containing the recombineering machinery) by electroporation. Restriction digests of the electroporated clones were compared to the original BAC, and confirmed integration of the BAC in EL350 clones G and H (Figure 5.12 A). PCR using the 5' and 3' recombineering arm primers confirmed the correct Podocin sequence was present on the BAC (Figure 5.12 B & C).

5.5.5 *Recombineering the GCT2iP5'3' vector into the Podocin BAC*

The GCT2iP5'3' vector was recombineered into the podocin BAC using previously published protocols (Sharan, Thomason et al. 2009). The EL350 cells containing the Podocin BAC were induced at 42°C to activate their recombination machinery and the linearised vector introduced via electroporation. Induced cells electroporated with DNA were grown overnight on kanamycin selection. Control electroporations of un-induced cells, cells with no DNA added and cells grown on no selection were used to verify cell viability, and specificity of the selection.

5.5.6 *Confirmation of correct integration of the recombineering arms*

PCR primers were designed to demonstrate correct integration of the GCT2iP5'3' vector into the Podocin BAC (Figure 5.13 A). Clone B contained both the 5' and 3' arm in the correct orientation (Figure 5.13 B & C). Re-digestion with *Hin*dIII and *Bam*HI confirmed the continued presence of the complete *Podocin* BAC (Figure 5.13 D).

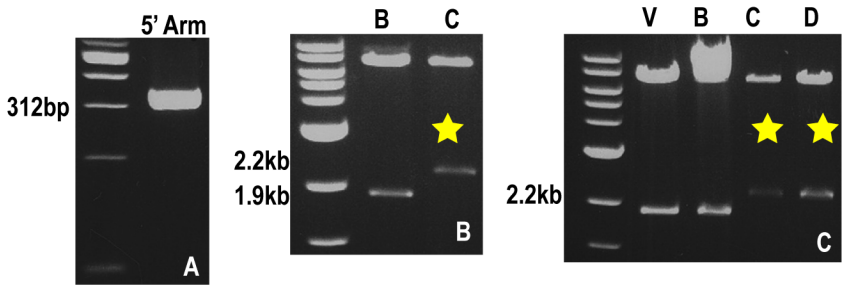

FIGURE 5.10: VERIFYING THE INCORPORATION OF THE RECOMBINEERING ARMS

A) 5' recombineering arm; B) *Nde*I/*Sal*I double digest confirming presence of 5' arm in clone C (2.2kb band). Clone B demonstrates the empty vector; C) *Nde*I/*Xho*I double digest confirming presence of 5' arm in clones C & D (2.2kb band). V=Vector; D) Star represents correct pattern.

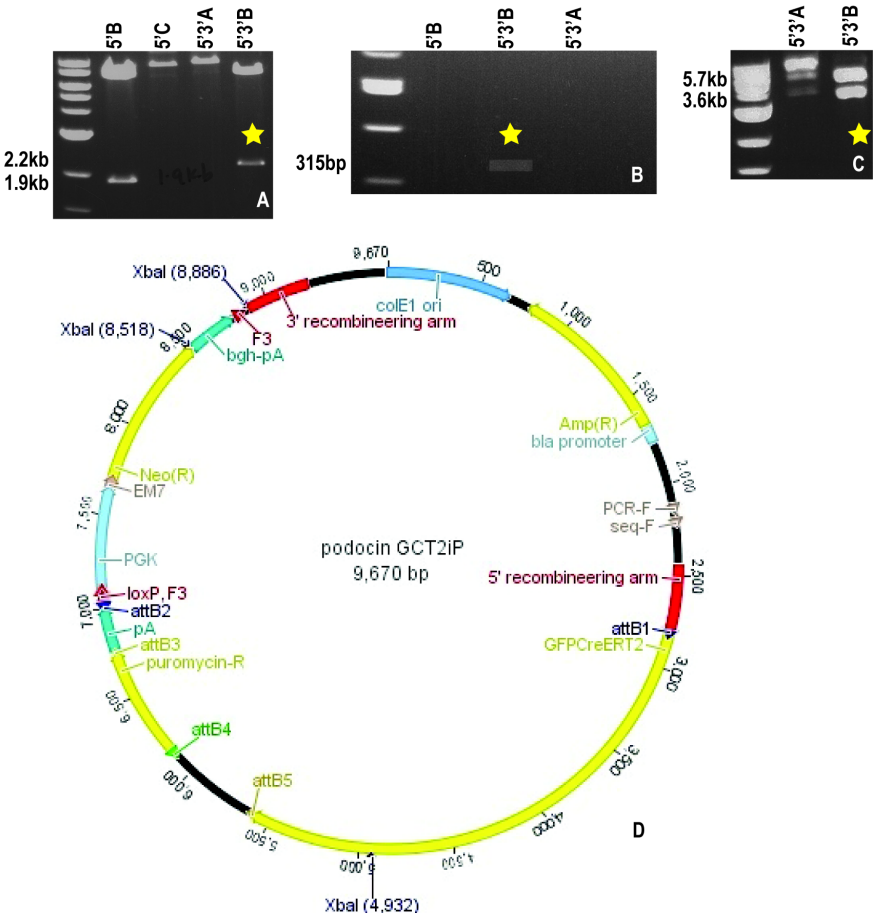

FIGURE 5.11: RECOMBINEERING IN THE 3' ARM

A) *Nde*I/*Xho*I digest confirms continued presence of 5' arm (2.2kb band). 5'B = Clone B from 5' recombineering (empty); 5'C = correctly integrated 5' arm in Clone C; 5'3'A = incorrect clone A following recombineering of 3'arm; 5'3'B = correct vector containing 5' recombineering arm. B) *Pac*I/*Asc*I digest demonstrating 315bp 3' arm in 5'3'B. C) *Xba*I digest to demonstrate correct integration of both 5' and3' arms into 5'3'B (bands at 5.7kb & 3.6kb). D) Restriction digest map

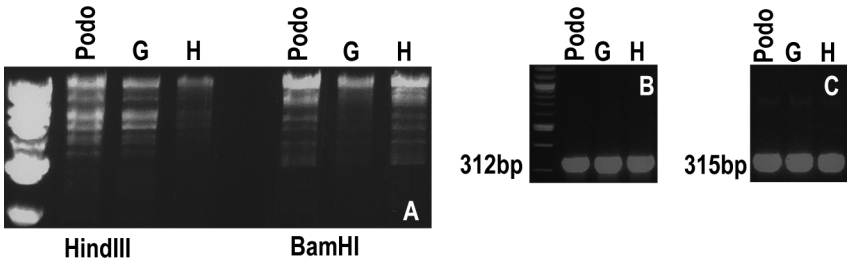

FIGURE 5.12: CONFIRMING THE PODOCIN BAC

A) *Hin*dIII and *Bam*HI restriction digest patterns. EL350 Clones G & H demonstrate the same digestion pattern as the original RP23 Podocin BAC (Lipska, Ranchin et al.). B) Amplification of 5' recombineering arm to demonstrate presence of Podocin sequence in the BAC. C) Amplification of 3' recombineering arm to demonstrate *Podocin sequence* in the BAC

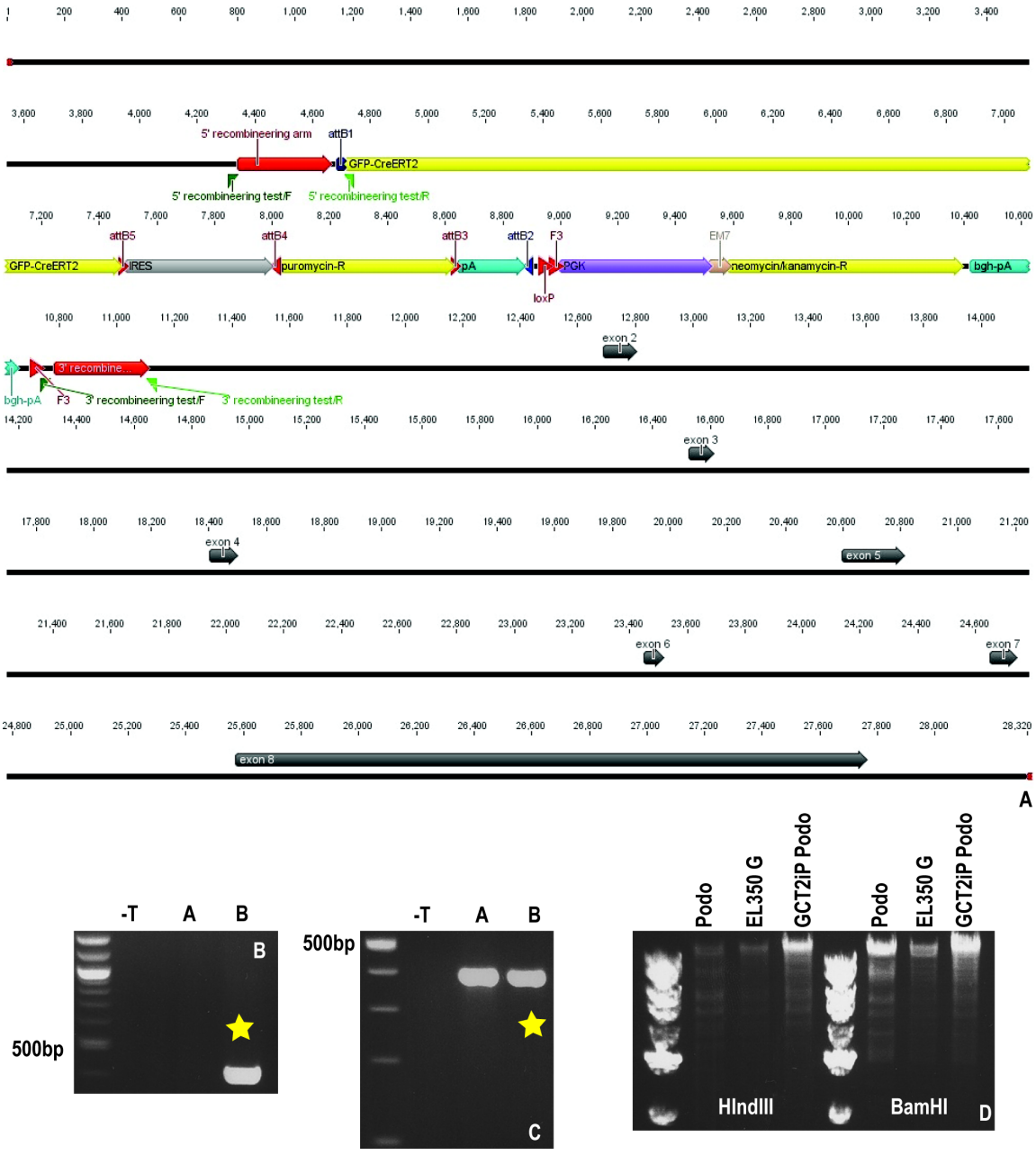

FIGURE 5.13: RECOMBINEERING THE VECTOR INTO THE PODOCIN BAC

A) Primer design to confirm correct integration and orientation of the vector into the Podocin BAC. B) Correct integration of 5' arm in B. C) Correct integration of 3' arm in B; D) Restriction digests confirm the continued presence of the complete Podocin BAC

5.5.7 *Removal of the BAC LoxP site*

The RP23 Podocin BAC contained a LoxP site in the backbone, which required removal, as a further LoxP site was also present in the inserted vector (Figure 5.14 A). The presence of two LoxP sites would allow recombination and inactivation of the vector upon Cre-recombinase activation. To select for recombinants in which the LoxP site was removed, it was replaced with an ampicillin cassette (lost from the original vector).

The ampicillin cassette was amplified from plasmid template pRosa26miWt1-406 by PCR, using primers containing sequence homology to the BAC backbone surrounding the LoxP sites (Figure 5.14 B).

The PCR product containing the amplified ampicillin cassette was used to recombineer the GCT2iP Podocin-BAC in EL350 cells as previously. PCR was used to verify the correct integration of the ampicillin cassette (Figure 5.15).

Unfortunately, a number of attempts resulted in incorrect integration of the ampicillin cassette elsewhere in the BAC backbone. The protocol was optimized with the addition of a *Dpn*I digestion, to remove any remaining plasmid DNA that may have been integrating incorrectly, and the addition of chloramphenicol selection (to ensure the presence of the complete BAC).

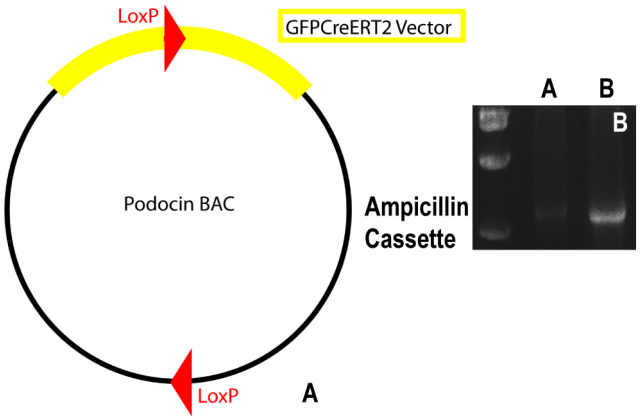

FIGURE 5.14: REMOVING THE LOXP SITES

A) Schematic representation of LoxP sites. B) Amplification of the ampicillin cassette. A= with DMSO, B= without DMSO

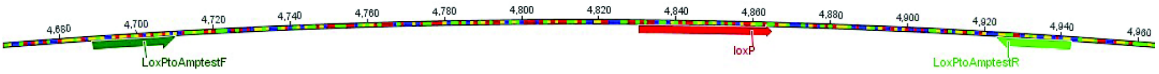

FIGURE 5.15: VERIFYING THE CORRECT INTEGRATION OF AMPICILLIN USING PCR

5.5.7.1 Troubleshooting Removal of the LoxP Cassette

Despite optimizing the protocol, it still proved impossible to recombineer the LoxP site and Ampicillin cassette correctly. To troubleshoot, all previous steps were reconfirmed to ensure the working GCT2iP Podocin BAC construct was correct. This demonstrated:

1) Presence of the podocin BAC
2) Presence of both 5' and 3' recombineering arms
3) Presence of the GFPCreERT2 cassette

The original Podocin BAC was used as a control to ensure there was no anomaly in the original BAC that was preventing correct recombination. Recombination of the ampicillin cassette into the original BAC was straightforward. With all components of the GCT2iP5'3' Podocin BAC confirmed to be correct, and the recombination protocol optimized, successful recombination was eventually achieved, and PCR of clones B1 and B2 demonstrated correct integration of the ampicillin cassette (Figure 5.16 A). However, further recombination experiments, using serial dilutions of DNA, were required to generate cells only containing one copy of the recombineered BAC (Figure 5.16 B). The final correct clone **'B2ACK'** was tested once again to ensure the presence of all the correct components (BAC digestion pattern, 5' and 3' recombineering arms, GFP-CreERT2 construct). Once verified, the construct was stored as glycerol stocks and could be used to generate transgenic animals (Figure 5.16 C)

This completed construct is referred to as **GCT2iP-Podocin-BAC**.

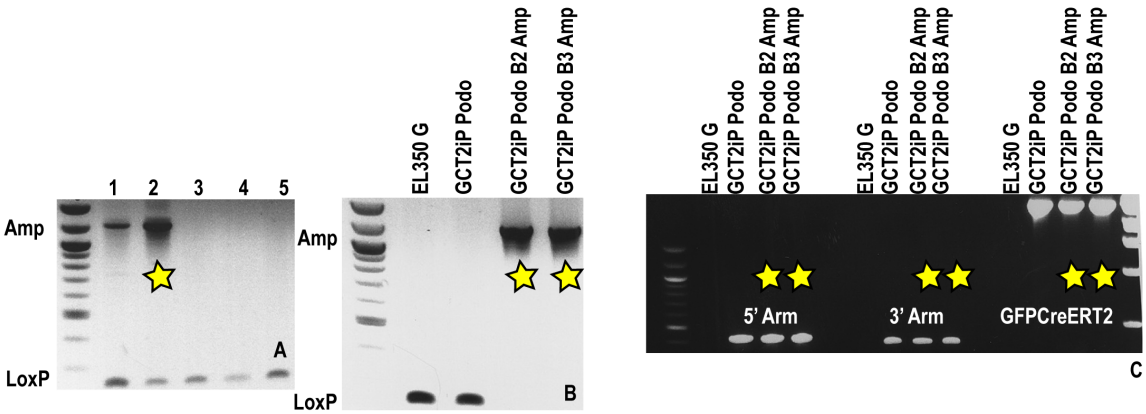

FIGURE 5.16: THE RECOMBINEERED BAC

A) PCR demonstrating correctly recombineered ampicillin cassette; B) Single copy number BAC containing ONLY the ampicillin cassette; C) confirming the correctly integrated components of the construct. Stars indicate correct construct

5.6 GENERATION OF THE PODOCIN-GFPCREERT2 MOUSE

5.6.1 BAC DNA MICROINJECTION

The initial strategy to generate transgenic animals was to use microinjection of BAC DNA into the oocyte. This would be the quickest and most efficient method, but could be limited by position and copy number effects.

EL350 cells containing clone the GCT2iP-Podocin-BAC were grown up for 20 hours at 32° to maxi-prep. DNA extraction was performed using the Qiagen Large Construct Kit.

The extracted DNA was digested overnight with PI-*Sce*I for linearization of the BAC. The enzyme was denatured and the DNA ethanol precipitated. It was prepared for microinjection by diluting to a concentration of 0.5ng/μl in microinjection buffer and kept at on ice until use.

DNA microinjection was performed by Paul Devenney. Both wild type (CD1) and $Wt1^{co/co}$ dams were used. This strategy was used to maximize both the efficiency of BAC DNA integration to make founders and also to limit the number of downstream breedings. CD1 dams tend to have larger litters, increasing the likelihood of finding transgenic founders. However, CD1 offspring would require 2 generations of crosses to generate *Podocin-Cre*$Wt1^{co/co}$ experimental animals and increase the heterogeneity in the genetic background (as CD1 mice are outbred). $Wt1^{co/co}$ dams tend to have smaller litters, but experimental animals could be generated within one generation, significantly reducing breeding times.

Microinjected offspring were born and earclipped at 2-3 weeks of age for genotyping. Offspring were identified by the prefix 'B2ACK' (referring to GCT2iP-Podocin-BAC Clone B2 Amp^R $Chlor^R$ Kan^R) and serial numbers corresponding with ear-notches. Validated genotyping PCRs for detection of Cre-recombinase and the GFP cassette were used. Positive founders were then mated with CD1 mice for phenotypic analysis, before crossing with $Wt1^{co/co}$ females.

5.6.1.1 Summary of BAC microinjections and offspring generated

TABLE 5.1: MICROINJECTION INTO WILD TYPE (CD1)

Injection Date	**Date of Birth**	**Pups born**	**Animal Numbers**	**Positive genotypes**
21.02.2011	13.03.2011	25	B2ACKwt 1-25	**B2ACKwt 9 Male**
25.08.2011	15.09.2011	26	B2ACKwt 26-51	All negative
10.9.2011	29.11.2011	11	B2ACKwt 68-81	*B2ACKwt 74 Male* *B2ACKwt 75 Female*
1.12.11	21.12.11	53	B2ACKwt 83-135	*B2ACKwt 85,86,91,99,114,128,132*
	TOTAL	115		**1 strong positive founder**
				9 equivocal founders

TABLE 5.2: MICROINJECTION INTO *WT1*$^{CO/CO}$

Injection Date	**Date of Birth**	**Pups born**	**Animal Numbers**	**Positive genotypes**
01.02.2011	24.02.2011	8	B2Ampco 1-8	*B2Ampco 2 Male*
22.02.2011	14.03.2011	26	B2ACKco 1-26	**B2ACKco 23 Male**
29.09.2011	20.10.2011	12	B2ACKco 35-44	*B2ACKco 35, 36, 37, 44 Male*
	TOTAL	46		**1 strong positive founder**
				5 equivocal founders

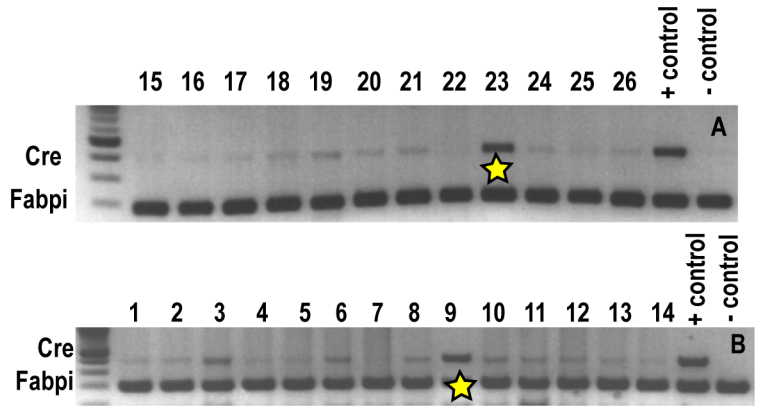

FIGURE 5.17: CRE GENOTYPING OF POTENTIAL FOUNDERS

Cre genotyping of strong positive founders A) B2ACKco (DNA microinjection into $Wt1^{co/co}$ oocytes. Male 23 is positive; B) B2ACKwt (DNA microinjection into CD1 oocytes). Male 9 is positive. Strongly positive founders indicated by stars

5.6.1.2 Characterization of *Podocin*-GFP-CreERT2 founders generated by BAC DNA

The strongly positive founder males were crossed with CD1 females, in order to rapidly analyse the phenotype of the offspring. Embryos were taken for analysis at E16.5, the earliest date where plentiful mature podocytes would be present. Embryonic kidneys were dissected and analysed whole mount for expression of GFP in the podocyte. Podocyte specific GFP expression would verify that the BAC was both being passed through the germline and being expressed correctly. Analysis of GFP expression in 56 embryos (from both strong founders B2ACKco23 and B2ACKwt9) using whole mount fluorescence microscopy, confocal microscopy on fixed kidneys, and FACs analysis of digested kidney tissue did not reveal any detectable GFP expression.

Initial genotyping PCR of embryonic tail tips for both Cre and GFP (i.e. presence of the transgene) was equivocal, with only faint bands present, despite multiple experimental repeats. It was therefore unclear whether the offspring were actually carrying the transgene. To ensure the lack of GFP expression was not due to weak activity by the Podocin promoter, the putative founder males were crossed with $R26R^{YFP/YFP}$ reporter females. Any Cre-positive offspring, plus Cre-negative littermate controls, could be injected with tamoxifen to analyse the Podocin-CreERT2-activity in the kidney via expression of YFP. However, although each putative founder male generated an YFP litter, at genotyping none of the offspring were Cre-positive so were not analysed further.

Further litters were generated, crossing with CD1 females (to maximize the number of offspring) and earclipped and genotyped at weaning. Three litters per putative founder male were generated and genotyped for Cre, however, none of the offspring appeared to carry the transgene.

During this time, a *Six2*-Cre-GFP transgenic line had been generated by my colleague, Karamjit Singh Dolt, which expressed both GFP and Cre in the *Six2*-positive renal precursor cells (Dolt, Lawrence et al. 2013). This implied the gateway recombineering construct and DNA microinjection technique were both viable. However, via DNA microinjection I was unable to generate founders who were able to transmit the transgene into the germline.

5.6.2 *Random integration of BAC into ES cells*

The secondary method to generate the Podocin-GFP-CreERT2 transgenic line was to use random integration of the GCT2iP-Podocin BAC into ES cells. This would prove faster than endogenous targeting into ES cells, but could still be influenced by positional effects.

Two rounds of DNA electroporation into ES cells were performed. Unfortunately the initial attempt had to be discarded due to contamination in the original ES cell culture. The second attempt did not yield any viable clones, due to a high level of differentiation amongst any surviving cells.

5.6.3 *Endogenous Targeting of GCT2iP-Podocin BAC into Embryonic Stem Cells*

Endogenous Targeting of the GCT2iP vector would allow specific integration of the vector into Exon 1 of the endogenous Podocin locus, thus removing any positional or copy number effects, such as the influence of nearby alien enhancers or insulators. However, endogenous targeting is the most prolonged method of generating transgenic lines, so was a contingency plan if BAC DNA microinjection was unsuccessful.

Endogenous Targeting involved a number of steps (Dolt, Lawrence et al. 2013):

1. Amplification of plasmid pMCS-DTA with PCR primers containing 50nt of homology to the GCT2iP-Podocin construct to make the Retrieval Arms (Figure 5.18 A).

2. Recombineering of the GCT2iP-Podocin BAC vector into the amplified plasmid pMCS-DTA DNA in EL350 cells (positive selection with ampicillin, negative selection with the diphtheria toxin) to create the Retrieval Vector (Figure 5.18 B)

3. Design and validation of 5' and 3' probes to differentiate between correctly targeted and wild type DNA

While still pursuing the generation and characterization of the Podocin-GFP-CreERT2 mouse line by DNA microinjection techniques, I completed a number of steps towards endogenous targeting:

- The endogenous targeting probes were designed and validated on wild type DNA (Figure 5.19 A)
- The pMCS-DTA plasmid was sequenced to confirm the correct sequence for cloning
- The pMCS-DTA plasmid was amplified with PCR primers containing the 50nt Retrieval Arms homologous to the GCT2iP-Podocin construct
- The GCT2iP-Podocin vector was recombineered into the amplified pMCS-DTA plasmid containing the retrieval arms and selected on kanamycin and ampicillin. Restriction digests were used to confirm correct integration of the construct into the amplified pMCS-DTA DNA (Figure 5.19 B). However, despite multiple attempts no correctly recombineered constructs were obtained.

At this stage, late in the project, it was decided not to pursue generating the Podocin-GFP-CreERT2 transgenic line further, as discussed below. Therefore, alternative methods were attempted in order to limit *Wt1* deletion to the glomerulus.

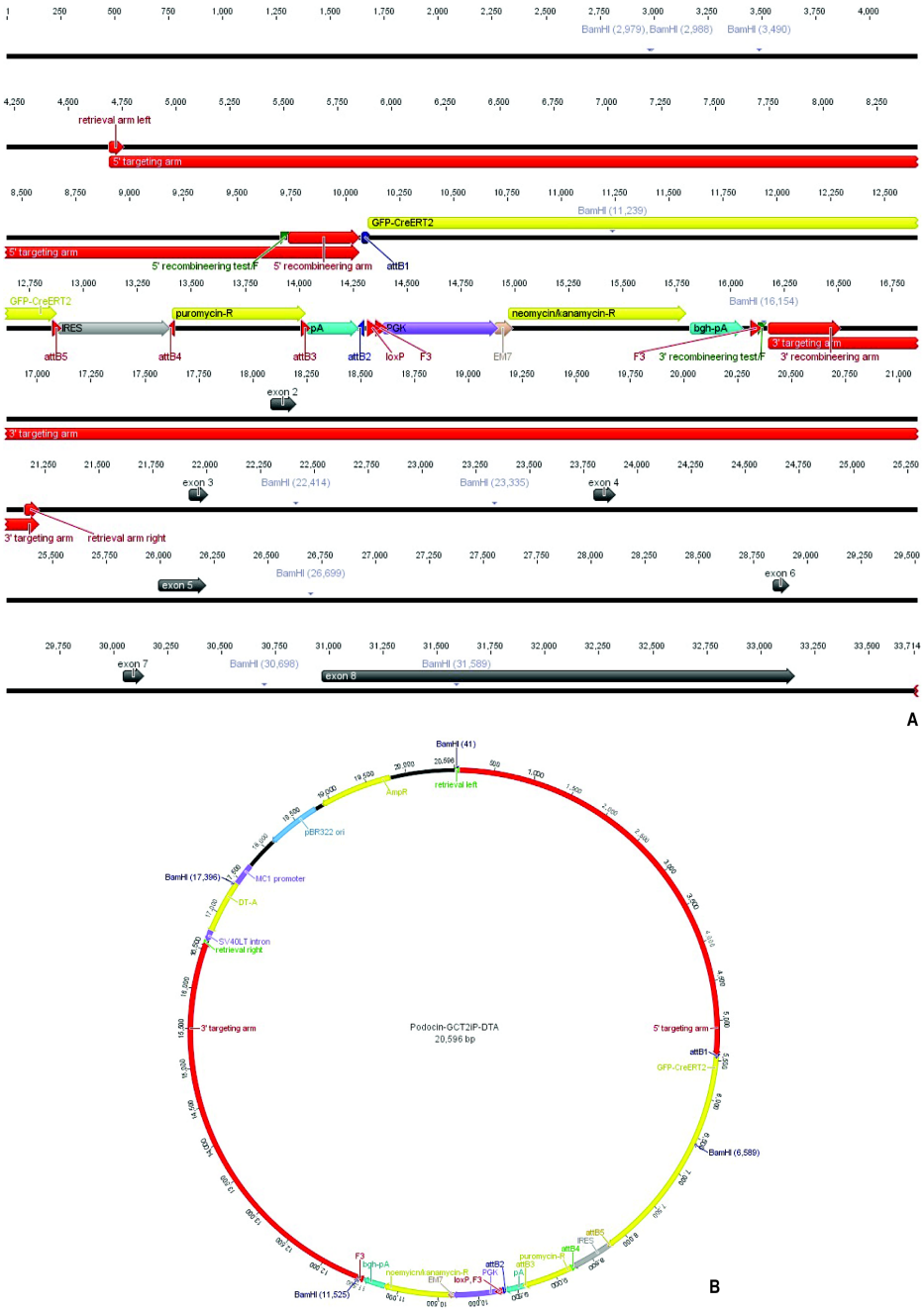

FIGURE 5.18: ENDOGENOUS TARGETING

A) Retrieval Primer Design; B) GCT21P Podocin vector recombineered into pMCS-DTA

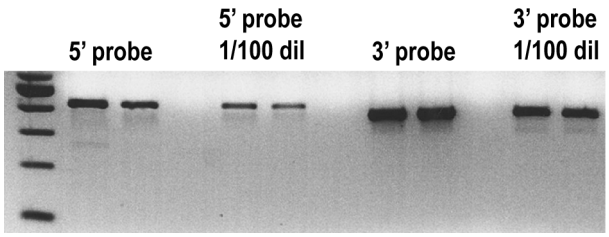

FIGURE 5.19: VALIDATING THE PROBES

Amplifying the 5' and 3' probes on wild type DNA. Probes amplified using neat and diluted maxi-prepped DNA.

5.7 USING *NESTIN*-CREERT2 AS A METHOD OF GLOMERULAR-SPECIFIC CRE-RECOMBINATION

Nestin is an intermediate filament protein that was originally identified in the central nervous system, where it is expressed in the neural stem / progenitor cell compartment (Wagner, Wagner et al. 2006). Outwith the developing central nervous system, Nestin has also been identified in the developing heart, testis and kidneys, and in muscle pre-cursors (Mohseni, Sung et al. 2011). Interestingly, Nestin continues to be expressed in the adult kidney, where its expression is restricted to the glomerulus (Wagner, Wagner et al. 2006), particularly the podocyte (Zou, Yaoita et al. 2006).

The lab had previously used a constitutional *Nestin*-Cre to successfully delete *Wt1* from the developing kidney (Rigby, Leitch et al. 2008). This resulted in halted nephrogenesis, due to a failure to proceed through mesenchymal to epithelial transition, and early death. Using a tamoxifen-inducible Cre would allow targeted deletion of *Wt1* in the adult glomerulus, predominantly in the podocyte, thus avoiding any potential confounding extra-renal effects and the embryonic lethality of constitutional deletion. A *Nestin*-CreERT2 mouse model was already available in the lab, which had been previously used successfully to permanently label neural progenitor cells when combined with a Z/EG reporter strain (Carlen, Meletis et al. 2006). However, expression of the transgene in the kidney had not been formally investigated.

Nestin-CreERT2 mice were crossed with an $R26R^{YFP/YFP}$ reporter strain to generate *Nestin*-$CreERT2^{YFP/YFP}$ offspring. In order to activate the Cre-recombinase, adult mice (Cre positive n=4, Cre negative n=3) were injected with tamoxifen 1mg/40g body weight for either 3 days or 5 days. Cre-negative littermates were used as control animals. Mice were sacrificed 1 week after tamoxifen injection and the kidneys harvested and fixed in paraffin and for cryopreservation for analysis of YFP expression.

No endogenous YFP expression could be detected on cryopreserved kidney sections using a fluorescent microscope (Figure 5.20). Immunoreactivity for YFP was also undetectable using a GFP antibody (Abcam ab6556) indicating little or no expression of the transgene and Cre activity in the kidney, rendering this model unsuitable for use as a tissue-specific Cre line.

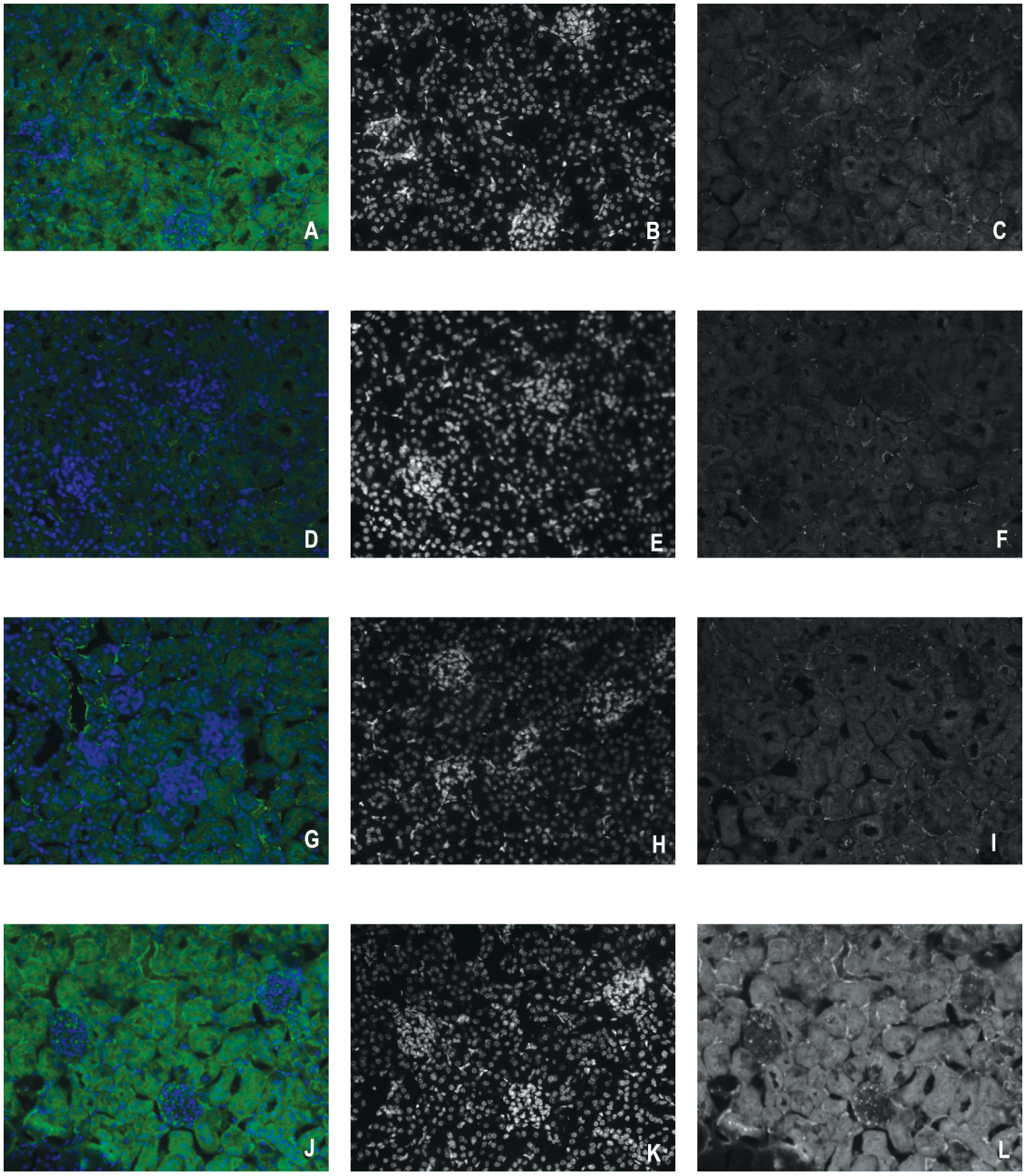

FIGURE 5.20: IMMUNOFLUORESCENCE FOR YFP EXPRESSION FOLLOWING CRE-INDUCTION IN *NESTIN*-CREERT2 YFP/YFP MICE

Immunofluorescence for YFP expression following Cre-induction in *Nestin*-CreERT2 YFP/YFP mice using a GFP secondary antibody A) Cre-positive male 1mg/40g BW x 3 days, merge. B) DAPI. C) FITC. D) Cre-negative control male 1mg/40g BW x 3 days, merge. E) DAPI. F) FITC. G) Cre-positive female 1mg/40g BW x 5 days, merge. H) DAPI. I) FITC. J) Cre-negative control female 1mg/40g BW x 5 days. H) DAPI. I) FITC.

No endogenous or immunofluorescently detected YFP is found in the glomerulus indicating the transgene is not active in the kidney.

5.8 Discussion

5.8.1 BAC recombineering was unsuccessful in generating an inducible podocyte-specific Cre transgenic line.

BAC recombineering was chosen as the method of genetic engineering, as it provides fast, flexible and efficient cloning in order to generate the desired construct, and avoids some of the limitations of traditional cloning techniques, such as the need for specific restriction sites flanking the gene of interest (Sharan, Thomason et al. 2009).

The use of Gateway recombination cloning technology (Invitrogen Gateway® Multisite Cloning) allowed flexible and reversible cloning, as up to 4 fragments could be inserted or replaced into the vector, according to the requirements of the construct (Sasaki, Sone et al. 2004).

However, the previous podocyte-specific Cre models mentioned earlier were generated using traditional cloning techniques using short promoter element transgenes (Eremina, Wong et al. 2002, Juhila, Roozendaal et al. 2006). These methods are limited by the requirement for unique restriction sites in both the cloning construct and the target genomic DNA. Also, they are less amenable to the manipulation of larger DNA fragments, such as the dual promoter-reporter construct (Copeland, Jenkins et al. 2001). Therefore, BAC recombineering was chosen instead as it provided a faster, more efficient and more flexible method of generating the transgene.

Generation of the construct proved relatively straightforward, apart from a few extra optimisation steps, and the construct was verified rigorously to ensure it contained all the correct constituents.

However, after several rounds of BAC DNA microinjection only two strong potential founders were generated. Neither of these appeared to pass the Podocin-GFP-CreERT2 transgene into the germline. Two rounds of random integration of the BAC DNA into ES cells had failed to yield any positive clones thus far, and although initial steps towards endogenous targeting of the

construct into ES cells had been completed, it was decided not to proceed further with alternative approaches of generating the transgenic line for two reasons.

Firstly, although the original putative *Podocin*-GFP-CreERT2 founders had been generated in a timely manner, the breedings needed to generate *Podocin*-GFP-CreERT2 positive offspring meant that time was limited to generate this line using other methods.

Secondly, although the original GFP-CreERT2 construct had been used successfully to generate a number of transgenic lines, information from collaborators revealed that others had also experienced problems with it. McMahon *et al* originally used this construct as a knock-in to the *Six2* locus, and demonstrated correct endogenous GFP expression and tamoxifen-inducible Cre activity in the *Six2*-positive nephron progenitor cells. The authors also expressed this construct at the *Wnt4* locus, although the GFP expression could only be detected with immunofluorescence (Kobayashi, Valerius et al. 2008). Subsequently, this construct has also been expressed at the *FoxD1* locus, where specific GFP and Cre expression have been demonstrated (Humphreys, Lin et al. 2010).

However, other mouse strains using this construct have not demonstrated full, or specific, expression patterns. For example, the *S100*-GCE (GFP-CreERT2 under control of the S100b promoter) mouse line does not demonstrate detectable endogenous GFP expression, although GFP protein can be detected immunohistochemically in some sites of S100b expression. Cre-activity is only found in a subset of these (McMahon, Aronow et al. 2008). The *TMEM100*-GCE strain (GFPCreERT2 construct expressed in the *Tmem100* domain) also showed variable expression, with a number of founder strains failing to express either GFP or the transgene (McMahon, Aronow et al. 2008).

Given the time constraints and concern regarding the efficacy of the GFP-CreERT2 construct, it was decided to stop further work on generating a novel *Podocin*-GFP-CreERT2 line, and to pursue an alternative strategy.

5.8.2 Alternative approaches to generating a podocyte-specific model of *Wt1* loss

The available *Nestin*-CreERT2 mouse line was analysed for expression of the transgene within the kidney, but, when crossed with a reporter strain, no detectable Cre-activity could be detected within the kidney. Therefore, this model would not offer glomerular-specific Cre-activity to limit *Wt1* deletion to the glomerulus. In fact, other Cre lines made with this Nes element have also not been found to express within the kidney, or anywhere outside the neuronal system (Meletis, Barnabe-Heider et al. 2008).

5.8.3 Using the *Podocin-iCreERT2* transgenic line to generate a podocyte specific model of *Wt1* loss

During the course of this project a paper was published describing a new podocyte-specific Cre line, which utilised a tamoxifen inducible Cre. This used an iCre-ERT2 construct under control of the human Podocin *(NPHS2)* promoter (Wang, Wang et al. 2010). The expression of Cre-recombinase in this construct was enhanced by applying mammalian codon usage, and reducing the high CpG content of the prokaryotic coding sequence, as this is vulnerable to epigenetic silencing (Shimshek, Kim et al. 2002). By crossing these mice with $R26R^{LacZ}$ reporter mice, podocyte specific Cre-activity was demonstrated after induction with tamoxifen.

When crossed with $Wt1^{co/co}$ mice, these mice would allow temporal and spatial control of Cre activity, thus limiting *Wt1* deletion to the adult podocyte and avoiding any potential extra-renal confounding effects.

Given the proven efficacy of this model, it was decided to import these mice for breeding with the *Wt1* conditional mice to generate the podocyte specific model of *Wt1* loss.

Importation of this line was greatly delayed due to the presence of MHV in the parent colony, so it could not be imported directly to the MRC IGMM animal unit. Therefore, the line is being re-derived by the Biomedical Research Resources department at the University of Edinburgh.

Once the *Podocin*-iCreERT2 animals are available, they will be crossed with $Wt1^{co/co}$ mice in order to generate the model of tamoxifen-inducible podocyte-specific *Wt1* deletion.

Unfortunately, given that generating a *Podocin*-GFP-CreERT2 line was unsuccessful, and importing the *Podocin*-iCreERT2 line has been unexpectedly prolonged, this has not been possible during the course of this PhD project, but will form the basis of future work.

5.9 CONCLUDING REMARKS

Generation of an inducible Podocyte-specific promoter-reporter transgenic mouse line was unsuccessful during the course of this project. BAC recombineering provided an efficient and flexible method of generating the transgenic construct, which was designed to provide not only Podocyte-specific Cre activity, but also fluorescent labeling of mature podocytes, and the capacity to trace *Wt1*-deleted podocytes specifically (see Figure 4.1).

Although generation of the construct was successful, BAC DNA microinjection did not produce any founder animals that were able to pass the transgene into the germline. As previously mentioned, microinjection leads to the random integration of target DNA, which can affect expression due to positional effects. However, transgenic efficiency is estimated at 5-30% (Rossant, Nutter et al. 2011), so given the number of microinjection attempts it is surprising no successful founders were generated. Successful generation of transgenic animals has been achieved using an alternative Six2-driven construct, implying no inherent problem in either the construct backbone or microinjection method (Dolt, Lawrence et al. 2013).

Ideally, the construct would have been used to generate mice using targeted integration into ES cells, which would have avoided any positional or copy number effects. However, given the concerns identified during the course of this project regarding the efficacy of the original GFP-CreERT2 construct, and the limited time available, this was not taken further.

As a successful podocyte-specific-Cre transgenic line was published during the course of this project, this will be used to take this work further and confirm the effects of *Wt1*-deletion in the podocyte.

6 General Discussion

6.1 The findings from this thesis can be summarised as follows:

6.1.1 The generation and In-vitro analysis of Wt1-mutant podocytes:

- Analysis of conditionally immortalised podocytes carrying *WT1* mutations from patients with DDS, demonstrates some alteration of the epithelial-mesenchymal balance, although there is significant variability between cell lines. Cell line DDS3 in particular, demonstrated marked upregulation of the mesenchymal driver, Snail, a known transcriptional target of Wt1, and also exhibited the most mesenchymal characteristics.

- Although these podocytes have been affected by *WT1* mutations throughout their development, rather than being a model of *WT1*-loss only in the adult, they offer a human comparison to the phenotype exhibited in the *Wt1*-conditional mouse. They provide supporting evidence of a role for *WT1* in maintaining the epithelial-mesenchymal balance in the podocyte

- Attempts to generate an *in vitro* model of Wt1 deletion in the podocyte met with only limited success but established that conditionally immortalised *CreERWt1*$^{co/GFP}$ podocytes generated from the *in vivo Wt1*-conditional model did not provide a robust model of *Wt1* deletion *in vitro*. Although *Wt1*-deletion could be clearly demonstrated at the DNA level, this was not translated into detectable changes in mRNA or protein expression. Perhaps as a consequence of their compound heterozygosity, or 'leaky' Cre-recombination, these cells only expressed low levels of *Wt1* prior to induction of Cre-recombinase activity, which may have accounted for this.

- Lentiviral mediated RNAi is an effective and flexible method of *Wt1* knockdown in conditionally immortalised podocytes and is possible in both differentiated and undifferentiated cells.

- *Wt1* is essential for the differentiation of podocytes in culture. Proliferating *Wt1*-knockdown conditionally immortalised podocytes are unable to differentiate.

6.1.2 Using a dose-limited model of conditional Wt1-deletion in the adult mouse, it was established that:

- *Wt1* is an essential gene in the adult mouse, and *Wt1*-deletion leads to early death
- *Wt1* deletion in the adult kidney leads to failure of the glomerular filtration barrier, leading to heavy albuminuria, hypoalbuminaemia and oedema, equivalent to human nephrotic syndrome
- *Wt1* deletion in adult kidney leads to severe and progressive damage to both podocytes and parietal epithelial cells
- This podocyte damage is associated with loss of key podocyte proteins, including a profound loss of nephrin expression. This is consistent with the failure of the slit diaphragm indicated by the heavy albuminuria.
- *Wt1*-deletion leads to an alteration in the expression of key regulators and markers of the epithelial-mesenchymal balance in podocytes
- Following *Wt1*-deletion, there is re-expression of *Wnt4* in the glomerulus, which is usually only expressed during renal development.
- The phenotype following *Wt1*-deletion is more severe than other models of podocyte injury.
- This model represents a robust, inducible model of severe glomerular injury, which would provide a good model for drug therapies.
- Given that *Wt1*-expression is focused within the podocyte, the effects of *Wt1*-deletion using a ubiquitously expressed Cre are unlikely to be due to extra-renal effects. However, using a podocyte-specific Cre would confirm these findings absolutely.

6.1.3 *Podocyte-specific Wt1 deletion in-vivo*

- BAC recombineering to generate a Podocin-Cre promoter-reporter mouse line was unsuccessful. This may have been due to positional or copy-number effects due to random integration of the construct, or perhaps due to unreliability of the original GFP-CreERT2 construct. There was not sufficient time during the project to successfully use endogenous targeting in ES cells to generate the model.

- Gateway recombineering did provide a flexible tool to generate the GFP-CreERT2 promoter-reporter construct (Dolt, Lawrence et al. 2013)

6.2 How do the findings from this thesis build upon previous work and how can they contribute to further understanding of podocyte biology?

Underlying this work is the central premise that kidney disease affecting the glomerulus is almost always progressive in nature and leads to an eventual requirement for renal replacement therapy, be that in the form of transplantation or dialysis. Key to this process is the understanding that glomerular numbers are finite, with very limited potential for regeneration of glomerular cells, let alone whole glomeruli. An understanding of the biology of the glomerulus, both in health and disease, is fundamental to identify pathways that could lead to clinical targets to slow progression of disease, or even encourage repair or regeneration.

Podocyte injury is the major mechanism of progressive glomerular damage, so podocytes remain a topic of intense interest in the field of kidney research. This thesis has looked at the role of *WT1* in the adult podocyte. Given the limitations of previous animal models, little research had been done on the role of *WT1* in the podocyte, despite the fact it remains the main focus of *WT1* expression in the adult.

The work in thesis has demonstrated the essential role of *Wt1* in the adult kidney, with *Wt1*-deletion leading to severe podocyte injury and failure of the glomerular filtration barrier. There is a profound loss of expression of key podocyte genes immediately following *Wt1*-loss. Preliminary data suggests this does not correspond directly to an equivalent loss of podocyte cells from the glomerulus, which would support a role for *Wt1* in podocyte differentiation. This theory is supported by the requirement for *Wt1* for podocyte differentiation *in vitro*. Other researchers have also demonstrated that podocytes carrying the *Wt1*-mutations of DDS have characteristics of earlier developmental stages (Schumacher, Jeruschke et al. 2007). Interestingly, this model of *Wt1*-deletion appears more severe than other models of podocyte injury, although conditional models of podocyte gene deletions remain limited. Certainly, it seems more severe than a model of conditional inactivation of podocin (Mollet, Ratelade et al. 2009). This would fit with an upstream role for *Wt1* in podocyte differentiation, although this remains speculation at this stage.

Increasing evidence is emerging for a role for *Wt1* in maintaining the balance of epithelial and mesenchymal characteristics in cells. Novel *Wt1* expression has been associated with phenotypic changes in such cells following injury (Smart, Bollini et al. 2011, Chau and Hastie 2012, Li, Wang et al. 2013). Novel *Wt1* expression is also demonstrated in parietal epithelial cells as they migrate onto the glomerular tuft in response to injury (Appel, Kershaw et al. 2009, Ohse, Vaughan et al. 2010). This study demonstrates changes in the epithelial and mesenchymal characteristics of *Wt1*-deleted podocytes. This merits further investigation in order to verify whether Wt1 is an upstream regulator of this epithelial-mesenchymal balance. Wt1 expression at a low level has been demonstrated in parietal epithelial cells (Kabgani, Grigoleit et al. 2012), so it may be that a change in *Wt1* expression is responsible for the phenotypic changes required for parietal cell precursors to become podocytes.

At a practical level, this study has demonstrated that RNAi can be used to knock down *Wt1* in conditionally immortalized podocytes *in vitro*. Unfortunately, as *Wt1* knockdown cells are unable to differentiate, they do not provide a viable tool to study the mechanistic aspects of Wt1 loss. However, these optimized transduction techniques could be used with inducible RNAi constructs, circumventing this problem.

Furthermore, this study has confirmed that the *Wt1*-deletion model provides a robust and reproducible model of severe podocyte injury, which holds potential for testing therapeutic strategies to ameliorate podocyte damage.

6.3 FUTURE WORK

6.3.1 PODOCYTE-SPECIFIC WT1-DELETION

A major disappointment during this period of study was the failure to generate a podocyte-specific promoter-reporter Cre line. This model would have allowed the easy identification of podocytes, and the permanent labelling of cells (podocytes) in which Cre had been active, thus facilitating accurate fate-tracing of *Wt1*-deleted cells. However, although gateway recombineering allowed relatively straightforward generation of an appropriate Podocin-GFP-CreERT2 construct, BAC DNA microinjection did not generate any founder animals that were able to transmit the transgene into the germline. There was insufficient time to pursue alternative methods to generate this model, such as gene targeting in ES cells.

During the course of this study, a more suitable model was published that allowed tamoxifen-inducible Cre-recombination under the control of the Podocin-promoter (Wang, Wang et al. 2010). Given concerns about the efficacy of eGFP-CreERT2 construct (see Chapter 5), it was decided to import this strain to cross with the *Wt1*-conditional mouse. However, delays were caused due to the presence of MHV in the parent colony, so crosses could not be undertaken before the end of this study period.

The original mouse model was crossed with an ubiquitously-expressed Cre line as the sites of *Wt1*-expression, and therefore effects of *Wt1*-deletion, were thought to be so limited. However, as discussed earlier, a number of extra-renal phenotypes were observed which could theoretically influence the renal effects. Given the high focus of Wt1-expression in the podocyte, and the absence of any observed phenotype (such as systemic inflammation) that would be likely to affect the kidney, it is extremely unlikely that the renal phenotype documented is an artifact, or secondary to any of the extra-renal effects. However, to prove this conclusively, this line will need to be crossed with the podocyte-specific Cre to limit *Wt1*-deletion to the podocyte.

As well as confirming the findings detailed in this study, close analysis of the renal effects will be undertaken. *Wt1*-deletion led to severe injury to both podocytes and parietal epithelial cells. Limiting *Wt1*-deletion to the podocyte will help differentiate whether the PEC damage is

primary (confirming the importance of Wt1 expression in PECs) or a secondary effect to the podocyte damage.

Techniques to analyse *Wt1*-deleted glomeruli and podocytes were optimized during the course of this project, so analysis of future experimental animals will be more rapid and efficient. In particular, a technique to facilitate FACS of GFP positive podocytes has been optimized. This will allow early analysis of isolated podocytes if crossed with the $Wt1^{co/GFP}$ line.

The promoter-reporter construct originally generated would have both identified podocytes and allowed identification of cells in which Cre had been active, if further crossed with a reporter strain. Unfortunately, the new line would not offer the same specific lineage tracing opportunities. However, crossing it with the $Wt1^{co/GFP}$ line and a further reporter strain would allow tracing of *Wt1* positive cells, which, if FACS sorted from isolated glomeruli, would be virtually all podocytes. FACS would allow identification and analysis of individual podocytes, allowing direct comparison between those cells in which Cre had been active and *Wt1* deleted and normal podocytes. Novel technologies to analyse small amounts of experimental tissue e.g. RNeasy Micro Kit (Qiagen 74004) or Fluidigm single-cell analysis (Citri, Pang et al. 2012) , would allow specific analysis of *Wt1*-deleted podocytes and increase the number of biological replicates, as less tissue would be required from each experimental animal.

6.3.2 Further investigation of the effects of Wt1 deletion on the epithelial-mesenchymal characteristics of podocytes

Wt1-deletion led to alterations in the epithelial-mesenchymal balance of podocytes, with a rapid and early increase in the mesenchymal drivers, particularly Snail, followed by an increase in mesenchymal genes such as vimentin, desmin and fibronectin. Intriguingly, these changes were not accompanied with a decrease in epithelial markers P-cadherin and Zo-1. The next stage in analysing these results would be to investigate the ultra-structural changes accompanying these changes in gene expression. Scanning electron microscopy of *Wt1*-deleted podocytes will allow analysis of cell-cell junctions and foot process effacement. Given the profound failure of the glomerular filtration barrier accompanying these changes, they are likely to be dramatic. Changes in protein distribution in *Wt1*-deleted podocytes are also likely to be pertinent.

6.3.3 Further Investigation of the effects of Wt1 deletion on podocyte differentiation

One of the most interesting findings in this thesis was the observation that Wt1 deletion lead to re-expression of Wnt4 in the glomerulus. During kidney development it has been demonstrated that Wt1 positively regulates Wnt4 expression by maintaining the chromatin at the Wnt4 locus in an active state and by recruitment of the co-activators Cbp and p300 (Rigby, Leitch et al. 2008). Data generated during this study appeared to indicate that later in development Wt1 switched to a repressive role, however, this had not been confirmed until now. As discussed below, it is unclear whether Wt1 acts as a direct transcriptional regulator for a number of podocyte genes, or whether it behaves as a master regulator of podocyte differentiation. Certainly these data hint that Wt1 loss results in a dedifferentiation phenotype consistent with an earlier developmental stage. Therefore, a microarray to analyse the effects of Wt1 deletion on other developmental pathways would provide useful information to answer this fundamental question.

6.3.4 How does Wt1-loss cause the effects demonstrated

A key gap in the understanding of *Wt1* activity in the kidney is exactly how it influences the podocyte phenotype. *Wt1*-loss in this model is associated with re-expression of *Wnt4*, consistent with re-activation of developmental pathways, with alterations in the epithelial-mesenchymal balance including increased expression of the mesenchymal driver Snail and with loss of key podocyte markers, including nephrin, podocin and podocalyxin. The question remains whether these effects are independent, or whether *Wt1* plays a fundamental upstream role in podocyte differentiation, which is reprogrammed following *Wt1*-loss. Certainly, there is evidence that *Wt1* directly regulates some of the podocyte genes that are affected. Both podocalyxin and nephrin contain Wt1 binding elements within their respective promoters, and *Wt1* has been shown to directly regulate their transcription in cell lines *in vitro*. However, the same cannot be said of podocin, the expression of which also decreases rapidly following *Wt1*-deletion. Podocin is a constituent of the slit diaphragm, so it is possible that its loss is secondary to slit diaphragm breakdown, indicated by the loss of nephrin and failure of the GFB. It must also be mentioned that no studies have yet been done looking for direct transcriptional regulation of podocin by

Wt1. However, gene expression profiling in *Wt1* mutant glomeruli did not identify early changes in podocin expression consistent with a direct regulatory role (Ratelade, Arrondel et al. 2010).

It is already known that *Wt1* directly regulates the transcription of Snail, activating the Snail promoter during cardiac development to facilitate epithelial to mesenchymal transition of epicardial cells (Martinez-Estrada, Lettice et al. 2010). The role of *Wt1* in regulating Snail in the kidney is not well understood, but as this study demonstrates, following *Wt1* deletion, and in human podocytes containing Wt1 mutations, Snail is upregulated.

With regard to *Wnt4*, the dichotomous role of *Wt1* is better understood, as *Wt1* is able to activate *Wnt4* in the kidney, but repress it in the epicardium, due to the recruitment of co-activators and repressors and alterations in the chromatin formation from active to repressed states (Rigby, Leitch et al. 2008). These contrasting effects are even thought to act in a temporal as well as a spatial manner, with *Wt1* potentially switching to a repressive role in adult kidney, supported by the findings in this study.

The next step to establish exactly how *Wt1* is affecting the expression of so many genes would be to use ChIP to demonstrate which targets *Wt1* is directly binding to transcriptionally regulate, and which are downstream effects. It may be possible that *Wt1* loss leads to a fundamental change in podocyte differentiation, so the loss of podocyte gene expression is downstream of this. However, it is equally possible that *Wt1* has a direct effect on the podocyte genes themselves, as well as an effect on the epithelial-mesenchymal balance. Using ChIP would help differentiate between these two scenarios and clarify whether Wt1 is directly or indirectly causing the effects demonstrated.

6.3.5 Generation of a useable model of Wt1-loss in podocytes in vitro

This study demonstrated that RNAi proved a viable method of knocking down *Wt1* in podocytes. However, in two entirely independent experiments, *Wt1* knockdown meant that conditionally immortalized podocytes were unable to differentiate. Although RNAi in differentiated cells was possible, by definition they could not be expanded, and the transduction protocol appeared to affect the phenotype of the differentiated cells. Therefore, the next step will be to use an inducible lentiviral vector such as the TRIPZ Inducible Lentiviral Construct (thermo-scientific).

This system will allow straightforward transduction of proliferating cells, which can be easily expanded, as well as inducible RNAi so *Wt1* can be knocked down in differentiating and / or differentiated cells. This system will complement the *in vivo* model by facilitating mechanistic studies while limiting the number of experimental animals.

This thesis has demonstrated some of the shortfalls of studying podocytes in vitro, and highlighted that expression of Wt1 in podocyte cell lines is artificially low, which may explain the low levels of nephrin expression documented (Chittiprol, Chen et al. 2011). However, this could be utilised by harnessing these cells as a 'low-Wt1' system, and overexpressing Wt1 within them, in order to attempt to drive them more towards podocyte differentiation. Wt1 rescue and overexpression experiments are complex as little is known about the relative dose and isoform ratios required. However, in a single cell-type system, expression of different levels of either human or murine Wt1 via adenoviral vectors (Wada, Pippin et al. 2005) may 'drive' podocyte differentiation further, and increase expression of key podocyte genes such as nephrin. This would answer an important question in itself regarding the role of *Wt1* as an upstream regulator of podocyte differentiation, as well as perhaps ensuring in vitro podocyte systems behaved more similarly to the *in vivo* setting.

6.4 Concluding Remarks

Using a conditional model of *Wt1*-loss, this study has established the importance of *Wt1* in the adult podocyte. *Wt1* loss leads to failure of the glomerular filtration barrier, and marked changes to the podocyte phenotype, including loss of specific podocyte gene expression and an alteration of the epithelial-mesenchymal balance. This has been supported by the analysis of human podocytes carrying *Wt1* mutations, which also demonstrate abnormalities of the epithelial-mesenchymal balance. These intriguing changes suggest a fundamental role for *Wt1* in podocyte differentiation. This is supported by the observation that *Wt1* expression is turned on in parietal epithelial cells as they migrate onto the glomerular tuft to differentiate into podocytes (Appel, Kershaw et al. 2009). As the central premise underlying this work is the need to halt the progression of glomerular disease, this study offers a potential target to influence the podocyte dedifferentiation response to injury and the progressive damage that results from this, with the potential that influencing *Wt1* expression could even allow for increased podocyte regeneration, as has been noted in other organs, notably the heart (Smart, Bollini et al. 2011).

7 MATERIALS AND METHODS

7.1 METHODS OVERVIEW

7.1.1 CELL CULTURE

All cell culture experiments were performed independently, with the exception of Wt1 knockdown in M15 cells, using the original Wt1-17/46/52 vectors, which was done in collaboration with Mara Artibani, PhD student, Hastie Group, IGMM.

Podocyte cell culture techniques were learned at the Saleem Labroratory, Academic Renal Unit, University of Bristol, under the supervision of Lan Ni, Research Technician.

ES cell culture techniques were taught and supervised by Joan Slight, Research Assistant, Hastie Group, IGMM

7.1.2 ANIMAL EXPERIMENTS

I performed all animal experiments myself (PIL 60/12595), under the supervision of Anna Thornburn and Rachel Berry (Research Assistants, Hastie Group, IGMM) and BRF or TGU staff. This included IP injection, daily assessment and body score analysis, urine collection, blood collection and tissue harvesting and euthanasia under terminal anaesthesia.

7.1.3 CLONING

Gateway recombineering was carried out independently following the protocol described by Sharan *et al*, 2009. Optimisation of cloning steps was carried out in collaboration with Karamjit Singh-Dolt, Postdoctoral Researcher, Hastie Group, IGMM. Sequence analysis was carried out using Geneious software in collaboration with Peter Hohenstein.

7.1.4 *Analysis*

RNA, DNA and protein and analyses were carried out independently using established labroratory techniques. Histological techniques were taught by Alyson Ross, Histology Research Assistant, MRC IGMM. Immunohistochemistry and immunofluorescence were taught by Rachel Berry. Imaging techniques and analysis were taught by Paul Perry and Matt Pearson, Imaging and Microscopy, MRC IGMM and on the Confocal and Advanced Light Microscopy Course, University of Edinburgh. I subsequently undertook all experimental analysis and optimisation of protocols based on these techniques independently.

7.2 Experiments done by others

7.2.1 *Cell Culture*

Generation of podocyte cell lines and cell culture of DDS podocytes was undertaken in Bristol, with cells sent to Edinburgh for further culture and/or analysis.

7.2.2 *Animal Experiments*

Animal care and plug checking was undertaken by BRF and TGU staff. Matings were set up by Anna Thornburn, Rachel Berry and Paul Devenney (Research Assistants, Hastie Group, IGMM). Earclips and preliminary genotyping were carried out by Anna Thornburn. I confirmed genotyping in experimental animals myself. Schedule 1 killings were performed by animal unit staff.

Pronuclear microinjection of transgenic DNA was performed by Paul Devenney.

7.2.3 *Cloning*

Stabilisation of the Destination Vector by altering the order of the restriction sites at the Multiple Cloning Site was done by Karamjit Singh-Dolt.

7.2.4 *Analysis*

Urine and Serum analysis was carried out by Forbes Howie, Chief Biomedical Scientist at the University of Edinburgh Clinical Biochemistry Section.

FACS analysis was carried out by Elisabeth Freyer, MRC, IGMM using FlowJo software.

7.3 CELL CULTURE

7.3.1 GENERATION OF HUMAN PODOCYTE CELL LINES

Wild type conditionally immortalised human podocytes (AB)(Loonstra, Vooijs et al. 2001)(Loonstra, Vooijs et al. 2001)(Loonstra, Vooijs et al. 2001)(Loonstra, Vooijs et al. 2001)(Loonstra, Vooijs et al. 2001)(Loonstra, Vooijs et al. 2001)(Loonstra, Vooijs et al. 2001)(Loonstra, Vooijs et al. 2001)(Loonstra, Vooijs et al. 2001) (Loonstra, Vooijs et al. 2001) were generated and cultured by the Saleem laboratory, as previously described (Saleem, O'Hare et al. 2002). These cells proliferate at 33°C and enter growth arrest (a situation analogous to the *in vivo* phenotype) at 37°C. The expression of podocyte specific proteins such as nephrin, podocin and synaptopodin in a mature distribution can be detected within 14 days. Additionally these cells have been transfected with the catalytic subunit of the human telomerase gene, hTERT, rendering them more stable to additional passages (O'Hare, Bond et al. 2001). Cells were used between passage 10-18 for this study. The mutant cell lines were derived from children with Denys Drash syndrome, with full institutional ethical approval (Academic Renal Unit, University of Bristol), whose kidneys were removed for therapeutic purposes. Podocytes were isolated from sieved glomeruli, grown to confluence and simultaneously transfected with the temperature sensitive SV40 (tsSV40) construct and hTERT, exactly as previously described (Saleem, O'Hare et al. 2002). After antibiotic selection, cells were sub-cloned.

All cells were cultured in the Saleem laboratory. Cells preserved in RNA later, or cDNA prepared in the Saleem laboratory, were used for the analysis undertaken in this project.

At least 2 biological replicates were used for each experiment, each sample was analysed in triplicate per experiment and each experiment was performed at least 3 times.

7.3.2 GENERATION OF MURINE PODOCYTE CELL LINES

To generate *CreERWt1*$^{co/GFP}$ immortalized podocytes, *CreERWt1*$^{GFP/+}$ mice were crossed with the H-2KbtsA58 "immorto" mice carrying a temperature-sensitive simian virus 40 (SV40) large T antigen (Jat, Noble et al. 1991). *CreERWt1*$^{GFP/+}$/Immorto+ mice were mated with *Wt1* $^{co/co}$ mice to generate *CreERWt1* $^{co/gfp}$ /Immorto+ offspring (Martinez-Estrada, Lettice et al. 2010).

Podocyte cell lines were generated from *CreERWt1*$^{co/gfp}$ /Immorto+ mice, in the laboratory of Moin Saleem (Academic Renal Unit, Southmead Hospital, Bristol) as previously described (Saleem, O'Hare et al. 2002).

A second cell line of "wild type" murine podocytes (WTpodo), generating from mice carrying the immorto-allele, was a kind gift from Jochen Reiser, University of Miami (Shankland, Pippin et al. 2007).

7.3.3 PODOCYTE CELL CULTURE

Cells were grown at permissive temperatures (33°C and 5% CO_2) in RPMI-1640 (Sigma R8758) supplemented with 10% heat-inactivated Foetal Calf Serum (FCS), insulin, transferrin, selenium (Sigma I-3146) and 50units/ml recombinant murine interferon-gamma (Peprotech). Media was changed every 2-3 days. Particular care was taken to avoid cells reaching confluency, as this has been associated with transformation of cells so they are unable to differentiate. Podocytes were differentiated on Collagen-I coated flasks at 38°C and 5% CO_2, without interferon gamma, over a period of 14 days. During this time they stopped proliferating and developed the characteristic flattened, arborised appearance of differentiated podocytes in culture (Shankland, Pippin et al. 2007). Immunofluorescence and Quantitative RT-PCR was used to confirm expression of key podocyte markers. Cells were only used up to passage 20, as prolonged passages can affect reliability of results (Shankland, Pippin et al. 2007), (Moin Saleem, personal communication).

7.3.4 Splitting Cells

Cells were washed twice with PBS to remove residual media and incubated with 1-2ml Trypsin at 37°C for 5 minutes. The trypsin was deactivated with media and the cell suspension centrifuged to form a cell pellet. The trypsin-containing supernatant was removed and the pellet resuspended in 1-2ml culture media, and re-plated at the desired dilution, following quantification using a hemacytometer.

7.3.5 Cryopreservation

2x Freezing Media

- 50% Culture Media
- 20% DMSO (dimethyl sulfoxide)
- 30% FCS

Cells were trypsinised and re-suspended to a single-cell suspension in 1ml culture media, as above. 0.5ml cell suspension was mixed with 0.5ml freezing mix and kept on ice, while being transported immediately to a -80°C freezer. After overnight storage at -80ºC they were transferred to long-term storage in liquid nitrogen.

7.3.6 Induction of Cre-Recombinase

Cre-recombinase was induced by the addition of 4OH-tamoxifen to culture media. 4-Hydroxy tamoxifen (Sigma H7904) was diluted in ethanol to make a 1mM stock solution. This was diluted further to reach the final desired concentration in culture media. Control cultures were treated with carrier (ethanol) alone.

7.3.7 *Caspase Apoptosis Assay*

The Caspase-Glo 3/7 assay (Promega G8090) was carried out according to manufacturer's instructions. This assay consists of a pro-luminescent caspase-3/7 DEVD-aminoluciferin substrate and a thermostable luciferase. The Caspase-Glo 3/7 Buffer and Substrate were mixed just prior to use. Equal volumes of Caspase-Glo 3/7 Reagent were added to treated or vehicle-treated cells and mixed gently. Following cell lysis, cellular caspase cleaved the substrate to allow release of free aminoluciferin. Consumption of aminoluciferin by the luciferase generated a 'glow' signal proportional to the degree of Caspase activity. Luciferase signal was measured on a Fluostar Omega plate reader.

After optimisation of conditions, 20,000 cells per well were plated and incubated overnight. Cells were incubated in tamoxifen or vehicle (ethanol = negative control) for 24 hours prior to the caspase assay being performed. Time points at between 1 and 3 hours after cell lysis were analysed to record maximum caspase activity.

Three biological replicates were carried out per experiment and each experiment repeated three times. Luminescence was corrected for blank (no-cell control) signal, which was subtracted from each luminescence reading. All experiments were carried out at 20°C.

7.3.8 *Time-lapse photography*

Time-lapse photography was carried out using a Nikon TiE (Perfect Focus System) microscope with NIS-Elements 4.0, equipped with an incubation chamber at 37°C, 100% humidity, and 5% CO_2. Cells were grown in a 6-well plate and 6 areas were randomly identified per well. Serial images were taken every 15 minutes across each area, over 72 hours.

7.3.9 FACS ANALYSIS OF CELL CULTURES

Cells were washed, trypsinised and resuspended in 1ml PBS + 0.5% FCS for flow cytometry. FACS analysis for expression of endogenous GFP expression was carried out by Elisabeth Freyer, MRC HGU Core Technical Services, using a FACS Flow Cytometer. Data were analysed using FlowJo software. Parameters were set for each run using GFP negative control cells.

7.3.10 M15 CELL CULTURE

M15 (murine mesonephric cells) were grown at 37ºC and 5% CO2 in DMEM (Sigma D567) supplemented with 10% FCS, glutamine and penicillin / streptomycin. Cells were split and frozen down as above.

7.4 RNA INTERFERENCE

7.4.1 LENTIVIRAL RNA INTERFERENCE USING THE EXPRESSION ARREST GIPZ LENTIVIRAL SHRNAMIR KIT.

The Thermo Scientific Open Biosystems Expression Arrest GIPZ Lentiviral shRNAmir kit was used as per manufacturer's instructions. Three *Wt1* knockdown constructs were used Wt1-17, Wt1-46 and Wt1-52, which were all predicted to bind in exons 3 and 4 and to knock down all relevant *Wt1* isoforms. Control constructs consisted of a non-silencing construct (N-S) and positive off-target control constructs (GAPDH and EG5) (Table 6.1)

.

TABLE 7.1: LENTIVIRAL SHRNAMIR KIT KNOCKDOWN VECTORS

RHS 4346	Non-silencing GIPZ Lentiviral shRNAmir Control
RHS 4371	GAPDH GIPZ Lentiviral shRNAmir positive control
RHS 4480	EG5 GIPZ Lentiviral shRNAmir positive control (mitotic phenotype)
V3LHS 380352	Wt1 Lentiviral shRNAmir Construct – binds exon (Wt1-52)
V2LHS 11417	Wt1 Lentiviral shRNAmir Construct – binds exon (Wt1-17)
V2LHS 33746	Wt1 Lentiviral shRNAmir Construct – binds exon (Wt1-46)

The shRNAmir vector contained a short hairpin RNA construct to express the human microRNA-30 transcript and included a Drosha processing site to increase knockdown efficiency. Dual selectable markers (GFP and puromycin resistance) allowed specific selection of transfected cells.

For transfection of shRNA, HEK293 cells were plated at equal densities the day prior to transfection. 2µg shRNA DNA was diluted in 1ml serum free media, and 10µg Arrest-In transfection reagent added. This was incubated for 20 minutes at room temperature and then

added to the plated cells. Cells were incubated for 5-6 hours at 37ºC and then normal media added. After culturing for 24 hours, puromycin selection was added. Following puromycin selection for one week, cells were sorted using FACS for GFP expression.

Transfection and viral production was carried out in HEK293 cells. Transduction of target cells was carried out in both permissive and differentiated WTpodo and M15 cells. Puromycin selection was titrated according to a previously generated puromycin kill curve. The WTpodo cell line proved highly sensitive to puromycin selection so only 0.3µg/ml of puromycin was required.

7.4.2 Optimised Lentiviral RNAi using alternative pGIPZ vectors

Previously verified Wt1 and control vectors were used to optimise Wt1 knockdown via RNAi (Rigby, Leitch et al. 2008) - see Table 6.2.

TABLE 7.2: OPTIMISED LENTIVIRAL RNAI KNOCKDOWN VECTORS

miWt1-1600/TOP	tgctgtttcacacctgtgtgtctcctgttttggccactgactgacaggagacacaggtgtgaaa
miWt1-1600/ BOTTOM	cctgtttcacacctgtgtctcctgtcagtcagtggccaaaacaggagacacacaggtgtgaaac
LacZ/TOP	tgctgaaatcgctgatttggtagtcgttttggccactgactgacgactacacatcagcgattt
LacZ/BOTTOM	cctgaaatcgctgatgtgtagtcgtcagtcagtggccaaaacgactacacaaatcagcgatttc

7.4.2.1 Lentiviral packaging in SODK3 cells

Trans-lentiviral packaging was performed in SODK3 cells, according to previously published methods (Cockrell, Ma et al. 2006). Trans-lentiviral packaging proteins and GFP were expressed from a Tet-off (tTA) system, meaning cells were cultured in the presence of 1µg/ml doxycline to inhibit expression. SODK3 cells were cultured in DMEM-HIGH (Sigma 51435C) containing 10% FCS, Glutamine, penicillin / streptomycin, 1µg/ml puromycin and 600µg/ml neomycin.

To activate the packaging system, SODK3 cells were split and doxycycline was withdrawn. FACS sorting for GFP expression (top 15% GFP-expressing cells) confirmed expression of the packaging proteins. Activated cells were plated onto poly-L-lysine coated plates and transfected

with the lentiviral construct using FuGENE® HD Transfection Reagent. After overnight transfection, non-selective media containing 5mM sodium butyrate was added, and changed after 24 hours. Viral containing supernatant was harvested after 72 hours, spun down to remove cell debris, and either used immediately to transduce target cells or stored at -80ºC.

7.4.2.2 Transduction of Target cells

Target cells were grown until approximately 70% confluent. Media was removed, and cells transduced with viral-containing supernatant and 4μg/ml polybrene overnight. After 24 hours with no selection, puromycin was added according to sensitivity of target cells (established using a puromycin kill curve: M15 5μg/ml; WTpodo 0.3μg/ml). Transduced target cells were selected on puromycin for at least one week, before FACS sorting for GFP expression (surrogate marker of shRNA expression). The top 10% GFP expressing cells (equivalent to maximal expression of shRNA) were selected and grown on in continuing puromycin selection to ensure ongoing stable expression of the lentiviral construct.

7.5 MOUSE LINES

7.5.1 CREERWT1$^{CO/CO}$

Wt1 conditional knockout mice (referred to as *Wt1*$^{co/co}$) were generated via ES cell targeting, using a targeting vector containing loxP sites flanking Exon1 (Martinez-Estrada, Lettice et al. 2010). Crossbreeding with the *CreER mouse* (A kind gift of Sue Monkley, University of Leicester) generated the *CreERWt1*$^{co/co}$ mouse line, facilitating tamoxifen mediated Cre-recombination and excision of Exon 1 of *Wt1,* to prevent translation of functional Wt1 protein in the adult mouse.

7.5.2 CREERWT1$^{CO/GFP}$

Crossbreeding the *CreER Wt1*$^{co/co}$ line with a knock-in Wt1-GFP mouse line (Hosen, Shirakata et al. 2007) produced the *CreERWt1*$^{co/GFP}$ line, containing both an inducible *Wt1*-conditional allele and a knock-in GFP allele to express GFP at sites of *Wt1* expression (Rigby, Leitch et al. 2008, Martinez-Estrada, Lettice et al. 2010).

7.5.3 CREER

Using the *CreER mouse* (Hayashi and McMahon 2002) provided a control line to check for the effects of Cre-toxicity (Loonstra, Vooijs et al. 2001). This line contained a ubiquitously expressed Cre-recombinase but no LoxP sites.

7.5.4 CREER26R$^{YFP/YFP}$

The ubiquitously expressed *CreER* line was crossed with a *Rosa26*$^{YFP/YFP}$ reporter mouse (*R26R*$^{YFP/YFP)}$ to produce YFP expression at sites of Cre-recombination. This would confirm sites of Cre-activity within the kidney. It also provided a control for the effects of Cre-activity without *Wt1* deletion.

7.5.5 *NESTINCREERT2 R26R$^{YFP/YFP}$*

NestinCreERT2 mice (Carlen, Meletis et al. 2006) were crossed with the *R26R$^{YFP/YFP}$* line to generate *NestinCreERT2R26R$^{YFP/YFP}$*. Nestin is expressed within the adult glomerulus, particularly the podocyte (Kirik and Korzhevskii 2009, Sakairi, Abe et al. 2010), so this line would potentially provide glomerular-specific Cre-activity and therefore limit *Wt1* loss to the kidney, while awaiting generation of a Podocyte-specific Cre-line.

7.6 Animal Experiments

7.6.1 Animal Husbandry

Mice were housed in one of two facilities

1) Barrier Facility – Transgenic Unit (TGU), MRC Human Genetics Unit

2) Semi-Barrier Facility – Biomedical Research Facility (BRF), University of Edinburgh.

Animals were housed in 12 hours of daylight, at constant temperature (21°C) and humidity (53%). All animal procedures were carried out under Home Office License, and with respect to the 3Rs principles of Reduction, Refinement and Replacement in animal experiments.

Animal care was undertaken by TGU & BRF staff, who also undertook plug-checking and assisted with intra-peritoneal injection and humane killing of experimental animals.

All matings were set up by Anna Thornburn, Rachel Berry and Paul Devenney. Every morning, females in breeding pairs were checked for the presence of vaginal plugs, and positive plugs were staged as 0.5dpc (days post-coital).

Mice were earclipped by Anna Thornburn for identification and genotyping purposes.

7.6.2 Tamoxifen administration

10mg/ml stock solution of tamoxifen (Sigma T5648) and glyceryl trioctanoate (Sigma T9126) was prepared, and divided into aliquots, which were kept in the dark at -20°C until use. When required, aliquots of tamoxifen were defrosted and mixed thoroughly. Mice were injected intra-peritoneally, using a 1ml sterile syringe, according to the appropriate dosing schedule.

7.6.3 *Clinical assessment following tamoxifen administration (Wt1 deletion)*

Mice were observed daily for clinical deterioration and scored for clinical status using a modified clinical distress scoring system (Lloyd, M.H. & Wolfensohn, S.E. 1999). Mice were humanely sacrificed once they reached a score of 14, but in practice, mice deteriorated very quickly over a period of 24 hours and were sacrificed as soon as this was noted.

7.6.4 *Urine and Serum Analysis*

7.6.4.1 Urine collection

Urine was collected via metabolic cages or spontaneous voiding. For metabolic cages, animals were habituated for 48-72 hours prior to the experiment. Urine was collected over a period of 24 hours.

For spontaneous voiding, animals were scruffed and spontaneously voided urine collected in an eppendorff tube.

Urine was centrifuged to pellet debris and frozen at -20°C until analysed.

7.6.4.2 Serum Collection

Animals were euthanased using CO2 inhalation and blood collected via cardiac puncture. After clotting on ice for 20minutes, blood was spun at full speed for 30minutes at 4°C. The serum supernatant was removed and stored at -20°C until analysed.

7.6.4.3 Serum and Urine Analysis

Serum and urine analysis was carried out in batches by by Forbes Howie, Chief Biomedical Scientist at the Edinburgh University Clinical Biochemistry Section.

Serum and Urine Creatinine**:**

- Creatinine was determined using the creatininase/creatinase specific enzymatic method (Borner, Szasz et al. 1979), utilising a commercial kit (Alpha Laboratories Ltd.

Eastleigh, UK) adapted for use on a Cobas Fara centrifugal analyser (Roche Diagnostics Ltd, Welwyn Garden City, UK). Within run precision was CV < 3% while intra-batch precision was CV < 5%.

Serum and Urine Urea:

- A commercial kit from Randox Laboratories Ltd. Crumlin, UK, was used on a Cobas Fara centrifugal analyser (Roche Diagnostics Ltd, Welwyn Garden City, UK) in order to detect urea concentration as described below. Hydrolysis of urea in the presence of water and urease produces ammonia and carbon dioxide. The resultant ammonia combines with α-oxogluterate and NADH in the presence of glutamate-dehydrogenase to yield glutamate and NAD. NAD production is monitored at 340 nm. Within run precision was CV < 3% while intra-batch precision was CV < 5%.

Immunoturbimetric Albumin Method:

- Mouse urine albumin measurements were determined using a commercial Microalbumin Kit (Olympus Diagnostics Ltd, Watford, UK) on a Cobas Fara centrifugal analyser (Roche Diagnostics Ltd, Welwyn Garden City, UK). This immunoturbidimetric assay is standardised against purified mouse albumin standards (Sigma Chemical Co. Poole, UK) with samples diluted in phosphate buffer saline.

Serum Albumin:

- Mouse serum albumin measurements were determined using a commercial serum albumin kit (Alpha Laboratories Ltd., Eastleigh, UK) on a Cobas Fara centrifugal analyser (Roche Diagnostics Ltd, Welwyn Garden City, U.K. Within run precision was CV < 2.5% while intra-batch precision was CV < 4%.

7.6.4.4 Coomassie Blue

Equal quantities of mouse urine were loaded onto SDS-Polyacrylamide Gels, with known quantities of Bovine Serum Albumin as reference. Following electrophoresis gels were washed three times in 200ml dH_2O, then stained for one hour with shaking in 50ml Coomassie Blue (BioRad Bio-Safe Coomassie Stain 161-0786). Gels were rinsed three times for at least 30 minutes in dH_20 to remove residual stains. Bands were visualized on a light box, and photographed.

7.6.5 TISSUE HARVESTING

Animals were culled humanely by cervical dislocation or CO2 inhalation. At necroscopy, macroscopic assessment of the major organs was undertaken and kidneys were removed and washed in HBSS or PBS to remove red blood cells. If for histological analysis, the capsule was removed and the kidney fixed in 4%PFA. If for RNA, DNA or protein analysis, the capsule was removed and kidney cortex immediately processed for glomerular isolation or stored in RNAlater (Invitrogen AM7021).

7.6.6 GLOMERULAR ISOLATION

Glomerular isolation was achieved using a serial sieving technique. Fresh kidneys were dissected into ice-cold HBSS (Gibco/Invitrogen 24020-133), decapsulated and minced. After rinsing thoroughly with fresh HBSS, the pieces were pushed through a 100µm cell strainer (BD Falcon 352360) into a chilled beaker. HBSS was added to as total of 6mls, and this was divided between 2 chilled 15ml falcon tubes. 2.2ml Percoll (Amersham 17-0891-02) was added to each tube. The samples were spun at 400rpm for 10 minutes at 4ºC, to separate glomeruli across the Percoll gradient. The presence of glomeruli in the top of the gradient was verified microscopically. The top 1-2mls was removed and passed again through a 100µm cell strainer to catch any large tubule fragments. The filtrate was then passed through a 40µm cell strainer (BD Falcon 352340) to trap the glomeruli. Glomeruli were lysed directly on the cell strainer for RNA, DNA and protein extraction.

7.6.7 FACS ANALYSIS OF KIDNEY CELLS

A number of methods were tested in order to attempt to generate a single cell suspension of GFP-positive podocytes:

7.6.7.1 Method 1 (Velecela, Lettice et al. 2013)

Fresh kidneys were dissected into ice-cold HBSS, de-capsulated and minced. After rinsing thoroughly with fresh HBSS, the pieces were pushed through a 100μm cell strainer into a chilled 50ml Falcon tube. Cells were spun at 1000rpm for 5 minutes, the supernatant removed, and the cell pellet re-suspended in 1ml chilled HBSS. Cells were washed a further two times, and the cell pellet re-suspended in at least twice the volume of Trypsin / Versene (without phenol red) 1:10. Cells were incubated at 37° with agitation for 10 minutes. The trypsin supernatant was removed and the Trypsin neutralised with 1ml DMEM + 10% FCS. The digested tissue was passed through a 40um cell sieve and further dissociated using 200ul pipette tip. After gentle centrifugation (1000rpm 5 mins) the cell pellet was resuspended in PBS + 10%FCS 0.5mls for FACs.

FACS analysis of kidney tissue processed using this method revealed a large majority of dead cells / debris and no identifiable GFP-positive population.

7.6.7.2 Method 2 (Valente, Henrique et al. 2011)

Fresh kidneys were dissected into ice-cold HBSS, decapsulated and chopped into $3mm^3$ cubes. After rinsing thoroughly with fresh HBSS until the supernatant ran clear, the pieces were minced finely with sterile scalpels. Tissue pieces were re-suspended in collagenase (1mg/ml final solution – made up as 2mg/ml in MEM then added 50:50 to prewarmed media immediately prior to use) and incubated for 20-30mins at 37° with agitation. The digested tissue was passed through a 100um cell sieve into a chilled 50ml falcon tube and pelleted. The supernatant was removed and the pellet re-suspended in at least twice the volume of Trypsin / Versene 1:10 (without phenol red). The trypsin suspension was incubated at 37° with agitation for 10 minutes. 1ml DMEM + 10% FCS was added to neutralize the Trypsin and any residual clumps dissociated using a 200μl pipette tip. The cells were pelleted and re-suspended in 0.5mls PBS + 10%FCS for FACS

Using this method, only a tiny GFP population (30/50000 cells) was identified via FACS, which was too small for further analysis

7.6.7.3 Method 3: Dispase disaggregation of tissues (Li, Ma et al. 2011), (Richard Mort, personal communication)

Fresh kidneys were dissected into ice-cold HBSS, de-capsulated and chopped into $1mm^3$ cubes then rinsed thoroughly in HBSS. The cubes were passed through a 100um cell sieve then pelleted. The cell pellet was re-suspended in dispase II (Gibco/Invitrogen 17105-041) and incubated for 20 minutes at 37° with agitation. The mixture was vortexed then spun at 2000rpm for 5mins and the supernatant removed. The pellet was re-suspended in 0.5mls PBS + 10%FCS for FACS analysis.

This method generated only a very small GFP positive population of 10/50000 cells only.

7.6.7.4 Method 4 (Welsh, Hale et al. 2010)

Kidneys were removed, de-capsulated and minced in ice-cold HBSS, then passed through a 100µm cell sieve. The sieved tissue was then passed through a 40µm cell sieve to collect the de-capsulated glomeruli. The glomeruli were collected by rinsing the sieve surface into two 1.5ml eppendorf tubes and centrifuged at 4 ^{0}C at 500G for 5mins. The supernatant was discarded and the two pellets (generated from the two kidneys from an individual mouse) were combined and re-suspended in 1ml Digest Buffer. The glomeruli were incubated in Digest Buffer for one hour in a rotating oven, then passed through a FACS tube filter lid (BD Falcon 352235). The glomeruli were washed twice in Basic Buffer and then resuspended in FACS buffer for FACS analysis, and collected in RNA later.

Using both kidneys, each mouse generated 3000-10000 positive cells to use for further analysis.

Digest buffer:

- DMEM
- 1mM EDTA
- 1mg/ml Collagenase I
- 1mg/ml Collagenase IV
- 1mg/ml Collagenase V
- DNAse (5uL/5ml) (100 Units/ml from Invitrogen)
- 3% BSA

Digest Buffer Stock

- DMEM 100ml
- EDTA 1mM 0.029g
- BSA 3% 3g

Digest Buffer to use: Add to 5ml

- Collagenase I (C1639) 1mg/ml 100ul
  (50mg/ml HBSS = 5mg/100ul)
- Collagenase IV (C 1889) 1mg/ml 100ul
  (50mg/ml HBSS = 5mg/100ul)
- Collagenase V (C9263) 1mg/ml 100ul
  (50mg/ml HBSS = 5mg/100ul)
- DNAse 0.5-1ul 2U/ul

Basic Buffer:

- DMEM 50ml
- Hepes 25mM 1.25ml of 1M stock in 50ml

FACS buffer:

- DMEM 50ml
- EDTA 1mM 0.0146g
- BSA 3% 1.5g
  Before use
- DNAse 0.5-1ul 2U/ul

7.6.7.5 Embryonic kidney

Whole embryonic kidney (E16.5-18.5) was mechanically dissociated between two sterile microscope slides and then digested in trypisn:versene 1:10 with agitation at 37°C. Every 10 minutes, dissolved cells were removed from the supernatant and removed to a fresh tube, where the trypsin was deactivated with MEM (Sigma M2279) containing 10%FCS. The tryspin: versene solution was replaced and the digestion continued until all solid material had dissolved. Following deactivation with media plus 10% FCS the cells were pelleted with gentle centrifugation (1000rpm 5 mins) and the cell pellet was resuspended in PBS + 10%FCS 0.5mls for FACs.

7.7 CLONING USING GATEWAY RECOMBINEERING

All Gateway reactions were carried out as described in the manual of the MultiSite Gateway® Pro Plus kit (Invitrogen). In summary, the constituent fragments were PCR amplified, cloned into the appropriate pDONR vector and verified by restriction digests and/or sequencing (Dolt, Lawrence et al. 2013).

Primers and PCR reactions are listed in Table 6.3 below.

7.7.1 PCR AMPLIFICATION OF THE EGFPCREERT2 CONSTRUCT

PCR amplification of the *eGFPCreERt2* construct was carried out according to manufacturer's instructions using PWO Superyield DNA polymerase (Roche) and the GC-rich buffer. The PCR product was run on a 0.8% gel. The remaining 40µl PCR reaction was diluted in TE and then precipitated using PEG magnesium. After centrifugation the DNA pellet was air-dried and resuspended in 50µl TE, and the concentration checked using Nanodrop. The PCR product was sequenced to ensure correct amplification (Sequencing primers are listed in Table 6.4).

7.7.2 BP REACTION

1.5µl (150ng) pDONR vector was combined with equal quantities purified DNA (150ng) and made up to a total volume of 8µl with TE. 2µl of BP clonase was added and the reaction left to proceed at room temperature overnight.

7.7.3 LR REACTION

150ng Entry Clone A1 was combined with equal quantities (150ng) Destination Vector A1, and the total volume made up to 8µl with TE. 2µl LR plus clonase was added and the reaction left to proceed at room temperature overnight.

7.7.4 PCR AMPLIFICATION OF THE RECOMBINEERING ARMS

7.7.4.1 BAC Miniprep

A modified version of the standard Qiagen Mini-prep protocol was used to purify BAC DNA (Sharan, Thomason et al. 2009). In brief, a single colony was picked and grown up in 5ml LB containing appropriate antibiotic selection at 37° with vigorous shaking, overnight. Bacterial cells were pelleted by centrifugation and the supernatant discarded. 100µl of chilled resuspension buffer P1 was added and the solution chilled on ice for 5 minutes. 200µl of lysis buffer P2 was then added and the mixture incubated for a further 5 minutes on ice. 150µl of neutralisation buffer N3 was added and the solution inverted to mix. After a further 5 minutes incubation on ice, the solid material was pelleted and the DNA-containing supernatant transferred to a clean tube. DNA was precipitated with 2 volumes of 95% ethanol and left on ice for 30 minutes. BAC DNA was pelleted, washed in 70% ethanol, air dried and re-suspended in TE.

7.7.4.2 PCR of the recombineering arms

Novagen KOD Hotstart DNA polymerase, with proof reading capabilities, was used to amplify the recombineering arms from the original template podocin BAC DNA. The PCR reaction was carried out according to manufacturer's instructions, using 1µl mini-prepped podocin BAC DNA as the template, plus 10% betaine. Primers are listed in Table 6.3. As no PCR product was generated, a further PCR reaction was attempted, with previously confirmed primers, to try to verify the presence of the podocin sequence within the BAC (see Table 6.3).

Following failure of the original BAC to generate a PCR product, Invitrogen Fast Start High Fidelity PCR system was used according to manufacturer's instructions, using 1µl of the new PR23 BAC DNA as template and including 2µl DMSO in the reaction.

7.7.5 RECOMBINEERING

Recombineering was carried out based on previously published protocols (Sharan, Thomason et al. 2009). In brief, the recombination machinery in EL350 cells were induced by incubating the cells at 42°C for 15 minutes. Control cells were kept at 32º. Induced and control cells were then chilled on ice for 10 minutes and spun down at 4º. Cells were washed 4 times in chilled dH2O and re-suspended in a final volume of 200µl ice-cold dH2O.

DNA was added to the induced electrocompetent cells, and control reactions were carried out in parallel with no DNA and with un-induced cells. Both experimental and control reactions were electroporated at 1.8kV, 25µF capacitance and 200Ω resistance. 1ml chilled Lo-Salt LB Lennox media was added immediately after electroporation. Cells were incubated for 2 hours at 32º with no selection, and then plated, at serial dilutions, on kanamycin selection, or without antibiotic selection to demonstrate cell viability. Cultures were then grown up overnight at 32º. Only induced cells electroporated with DNA were expected to produce colonies on selection.

PCR using the Invitrogen Fast Start High Fidelity PCR system was used to detect correct integration of the recombineering construct into the podocin BAC (see Table 6.3).

The ampicillin cassette to replace the extra LoxP site on the Podocin BAC was amplified by PCR, using Invitrogen Platinum Taq (see Table 6.3). The PCR product was recombineered into the GCT2iP Podocin-BAC as above, and correct integration verified using PCR.

TABLE 7.3: RECOMBINEERING PRIMERS

NAME	PRIMER	RESULT
eGFP-CreERT2-attB1-F	ggggacaagtttgtacaaaaaagcaggcttaaccatgggtgagcaagggcgag	eGFP-CreERT2 fragment
eGFP-CreERT2-attB1-R	ggggacaacttttgtatacaaagttgttcaagctgtggcagggaa	
Nphs2 5 NdeI/F	gcgcCATATGcacctaagcagagcctgc	5' Recombineering Arm
Nphs2 5 SalI/R	gcgcGTCGACtctcaatgcagcggtgca	
Nphs2 3 PacI/F	gcgcTTAATTAAtggaaggtagatcccacgag	3'Recombineering Arm
Nphs2 3 AscI/R	tataGGCGCGCCggaagaggaggcacaaggtt	
PodocinPE/R	tccgcgccctcctctccatggtcagagctg	2.5kb Podocin promoter
PodocinPE/F	actctagagccctcctatttagtctctctgccacc	
PodocinHA/F	tgaattcgagagaggaggggcgcggagc	Podocin cDNA
PodocinHA/R	tattaagcttatataacatgggagagtc	
5' recombineering test/F	tagtgcagtgtgttctgtc	Correct integration
5' recombineering test/R	ctcgcccttgctcaccat	5' arm
3' recombineering test/F	ggtcatagctgtttcctgg	Correct integration
3' recombineering test/R	ttaagactgattggcaagga	3' arm
LoxPAmpF	gcttatcgatgataagctgtcaaacatgagaattgatccggaacccttaatcttacaatttaggtggcact	Ampicillin cassette
LoxPAmpR	tccgatgcaagtgtgtcgctgtcgacggtgaccctatagtcgagggacctaatatgagtaaacttggtctga	
AmpTestF	gtgccgaggatgacgatgagc	Correct integration
AmpTestR	ccgtgccggcacgttaacc	ampicillin cassette

TABLE 7.4: EGFP-CREERT2 SEQUENCING PRIMERS

eGFP-CReERT2-seq/F1:	aagggcgaggagctgttca	eGFP-CreERT2-seq/R1	tcaagctgtggcagggaa
eGFP-CreERT2-seq/F2	ttcaaggacgacggcaac	eGFP-CreERT2-seq/R2	cttggccatcaggtggat
eGFP-CreERT2-seq/F3	agtccgccctgagcaaaga	eGFP-CreERT2-seq/R3	gccagacgagaccaatca
eGFP-CreERT2-seq/F4	atgcttctgtccgtttgc	eGFP-CreERT2-seq/R4	cttggccaaaggttggca
eGFP-CreERT2-seq/F5	caggttcgttcactcatg	eGFP-CreERT2-seq/R5	gcgagttgatagctggct
eGFP-CreERT2-seq/F6	aaaaatggtgttgccgcg	eGFP-CreERT2-seq/R6	cagattacgtatatcctg
eGFP-CreERT2-seq/F7	agccatctgctggagaca	eGFP-CreERT2-seq/R7	ccggttattcaacttgca
eGFP-CreERT2-seq/F8	ctagaatgtgcctggcta	eGFP-CreERT2-seq/R8	gtgatcgcgcttctcgtt
eGFP-CreERT2-seq/F9	ctggacaagatcacagac	eGFP-CreERT2-seq/R9	tcgccctcgaacttcacct
eGFP-CreERT2-seq/F10	gcaaaagtattacatcac	eGFP-CreERT2-seq/R10	tcgaccaggatgggcacc

7.8 GENERATING THE PODOCIN-GFPCREERT2 MOUSE

7.8.1 MICROINJECTION OF BAC DNA INTO THE PRONUCLEUS OF FERTILISED MOUSE OOCYTES

EL350 bacteria containing the GCT2iP-Podocin BAC clone 'B2ACK' construct were grown up for 20 hours at 32° with shaking, in ampicillin and kanamycin selection.

The Qiagen Large Construct Kit (Qiagen 12462) was used for DNA extraction, according to manufacturers instructions.

In brief, the bacteria were pelleted by centrifugation and re-suspended in 20ml buffer P1. 20ml buffer P2 was added to lyse the cells, and the mixture incubated at room temperature for 5 minutes. 20ml chilled buffer P3 was added to precipitate genomic DNA and cellular proteins, and the mixture incubated on ice for 10 minutes. After centrifugation at ≥20,000g for 30 minutes at 4°C the lysate was removed and passed through a filter paper. DNA was precipitated by adding 0.6 volumes room-temperature isopropanol, and pelleted by centrifugation at ≥15,000g for 30 minutes at 4°C. The supernatant was discarded and the DNA pellet washed with 5ml 70% ethanol. After air-drying, the DNA pellet was re-dissolved in 9.5ml Buffer EX. 200µl ATP-dependent exonuclease and 300µl ATP solution were added to the dissolved DNA, to digest any genomic or nicked BAC DNA.

10ml of Buffer QS was added to the exonuclease-digested DNA and then the whole mixture passed through a Qiagen-tip 500 column. The bound DNA was washed twice with 30ml Buffer QC and then eluted in 15ml pre-warned Buffer QF. DNA was precipitated again using 0.7 volumes room-temperature isopropanol and centrifuged for 30 minutes at ≥15,000g. The resultant pellet was washed in 70% ethanol, air dried and resuspended in 200µl TE, and the concentration checked on Nanodrop.

DNA was diluted to a final concentration of 0.5ng/µl in microinjection buffer.

1000x Polyamines Mix

- 30mM Spermine
- 70mM Spermidine

  Stored at -20°C

Microinjection Buffer

- 10mM TrisHCl (pH 7.5)
- 0.1mM EDTA (pH8)
- 100mM NaCl
- 1x polyamines mix
- dH20 to total volume 50ml

  Filter sterilize

7.8.1.1 Pronuclear Injection

Pronuclear injection of BAC DNA was performed by Paul Devenney, Research Assistant, MRC HGU, according to previously published methods (Cho, Haruyama et al. 2009). Female CD1 or $Wt1^{co/co}$ mice were super-ovulated by injecting intra-peritoneally with pregnant mare's serum gonadotrophin 2 days prior to human chorionic gonadotrophin and matings. Matings were set up late afternoon with one male to one female. Successful matings were verified by checking for the presence of vaginal plugs the following morning, and fresh fertilized eggs harvested from the plugged female mice.

The plugged female mice were culled by cervical dislocation and the entire ovary and oviduct removed, and incubated in M2 medium (Sigma M7167). Zygotes were released by dissecting the ampulla in M2 media containing hyaluronidase (1.5mg hyaluronidase (Sigma H3884) in 5ml M2 medium). The eggs separated from the cumulus in the hyaluronidase and were transferred, using a mouth pipette, to fresh M2 media for washing. Embryos were washed 4 times, and any abnormal or unfertilised eggs discarded. Washed eggs were incubated in M16 media (Sigma-M7292) at 37°C until ready for implantation into recipient mice.

BAC DNA was microinjected at a concentration of 0.5-1ng/µl. A holding pipette was used to immobilise the zygote, and DNA injected into the pronucleus. The microinjected zygotes were

transferred to fresh M16 media and incubated at 37ºC until ready to be injected into pseudo-pregnant recipients.

Pseudo-pregnant females were generated by mating CD1 females with vasectomised males 1 day before embryo surgery. Pseudo-pregnant females were anaesthetised and 20 injected zygotes were transferred into the oviduct and to the ampulla. The oviduct was replaced into the body cavity and the skin wound repaired. Mice were allowed to recover from anaesthetic and to deliver the pups normally at E20-21.

7.8.2 GENE TARGETING IN ES CELLS

7.8.2.1 Random Integration into ES cells

7.8.2.1.1 Preparation of DNA for electroporation

The GCT2iP-Podocin (still containing the LoxP site) BAC DNA was extracted using the Qiagen Large Construct Kit (Qiagen 12462) as above. 25µg BAC DNA was digested with *PISceI* overnight, denatured, and ethanol precipitated.

7.8.2.1.2 Electroporation of BAC DNA into ES cells (random integration)

E14 cells were grown up and split the day prior to electroporation. Cells were washed, trypsinised and re-suspended, and then counted, to give 10^7 cells to be electroporated with 25µg BAC DNA. The DNA was added to one aliquot of cells, and a further 10^7 cells kept as a minus DNA control. After incubation on ice for 15 minutes the cells were transferred to a pre-chilled 4mm cuvette and electroporated at 0.8volts. Cells were allowed to recover on ice for 15minutes and then plated on gelatin-coated plates on standard ES culture media. The following day, neomycin selection was added, and the cells maintained on neomycin selection until day 10, when clones could be picked.

7.8.2.2 Endogenous Targeting into ES cells

7.8.2.2.1 Amplification of the pMCS-DTA plasmid to produce the retrieval arms

The plasmid template pMCS-DTA was linearised using a *SmaI* restriction digest. After the enzyme was denatured at 65°C the linearised plasmid was used as a template for PCR amplification to produce the retrieval arms.

Primers are listed in Table 6.5

TABLE 7.5: ENDOGENOUS TARGETING PRIMERS

NAME	PRIMER	RESULT
Pod-retrieval-L	agggtcaatgtcgagaaggacttatctcctatgataaggaattacttcgctctagaactagtggatccc	Retrieval Arm L
Pod-retrieval-R	tgggggaaccacttgccttggtgtagagaggaggtcagaacctcaggtcttgcaggaattcgatatcaag	Retrieval Arm R
5'probe1/F	taagccattcttgcctaaaac	Endogenous targeting
5'probe1/R	tctgggtaggttttactcc	Probe 5’
3’probe2/F	ctttaggttgtgcaagagta	Endogenous targeting
3’probe2/R	agctccatgacttaatctg	Probe 3’

7.9 MICROBIOLOGY

7.9.1 CULTURE METHODS

All microbiological procedures were carried out using aseptic technique. These included preparation of agar plates, culturing, picking colonies and making glycerol stocks for long term storage. Agar plates were prepared by melting agar at low power in the microwave and then cooling to 55°C. Appropriate antibiotics were added for bacterial selection (Kanamycin 50µg/ml, ampicillin 50µg/ml. Chloramphenicol 12.5 µg/ml).

Liquid cultures were grown in LB broth with appropriate antibiotic selection, at the recommended temperature, with vigorous shaking. Plated cultures were grown on air-dried agar plates, containing appropriate antibiotic selection, and grown overnight at 37°C or 30°C, accordingly.

For mini-prep, a single colony was picked and used to inoculate 5ml LB containing appropriate antibiotic selection. Plasmid DNA was extracted the following day after incubation overnight with vigorous shaking.

For maxi-prep, 500µl from an overnight 5ml starter culture (as above) was grown for 16-20hours in 400ml LB containing appropriate antibiotic selection.

7.9.2 BACTERIAL TRANSFORMATION VIA HEAT SHOCK

Maximum Efficiency STBL2 competent cells (Invitrogen 10268-019), or "one shot" DH5α competent cells (Invitrogen 12297-016) were transformed by heat shock according to the manufacturers recommendations. One vial of bacteria was thawed on ice for 10 minutes. 1µl proteinase K was added to the digested DNA (1-10ng), mixed, then added to the thawed cells. The vial was incubated on ice for 30 minutes and then heat-shocked at 42°C for 45econds. The vial was immediately placed on ice for 2 minutes, and then 250µl warmed SOC media added. After incubation at 30ºC for one hour, the transformed bacteria were plated on agar plates on appropriate selection and grown overnight at 30ºC.

7.9.3 *Bacterial transformation via electroporation*

Electroporation of BAC DNA was carried out in EL350 cells according to previously published protocols (Sharan, Thomason et al. 2009). In brief, a single EL350 colony was grown up overnight at 32ºC in 5ml LB. 0.5ml of this culture was then added to a 25ml flask and grown for 3-4 hours until it reached an OD_{600} of 0.5-0.6. The bacterial cells were spun down for 10 minutes and then washed 4 times in ice-cold water. The washed pellet was re-suspended in a final volume of 100µl ice cold H2O. 100ng of BAC DNA was mixed with 50µl electrocompetent cells and chilled on ice for 5 minutes, before transferring the mixture into a cuvette. BAC DNA was introduced into the electrocompetent cells by electroporation at 1.8kV, 25µF capacitance and 200Ω resistance. Control electroporations with no DNA were also performed. Immediately after electroporation, 1ml chilled LB was added and the mixture transferred to a sterile culture tube and grown without selection for one hour at 32º. Cells were spun down and the pellet re-suspended in 200µl LB and plated on chloramphenicol selection. Plates were grown up overnight at 32º and only the BAC DNA electroporation plates should have grown colonies.

7.9.4 *Reagents prepared by the MRC HGU Core Scientific Services*

Luria-Bertani (Natoli, McDonald et al.) Broth

- 10g Tryptone
- 5g yeast extract
- 10g NaCl
- 1g Glucose
- Made up to 1000ml in dH20 and autoclaved

Agar

- 1l LB broth
- 15g Agar
- Autoclaved

7.9.5 MAINTENANCE OF ES CELLS IN CULTURE

Aseptic technique was used for all procedures using ES cells, which were grown in culture without antibiotics. ES cells were grown in specialized culture media on gelatin-coated plates, at 37°C in 5%CO2.

Culture Media

- Glasgow MEM (Gibco, BHK-21) 500ml
- FCS (Globalpharm) 10% final volume
- Glutamine (Gibco) 0.3% final volume
- MEM non-essential amino acids (Sigma) 0.1mM
- Sodium Pyruvate (Sigma) 1mM
- B-Mercaptoethanol (Sigma) 0.1mM

7.9.5.1 Gelatin-coated Plates

Plates were coated with 0.1% Gelatin solution (Sigma) and incubated at 37º for at least 15 minutes. Prior to plating cells, the gelatin solution was removed and replaced with media.

7.9.5.2 Splitting Cells

Cells were washed twice with PBS to remove any residual media and then incubated with 1ml Trypsin (Sigma) at 37°C for 5 minutes. The trypsin was deactivated with 9ml media and the cells placed in a 15ml falcon tube. A cell pellet was produced by centrifugation for 5minutes at 1000rpm. The trypsin-containing supernatant was removed and the pellet re-suspended in 1-2ml culture media, and re-plated at the desired dilution.

7.9.5.3 Cryopreservation

- 2X Freezing Media
- 20% DMSO (dimethyl sulfoxide)
- 80% FCS

Cells were trypsinised and re-suspended to a single-cell suspension in 1ml culture media, as above. 0.5ml cell suspension was mixed with 0.5ml freezing mix and kept on ice, while being transported immediately to a -80°C freezer. After overnight storage at -80ºC they were transferred to long-term storage in liquid nitrogen.

7.10 RNA

7.10.1 RNA ANALYSIS

Experimental conditions were maintained to avoid contamination of sample RNA and degradation by RNAses. Surfaces and equipment were cleaned with 70% ethanol followed by RNAZap (Ambion AM9782), to inactivate any environmental RNAses. All RNA work was carried out using barrier tip pipettes, and reagents were RNAse free and used solely for RNA work. RNA was stored for as short a time as possible at -80ºC and kept on ice or dry ice when in use, to prevent degradation. Tissues that were not processed immediately were preserved in RNAlater (Applied Biosystems AM7024), kept at 4ºC overnight and then stored at -20°C long term.

7.10.2 RNA ISOLATION

Isolation of RNA from cells and tissues was performed according to manufacturer's instructions using the RNeasy Mini Kit (Qiagen 74104) or AllPrep DNA/RNA/Protein Mini Kit (Qiagen 80004). DNAse digestion was performed when using the RNeasy kit. RNA was eluted in 30-40µl RNA free water

7.10.3 MEASURING RNA CONCENTRATION

RNA concentration was measured using a Nanodrop 2000 Spectrophotometer (Thermo Scientific Micro-Volume UV-Vis Spectrophotometer).

7.10.4 cDNA Synthesis

cDNA was synthesized from a specified amount of total starting RNA (between 2-10µg). RNA was transcribed using AMV reverse transcriptase (Roche 11495062001) and oligo d(T) priming. 4µl AMV Reverse Transcriptase 5x Reaction Buffer, 1.25µl RNAse free dNTPs, 0.25µl RNAse inhibitor (Roche 03335399001), 1µl oligo d(T) and 1µl AMV reverse transcriptase were added to the appropriate volume of RNA (made up to 12.5µl with RNAse free water). After incubation at 48°C for 2 hours the resulting cDNA was diluted to a concentration of 10ng/µl. 2µl of diluted cDNA was used per Real Time PCR reaction.

7.10.5 Real Time PCR

Quantitative (Real Time) PCR reactions were carried out using the Roche Lightcycler 480 system. Assays were designed using the Universal Probe Library Assay Design Centre (Roche) and using Universal Probe Library probes and primers. Primers were supplied as lyophilised powders and rehydrated in TE to a stock solution of 100µM. Working solutions of 20µM were made for use in individual PCR reactions. The PCR reaction was carried out according to manufacturers recommendations, using 0.2µl forward primer (target gene), 0.2µl reverse primer (target gene), 0.2µl target probe, 0.05-0.2µl forward and reverse primers (reference gene), 0.05-0.2µl reference probe, 5µl Lightcycler Master Mix (Roche 04-887-301-001) and made up to 8µl with RNAse free dH2O. 2µl of cDNA was added to make a total volume of 10µl. Relative expression of each target gene was quantified against a reference gene (*GAPDH* for mouse, *ACTB* for human). Each experiment was performed and analysed in triplicate, and standard error of the mean was calculated. To aid comparison between experimental groups, results were expressed relative to matched controls, which were arbitrarily assigned a value of 1. Primers and probes are listed in Table 6.6.

TABLE 7.6: Q-RT-PCR HUMAN PRIMERS

HUMAN			
TRANSCRIPT	**FORWARD PRIMER**	**REVERSE PRIMER**	**PROBE**
WT1	agctcaaaagacaccaaaggag	gggagaactttcgctgacaa	47
WT1 (exon7/exon8 - detecting all isoforms)	agctgtcccacttacagatgc	ccttgaagtcacactggtatgg	4
Snail	gctgcaggactctaatccaga	atctccggaggtgggatg	11
Slug	acagcgaactggacacacat	gatggggctgtatgctcct	73
TGFβ1	cacgtggagctgtaccagaa	cagccggttgctgaggta	72
Vim (Vimentin)	aaagtgtggctgccaagaac	agcctcagagaggtcagcaa	16
Desmin	gcgtgacaacctgatagacg	tctcttagttggatttcctcctgt	110
MMP9	tcttccctggagacctgaga	gccacccgagtgtaaccata	53
Col1	atgttcagctttgtggacctc	ctgtacgcaggtgattggtg	15
Fn1A (Fibronectin A)	caccacagccatctcacatt	cttccaacggcctacagaat	39
Fn1B (Fibronectin B)	cggctacatcatcaagtatgaga	tattcggttcccggttcc	52
Zo-1	tgcaagtagagagaggagcttg	tgccaatcgaagaccatattc	11
Wnt 4	aggtggtgacgcaaggtg	cctgacctgctttctgtcagt	25

TABLE 7.7: Q-RT-PCR MOUSE PRIMERS

MOUSE			
TRANSCRIPT	**FORWARD PRIMER**	**REVERSE PRIMER**	**PROBE**
Wt1 (exon 8 / exon 9)	caccaaaggagacacacagg	gggaaaactttcgctgacaa	47
Wt1 (exon 1 / exon 2)	caggatgttccccaatgc	gaaagtgaccgtgctgtatcc	27
Nephrin	ccatcctcccagagatgttc	ttctccatgtcgtccaggtt	101
Podocin	ccatctggttctgcataaagg	ccaggacctttggctcttc	38
Synaptopodin	gtagccaggtgagccaagg	ttttcggtgaagcttgtgc	67
Podocalyxin	cctgcatctcactcccataat	tctgttgatgttgtggcactt	21
ZO-1	gccagatatctatcagattgcaaaa	gatgccagagctacgatgg	95
Snail	cttgtgtctgcacgacctgt	caggagaatggcttctcacc	71
Slug	atccttggggcgtgtaagt	tgaaccactgtgatccttgg	6
Zeb-1	gccagcagtcatgatgaaaa	tatcacaatacgggcaggtg	48
Vimentin	ccaacctttttcttccctgaa	tgagtgggtgtcaaccagag	109
Fibronectin	gatgccgatcagaagtttgg	ggttgtgcagatctcctcgt	46
Desmin	gccacctaccggaagctact	gcagagaaggtctggataggaa	15
P-cadherin	ggaagggtggtttcatcctc	aggaggagtgccagtagaagg	56
Wnt4	ctggactccctccctgtctt	atgcccttgtcactgcaaa	62
Wnt7b	gcgtcctctacgtgaagctc	tcttgttgcagatgatgttgg	49

7.11 Protein

7.11.1 Protein Extraction

Total protein lysates from experimental tissues and cells were prepared using the commercially available cOmplete Lysis-M Kit (Roche 04719956001) or the AllPrep DNA/RNA/Protein Mini Kit (Qiagen 80004). Following RNA binding, protein was precipitated using Buffer APP, and precipitated proteins pelleted by centrifugation. The pellet was re-dissolved in buffer ALO and denatured at 95°C for 5 minutes.

7.11.2 Measuring Protein Concentration

Protein concentration was quantified using the commercially available BCA Protein Assay Kit (Thermo Scientific) in which your protein of interest is compared to albumin dilutions of known concentration. Each measurement was performed in duplicate and assays were read on a FluoStar Omega Plate Reader (BMG Labtech).

7.11.3 Western Blot

Protein samples of known concentration were mixed with 2x Loading Buffer and incubated at 95ºC for 5 minutes, then cooled on ice. Proteins were separated using gel electrophoresis using either commercially available ready-made Tris-Glycine Gels (1mm x 15 wells, Invitrogen) or hand poured gels. A pre-stained protein marker (New England Biolabs Prestained Protein Marker, Broad Range (7-175 kDa) P7708V) was used to quantify the size of the resultant bands. Proteins were transferred to Amersham Hybond-P blotting membrane (GE Healthcare) using a compressed transfer stack consisting of 3 buffer pads, whatmann paper, the gel, blotting membrane (which had been incubated in methanol for 10 minutes), whatmann paper and 3 further buffer pads, all soaked in transfer buffer. Transfer was carried out at 12volts in a transfer tank for 1hr.

After transfer, the membrane was blocked for 1 hour in 10% Fat Free Milk Powder (marvel) in TBST at room temperature. Incubation with the primary antibody, diluted in 5% milk/TBST, was carried out overnight at 4ºC.

The following day, the membrane was washed 3 x 20 mins in TBST and then incubated in secondary antibody, diluted in 5%milk/TBST for 1 hour at room temperature. The membrane was then washed a further 3 times in TBST.

Protein detection was carried out using the ECL-Plus Kit (GE Healthcare) as per manufacturer's instructions.

To ensure equal loading the membrane was stripped using stripping buffer, then washed 2x20min with TBST before re-probing with another primary antibody for a housekeeping gene.

Loading Buffer (2x)

- 10% SDS 4ml
- Glycerol 2ml
- Tris (1M pH 6.8) 1.2ml
- DTT (1M) 2ml
- Bromophenol Blue 10µl
- dH20 700 µl

Transfer Buffer

- Glycine 28.8g
- Tris 5.8g
- Methanol 400ml

  Final volume brought to 2000ml with dH2O

TBST

- 50mM TrisHCl pH 7.5
- 150mM NaCl
- 0.1% Tween (Sigma)

Stripping Buffer

- 100mM β-mercaptoethanol
- 2% SDS
- 62.5mM TrisHCl pH 6.7

TABLE 7.8: ANTIBODIES USED IN WESTERN BLOT

Target			**Concentration**
WT1	Santa-Cruz C19	Sc-192	1/5000

7.12 DNA

7.12.1 Isolation of Genomic DNA for Genotyping of Experimental Animals

Earclips were taken from mice at weaning for identification purposes and to isolate DNA for genotyping. Genomic DNA extraction was carried out using the HOTSHOT method. Earclips were incubated in 75µl 25mMNaOH, 0.2mM EDTA at 95°C for 30 minutes. Following cooling to room temperature, the solution was neutralized with 75µl 40mM Tris.HCl and vortexed (Truett, Heeger et al. 2000). Genotyping of embryos was carried out using the same method but using tailtips.

7.12.2 Isolation of Genomic DNA from Tissues stored in RNA Later

Isolation of Genomic DNA from Tissues stored in RNA Later (Invitrogen AM7020) was carried out according to manufacturer's instructions. RNALater preserved tissue was minced finely and digested in 1.5ml digestion buffer (60 mM Tris pH 8.0; 100 mM EDTA; 0.5% SDS) with Proteinase K added to a final concentration of 500µg/ml. After mixing by inversion, samples were incubated at 55°C for 4-24 hours with rotation, until little cellular material remained.

Samples were divided into 2 equal aliquots, and then equal volumes of 50:50 phenol/chloroform (Sigma P2069) were added. Samples were mixed for 2 minutes by inversion. After centrifuging at high speed for 10 minutes the aqueous (upper) phase was removed to a new tube using a wide-bore pipette tip. The phenol/chloroform extraction was carried out a total of 3 times, and repeated if the upper: lower interface remained dirty.

The final extraction was carried out with choloroform, and the upper phase removed to a fresh eppendorff tube. 1/10 volume 3M sodium acetate (pH 5.2) and 1 volume 95% ethanol was added and mixed by gentle inversion. After centrifugation for 10 minutes at high speed the DNA pellet was washed in 70% ethanol for 5 minutes and allowed to air-dry overnight.

DNA was re-suspended overnight in TE at 4° and quantified by spectrophotometry

7.12.3 DNA EXTRACTION

7.12.3.1 DNA Extraction using the Qiagen AllPrep DNA/RNA/Protein Mini Kit

DNA extraction using the Qiagen AllPrep DNA/RNA/Protein Mini Kit (80004) was carried out as per manufacturers instructions. Tissues were lysed and homogenized in a highly denaturing guanidine-isothiocyanate containing buffer (RLT plus β-mercaptoethanol) to denature DNases, RNAses and proteases. The lysate was passed through an AllPrep DNA spin column to bind DNA. After washing, the DNA was eluted in 100µl Buffer EB and quantified by spectrophotometry.

7.12.3.2 DNA extraction using DirectPCRLysis Reagent

DNA was extracted from cells using DirectPCR Lysis Reagent (Viagen Biotech 301-C) according to manufacturer's instructions. Cells were suspended in DirectPCR Lysis Reagent and 0.2mg/ml Proteinase K and incubated overnight at 55ºC until no clumps remained. Crude lysates were then incubated at 80ºC for 1 hour. Debris was pelleted by centrifugation for 15 seconds. 1µL supernatant used as template per PCR reaction.

7.12.3.3 DNA Extraction from BACs

DNA was extracted from BACs using a modified method using reagents from the Qiagen Maxi-Prep kit (Qiagen 12163) (Sharan, Thomason et al. 2009). In brief, for mini-prep, bacterial cells containing the BAC were grown up overnight at 30°C with shaking in 5ml LB containing appropriate antibiotic selection. For maxi-prep, the 5ml starter culture was used to inoculate 400ml LB containing appropriate antibiotic selection and grown up for a further 16-20 hours.

After cells were pelleted and supernatant removed they were re-suspended in chilled buffer P1 and then lysed in buffer P2. After incubation on ice for 5 minutes, buffer P3 was added to precipitate the lysate, which was then incubated on ice for 5-20 minutes. After centrifugation, the supernatant was removed and transferred to a clean tube. 2 volumes 95% ethanol were added and the mixture incubated on ice for 30 minutes, then centrifuged for 10 minutes at 4°C. The pellet was washed in 70% ethanol, air dried and then suspended in 50-200µl TE.

7.12.3.4 DNA extraction from plasmids

Qiagen Plasmid Kits (Plasmid Mini Kit [Qiagen 27106] for up to 20µg DNA and Plasmid Maxi Kit [Qiagen 12163] for up to 500µg DNA) were used to isolate plasmid DNA, according to the manufacturer's instructions.

For mini-prep, a single colony was picked and 5ml LB containing appropriate antibiotic selection was inoculated with bacteria. Plasmid DNA was extracted the following day after incubation overnight with vigorous shaking.

For maxi-prep, 500µl from an overnight 5ml starter culture (as above) was for 16-20hours in 400ml LB containing appropriate antibiotic selection.

7.12.4 Measuring DNA Concentration

DNA concentration was measured using a Nanodrop 2000 Spectrophotometer (Thermo Scientific Micro-Volume UV-Vis Spectrophotometer.

7.12.5 DNA Precipitation

1 volume of DNA sample as mixed with 1/10 volume 3M Sodium Acetate and 2.5 volumes cold 100% ethanol. The solution was mixed well and kept at -20°C for 20minutes. After centrifugation at maximum speed at 4°C for 15minutes the DNA pellet was washed in 70% ethanol and then air-dried. The pellet was re-suspended in 30µl TE and the concentration checked on Nanodrop.

7.12.6 Digestion with Restriction Enzymes

Digestion with Restriction Enzymes was carried out in a suitable buffer and incubated at an appropriate temperature according to the manufacturer's recommendations. The standard method was to digest 0.1µg - 5µg DNA in a total volume of 20-100µl, with approximately 10-fold excess of enzyme (assuming at 37° 1U restriction enzyme cuts 1µg DNA in 1 hour). The final volume was made up using dH20 to a level at least 10-fold more than the volume of enzyme in order to avoid excess glycerol inhibiting the digestion. Multi-digest reactions were combined according to the manufacturers recommendations.

7.12.7 DNA Ligation

Appropriate quantities of DNA were combined with Roche T4 DNA ligase (0716359001) and the supplied 10x buffer plus dH2O to a total volume of 30µl. The reaction was left to proceed at 16°C overnight.

7.12.8 DNA purification

DNA was purified using QIAquick PCR purification kit (Qiagen 28104) according to manufacturer's instructions. High salt binding buffer was added to the PCR product, before application and binding to the spin column, in order to promote adsorbtion of DNA to the column membrane. Following washing to remove impurities such as excess primer, the pure DNA was eluted in low-salt buffer.

TABLE 7.9: RESTRICTION DIGESTS

Restriction Enzyme	**Buffer**	**Incubation Temperature**	**Manufacturer**
EcoRI	SuRE/Cut H	37	Roche
HindIII	SuRE/Cut B	37	Roche
PstI	SuRE/Cut H	37	Roche
PacI	NEBuffer1	37	NEB
AscI	NEBuffer4	37	NEB
SalI	SuRE/Cut H	37	Roche
NdeI	NEBuffer4	37	NEB
BamHI	SuRE/Cut B	37	Roche
DpnI	SuRE/Cut A	37	Roche
XbaI	SuRE/Cut H	37	Roche
P1-SceI	NEBuffer-PI-SceI	37	NEB
NdeI/SalI	NEBuffer3	37	NEB
NdeI/XhoI	NEBuffer4	37	NEB
PacI/AscI	NEBuffer4	37	NEB

7.13 Polymerase Chain Reaction (PCR)

7.13.1 Deoxyribonucleotide triphosphates (dNTPs)

Invitrogen 100mM dNTP kit PCR Grade (10297-018) was used to make a working stock containing dATP, dCTP, DTTP, DGTP. 100µl of each dNTP was added to 4.6ml dH20 to make a 2mM working solution. 0.2mM dNTPs was used per PCR reaction.

7.13.2 Primers

Primers were designed using either the Primer 3 Programme (http://primer3.sourceforge.net/) or using Geneious Pro software. Oligonucleotides were purchased as lyophilized desalted compounds and reconstituted to make a sterile 100µM stock solution with TE Buffer and stored at -20°. Diluted working solutions were used in PCR reactions to a final concentration of 0.25µM (unless otherwise specified).

7.13.3 Other Reagents

Taq DNA Polymerase (Invitrogen 10342-053) or Platinum Taq DNA Polymerase (Invitrogen 11304-011) were used, in combination with their supplied 10x buffer, depending on the region to be amplified, and purpose of the resulting PCR product. Mg2+ (Invitrogen) was added to a final concentration of 2.5mM. The reaction volume was made up to a final volume of 20 or 25µl with dH20.

7.13.4 Purification of PCR Products

PCR products were purified using the Qiagen QIAQuick PCR Purification Kit (28104) as above. 50µl of PCR product was diluted with 5 volumes Buffer PB, and spun through the QIAQuick spin column. The bound DNA was washed in 750µl BufferPE and eluted in 30µl sterile water. DNA concentration was checked using Nanodrop.

TABLE 7.10: PCR PRIMERS

Genotyping	**Forward Primer**	**Reverse Primer**	**DNA Polymerase**	**PCR Programme**
Wt1	tgggcatttctgctaagcg	taagagtcaacgcctgtgg	Taq	Geno56
		agctgcggggtcactttag	Taq	
Cre	gcattaccggtcgagcaacgagtgatgag	gagtgaacgaacctggtcgaaatcagtgcg	Platinum Taq	Geno58
Fabpi (housekeeping)	tggacaggactggacctctgctttcctaga	tggacaggactggacctctgctttcctaga	Platinum Taq	Geno58
GFP	gcctgaagaacgagatcagc	ggcagcttgaattcctctca	Taq	Wt1-GFP
Rosa26	ggcttaaaggctaacctgatgtg	ggagcgggagaaatggatatg	Taq	MTRosa

TABLE 7.11: PCR CONDITIONS

	Temperature (°C)	Incubation Time	Cycles
Geno 58	94	2 min	
	94	15s	
	58	30s	35 cycles
	72	1 min	
	72	5 min	
	4	10 min	
Geno 56	94	2 min	
	94	15s	
	56	30s	35 cycles
	72	1 min	
	72	5 min	
	4	10 min	
MT Rosa	94	4 min	
	94	1 min	
	60	45s	30 cycles
	72	1 min	
	72	10 min	

WT1-GFP	94	3 min	
	94	30s	
	58	30s	35 cycles
	72	1 min	
	72	5 min	

7.13.5 GEL ELECTROPHORESIS

Agarose gel electrophoresis was used to separate DNA / PCR fragments according to size. Gels were prepared by melting the appropriate amount of agarose (according to the desired gel density) in 1x TBE buffer by heating in a microwave. The percentage of agarose used was dependent upon the size of the fragments to be separated. After cooling a little, ethidium bromide (BDH 10mg/ml) was added to a final concentration of 50µg/100ml and the gel left to set.

DNA was mixed with 10x Loading Buffer (3ml glycerol; 1ml 10xTBE; 6ml dH20; Bromophenol Blue (Sigma)) and loaded onto the gel. Electrophoresis was carried out in 1xTBE buffer and run at 70-150V. DNA fragments were visualized under UV illumination and photographed on a BioDocit (UVP) Imaging System. Fragment size was determined by comparison to a DNA ladder, either 100bp DNA Ladder (NEB N3231L) or 1kb DNA ladder N3232L.

7.14 HISTOLOGY

7.14.1 PARAFFIN FIXATION

Mice were sacrificed by cervical dislocation or CO2 inhalation. Kidneys were removed, de-capsulated and rinsed in PBS to remove excess blood. They were then fixed in 4%PFA (4g paraformaldehyde (Sigma 158127-500G) in 100ml PBS) overnight at 4°C. The following day, kidneys were washed twice in PBS for 15 minutes each time, and then taken through serial dilutions of ethanol (15minutes 25% ethanol, 15mins 50% ethanol, 15mins 75% ethanol) and then stored in 70% ethanol. Kidneys were embedded in paraffin, using 30minute cycles on an automated TissueTekVIP 5 Jr machine. Samples containing either GFP or YFP were processed immediately to avoid loss of the signal. Tissue blocks were sectioned at 4μM and baked at 50ºC for at least one hour prior to staining.

E18.5 embryos were decapitated and fixed in 4% PFA overnight. They following day they were trimmed to give a suitable tissue block to include the kidneys and fixed again in 4% PFA overnight. After washing in serial dilutions of ethanol (as above) fixed tissue blocks were paraffin embedded using 90minute cycles. Sections were cut at 4μM and baked at 50ºC for at least one hour prior to staining.

7.14.2 CRYOPRESERVATION

Mice were sacrificed by cervical dislocation or CO2 inhalation. Kidneys were removed, de-capsulated and rinsed in PBS to remove excess blood. They were then fixed in 4%PFA overnight at 4°C. The following day, kidneys were washed twice in PBS for 15 minutes each time, then dehydrated in 5% sucrose in PBS for 45minutes and then 20% sucrose in PBS until the tissue sank (usually overnight). Tissue samples were foxed in OCT (Tissue-Tek 25608-930) and stored at -80ºC. Cryosectioning was done at 10μM and slides allowed to thaw before use

7.14.3 HISTOLOGICAL STAINING

All histological staining techniques were carried out using standard protocols based on methods described in "The Theory and Practice of Histological Techniques", 3rd Edition, Bancroft and Stevens. These included:

7.14.3.1 Haematoxylin and Eosin Staining (H&E)

Harris' Haematoxylin

- Haematoxylin 10g
- Absolute Alcohol 100ml
- Potassium Alum 200g
- Distilled Water 2000ml
- Mercuric Oxide 5g

Eosin

- 3 parts 1% Aqueous Eosin Y
- 1 part 1% Ethanol
- 0.05% Acetic Acid
- (filtered before use)

Slides were de-waxed in xylene and then hydrated in serial dilutions of ethanol, before washing in distilled water. Slides were stained in haematoxylin for 4 minutes, rinsed and differentiated in acid/alcohol for a few seconds. After a further wash, slides were blued in lithium carbonate solution, before a 5 minute wash. Slides were stained in eosin for 3 minutes and briefly rinsed. After two washes in 100% ethanol, slides were cleared in xylene, before mounting in DPX mountant (Leica 3808600ED) and left to dry overnight.

7.14.3.2 Periodic Acid Schiff Staining for glycogen (glomerular basement membrane)

Slides were de-waxed and brought to distilled water as above. Using the Sigma PAS Kit (395B), slides were treated with periodic acid for 5 minutes then washed well in several changes of distilled water. Slides were immersed in Schiff's solution for 15 minutes before washing in running water for a further 10 minutes. Nuclei were blued in Harris Haematoxylin (as above). Following a rinse in distilled alcohol, slides were cleared in xylene and mounted in DPX.

7.14.3.3 Masson Trichome Staining for collagen deposition

Celestine Blue

- Celestine Blue B 2.5g
- Ferric Ammonium sulphate 25g
- Glycerin 70ml
- dH20 500ml

Acid fuchsin solution

- Acid fuchsin 0.5g
- Glacial acetic Acid 0.5ml
- dH20 100ml

Phosphomolybdic Acid

- Phosphomolybdic Acid 1g
- dH20 100ml

Methyl Blue

- Methyl Blue 2g
- Glacial acetic acid 2.5ml
- dH20 100ml

Sections were de-waxed and bought to distilled water. Nuclei were stained using Celestin-blue-haemalum and differentiated with 1% acid/alcohol. After washing well, sections were stained in acid fuchsin solution for 5 minutes and then rinsed in distilled water. The sections were then treated with phosphomolybdic acid solution for 5 minutes, drained, and stained with methyl blue for a further 5 minutes. After rinsing in distilled water, slides were treated with 1% acetic acid for 2 minutes. After dehydration in ethanol and clearing in xylene, sections were mounted in DPX.

Control and mutant matched sections were processed in parallel to avoid batch differences. Stained sections were kept at room temperature in the dark to avoid fading.

A modified glomerular injury score was used to semi-quantitaively compare the degree of glomerular injury. 30 randomly selected glomeruli were scored blindly as to the degree of glomerular injury (podocyte and/or parietal cell vacuolation and injury, loss of glomerular capillary loop architecture, glomerular hypercellularity). Scoring was as follows: Score 0 = no damage, 1 = 0-25% epithelial cells/glomerulus affected, 2 = 25-50%. 3 = 50-75%, 4 = 75-100%.

7.14.4 IMMUNOHISTOCHEMISTRY

7.14.4.1 Immunoperoxidase

Immunohistochemistry with antigen retrieval was carried out as previously described (Martinez-Estrada, Lettice et al. 2010). 4μM sections were de-waxed by immersing in xylene overnight, and then taken through 3 washes 100% ethanol and 2 washes 96% ethanol for 10 minutes each. Samples were blocked for endogenous peroxidase for 30 minutes. Antigen retrieval was achieved using a pressure cooker method in which slides were boiled in TEG buffer (10mM Tris and 0.5mM EGTA, pH9) and pressure-cooked for 4 minutes. After cooling, slides were incubated in 50mM NH4Cl in PBS then blocked in 1% BSA; 0.2% gelatin and 0.05% saponin three times for 10 minutes each. Samples were incubated in the primary antibody diluted in 0.1%BSA + 0.3% Trition-X-100 in PBS overnight at 4°. The following day, cells were washed in 0.1% BSA; 0.2% gelatin and 0.05% saponin three times for 10 minutes each and then incubated with antiperoxidase secondary antibody diluted in 0.1%BSA + 0.3% Trition-X-100 in PBS for 1 hour at room temperature. After further washing in 0.1% BSA; 0.2% gelatin and 0.05% saponin slides were incubated with DAB for 10 minutes in the dark. After washing off excess DAB cells were counterstained with Mayers Haemalum, dehydrated and mounted in Depex.

7.14.4.2 Immunofluorescence on frozen tissue sections

OCT cryopreserved tissue samples were cut at 10μM slices and thawed for 20 minutes. Sections were washed three times in PBS for 10 minutes each, and then permeabilised on 0.25% Triton-X in PBS for 10 minutes at room temperature. Sections were washed again in PBS another three times for 10 minutes each, and then blocked for 1 hour at room temperature in 2% BSA in PBS. Sections were incubated overnight with the primary antibody, diluted in 2% BSA, at 4°C. The following day, sections were washed three times in PBS for 10 minutes, and then incubated with a fluorescence-conjugated secondary antibody, diluted in 2% BSA for 1 hour in the dark. After three further washes in PBS for 10 minutes each, slides were mounted in Vectashield Hardset Mounting Medium with DAPI (Vector Laboratories H-1500) and stored at 4ºC in the dark.

7.14.4.3 Immunofluorescence on paraffin sections

Paraffin sections were prepared for immunofluorescence as per the immunoperoxidase method. However, following incubation with the primary antibody and the three washes with PBS, sections were incubated with fluorescence conjugated secondary antibody in the dark for one hour. Sections were then washed three times in PBS, and three times in dH20 before mounting in Vectashield Hardset Mounting Medium with DAPI (Vector Laboratories H-1500). Sections were stored long term at 4°C in the dark.

7.14.4.4 Immunofluorescence on cells

For immunofluorescence cells were grown on collagen-coated coverslips. Culture media was removed and cells were fixed in 2% PFA for 20 minutes. After washing in PBS, cells were permeabilised in 0.5% Triton-X100 in PBS for 5 minutes and washed again in PBS. Cells were then blocked in 2%BSA for 1 hour at room temperature. Incubation with the primary antibody, diluted in 2% BSA was carried out at 4°C overnight. The following day, samples were washed three times in PBS and then incubated with the appropriate secondary fluorescence-conjugated antibody in the dark for 1 hour. After three further 30 minute washes in PBS, coverslips were mounted with Vectashield with DAPI (H-1200) and stored at 4ºC in the dark (Martinez-Estrada, Lettice et al. 2010).

TABLE 7.12: ANTIBODIES

Antibody	**Manufacturer**	**Product**	**IP**	**IF**
WT1	Santa Cruz	C19 D1703	1/2000	1/4000
Synaptopodin	Progen	G1D4	1/100	1/250
Podocalyxin	R&D Systems	AF1556	1/100	1/500
Podocin	Sigma	PO372		1/250
PhosphohistoneH3	Cell signaling	P701	1/500	
Cleaved Caspase 3	Cell signalling	P661	1/100	
F4/80	Caltag	MF48000	1/250	
GFP	Abcam	Ab6556	1/500	1/1000

7.15 MICROSCOPY

Slides were visualized using a Zeiss Axioplan 2 microscope.

7.15.1 QUANTIFICATION OF CRE-RECOMBINATION EVENTS

Paraffin fixed tissue from *CreER R26R*$^{YFP/YFP}$ mice injected with either 1mg/40g BW or 4mg/40g BW tamoxifen for 5 days (n=2 for each dose) was stained with anti-GFP antibody (which detected YFP protein expression) using the immunoperoxidase protocol as above. The whole slide was imaged using Dotslider at x40 magnification. In a blinded fashion, the total number of stained cells in 20 randomly selected glomeruli from each animal were counted, and divided by the total number of nuclei per glomerulus to quantify the number of Cre-recombination events pre glomerulus.

7.15.2 QUANTIFICATION OF WT1 STAINING

Following immunohistochemistry for Wt1, the number of Wt1 positive cells per glomerulus were counted in 30 randomly selected glomeruli in different microscopic fields for each sample.

7.15.3 GLOMERULAR INJURY

The proportion of injured glomeruli / total glomeruli was counted across 30 randomly selected x10 magnification microscopic fields.

7.15.4 HISTOLOGICAL SCORE

A modified histological scoring method (Suzuki, Matsusaka et al. 2009) was used to semi-quantitatively assess the level of glomerular injury across 30 randomly selected glomeruli across different microscopic fields, examined at x40 magnification (Score 0 = no damage, 1 = 0-25% glomerular volume, 2 = 25-50%. 3 = 50-75%, 4 = 75-100%).

7.16 Bioinformatics

Frequently used websites are listed below in Table 6.13

7.17 Statistical Methods

Statistics were carried out using the statistical programme SigmaPlot 11. Results are expressed as mean +/- S.E.M (depicted by error bars). Data were tested and analysed using Students T-test for parametric data unless stated otherwise. Multiple groups were analysed using a one-way ANOVA. P values <0.05 were considered significant. Mann-U-Whitney test was used to test significance in non-parametric data.

TABLE 7.13: BIOINFORMATICS

Name	**Purpose**	**URL**
UPL Assay Design Centre	Designing primers and probes for real time PCR	http://www.roche-applied-science.com/sis/rtpcr/upl/index.jsp?id=UP030000
Primer3	Designing PCR primers	http://primer3.sourceforge.net
Ensembl	Genome Browser	http://www.ensembl.org/index.html
NCBI	Searching for articles	http://www.ncbi.nlm.nih.gov/pubmed

7.18 Solutions prepared by the MRC HGU Core Scientific Services

Phosphate Buffered Saline (PBS)

- NaCl 8g
- KCl 0.2g
- Na2HPO4 1.44g
- KH2PO4 0.24g
- Dissolve in 800ml dH20
- Adjust pH to 7.4
- Bring final volume to 1000ml with dH20

Tris HCL

- Dissolve Tris (hydroxymethyl) aminomethane in sterile water
- Adjust pH with HCl

EDTA

- Dissolve ethyldiaminetetraacetic acid di-sodium salt in sterile water
- Add solid NaOH to adjust pH to 8.0

TE Buffer

- 10mM Tris.HCl (pH 7.5)
- 1mM EDTA

TBE Buffer (20x Stock)

- Tris (hydroxymethyl) aminomethane 242g
- Glacial acetic acid 57.1ml
- 0.5M EDTA 100ml
- Bring volume to 1000ml with dH2O

Trypsin

- Tryspin 1:250 2g
- Phenol Red 5ml
- Penicillin 0.06g
- Streptomycin 0.13g
- Make up to 1000ml in PBS
- Adjust pH to 7.3 using NaHCO3

Versene

- Dulbeccos Tablets 10
- Sodium EDTA 0.4g
- 0.2% Phenol Red 5ml
- Make up to 1000ml with dH2O

APPENDIX

CONFERENCE PRESENTATIONS AND PUBLICATIONS DURING THE COURSE OF THIS THESIS

Miller-Hodges, E. and P. Hohenstein (2012). "WT1 in disease: shifting the epithelial mesenchymal balance." J Pathol 226(2): 229-240

Dolt, K. S., M. L. Lawrence, E. Miller-Hodges, J. Slight, A. Thornburn, P. S. Devenney and P. Hohenstein (2013). "A Universal Vector for High-Efficiency Multi-Fragment Recombineering of BACs and Knock-In Constructs." PLoS One 8(4): e62054

Miller-Hodges, E, Hohenstein P and Hastie, N. *"Wt1* is critical for maintenance of the epithelial-mesenchymal balance in podocytes". In: Renal Association Conference; 2012 Jun 12-14; Gateshead. Abstract 31. Awarded the Amgen Bursary

REFERENCES

(2007). "KDOQI Clinical Practice Guidelines and Clinical Practice Recommendations for Diabetes and Chronic Kidney Disease." Am J Kidney Dis **49**(2 Suppl 2): S12-154.

Adams, D. J. and L. van der Weyden (2008). "Contemporary approaches for modifying the mouse genome." Physiol Genomics **34**(3): 225-238.

Appel, D., D. B. Kershaw, B. Smeets, G. Yuan, A. Fuss, B. Frye, M. Elger, W. Kriz, J. Floege and M. J. Moeller (2009). "Recruitment of podocytes from glomerular parietal epithelial cells." J Am Soc Nephrol **20**(2): 333-343.

Armstrong, J. F., K. Pritchard-Jones, W. A. Bickmore, N. D. Hastie and J. B. Bard (1993). "The expression of the Wilms' tumour gene, WT1, in the developing mammalian embryo." Mech Dev **40**(1-2): 85-97.

Asahina, K., B. Zhou, W. T. Pu and H. Tsukamoto (2011). "Septum transversum-derived mesothelium gives rise to hepatic stellate cells and perivascular mesenchymal cells in developing mouse liver." Hepatology **53**(3): 983-995.

Auber, F., C. Jeanpierre, E. Denamur, F. Jaubert, G. Schleiermacher, C. Patte, S. Cabrol, G. Leverger, C. Nihoul-Fekete and S. Sarnacki (2009). "Management of Wilms tumors in Drash and Frasier syndromes." Pediatr Blood Cancer **52**(1): 55-59.

Aucella, F., L. Bisceglia, P. De Bonis, M. Gigante, G. Caridi, G. Barbano, G. Mattioli, F. Perfumo, L. Gesualdo and G. M. Ghiggeri (2006). "WT1 mutations in nephrotic syndrome revisited. High prevalence in young girls, associations and renal phenotypes." Pediatr Nephrol **21**(10): 1393-1398.

Barbaux, S., P. Niaudet, M. C. Gubler, J. P. Grunfeld, F. Jaubert, F. Kuttenn, C. N. Fekete, N. Souleyreau-Therville, E. Thibaud, M. Fellous and K. McElreavey (1997). "Donor splice-site mutations in WT1 are responsible for Frasier syndrome." Nat Genet **17**(4): 467-470.

Barbosa, A. S., C. G. Hadjiathanasiou, C. Theodoridis, A. Papathanasiou, A. Tar, M. Merksz, B. Gyorvari, C. Sultan, R. Dumas, F. Jaubert, P. Niaudet, C. A. Moreira-Filho, C. Cotinot and M. Fellous (1999). "The same mutation affecting the splicing of WT1 gene is present on Frasier syndrome patients with or without Wilms' tumor." Hum Mutat **13**(2): 146-153.

Barker, N., J. H. van Es, J. Kuipers, P. Kujala, M. van den Born, M. Cozijnsen, A. Haegebarth, J. Korving, H. Begthel, P. J. Peters and H. Clevers (2007). "Identification of stem cells in small intestine and colon by marker gene Lgr5." Nature **449**(7165): 1003-1007.

Benetti, E., G. Caridi, C. Malaventura, M. Dagnino, E. Leonardi, L. Artifoni, G. M. Ghiggeri, S. C. Tosatto and L. Murer "A novel WT1 gene mutation in a three-generation family with progressive isolated focal segmental glomerulosclerosis." Clin J Am Soc Nephrol **5**(4): 698-702.

Bockenhauer, D., W. van't Hoff, G. Chernin, S. F. Heeringa and N. J. Sebire (2009). "Membranoproliferative glomerulonephritis associated with a mutation in Wilms' tumour suppressor gene 1." Pediatr Nephrol **24**(7): 1399-1401.

Borner, U., G. Szasz, W. Bablok and E. W. Busch (1979). "[A specific fully enzymatic method for creatinine: reference values in serum (author's transl)]." J Clin Chem Clin Biochem **17**(11): 679-682.

Boute, N., O. Gribouval, S. Roselli, F. Benessy, H. Lee, A. Fuchshuber, K. Dahan, M. C. Gubler, P. Niaudet and C. Antignac (2000). "NPHS2, encoding the glomerular protein podocin, is mutated in autosomal recessive steroid-resistant nephrotic syndrome." Nat Genet **24**(4): 349-354.
Brenner, B. M., T. W. Meyer and T. H. Hostetter (1982). "Dietary protein intake and the progressive nature of kidney disease: the role of hemodynamically mediated glomerular injury in the pathogenesis of progressive glomerular sclerosis in aging, renal ablation, and intrinsic renal disease." N Engl J Med **307**(11): 652-659.
Bugeon, L., A. Danou, D. Carpentier, P. Langridge, N. Syed and M. J. Dallman (2003). "Inducible gene silencing in podocytes: a new tool for studying glomerular function." J Am Soc Nephrol **14**(3): 786-791.
Burn, S. F., A. Webb, R. L. Berry, J. A. Davies, A. Ferrer-Vaquer, A. K. Hadjantonakis, N. D. Hastie and P. Hohenstein (2011). "Calcium/NFAT signalling promotes early nephrogenesis." Dev Biol **352**(2): 288-298.
Burns, W. C. and M. C. Thomas (2010). "The molecular mediators of type 2 epithelial to mesenchymal transition (EMT) and their role in renal pathophysiology." Expert Rev Mol Med **12**: e17.
Caricasole, A., A. Duarte, S. H. Larsson, N. D. Hastie, M. Little, G. Holmes, I. Todorov and A. Ward (1996). "RNA binding by the Wilms tumor suppressor zinc finger proteins." Proc Natl Acad Sci U S A **93**(15): 7562-7566.
Carlen, M., K. Meletis, F. Barnabe-Heider and J. Frisen (2006). "Genetic visualization of neurogenesis." Exp Cell Res **312**(15): 2851-2859.
Carroll, T. J., J. S. Park, S. Hayashi, A. Majumdar and A. P. McMahon (2005). "Wnt9b plays a central role in the regulation of mesenchymal to epithelial transitions underlying organogenesis of the mammalian urogenital system." Dev Cell **9**(2): 283-292.
Chau, Y. Y., D. Brownstein, H. Mjoseng, W. C. Lee, N. Buza-Vidas, C. Nerlov, S. E. Jacobsen, P. Perry, R. Berry, A. Thornburn, D. Sexton, N. Morton, P. Hohenstein, E. Freyer, K. Samuel, R. van't Hof and N. Hastie (2011). "Acute multiple organ failure in adult mice deleted for the developmental regulator Wt1." PLoS Genet **7**(12): e1002404.
Chau, Y. Y. and N. D. Hastie (2012). "The role of Wt1 in regulating mesenchyme in cancer, development, and tissue homeostasis." Trends Genet **28**(10): 515-524.
Cheng, H., X. Fan, G. W. Moeckel and R. C. Harris (2011). "Podocyte COX-2 exacerbates diabetic nephropathy by increasing podocyte (pro)renin receptor expression." J Am Soc Nephrol **22**(7): 1240-1251.
Chernin, G., V. Vega-Warner, D. S. Schoeb, S. F. Heeringa, B. Ovunc, P. Saisawat, R. Cleper, F. Ozaltin, F. Hildebrandt and G. P. N. S. G. Members of the (2010). "Genotype/phenotype correlation in nephrotic syndrome caused by WT1 mutations." Clin J Am Soc Nephrol **5**(9): 1655-1662.
Chittiprol, S., P. Chen, D. Petrovic-Djergovic, T. Eichler and R. F. Ransom (2011). "Marker expression, behaviors, and responses vary in different lines of conditionally immortalized cultured podocytes." Am J Physiol Renal Physiol **301**(3): F660-671.
Cho, A., N. Haruyama and A. B. Kulkarni (2009). "Generation of transgenic mice." Curr Protoc Cell Biol **Chapter 19**: Unit 19 11.
Cilloni, D., E. Gottardi, F. Messa, M. Fava, P. Scaravaglio, M. Bertini, M. Girotto, C. Marinone, D. Ferrero, A. Gallamini, A. Levis and G. Saglio (2003). "Significant correlation between the degree

of WT1 expression and the International Prognostic Scoring System Score in patients with myelodysplastic syndromes." J Clin Oncol **21**(10): 1988-1995.
Citri, A., Z. P. Pang, T. C. Sudhof, M. Wernig and R. C. Malenka (2012). "Comprehensive qPCR profiling of gene expression in single neuronal cells." Nat Protoc **7**(1): 118-127.
Cockrell, A. S., H. Ma, K. Fu, T. J. McCown and T. Kafri (2006). "A trans-lentiviral packaging cell line for high-titer conditional self-inactivating HIV-1 vectors." Mol Ther **14**(2): 276-284.
Copeland, N. G., N. A. Jenkins and D. L. Court (2001). "Recombineering: a powerful new tool for mouse functional genomics." Nat Rev Genet **2**(10): 769-779.
Coppes-Zantinga, A. R. and M. J. Coppes (1999). "The eponym "Wilms": a reminder of a surgeon's lifelong contributions to medicine." Med Pediatr Oncol **32**(6): 438-439.
Coresh, J., B. C. Astor, T. Greene, G. Eknoyan and A. S. Levey (2003). "Prevalence of chronic kidney disease and decreased kidney function in the adult US population: Third National Health and Nutrition Examination Survey." Am J Kidney Dis **41**(1): 1-12.
Dahan, K., M. Kamal, L. H. Noel, C. Jeanpierre, M. C. Gubler, N. Brousse and N. P. Mariaud de Serre (2007). "Small glomeruli in WAGR (Wilms Tumor, Aniridia, Genitourinary Anomalies and Mental Retardation) syndrome." Am J Kidney Dis **49**(6): 793-800.
Dai, C., D. B. Stolz, L. P. Kiss, S. P. Monga, L. B. Holzman and Y. Liu (2009). "Wnt/beta-catenin signaling promotes podocyte dysfunction and albuminuria." J Am Soc Nephrol **20**(9): 1997-2008.
Davidson, G., R. Dono and R. Zeller (2001). "FGF signalling is required for differentiation-induced cytoskeletal reorganisation and formation of actin-based processes by podocytes." J Cell Sci **114**(Pt 18): 3359-3366.
Davies, J. A., M. Ladomery, P. Hohenstein, L. Michael, A. Shafe, L. Spraggon and N. Hastie (2004). "Development of an siRNA-based method for repressing specific genes in renal organ culture and its use to show that the Wt1 tumour suppressor is required for nephron differentiation." Hum Mol Genet **13**(2): 235-246.
Davies, R. C., C. Calvio, E. Bratt, S. H. Larsson, A. I. Lamond and N. D. Hastie (1998). "WT1 interacts with the splicing factor U2AF65 in an isoform-dependent manner and can be incorporated into spliceosomes." Genes Dev **12**(20): 3217-3225.
Diep, C. Q., D. Ma, R. C. Deo, T. M. Holm, R. W. Naylor, N. Arora, R. A. Wingert, F. Bollig, G. Djordjevic, B. Lichman, H. Zhu, T. Ikenaga, F. Ono, C. Englert, C. A. Cowan, N. A. Hukriede, R. I. Handin and A. J. Davidson (2011). "Identification of adult nephron progenitors capable of kidney regeneration in zebrafish." Nature **470**(7332): 95-100.
Dolt, K. S., M. L. Lawrence, E. Miller-Hodges, J. Slight, A. Thornburn, P. S. Devenney and P. Hohenstein (2013). "A Universal Vector for High-Efficiency Multi-Fragment Recombineering of BACs and Knock-In Constructs." PLoS One **8**(4): e62054.
Donadelli, R., C. Zanchi, M. Morigi, S. Buelli, C. Batani, S. Tomasoni, D. Corna, D. Rottoli, A. Benigni, M. Abbate, G. Remuzzi and C. Zoja (2003). "Protein overload induces fractalkine upregulation in proximal tubular cells through nuclear factor kappaB- and p38 mitogen-activated protein kinase-dependent pathways." J Am Soc Nephrol **14**(10): 2436-2446.
Drossopoulou, G. I., N. E. Tsotakos and E. C. Tsilibary (2009). "Impaired transcription factor interplay in addition to advanced glycation end products suppress podocalyxin expression in high glucose-treated human podocytes." Am J Physiol Renal Physiol **297**(3): F594-603.
Dudnakova, T., L. Spraggon, J. Slight and N. Hastie (2010). "Actin: a novel interaction partner of WT1 influencing its cell dynamic properties." Oncogene **29**(7): 1085-1092.

Eremina, V., M. A. Wong, S. Cui, L. Schwartz and S. E. Quaggin (2002). "Glomerular-specific gene excision in vivo." J Am Soc Nephrol **13**(3): 788-793.
Erkan, E., P. Devarajan and G. J. Schwartz (2005). "Apoptotic response to albumin overload: proximal vs. distal/collecting tubule cells." Am J Nephrol **25**(2): 121-131.
Faul, C., M. Donnelly, S. Merscher-Gomez, Y. H. Chang, S. Franz, J. Delfgaauw, J. M. Chang, H. Y. Choi, K. N. Campbell, K. Kim, J. Reiser and P. Mundel (2008). "The actin cytoskeleton of kidney podocytes is a direct target of the antiproteinuric effect of cyclosporine A." Nat Med **14**(9): 931-938.
Fischbach, B. V., K. L. Trout, J. Lewis, C. A. Luis and M. Sika (2005). "WAGR syndrome: a clinical review of 54 cases." Pediatrics **116**(4): 984-988.
Fuchshofer, R., S. Ullmann, L. F. Zeilbeck, M. Baumann, B. Junglas and E. R. Tamm (2011). "Connective tissue growth factor modulates podocyte actin cytoskeleton and extracellular matrix synthesis and is induced in podocytes upon injury." Histochem Cell Biol **136**(3): 301-319.
Fukuda, A., L. T. Wickman, M. P. Venkatareddy, Y. Sato, M. A. Chowdhury, S. Q. Wang, K. A. Shedden, R. C. Dysko, J. E. Wiggins and R. C. Wiggins (2012). "Angiotensin II-dependent persistent podocyte loss from destabilized glomeruli causes progression of end stage kidney disease." Kidney Int **81**(1): 40-55.
Gao, F., S. Maiti, G. Sun, N. G. Ordonez, M. Udtha, J. M. Deng, R. R. Behringer and V. Huff (2004). "The Wt1+/R394W mouse displays glomerulosclerosis and early-onset renal failure characteristic of human Denys-Drash syndrome." Mol Cell Biol **24**(22): 9899-9910.
Gao, S. Y., C. Y. Li, T. Shimokawa, T. Terashita, S. Matsuda, E. Yaoita and N. Kobayashi (2007). "Rho-family small GTPases are involved in forskolin-induced cell-cell contact formation of renal glomerular podocytes in vitro." Cell Tissue Res **328**(2): 391-400.
Greka, A. and P. Mundel "Cell biology and pathology of podocytes." Annu Rev Physiol **74**: 299-323.
Greka, A. and P. Mundel (2012). "Cell biology and pathology of podocytes." Annu Rev Physiol **74**: 299-323.
Guo, J. K., A. Marlier, H. Shi, A. Shan, T. A. Ardito, Z. P. Du, M. Kashgarian, D. S. Krause, D. Biemesderfer and L. G. Cantley (2012). "Increased tubular proliferation as an adaptive response to glomerular albuminuria." J Am Soc Nephrol **23**(3): 429-437.
Guo, J. K., A. L. Menke, M. C. Gubler, A. R. Clarke, D. Harrison, A. Hammes, N. D. Hastie and A. Schedl (2002). "WT1 is a key regulator of podocyte function: reduced expression levels cause crescentic glomerulonephritis and mesangial sclerosis." Hum Mol Genet **11**(6): 651-659.
Haber, D. A., A. J. Buckler, T. Glaser, K. M. Call, J. Pelletier, R. L. Sohn, E. C. Douglass and D. E. Housman (1990). "An internal deletion within an 11p13 zinc finger gene contributes to the development of Wilms' tumor." Cell **61**(7): 1257-1269.
Hahn, H., Y. M. Cho, Y. S. Park, H. W. You and H. I. Cheong (2006). "Two cases of isolated diffuse mesangial sclerosis with WT1 mutations." J Korean Med Sci **21**(1): 160-164.
Halbesma, N., D. S. Kuiken, A. H. Brantsma, S. J. Bakker, J. F. Wetzels, D. De Zeeuw, P. E. De Jong and R. T. Gansevoort (2006). "Macroalbuminuria is a better risk marker than low estimated GFR to identify individuals at risk for accelerated GFR loss in population screening." J Am Soc Nephrol **17**(9): 2582-2590.
Hamer, R. A. and A. M. El Nahas (2006). "The burden of chronic kidney disease." BMJ **332**(7541): 563-564.

Hammes, A., J. K. Guo, G. Lutsch, J. R. Leheste, D. Landrock, U. Ziegler, M. C. Gubler and A. Schedl (2001). "Two splice variants of the Wilms' tumor 1 gene have distinct functions during sex determination and nephron formation." Cell **106**(3): 319-329.
Hanson, J., J. Gorman, J. Reese and G. Fraizer (2007). "Regulation of vascular endothelial growth factor, VEGF, gene promoter by the tumor suppressor, WT1." Front Biosci **12**: 2279-2290.
Hastie, N. D. (2001). "Life, sex, and WT1 isoforms--three amino acids can make all the difference." Cell **106**(4): 391-394.
Hawkins, P. (2002). "Recognizing and assessing pain, suffering and distress in laboratory animals: a survey of current practice in the UK with recommendations." Lab Anim **36**(4): 378-395.
Hayashi, S. and A. P. McMahon (2002). "Efficient recombination in diverse tissues by a tamoxifen-inducible form of Cre: a tool for temporally regulated gene activation/inactivation in the mouse." Dev Biol **244**(2): 305-318.
He, W., C. Dai, Y. Li, G. Zeng, S. P. Monga and Y. Liu (2009). "Wnt/beta-catenin signaling promotes renal interstitial fibrosis." J Am Soc Nephrol **20**(4): 765-776.
He, W., Y. S. Kang, C. Dai and Y. Liu (2011). "Blockade of Wnt/beta-catenin signaling by paricalcitol ameliorates proteinuria and kidney injury." J Am Soc Nephrol **22**(1): 90-103.
Heid, C. A., J. Stevens, K. J. Livak and P. M. Williams (1996). "Real time quantitative PCR." Genome Res **6**(10): 986-994.
Henao, D. E., A. P. Cadavid and M. A. Saleem (2013). "Exogenous vascular endothelial growth factor supplementation can restore the podocyte barrier-forming capacity disrupted by sera of preeclamptic women." J Obstet Gynaecol Res **39**(1): 46-52.
Herman-Edelstein, M., M. C. Thomas, V. Thallas-Bonke, M. Saleem, M. E. Cooper and P. Kantharidis (2011). "Dedifferentiation of immortalized human podocytes in response to transforming growth factor-beta: a model for diabetic podocytopathy." Diabetes **60**(6): 1779-1788.
Higashi, A. Y., T. Ikawa, M. Muramatsu, A. N. Economides, A. Niwa, T. Okuda, A. J. Murphy, J. Rojas, T. Heike, T. Nakahata, H. Kawamoto, T. Kita and M. Yanagita (2009). "Direct hematological toxicity and illegitimate chromosomal recombination caused by the systemic activation of CreERT2." J Immunol **182**(9): 5633-5640.
Hirschberg, R., S. Wang and G. M. Mitu (2008). "Functional symbiosis between endothelium and epithelial cells in glomeruli." Cell Tissue Res **331**(2): 485-493.
Hohenstein, P. and N. D. Hastie (2006). "The many facets of the Wilms' tumour gene, WT1." Hum Mol Genet **15 Spec No 2**: R196-201.
Holthofer, H., A. Miettinen, V. P. Lehto, E. Lehtonen and I. Virtanen (1984). "Expression of vimentin and cytokeratin types of intermediate filament proteins in developing and adult human kidneys." Lab Invest **50**(5): 552-559.
Hosen, N., T. Shirakata, S. Nishida, M. Yanagihara, A. Tsuboi, M. Kawakami, Y. Oji, Y. Oka, M. Okabe, B. Tan, H. Sugiyama and I. L. Weissman (2007). "The Wilms' tumor gene WT1-GFP knock-in mouse reveals the dynamic regulation of WT1 expression in normal and leukemic hematopoiesis." Leukemia **21**(8): 1783-1791.
Hostetter, T. H., J. L. Olson, H. G. Rennke, M. A. Venkatachalam and B. M. Brenner (1981). "Hyperfiltration in remnant nephrons: a potentially adverse response to renal ablation." Am J Physiol **241**(1): F85-93.

Hsu, H. H., S. Hoffmann, N. Endlich, A. Velic, A. Schwab, T. Weide, E. Schlatter and H. Pavenstadt (2008). "Mechanisms of angiotensin II signaling on cytoskeleton of podocytes." J Mol Med (Berl) **86**(12): 1379-1394.
Humphreys, B. D., S. L. Lin, A. Kobayashi, T. E. Hudson, B. T. Nowlin, J. V. Bonventre, M. T. Valerius, A. P. McMahon and J. S. Duffield (2010). "Fate tracing reveals the pericyte and not epithelial origin of myofibroblasts in kidney fibrosis." Am J Pathol **176**(1): 85-97.
Iijima, K., T. Someya, S. Ito, K. Nozu, K. Nakanishi, K. Matsuoka, H. Ohashi, M. Nagata, K. Kamei and S. Sasaki (2012). "Focal segmental glomerulosclerosis in patients with complete deletion of one WT1 allele." Pediatrics **129**(6): e1621-1625.
Ijpenberg, A., J. M. Perez-Pomares, J. A. Guadix, R. Carmona, V. Portillo-Sanchez, D. Macias, P. Hohenstein, C. M. Miles, N. D. Hastie and R. Munoz-Chapuli (2007). "Wt1 and retinoic acid signaling are essential for stellate cell development and liver morphogenesis." Dev Biol **312**(1): 157-170.
Inokuchi, S., I. Shirato, N. Kobayashi, H. Koide, Y. Tomino and T. Sakai (1996). "Re-evaluation of foot process effacement in acute puromycin aminonucleoside nephrosis." Kidney Int **50**(4): 1278-1287.
Ivanova, L., M. J. Butt and D. G. Matsell (2008). "Mesenchymal transition in kidney collecting duct epithelial cells." Am J Physiol Renal Physiol **294**(5): F1238-1248.
Jat, P. S., M. D. Noble, P. Ataliotis, Y. Tanaka, N. Yannoutsos, L. Larsen and D. Kioussis (1991). "Direct derivation of conditionally immortal cell lines from an H-2Kb-tsA58 transgenic mouse." Proc Natl Acad Sci U S A **88**(12): 5096-5100.
Jeanpierre, C., E. Denamur, I. Henry, M. O. Cabanis, S. Luce, A. Cecille, J. Elion, M. Peuchmaur, C. Loirat, P. Niaudet, M. C. Gubler and C. Junien (1998). "Identification of constitutional WT1 mutations, in patients with isolated diffuse mesangial sclerosis, and analysis of genotype/phenotype correlations by use of a computerized mutation database." Am J Hum Genet **62**(4): 824-833.
Juhila, J., R. Roozendaal, M. Lassila, S. J. Verbeek and H. Holthofer (2006). "Podocyte cell-specific expression of doxycycline inducible Cre recombinase in mice." J Am Soc Nephrol **17**(3): 648-654.
Kabgani, N., T. Grigoleit, K. Schulte, A. Sechi, S. Sauer-Lehnen, C. Tag, P. Boor, C. Kuppe, G. Warsow, S. Schordan, J. Mostertz, R. K. Chilukoti, G. Homuth, N. Endlich, F. Tacke, R. Weiskirchen, G. Fuellen, K. Endlich, J. Floege, B. Smeets and M. J. Moeller (2012). "Primary cultures of glomerular parietal epithelial cells or podocytes with proven origin." PLoS One **7**(4): e34907.
Kalluri, R. and R. A. Weinberg (2009). "The basics of epithelial-mesenchymal transition." J Clin Invest **119**(6): 1420-1428.
Karner, C. M., A. Das, Z. Ma, M. Self, C. Chen, L. Lum, G. Oliver and T. J. Carroll (2011). "Canonical Wnt9b signaling balances progenitor cell expansion and differentiation during kidney development." Development **138**(7): 1247-1257.
Kato, T., S. Mizuno and M. Kamimoto (2010). "The decreases of nephrin and nuclear WT1 in podocytes may cause albuminuria during the experimental sepsis in mice." Biomed Res **31**(6): 363-369.
Kerr, M., B. Bray, J. Medcalf, D. J. O'Donoghue and B. Matthews (2012). "Estimating the financial cost of chronic kidney disease to the NHS in England." Nephrol Dial Transplant **27 Suppl 3**: iii73-80.

Kestila, M., U. Lenkkeri, M. Mannikko, J. Lamerdin, P. McCready, H. Putaala, V. Ruotsalainen, T. Morita, M. Nissinen, R. Herva, C. E. Kashtan, L. Peltonen, C. Holmberg, A. Olsen and K. Tryggvason (1998). "Positionally cloned gene for a novel glomerular protein--nephrin--is mutated in congenital nephrotic syndrome." Mol Cell **1**(4): 575-582.
Kirik, O. V. and D. E. Korzhevskii (2009). "Expression of neural stem cell marker nestin in the kidney of rats and humans." Bull Exp Biol Med **147**(4): 539-541.
Kispert, A., S. Vainio and A. P. McMahon (1998). "Wnt-4 is a mesenchymal signal for epithelial transformation of metanephric mesenchyme in the developing kidney." Development **125**(21): 4225-4234.
Kobayashi, A., M. T. Valerius, J. W. Mugford, T. J. Carroll, M. Self, G. Oliver and A. P. McMahon (2008). "Six2 defines and regulates a multipotent self-renewing nephron progenitor population throughout mammalian kidney development." Cell Stem Cell **3**(2): 169-181.
Kohsaka, T., M. Tagawa, Y. Takekoshi, H. Yanagisawa, K. Tadokoro and M. Yamada (1999). "Exon 9 mutations in the WT1 gene, without influencing KTS splice isoforms, are also responsible for Frasier syndrome." Hum Mutat **14**(6): 466-470.
Kreidberg, J. A., H. Sariola, J. M. Loring, M. Maeda, J. Pelletier, D. Housman and R. Jaenisch (1993). "WT-1 is required for early kidney development." Cell **74**(4): 679-691.
Kretzler, M., V. P. Teixeira, P. G. Unschuld, C. D. Cohen, R. Wanke, I. Edenhofer, P. Mundel, D. Schlondorff and H. Holthofer (2001). "Integrin-linked kinase as a candidate downstream effector in proteinuria." FASEB J **15**(10): 1843-1845.
Kretzschmar, K. and F. M. Watt (2012). "Lineage tracing." Cell **148**(1-2): 33-45.
Kriz, W., B. Kaissling and M. Le Hir (2011). "Epithelial-mesenchymal transition (EMT) in kidney fibrosis: fact or fantasy?" J Clin Invest **121**(2): 468-474.
Kriz, W. and M. LeHir (2005). "Pathways to nephron loss starting from glomerular diseases-insights from animal models." Kidney Int **67**(2): 404-419.
Ladomery, M. R., J. Slight, S. Mc Ghee and N. D. Hastie (1999). "Presence of WT1, the Wilm's tumor suppressor gene product, in nuclear poly(A)(+) ribonucleoprotein." J Biol Chem **274**(51): 36520-36526.
Lahdenkari, A. T., K. Lounatmaa, J. Patrakka, C. Holmberg, J. Wartiovaara, M. Kestila, O. Koskimies and H. Jalanko (2004). "Podocytes are firmly attached to glomerular basement membrane in kidneys with heavy proteinuria." J Am Soc Nephrol **15**(10): 2611-2618.
Larsson, S. H., J. P. Charlieu, K. Miyagawa, D. Engelkamp, M. Rassoulzadegan, A. Ross, F. Cuzin, V. van Heyningen and N. D. Hastie (1995). "Subnuclear localization of WT1 in splicing or transcription factor domains is regulated by alternative splicing." Cell **81**(3): 391-401.
Lee, D. L., R. C. Webb and M. W. Brands (2004). "Sympathetic and angiotensin-dependent hypertension during cage-switch stress in mice." Am J Physiol Regul Integr Comp Physiol **287**(6): R1394-1398.
Lee, S. B. and D. A. Haber (2001). "Wilms tumor and the WT1 gene." Exp Cell Res **264**(1): 74-99.
Lemley, K. V., R. A. Lafayette, M. Safai, G. Derby, K. Blouch, A. Squarer and B. D. Myers (2002). "Podocytopenia and disease severity in IgA nephropathy." Kidney Int **61**(4): 1475-1485.
Li, A., Y. Ma, X. Yu, R. L. Mort, C. R. Lindsay, D. Stevenson, D. Strathdee, R. H. Insall, J. Chernoff, S. B. Snapper, I. J. Jackson, L. Larue, O. J. Sansom and L. M. Machesky (2011). "Rac1 drives melanoblast organization during mouse development by orchestrating pseudopod- driven motility and cell-cycle progression." Dev Cell **21**(4): 722-734.

Li, C. M., C. E. Kim, A. A. Margolin, M. Guo, J. Zhu, J. M. Mason, T. W. Hensle, V. V. Murty, P. E. Grundy, E. R. Fearon, V. D'Agati, J. D. Licht and B. Tycko (2004). "CTNNB1 mutations and overexpression of Wnt/beta-catenin target genes in WT1-mutant Wilms' tumors." Am J Pathol **165**(6): 1943-1953.
Li, Y., Y. S. Kang, C. Dai, L. P. Kiss, X. Wen and Y. Liu (2008). "Epithelial-to-mesenchymal transition is a potential pathway leading to podocyte dysfunction and proteinuria." Am J Pathol **172**(2): 299-308.
Li, Y., J. Wang and K. Asahina (2013). "Mesothelial cells give rise to hepatic stellate cells and myofibroblasts via mesothelial-mesenchymal transition in liver injury." Proc Natl Acad Sci U S A **110**(6): 2324-2329.
Lipska, B. S., B. Ranchin, P. Iatropoulos, J. Gellermann, A. Melk, F. Ozaltin, G. Caridi, T. Seeman, K. Tory, A. Jankauskiene, A. Zurowska, M. Szczepanska, A. Wasilewska, J. Harambat, A. Trautmann, A. Peco-Antic, H. Borzecka, A. Moczulska, B. Saeed, R. Bogdanovic, M. Kalyoncu, E. Simkova, O. Erdogan, K. Vrljicak, A. Teixeira, M. Azocar, F. Schaefer, C. the PodoNet, M. Azocar, L. M. Higuita, B. Ranchin, M. Fischbach, T. Davitaia, J. Gellermann, J. Oh, A. Melk, F. Schaefer, M. Wigger, N. Printza, P. Sallay, A. Gheissari, M. Noris, A. Pasini, G. Marco Ghiggeri, G. Ardissino, E. Benetti, F. Emma, B. Aoun, P. Abou-Jaoude, A. Jankauskiene, A. Wasilewska, E. Gacka, A. Zurowska, D. Drozdz, M. Tkaczyk, H. Borzecka, M. Silska, T. Jarmolinski, A. Firszt-Adamczyk, J. Ksiazek, E. Kuzma-Mroczkowska, A. Medynska, M. Szczepanska, A. Caldas Afonso, H. Jardim, R. Bogdanovic, R. T. Krmar, G. D. Simonetti, B. Saeed, A. Anarat, A. Balat, Z. E. Baskin, N. Cakar, O. Erdogan, B. Ozcakar, F. Ozaltin, O. Sakallioglu, O. Soylemezoglu, S. Akman, F. Gok, S. Caliskan, C. Candan, S. Emre, S. Mir, I. Akil, P. Ertan, O. Ozkaya, M. Kalyoncu, E. Simkova, E. Alhammadi and R. Sobko (2014). "Genotype-phenotype associations in WT1 glomerulopathy." Kidney Int.
Little, M., G. Holmes, W. Bickmore, V. van Heyningen, N. Hastie and B. Wainwright (1995). "DNA binding capacity of the WT1 protein is abolished by Denys-Drash syndrome WT1 point mutations." Hum Mol Genet **4**(3): 351-358.
Little, M. and C. Wells (1997). "A clinical overview of WT1 gene mutations." Hum Mutat **9**(3): 209-225.
Little, M. H., K. A. Williamson, M. Mannens, A. Kelsey, C. Gosden, N. D. Hastie and V. van Heyningen (1993). "Evidence that WT1 mutations in Denys-Drash syndrome patients may act in a dominant-negative fashion." Hum Mol Genet **2**(3): 259-264.
Liu, Y. "New insights into epithelial-mesenchymal transition in kidney fibrosis." J Am Soc Nephrol **21**(2): 212-222.
Liu, Y. (2010). "New insights into epithelial-mesenchymal transition in kidney fibrosis." J Am Soc Nephrol **21**(2): 212-222.
Loo, C. K., T. N. Pereira and G. A. Ramm (2012). "Abnormal WT1 expression in human fetuses with bilateral renal agenesis and cardiac malformations." Birth Defects Res A Clin Mol Teratol **94**(2): 116-122.
Loonstra, A., M. Vooijs, H. B. Beverloo, B. A. Allak, E. van Drunen, R. Kanaar, A. Berns and J. Jonkers (2001). "Growth inhibition and DNA damage induced by Cre recombinase in mammalian cells." Proc Natl Acad Sci U S A **98**(16): 9209-9214.
Macary, G., J. Rossert, P. Bruneval, C. Mandet, M. F. Belair, P. Houillier and J. P. Duong Van Huyen (2010). "Transgenic mice expressing nitroreductase gene under the control of the

podocin promoter: a new murine model of inductible glomerular injury." Virchows Arch **456**(3): 325-337.
Macconi, D., F. Sangalli, M. Bonomelli, S. Conti, L. Condorelli, E. Gagliardini, G. Remuzzi and A. Remuzzi (2009). "Podocyte repopulation contributes to regression of glomerular injury induced by ACE inhibition." Am J Pathol **174**(3): 797-807.
Machuca, E., G. Benoit, F. Nevo, M. J. Tete, O. Gribouval, A. Pawtowski, P. Brandstrom, C. Loirat, P. Niaudet, M. C. Gubler and C. Antignac (2010). "Genotype-phenotype correlations in non-Finnish congenital nephrotic syndrome." J Am Soc Nephrol **21**(7): 1209-1217.
Mao, X., Y. Fujiwara and S. H. Orkin (1999). "Improved reporter strain for monitoring Cre recombinase-mediated DNA excisions in mice." Proc Natl Acad Sci U S A **96**(9): 5037-5042.
Martinez-Estrada, O. M., L. A. Lettice, A. Essafi, J. A. Guadix, J. Slight, V. Velecela, E. Hall, J. Reichmann, P. S. Devenney, P. Hohenstein, N. Hosen, R. E. Hill, R. Munoz-Chapuli and N. D. Hastie (2010). "Wt1 is required for cardiovascular progenitor cell formation through transcriptional control of Snail and E-cadherin." Nat Genet **42**(1): 89-93.
Matsusaka, T., E. Sandgren, A. Shintani, V. Kon, I. Pastan, A. B. Fogo and I. Ichikawa (2011). "Podocyte injury damages other podocytes." J Am Soc Nephrol **22**(7): 1275-1285.
McCarty, G., O. Awad and D. M. Loeb (2011). "WT1 protein directly regulates expression of vascular endothelial growth factor and is a mediator of tumor response to hypoxia." J Biol Chem **286**(51): 43634-43643.
McKenzie, L. M., S. L. Hendrickson, W. A. Briggs, R. A. Dart, S. M. Korbet, M. H. Mokrzycki, P. L. Kimmel, T. S. Ahuja, J. S. Berns, E. E. Simon, M. C. Smith, H. Trachtman, D. M. Michel, J. R. Schelling, M. Cho, Y. C. Zhou, E. Binns-Roemer, G. D. Kirk, J. B. Kopp and C. A. Winkler (2007). "NPHS2 variation in sporadic focal segmental glomerulosclerosis." J Am Soc Nephrol **18**(11): 2987-2995.
McMahon, A. P., B. J. Aronow, D. R. Davidson, J. A. Davies, K. W. Gaido, S. Grimmond, J. L. Lessard, M. H. Little, S. S. Potter, E. L. Wilder and P. Zhang (2008). "GUDMAP: the genitourinary developmental molecular anatomy project." J Am Soc Nephrol **19**(4): 667-671.
Megremis, S., A. Mitsioni, I. Fylaktou, S. K. Tzeli, F. Komianou, C. J. Stefanidis, E. Kanavakis and J. Traeger-Synodinos "Broad and unexpected phenotypic expression in Greek children with steroid-resistant nephrotic syndrome due to mutations in the Wilms' tumor 1 (WT1) gene." Eur J Pediatr **170**(12): 1529-1534.
Meletis, K., F. Barnabe-Heider, M. Carlen, E. Evergren, N. Tomilin, O. Shupliakov and J. Frisen (2008). "Spinal cord injury reveals multilineage differentiation of ependymal cells." PLoS Biol **6**(7): e182.
Menke, A. L., I. J. A, S. Fleming, A. Ross, C. N. Medine, C. E. Patek, L. Spraggon, J. Hughes, A. R. Clarke and N. D. Hastie (2003). "The wt1-heterozygous mouse; a model to study the development of glomerular sclerosis." J Pathol **200**(5): 667-674.
Merkel, C. E., C. M. Karner and T. J. Carroll (2007). "Molecular regulation of kidney development: is the answer blowing in the Wnt?" Pediatr Nephrol **22**(11): 1825-1838.
Miller-Hodges, E. and P. Hohenstein (2012). "WT1 in disease: shifting the epithelial-mesenchymal balance." J Pathol **226**(2): 229-240.
Moeller, M. J. (2010). "Glomerular scarring: can we delay or even reverse glomerulosclerosis by RAAS inhibition?" Nephrol Dial Transplant **25**(7): 2101-2103.

Moeller, M. J., A. Soofi, I. Hartmann, M. Le Hir, R. Wiggins, W. Kriz and L. B. Holzman (2004). "Podocytes populate cellular crescents in a murine model of inflammatory glomerulonephritis." J Am Soc Nephrol **15**(1): 61-67.
Moffett, P., W. Bruening, H. Nakagama, N. Bardeesy, D. Housman, D. E. Housman and J. Pelletier (1995). "Antagonism of WT1 activity by protein self-association." Proc Natl Acad Sci U S A **92**(24): 11105-11109.
Mohseni, P., H. K. Sung, A. J. Murphy, C. L. Laliberte, H. M. Pallari, M. Henkelman, J. Georgiou, G. Xie, S. E. Quaggin, P. S. Thorner, J. E. Eriksson and A. Nagy (2011). "Nestin is not essential for development of the CNS but required for dispersion of acetylcholine receptor clusters at the area of neuromuscular junctions." J Neurosci **31**(32): 11547-11552.
Mollet, G., J. Ratelade, O. Boyer, A. O. Muda, L. Morisset, T. A. Lavin, D. Kitzis, M. J. Dallman, L. Bugeon, N. Hubner, M. C. Gubler, C. Antignac and E. L. Esquivel (2009). "Podocin inactivation in mature kidneys causes focal segmental glomerulosclerosis and nephrotic syndrome." J Am Soc Nephrol **20**(10): 2181-2189.
Morrison, A. A., R. L. Viney, M. A. Saleem and M. R. Ladomery (2008). "New insights into the function of the Wilms tumor suppressor gene WT1 in podocytes." Am J Physiol Renal Physiol **295**(1): F12-17.
Mundlos, S., J. Pelletier, A. Darveau, M. Bachmann, A. Winterpacht and B. Zabel (1993). "Nuclear localization of the protein encoded by the Wilms' tumor gene WT1 in embryonic and adult tissues." Development **119**(4): 1329-1341.
Natoli, T. A., A. McDonald, J. A. Alberta, M. E. Taglienti, D. E. Housman and J. A. Kreidberg (2002). "A Mammal-Specific Exon of WT1 Is Not Required for Development or Fertility." Molecular and Cellular Biology **22**(12): 4433-4438.
Niaudet, P. and M. C. Gubler (2006). "WT1 and glomerular diseases." Pediatr Nephrol **21**(11): 1653-1660.
Niksic, M., J. Slight, J. R. Sanford, J. F. Caceres and N. D. Hastie (2004). "The Wilms' tumour protein (WT1) shuttles between nucleus and cytoplasm and is present in functional polysomes." Hum Mol Genet **13**(4): 463-471.
O'Hare, M. J., J. Bond, C. Clarke, Y. Takeuchi, A. J. Atherton, C. Berry, J. Moody, A. R. Silver, D. C. Davies, A. E. Alsop, A. M. Neville and P. S. Jat (2001). "Conditional immortalization of freshly isolated human mammary fibroblasts and endothelial cells." Proc Natl Acad Sci U S A **98**(2): 646-651.
Ohse, T., R. Inagi, T. Tanaka, T. Ota, T. Miyata, I. Kojima, J. R. Ingelfinger, S. Ogawa, T. Fujita and M. Nangaku (2006). "Albumin induces endoplasmic reticulum stress and apoptosis in renal proximal tubular cells." Kidney Int **70**(8): 1447-1455.
Ohse, T., J. W. Pippin, A. M. Chang, R. D. Krofft, J. H. Miner, M. R. Vaughan and S. J. Shankland (2009). "The enigmatic parietal epithelial cell is finally getting noticed: a review." Kidney Int **76**(12): 1225-1238.
Ohse, T., J. W. Pippin, M. R. Vaughan, P. T. Brinkkoetter, R. D. Krofft and S. J. Shankland (2008). "Establishment of conditionally immortalized mouse glomerular parietal epithelial cells in culture." J Am Soc Nephrol **19**(10): 1879-1890.
Ohse, T., M. R. Vaughan, J. B. Kopp, R. D. Krofft, C. B. Marshall, A. M. Chang, K. L. Hudkins, C. E. Alpers, J. W. Pippin and S. J. Shankland (2010). "De novo expression of podocyte proteins in parietal epithelial cells during experimental glomerular disease." Am J Physiol Renal Physiol **298**(3): F702-711.

Pagtalunan, M. E., P. L. Miller, S. Jumping-Eagle, R. G. Nelson, B. D. Myers, H. G. Rennke, N. S. Coplon, L. Sun and T. W. Meyer (1997). "Podocyte loss and progressive glomerular injury in type II diabetes." J Clin Invest **99**(2): 342-348.
Palmer, R. E., A. Kotsianti, B. Cadman, T. Boyd, W. Gerald and D. A. Haber (2001). "WT1 regulates the expression of the major glomerular podocyte membrane protein Podocalyxin." Curr Biol **11**(22): 1805-1809.
Park, S., A. Bernard, K. E. Bove, D. A. Sens, D. J. Hazen-Martin, A. J. Garvin and D. A. Haber (1993). "Inactivation of WT1 in nephrogenic rests, genetic precursors to Wilms' tumour." Nat Genet **5**(4): 363-367.
Patek, C. E., S. Fleming, C. G. Miles, C. O. Bellamy, M. Ladomery, L. Spraggon, J. Mullins, N. D. Hastie and M. L. Hooper (2003). "Murine Denys-Drash syndrome: evidence of podocyte de-differentiation and systemic mediation of glomerulosclerosis." Hum Mol Genet **12**(18): 2379-2394.
Patek, C. E., M. H. Little, S. Fleming, C. Miles, J. P. Charlieu, A. R. Clarke, K. Miyagawa, S. Christie, J. Doig, D. J. Harrison, D. J. Porteous, A. J. Brookes, M. L. Hooper and N. D. Hastie (1999). "A zinc finger truncation of murine WT1 results in the characteristic urogenital abnormalities of Denys-Drash syndrome." Proc Natl Acad Sci U S A **96**(6): 2931-2936.
Patrakka, J., A. T. Lahdenkari, O. Koskimies, C. Holmberg, J. Wartiovaara and H. Jalanko (2002). "The number of podocyte slit diaphragms is decreased in minimal change nephrotic syndrome." Pediatr Res **52**(3): 349-355.
Pelletier, J., M. Schalling, A. J. Buckler, A. Rogers, D. A. Haber and D. Housman (1991). "Expression of the Wilms' tumor gene WT1 in the murine urogenital system." Genes Dev **5**(8): 1345-1356.
Peti-Peterdi, J. and A. Sipos (2010). "A high-powered view of the filtration barrier." J Am Soc Nephrol **21**(11): 1835-1841.
Philippe, A., S. Weber, E. L. Esquivel, C. Houbron, G. Hamard, J. Ratelade, W. Kriz, F. Schaefer, M. C. Gubler and C. Antignac (2008). "A missense mutation in podocin leads to early and severe renal disease in mice." Kidney Int **73**(9): 1038-1047.
Que, J., B. Wilm, H. Hasegawa, F. Wang, D. Bader and B. L. Hogan (2008). "Mesothelium contributes to vascular smooth muscle and mesenchyme during lung development." Proc Natl Acad Sci U S A **105**(43): 16626-16630.
Rao, M. K., J. Pham, J. S. Imam, J. A. MacLean, D. Murali, Y. Furuta, A. P. Sinha-Hikim and M. F. Wilkinson (2006). "Tissue-specific RNAi reveals that WT1 expression in nurse cells controls germ cell survival and spermatogenesis." Genes Dev **20**(2): 147-152.
Ratelade, J., C. Arrondel, G. Hamard, S. Garbay, S. Harvey, N. Biebuyck, H. Schulz, N. Hastie, M. Pontoglio, M. C. Gubler, C. Antignac and L. Heidet (2010). "A murine model of Denys-Drash syndrome reveals novel transcriptional targets of WT1 in podocytes." Hum Mol Genet **19**(1): 1-15.
Reeves, W., J. P. Caulfield and M. G. Farquhar (1978). "Differentiation of epithelial foot processes and filtration slits: sequential appearance of occluding junctions, epithelial polyanion, and slit membranes in developing glomeruli." Lab Invest **39**(2): 90-100.
Reiser, J., W. Kriz, M. Kretzler and P. Mundel (2000). "The glomerular slit diaphragm is a modified adherens junction." J Am Soc Nephrol **11**(1): 1-8.
Reiser, J., K. R. Polu, C. C. Moller, P. Kenlan, M. M. Altintas, C. Wei, C. Faul, S. Herbert, I. Villegas, C. Avila-Casado, M. McGee, H. Sugimoto, D. Brown, R. Kalluri, P. Mundel, P. L. Smith,

D. E. Clapham and M. R. Pollak (2005). "TRPC6 is a glomerular slit diaphragm-associated channel required for normal renal function." Nat Genet **37**(7): 739-744.
Relle, M., H. Cash, C. Brochhausen, D. Strand, J. Menke, P. R. Galle and A. Schwarting (2011). "New perspectives on the renal slit diaphragm protein podocin." Mod Pathol **24**(8): 1101-1110.
Rigby, R. E., A. Leitch and A. P. Jackson (2008). "Nucleic acid-mediated inflammatory diseases." Bioessays **30**(9): 833-842.
Rivera, M. N. and D. A. Haber (2005). "Wilms' tumour: connecting tumorigenesis and organ development in the kidney." Nat Rev Cancer **5**(9): 699-712.
Robert, B., X. Zhao and D. R. Abrahamson (2000). "Coexpression of neuropilin-1, Flk1, and VEGF(164) in developing and mature mouse kidney glomeruli." Am J Physiol Renal Physiol **279**(2): F275-282.
Ronconi, E., C. Sagrinati, M. L. Angelotti, E. Lazzeri, B. Mazzinghi, L. Ballerini, E. Parente, F. Becherucci, M. Gacci, M. Carini, E. Maggi, M. Serio, G. B. Vannelli, L. Lasagni, S. Romagnani and P. Romagnani (2009). "Regeneration of glomerular podocytes by human renal progenitors." J Am Soc Nephrol **20**(2): 322-332.
Rossant, J., L. M. Nutter and M. Gertsenstein (2011). "Engineering the embryo." Proc Natl Acad Sci U S A **108**(19): 7659-7660.
Ruester, C., S. Franke, T. Bondeva and G. Wolf (2011). "Erythropoietin protects podocytes from damage by advanced glycation end-products." Nephron Exp Nephrol **117**(1): e21-30.
Ruf, R. G., A. Lichtenberger, S. M. Karle, J. P. Haas, F. E. Anacleto, M. Schultheiss, I. Zalewski, A. Imm, E. M. Ruf, B. Mucha, A. Bagga, T. Neuhaus, A. Fuchshuber, A. Bakkaloglu and F. Hildebrandt (2004). "Patients with mutations in NPHS2 (podocin) do not respond to standard steroid treatment of nephrotic syndrome." J Am Soc Nephrol **15**(3): 722-732.
Ruf, R. G., M. Schultheiss, A. Lichtenberger, S. M. Karle, I. Zalewski, B. Mucha, A. S. Everding, T. Neuhaus, L. Patzer, C. Plank, J. P. Haas, F. Ozaltin, A. Imm, A. Fuchshuber, A. Bakkaloglu, F. Hildebrandt and A. P. N. S. Group (2004). "Prevalence of WT1 mutations in a large cohort of patients with steroid-resistant and steroid-sensitive nephrotic syndrome." Kidney Int **66**(2): 564-570.
Sakairi, T., Y. Abe, H. Kajiyama, L. D. Bartlett, L. V. Howard, P. S. Jat and J. B. Kopp (2010). "Conditionally immortalized human podocyte cell lines established from urine." Am J Physiol Renal Physiol **298**(3): F557-567.
Sakairi, T., Y. Abe and J. B. Kopp (2011). "TGF-beta1 reduces Wilms' tumor suppressor gene expression in podocytes." Nephrol Dial Transplant **26**(9): 2746-2752.
Saleem, M. A., M. J. O'Hare, J. Reiser, R. J. Coward, C. D. Inward, T. Farren, C. Y. Xing, L. Ni, P. W. Mathieson and P. Mundel (2002). "A conditionally immortalized human podocyte cell line demonstrating nephrin and podocin expression." J Am Soc Nephrol **13**(3): 630-638.
Saleem, M. A., J. Zavadil, M. Bailly, K. McGee, I. R. Witherden, H. Pavenstadt, H. Hsu, J. Sanday, S. C. Satchell, R. Lennon, L. Ni, E. P. Bottinger, P. Mundel and P. W. Mathieson (2008). "The molecular and functional phenotype of glomerular podocytes reveals key features of contractile smooth muscle cells." Am J Physiol Renal Physiol **295**(4): F959-970.
Samejima, K., K. Nakatani, D. Suzuki, O. Asai, H. Sakan, S. Yoshimoto, Y. Yamaguchi, M. Matsui, Y. Akai, M. Toyoda, M. Iwano and Y. Saito (2012). "Clinical significance of fibroblast-specific protein-1 expression on podocytes in patients with focal segmental glomerulosclerosis." Nephron Clin Pract **120**(1): c1-7.

Sasaki, Y., T. Sone, S. Yoshida, K. Yahata, J. Hotta, J. D. Chesnut, T. Honda and F. Imamoto (2004). "Evidence for high specificity and efficiency of multiple recombination signals in mixed DNA cloning by the Multisite Gateway system." J Biotechnol **107**(3): 233-243.
Schmidt-Ott, K. M. and J. Barasch (2008). "WNT/beta-catenin signaling in nephron progenitors and their epithelial progeny." Kidney Int **74**(8): 1004-1008.
Schumacher, V. A., S. Jeruschke, F. Eitner, J. U. Becker, G. Pitschke, Y. Ince, J. H. Miner, I. Leuschner, R. Engers, A. S. Everding, M. Bulla and B. Royer-Pokora (2007). "Impaired glomerular maturation and lack of VEGF165b in Denys-Drash syndrome." J Am Soc Nephrol **18**(3): 719-729.
Schumacher, V. A., U. Schlotzer-Schrehardt, S. A. Karumanchi, X. Shi, J. Zaia, S. Jeruschke, D. Zhang, H. Pavenstadt, A. Drenckhan, K. Amann, C. Ng, S. Hartwig, K. H. Ng, J. Ho, J. A. Kreidberg, M. Taglienti, B. Royer-Pokora and X. Ai (2011). "WT1-dependent sulfatase expression maintains the normal glomerular filtration barrier." J Am Soc Nephrol **22**(7): 1286-1296.
Shalamanova, L., F. McArdle, A. B. Amara, M. J. Jackson and R. Rustom (2007). "Albumin overload induces adaptive responses in human proximal tubular cells through oxidative stress but not via angiotensin II type 1 receptor." Am J Physiol Renal Physiol **292**(6): F1846-1857.
Shankland, S. J. (2006). "The podocyte's response to injury: role in proteinuria and glomerulosclerosis." Kidney Int **69**(12): 2131-2147.
Shankland, S. J., J. W. Pippin, J. Reiser and P. Mundel (2007). "Podocytes in culture: past, present, and future." Kidney Int **72**(1): 26-36.
Sharan, S. K., L. C. Thomason, S. G. Kuznetsov and D. L. Court (2009). "Recombineering: a homologous recombination-based method of genetic engineering." Nat Protoc **4**(2): 206-223.
Shih, N. Y., J. Li, V. Karpitskii, A. Nguyen, M. L. Dustin, O. Kanagawa, J. H. Miner and A. S. Shaw (1999). "Congenital nephrotic syndrome in mice lacking CD2-associated protein." Science **286**(5438): 312-315.
Shimshek, D. R., J. Kim, M. R. Hubner, D. J. Spergel, F. Buchholz, E. Casanova, A. F. Stewart, P. H. Seeburg and R. Sprengel (2002). "Codon-improved Cre recombinase (iCre) expression in the mouse." Genesis **32**(1): 19-26.
Shirato, I. (2002). "Podocyte process effacement in vivo." Microsc Res Tech **57**(4): 241-246.
Sim, E. U., A. Smith, E. Szilagi, F. Rae, P. Ioannou, M. H. Lindsay and M. H. Little (2002). "Wnt-4 regulation by the Wilms' tumour suppressor gene, WT1." Oncogene **21**(19): 2948-2960.
Sison, K., V. Eremina, H. Baelde, W. Min, M. Hirashima, I. G. Fantus and S. E. Quaggin (2010). "Glomerular structure and function require paracrine, not autocrine, VEGF-VEGFR-2 signaling." J Am Soc Nephrol **21**(10): 1691-1701.
Smart, N., S. Bollini, K. N. Dube, J. M. Vieira, B. Zhou, S. Davidson, D. Yellon, J. Riegler, A. N. Price, M. F. Lythgoe, W. T. Pu and P. R. Riley (2011). "De novo cardiomyocytes from within the activated adult heart after injury." Nature **474**(7353): 640-644.
Smeets, B., M. L. Angelotti, P. Rizzo, H. Dijkman, E. Lazzeri, F. Mooren, L. Ballerini, E. Parente, C. Sagrinati, B. Mazzinghi, E. Ronconi, F. Becherucci, A. Benigni, E. Steenbergen, L. Lasagni, G. Remuzzi, J. Wetzels and P. Romagnani (2009). "Renal progenitor cells contribute to hyperplastic lesions of podocytopathies and crescentic glomerulonephritis." J Am Soc Nephrol **20**(12): 2593-2603.
Smeets, B., C. Kuppe, E. M. Sicking, A. Fuss, P. Jirak, T. H. van Kuppevelt, K. Endlich, J. F. Wetzels, H. J. Grone, J. Floege and M. J. Moeller (2011). "Parietal epithelial cells participate in the formation of sclerotic lesions in focal segmental glomerulosclerosis." J Am Soc Nephrol **22**(7): 1262-1274.

Srinivas, S., T. Watanabe, C. S. Lin, C. M. William, Y. Tanabe, T. M. Jessell and F. Costantini (2001). "Cre reporter strains produced by targeted insertion of EYFP and ECFP into the ROSA26 locus." BMC Dev Biol **1**: 4.
Stark, K., S. Vainio, G. Vassileva and A. P. McMahon (1994). "Epithelial transformation of metanephric mesenchyme in the developing kidney regulated by Wnt-4." Nature **372**(6507): 679-683.
Steege, A., M. Fahling, A. Paliege, A. Bondke, K. M. Kirschner, P. Martinka, C. Kaps, A. Patzak, P. B. Persson, B. J. Thiele, H. Scholz and R. Mrowka (2008). "Wilms' tumor protein (-KTS) modulates renin gene transcription." Kidney Int **74**(4): 458-466.
Stefanidis, C. J. and U. Querfeld (2011). "The podocyte as a target: cyclosporin A in the management of the nephrotic syndrome caused by WT1 mutations." Eur J Pediatr **170**(11): 1377-1383.
Steffes, M. W., D. Schmidt, R. McCrery and J. M. Basgen (2001). "Glomerular cell number in normal subjects and in type 1 diabetic patients." Kidney Int **59**(6): 2104-2113.
Sugiyama, H. (2002). "Wilms tumor gene WT1 as a tumor marker for leukemic blast cells and its role in leukemogenesis." Methods Mol Med **68**: 223-237.
Sugiyama, H. (2010). "WT1 (Wilms' tumor gene 1): biology and cancer immunotherapy." Jpn J Clin Oncol **40**(5): 377-387.
Suh, J. H., G. Jarad, R. G. VanDeVoorde and J. H. Miner (2011). "Forced expression of laminin beta1 in podocytes prevents nephrotic syndrome in mice lacking laminin beta2, a model for Pierson syndrome." Proc Natl Acad Sci U S A **108**(37): 15348-15353.
Surendran, K., S. P. McCaul and T. C. Simon (2002). "A role for Wnt-4 in renal fibrosis." Am J Physiol Renal Physiol **282**(3): F431-441.
Suri, M., P. Kelehan, D. O'Neill, S. Vadeyar, J. Grant, S. F. Ahmed, J. Tolmie, E. McCann, W. Lam, S. Smith, D. Fitzpatrick, N. D. Hastie and W. Reardon (2007). "WT1 mutations in Meacham syndrome suggest a coelomic mesothelial origin of the cardiac and diaphragmatic malformations." Am J Med Genet A **143A**(19): 2312-2320.
Suzuki, T., T. Matsusaka, M. Nakayama, T. Asano, T. Watanabe, I. Ichikawa and M. Nagata (2009). "Genetic podocyte lineage reveals progressive podocytopenia with parietal cell hyperplasia in a murine model of cellular/collapsing focal segmental glomerulosclerosis." Am J Pathol **174**(5): 1675-1682.
Swetha, G., V. Chandra, S. Phadnis and R. Bhonde (2011). "Glomerular parietal epithelial cells of adult murine kidney undergo EMT to generate cells with traits of renal progenitors." J Cell Mol Med **15**(2): 396-413.
Takemoto, M., N. Asker, H. Gerhardt, A. Lundkvist, B. R. Johansson, Y. Saito and C. Betsholtz (2002). "A new method for large scale isolation of kidney glomeruli from mice." Am J Pathol **161**(3): 799-805.
Toyonaga, J., K. Tsuruya, H. Ikeda, H. Noguchi, H. Yotsueda, K. Fujisaki, M. Hirakawa, M. Taniguchi, K. Masutani and M. Iida (2011). "Spironolactone inhibits hyperglycemia-induced podocyte injury by attenuating ROS production." Nephrol Dial Transplant **26**(8): 2475-2484.
Truett, G. E., P. Heeger, R. L. Mynatt, A. A. Truett, J. A. Walker and M. L. Warman (2000). "Preparation of PCR-quality mouse genomic DNA with hot sodium hydroxide and tris (HotSHOT)." Biotechniques **29**(1): 52, 54.

Tsvetanova, B., L. Peng, X. Liang, K. Li, L. Hammond, T. C. Peterson and F. Katzen (2012). "Advanced DNA assembly technologies in drug discovery." Expert Opin Drug Discov **7**(5): 371-374.
Tuncdemir, M. and M. Ozturk (2011). "The effects of angiotensin-II receptor blockers on podocyte damage and glomerular apoptosis in a rat model of experimental streptozotocin-induced diabetic nephropathy." Acta Histochem **113**(8): 826-832.
Ullman-Cullere, M. H. and C. J. Foltz (1999). "Body condition scoring: a rapid and accurate method for assessing health status in mice." Lab Anim Sci **49**(3): 319-323.
Vajjhala, P. R., E. Macmillan, T. Gonda and M. Little (2003). "The Wilms' tumour suppressor protein, WT1, undergoes CRM1-independent nucleocytoplasmic shuttling." FEBS Lett **554**(1-2): 143-148.
Valente, M. J., R. Henrique, V. L. Costa, C. Jeronimo, F. Carvalho, M. L. Bastos, P. G. de Pinho and M. Carvalho (2011). "A rapid and simple procedure for the establishment of human normal and cancer renal primary cell cultures from surgical specimens." PLoS One **6**(5): e19337.
van den Berg, J. G., M. A. van den Bergh Weerman, K. J. Assmann, J. J. Weening and S. Florquin (2004). "Podocyte foot process effacement is not correlated with the level of proteinuria in human glomerulopathies." Kidney Int **66**(5): 1901-1906.
Van Keuren, M. L., G. B. Gavrilina, W. E. Filipiak, M. G. Zeidler and T. L. Saunders (2009). "Generating transgenic mice from bacterial artificial chromosomes: transgenesis efficiency, integration and expression outcomes." Transgenic Res **18**(5): 769-785.
Velecela, V., L. A. Lettice, Y. Y. Chau, J. Slight, R. L. Berry, A. Thornburn, Q. D. Gunst, M. van den Hoff, M. Reina, F. O. Martinez, N. D. Hastie and O. M. Martinez-Estrada (2013). "WT1 regulates the expression of inhibitory chemokines during heart development." Hum Mol Genet.
Venkatareddy, M., L. Cook, K. Abuarquob, R. Verma and P. Garg (2011). "Nephrin regulates lamellipodia formation by assembling a protein complex that includes Ship2, filamin and lamellipodin." PLoS One **6**(12): e28710.
Wagner, K. D., N. Wagner, A. Bondke, B. Nafz, B. Flemming, H. Theres and H. Scholz (2002). "The Wilms' tumor suppressor Wt1 is expressed in the coronary vasculature after myocardial infarction." FASEB J **16**(9): 1117-1119.
Wagner, N., H. Morrison, S. Pagnotta, J. F. Michiels, Y. Schwab, K. Tryggvason, A. Schedl and K. D. Wagner (2011). "The podocyte protein nephrin is required for cardiac vessel formation." Hum Mol Genet **20**(11): 2182-2194.
Wagner, N., K. D. Wagner, H. Scholz, K. M. Kirschner and A. Schedl (2006). "Intermediate filament protein nestin is expressed in developing kidney and heart and might be regulated by the Wilms' tumor suppressor Wt1." Am J Physiol Regul Integr Comp Physiol **291**(3): R779-787.
Wagner, N., K. D. Wagner, Y. Xing, H. Scholz and A. Schedl (2004). "The major podocyte protein nephrin is transcriptionally activated by the Wilms' tumor suppressor WT1." J Am Soc Nephrol **15**(12): 3044-3051.
Walker, C., F. Rutten, X. Yuan, H. Pass, D. M. Mew and J. Everitt (1994). "Wilms' tumor suppressor gene expression in rat and human mesothelioma." Cancer Res **54**(12): 3101-3106.
Wang, C., X. Liu, Z. Ke, Y. Tang, C. C. Li, C. M. Li, Z. Ye, J. Zhang and T. Lou (2012). "Mesangial medium from IgA nephropathy patients induces podocyte epithelial-to-mesenchymal transition through activation of the phosphatidyl inositol-3-kinase/Akt signaling pathway." Cell Physiol Biochem **29**(5-6): 743-752.

Wang, J., Y. Wang, J. Long, B. H. Chang, M. H. Wilson, P. Overbeek and F. R. Danesh (2010). "Tamoxifen-inducible podocyte-specific iCre recombinase transgenic mouse provides a simple approach for modulation of podocytes in vivo." Genesis **48**(7): 446-451.
Wang, L., G. C. Shearer, M. S. Budamagunta, J. C. Voss, A. Molfino and G. A. Kaysen (2012). "Proteinuria decreases tissue lipoprotein receptor levels resulting in altered lipoprotein structure and increasing lipid levels." Kidney Int **82**(9): 990-999.
Wang, Y., H. L. Yao, C. B. Cui, E. Wauthier, C. Barbier, M. J. Costello, N. Moss, M. Yamauchi, M. Sricholpech, D. Gerber, E. G. Loboa and L. M. Reid (2010). "Paracrine signals from mesenchymal cell populations govern the expansion and differentiation of human hepatic stem cells to adult liver fates." Hepatology **52**(4): 1443-1454.
Wasilewska, A. M., E. Kuroczycka-Saniutycz and W. Zoch-Zwierz (2011). "Effect of cyclosporin A on proteinuria in the course of glomerulopathy associated with WT1 mutations." Eur J Pediatr **170**(3): 389-391.
Waters, A. M., M. Y. Wu, T. Onay, J. Scutaru, J. Liu, C. G. Lobe, S. E. Quaggin and T. D. Piscione (2008). "Ectopic notch activation in developing podocytes causes glomerulosclerosis." J Am Soc Nephrol **19**(6): 1139-1157.
Wells, J., M. N. Rivera, W. J. Kim, K. Starbuck and D. A. Haber "The predominant WT1 isoform (+KTS) encodes a DNA-binding protein targeting the planar cell polarity gene Scribble in renal podocytes." Mol Cancer Res **8**(7): 975-985.
Welsh, G. I., L. J. Hale, V. Eremina, M. Jeansson, Y. Maezawa, R. Lennon, D. A. Pons, R. J. Owen, S. C. Satchell, M. J. Miles, C. J. Caunt, C. A. McArdle, H. Pavenstadt, J. M. Tavare, A. M. Herzenberg, C. R. Kahn, P. W. Mathieson, S. E. Quaggin, M. A. Saleem and R. J. Coward (2010). "Insulin signaling to the glomerular podocyte is critical for normal kidney function." Cell Metab **12**(4): 329-340.
Welsh, G. I. and M. A. Saleem (2010). "Nephrin-signature molecule of the glomerular podocyte?" J Pathol **220**(3): 328-337.
Wharram, B. L., M. Goyal, J. E. Wiggins, S. K. Sanden, S. Hussain, W. E. Filipiak, T. L. Saunders, R. C. Dysko, K. Kohno, L. B. Holzman and R. C. Wiggins (2005). "Podocyte depletion causes glomerulosclerosis: diphtheria toxin-induced podocyte depletion in rats expressing human diphtheria toxin receptor transgene." J Am Soc Nephrol **16**(10): 2941-2952.
Wiggins, J. E., M. Goyal, S. K. Sanden, B. L. Wharram, K. A. Shedden, D. E. Misek, R. D. Kuick and R. C. Wiggins (2005). "Podocyte hypertrophy, "adaptation," and "decompensation" associated with glomerular enlargement and glomerulosclerosis in the aging rat: prevention by calorie restriction." J Am Soc Nephrol **16**(10): 2953-2966.
Winn, M. P., P. J. Conlon, K. L. Lynn, M. K. Farrington, T. Creazzo, A. F. Hawkins, N. Daskalakis, S. Y. Kwan, S. Ebersviller, J. L. Burchette, M. A. Pericak-Vance, D. N. Howell, J. M. Vance and P. B. Rosenberg (2005). "A mutation in the TRPC6 cation channel causes familial focal segmental glomerulosclerosis." Science **308**(5729): 1801-1804.
Yakar, S., C. J. Rosen, W. G. Beamer, C. L. Ackert-Bicknell, Y. Wu, J. L. Liu, G. T. Ooi, J. Setser, J. Frystyk, Y. R. Boisclair and D. LeRoith (2002). "Circulating levels of IGF-1 directly regulate bone growth and density." J Clin Invest **110**(6): 771-781.
Yamaguchi, Y., M. Iwano, D. Suzuki, K. Nakatani, K. Kimura, K. Harada, A. Kubo, Y. Akai, M. Toyoda, M. Kanauchi, E. G. Neilson and Y. Saito (2009). "Epithelial-mesenchymal transition as a potential explanation for podocyte depletion in diabetic nephropathy." Am J Kidney Dis **54**(4): 653-664.

Yang, A. H., J. Y. Chen and B. F. Chen (2004). "The dysregulated glomerular cell growth in Denys-Drash syndrome." Virchows Arch **445**(3): 305-314.
Yang, W., J. Wang, L. Shi, L. Yu, Y. Qian, Y. Liu, W. Wang and S. Cheng (2012). "Podocyte injury and overexpression of vascular endothelial growth factor and transforming growth factor-beta 1 in adriamycin-induced nephropathy in rats." Cytokine **59**(2): 370-376.
Zeisberg, M. and J. S. Duffield (2010). "Resolved: EMT produces fibroblasts in the kidney." J Am Soc Nephrol **21**(8): 1247-1253.
Zhou, B., L. B. Honor, Q. Ma, J. H. Oh, R. Z. Lin, J. M. Melero-Martin, A. von Gise, P. Zhou, T. Hu, L. He, K. H. Wu, H. Zhang, Y. Zhang and W. T. Pu (2012). "Thymosin beta 4 treatment after myocardial infarction does not reprogram epicardial cells into cardiomyocytes." J Mol Cell Cardiol **52**(1): 43-47.
Zhou, B., Q. Ma, S. Rajagopal, S. M. Wu, I. Domian, J. Rivera-Feliciano, D. Jiang, A. von Gise, S. Ikeda, K. R. Chien and W. T. Pu (2008). "Epicardial progenitors contribute to the cardiomyocyte lineage in the developing heart." Nature **454**(7200): 109-113.
Zou, J., E. Yaoita, Y. Watanabe, Y. Yoshida, M. Nameta, H. Li, Z. Qu and T. Yamamoto (2006). "Upregulation of nestin, vimentin, and desmin in rat podocytes in response to injury." Virchows Arch **448**(4): 485-492.